INTERRELATIONSHIP BETWEEN LEAF DEVELOPMENT AND PHOTOREGULATION OF STARCH DEGRADING ENZYMES IN PEARL MILLET

(Pennisetum americanum).

A THESIS SUBMITTED FOR THE DEGREE OF
DOCTOR OF PHYLOSOPHY

By
K. I. MARAGATHA VALLY

SCHOOL OF LIFE SCIENCES
University of Hyderabad
HYDERABAD - 500 134
INDIA

FEBRUARY, 1994

ENROLLMENT NO. NL - 3856

UNIVERSITY OF HYDERABAD

CERTIFICATE

This is to certify that the thesis entitled "Interrelationship between leaf development and photoregulation of starch degrading enzymes in pearl millet (Pennisetum americanum)" is based on the results of the work done by Ms. K. J. Maragatha Vally for the degree of Doctor of Philosophy under my supervision. This work has not been submitted for any degree or diploma of any other University or Institution.

Prof. A. R. Reddy
Head
Department of Plant Sciences

Prof. R. P. Sharma
Supervisor
Prof. R P. SHARMA,
Dept. of Plant Sciences
School of Life Sciences,
University of Hyderabad.
HYDERABAD-500 134, INDIA

28-2-94
Prof. N. C. Subrahmanyam
Dean
School of Life Sciences

UNIVERSITY OF HYDERABAD

DECLARATION

I hereby declare that the work presented in this thesis has been carried out by me under the supervision of **Prof. R. P. Sharma** and that this has not been submitted for a degree or diploma in any other University

Dated :28 February, 1994
Place : Hyderabad

Vally. K.
K. J. Maragatha Vally

R.P. Sharma
Prof. R. P. Sharma
(Supervisor)

TO MY MOTHER

ACKNOWLEDGEMENTS

I express immense sense of gratitude to my supervisor Prof. R.P. Sharma whose guidance had been a constant source of encouragement at all stages of this work. I am greatly indebted for his suggestions and critical comments throughout my course. I gratefully acknowledge all the facilities provided by Prof. A.R Reddy, Head, Department of Plant Science, Prof.N.C. Subramanyam, Dean, School of Life Sciences and former Dean Prof. P.R.K. Reddy.

I owe my sincere gratitude to Dr. Aparna Datta Gupta for her timely help.

I record my sincere thanks to Dr. B. Sangeetha, Dr. V.A. Manga, Dr. Suverchala, and Ms. K. Joanny for comforting at many stages during this course. My due thanks to Dr. K. Subbaramaiah, Dr. K.Subbarao, Mr. Venkat, Ms. Selvi, Mr. Ramachandra Reddy and Rupali for their help and cooperation.

A lot of help was extended to me by Mr. Narayana Reddy and Janardhan Reddy. I am thankful to them.

I acknowledge CSIR for their financial support.

Nothing will be enough to express my indebtedness to my family members, for their unstinting cooperation and encouragement. Finally, I acknowledge, silent but firm backing of my husband with which I could complete this course successfully.

ABBREVIATIONS

A	= absorbance
ABA	= abscisic acid
B	= bundle sheath
BL	= blue light
BSA	• bovine serum albumin
cm	= centimeter
d	= day
D	= dark
DMSO	= dimethyl sulfonic acid
DNS	= dinitrosalicylic acid
DW	= distilled water
EDTA	= ethylene diamine tetraacetic acid
FRL	= far red light
GA_3	= gibberellic acid
gm/FW	= gram fresh weight
h	= hour
IAA	= Indole acetic acid
LHCP	= light harvesting chlorophyll a/b binding protein
LSU	= large subunit of RuBPCase
M	= **mesophyll** cells.
MDH	= **malate** dehydrogenase
MES	= 2-[N- **Morpholino**] ethanesulfonic acid
MW	= molecular weight
NADP	= **Nicotinamide** adenine dinucleotide phosphate
NET	= **NaCl** EDTA Tris buffer
NF	= Norflurazon
NP-40	= Nonidet P-40
mRNA	= messenger ribonucleic acid
nkat	= nano **katal**
PAGE	= polyacrylamide gel electrophoresis
PBS	= phosphate buffered saline
PEPC	• phospho **enol** pyruvate carboxylase
Pfr	= far-red light absorbing form of phytochrome
Pr	= red light absorbing form of phytochrome
PPO	= **2,5-diphenyl** oxazole
RL	= red light
Rubisco	= **rubulose-1,5-bisphosphate** carboxylase
SDS	= sodium dodecyl sulphate
SSU	= small subunit of RuBPCase
SRID	= single radial **immunodiffusion**
TCA	= trichloro acetic acid
UV	= ultra violet
v/v	= volume/volume
w/v	= weight/volume

CONTENTS

INTRODUCTION

CHAPTER 1

INTRODUCTION

Plant development is a complex process which basically comprises cell division, cell differentiation and growth. Unlike animals, where development is highly controlled and exactly specified, plant development and organization is extraordinarily plastic. Plant development is continuous and indeterminate since growth and differentiation are localized throughout the plant body at meristematic zones (Steeves and Sussex, 1989). The appearance of new organs such as leaves or flowers results from organized cell division and differentiation in these meristems (Medford, 1992). During the course of cell division in apical meristems, the organ primordias are initiated continually, constituting of a large number of cells, which act in synchrony to follow a programmed sequence of division, expansion and differentiation to form a determinate appendage such as the leaf. In most cases once an organ is differentiated and cell expansion is completed, it does not grow further, and performs its function till the onset of senescence. In this respect, monocot leaf development differs from development in other organs, as the monocot leaf is under a continuous state of differentiation, as it possesses a basal meristem which continuously contributes new cells at the leaf base.

Though the process of leaf initiation and development is genetically determined, the acquisition of a photoautotrophic mode of nutrition in the leaf is solely dependent on availability of an environmental factor-light. In the

absence of light, leaf development follows a strategy called scotomorphogenesis wherein leaves are yellow in color due to absence of chloroplasts, and plastid differentiates to etioplast. In the presence of light, a normal photomorphogenic development is initiated wherein the leaf develops normal chloroplasts. In higher plants, greening of leaves involves a series of distinct morphological and biochemical processes leading to differentiation of cells and organelles such as chloroplasts. Chloroplast development requires a complex interaction between nuclear and plastid genomes which is triggered by light and a chloroplast-derived plastidic signal. In addition, light is also required for photoreduction of protochlorophyllide to chlorophyll (Hoober, 1984). In C_4 plants leaf development is further accompanied by differentiation of two photosynthetic cell types viz., bundle sheath and mesophyll cells. The photosynthetic reactions are split between these two cell types with each cell type accumulating a specific complement of photosynthetic enzymes (Langdale and Nelson, 1991).

Leaves are the principal site of photosynthetic carbon fixation, depositing excess of fixed carbon in the chloroplast in the form of polymeric carbohydrates like starch, which is subsequently degraded and mobilized to different parts of the organism. The starch deposited in chloroplasts is mobilized via the action of starch degrading enzymes like amylases and phosphorylases. While there have been a number of investigations outlining photoinduced leaf development and chloroplast biogenesis in relation to synthesis of enzymes and proteins involved in trapping of light energy, carbon fixation and generating sugars etc., the development, extent and role of starch degrading enzymes during leaf development is poorly understood. Most

importantly, little is known about the influence of cellular position on development of these enzymes.

The monocot leaf offers an ideal system to study the interrelationship between cell development and intercellular regulation of cytosolic and plastidic enzymes. The monocot leaf lends itself best to study different developmental stages along the leaf axis, as it possesses a continuous gradient of maturing cells from the base to tip of the leaf. Moreover, parallel to the cell-differentiation gradient, a gradient of chloroplasts in different developmental states also exists from the base to the tip of these leaves. In the present study the relationship between leaf development and starch degrading enzymes was studied by using the leaves of monocotyledon plant, pearl millet (*Pennisetum americanum).* Being a C_4 plant, the pearl millet also possesses dimorphic chloroplasts. The studies were directed towards deciphering the interrelationships between cellular position, gradient of cell maturation, chloroplast differentiation and photoregulation of starch degrading enzymes, viz., amylases and phosphorylases. The possible role of these enzymes in mobilization of photosynthetically generated transitory starch was also examined.

REVIEW OF LITERATURE

CHAPTER 2

REVIEW OF LITERATURE

In land plants, the leaf is the site for trapping light energy via photosynthesis. To be fully effective as a photosynthetic organ, leaf has to trap light, with the inevitable consequence that it is also exposed to infrared wavelengths that causes heating, and to ultraviolet radiation that causes genetic damage (Dale, 1992). The development of the leaf lamina is an important process in relation to the interception of light and the accomplishment of photosynthetic competence (Leech and Baker, 1983). Though leaf development is genetically determined (Freeling, 1992; Freeling *et ed.,* 1992), the acquisition of photosynthesis and differentiation of leaf cells is triggered by an environmental factor-light. The several facets of leaf development influenced by light are seen most remarkably during de-etiolation of seedlings e.g., light-stimulated unrolling of cereal leaves (Virgin, 1989), and cotyledon or leaf expansion in dicot seedlings (Sangeetha and Sharma, 1988). Additionally, light also influences several metabolic processes in leaf cells via regulation of gene expression, and by controlling activities of enzymes regulating metabolic pathways. In the present review, the role of light in the development of the monocot leaf is summarized with particular emphasis on regulation of starch degrading enzymes.

2.1 LEAF DEVELOPMENT

In angiosperms, leaves originate at shoot apical meristems, which consist of three distinct cell layers L1, L2 and L3 from which plant organs are derived (Poethig, 1987). These layers have a distinct pattern of cell divisions, e.g., in the L1 layer, which is the outermost, cell division is anticlinal and gives rise to the epidermal tissue of the differentiating organ. The cells in the L2 layer divide mostly in the anticlinal plane, but also in the periclinal plane, and cells of the L3 layer divide both in anticlinal and periclinal planes. In monocots, leaves are derived from L1, L2 and L3 layers of apical meristems. In dicots, two tunica layers, L1 and L2, are present, out of which only the L1 layer contributes to epidermis, and the L2 and L3 layers give rise to the internal tissue of the leaf (Poethig, 1987; 1989).

In maize, cells from both L1 and L2 layers of the apical meristem divide to form the leaf primordium (Poethig, 1987). Subsequent growth occurs predominantly from a basal intercalary meristem, where polarized patterns of cell division and expansion produce the elongated structure characteristic of a mature leaf (Sharman, 1942). Clonal analysis has shown that the monocot leaf epidermis is derived from the L1 layer of the apex, whereas the internal leaf structures, vascular tissue, photosynthetic bundle sheath (B) and mesophyll (M) cells are derived primarily from the L2 layer (Poethig, 1987). At the leaf margins, both the epidermis and the internal tissue are often derived from the L1 layer (Langdale *et al.*, 1989). After the formation of leaf primordium further growth of the leaf is largely restricted to a basal meristem, and the leaf possesses a gradient of cell maturation, showing all stages of

development from the most immature at the base to the fully functional and differentiated cells at the tip of the leaf (Sharman, 1942).

2.1.1 Cell differentiation in C_4 plants

In C_4 plants, leaf development is more complex than in C_3 plants due to chloroplastic and cellular dimorphism. C_4 differentiation depends largely on cell position and light-induced signals. In C_4 monocot leaves, the cellular differentiation of 'kranz anatomy' is associated with the development of the basic framework of a vascular system. Vascular development is initiated as the midvein develops from procambium in the shoot apex and differentiates towards the tip of the leaf (acropetally), dividing leaf in half, longitudinally (Sharman, 1942; Esau, 1943). Once procambial meristems become discrete, veins enlarge as a result of periclinal (radial increase) and anticlinal (longitudinal increase) divisions within the procambial strand. As the leaf primordium expands, lateral (large, acropetal) and then intermediate (small, basipetal) veins progressively subdivide the leaf. The overall age-gradient in the vasculature is also seen from the tip (oldest) to the base of the leaf. Bundle sheath and mesophyll cells around the medium vein matures first (acropetally); cells around the lateral veins then develop both acropetally and basipetally. Finally, cells around the intermediate veins mature basipetally. This is the same order in which the cells become morphologically differentiated (Easu, 1943; Sharman, 1942; Russell and Evert, 1985).

The development of bundle sheath cells takes place from cell division of either procambial cells or ground meristematic cells of mesophyll. The

maturation of bundle sheath cells and mesophyll cells is closely linked to vascular development and follows vascular differentiation (Langdale *et al.*, 1987). The bundle sheath cells differentiates coordinately, partly from the outermost layer of the procambium, and partly from the adjacent ground meristem. These divisions generate 'half vein' units which comprise half of the bundle sheath cells around a vein and a single adjacent mesophyll cell (Langdale *et al.*, 1989). Dengler *et al.*, (1985, 1990) however, suggested that bundle sheath cells are derived entirely from procambial meristems, and mesophyll cells from ground meristem.

2.1.2 Regulation of leaf development

The identity of morphogenic factors which determine leaf initiation, and its distinction from reproductive organs is still unknown. A number of mutants have been described which are defective in leaf development, of these Knotted-1 (*Kn1*) gene of maize is quite interesting. The product *of Knl* gene is present in the nucleus of the shoot apical meristem cells, but is undetectable in leaf and floral organ primordia of wild-type plants (Freeling *et al.*, 1988; Smith *et al.*, 1992). Mutation at the *Knl* locus disrupts epidermal-layer development to give finger-like projections on leaf surface. To date, *Knl* is the first gene whose downregulation may be linked in some way to the earliest known events in leaf initiation. The *Knl* locus was cloned and its cDNA sequence shows a similarity to a homeo-domain protein present in animals, which acts as a transcriptional regulator controlling animal development (Vollbrecht *et al.*, 1991). The ecotopic expression of *theKnl* gene product in developing leaf blade interferes with normal leaf development: the regions expressing it differentiate

to the leaf sheath around the veins rather than the normal leaf blade. Similar to the *Kn1* gene product, ROUGH SHEATH-1 and LIGULELESS-3 genes also encode homeo-domain proteins in maize (Smith and Hake, 1992). Similarly, the production of juvenile leaves and adult leaves in maize is controlled by specific gene loci. In maize, juvenile leaves are shorter than adult leaves and possess epicuticular wax which is not present on adult leaves (Poethig, 1990). The mutations controlling juvenile-leaf production in maize act on apical meristems to delay its transformation to the floral stage and promote development of the juvenile leaf (Bassiri *et al.*, 1992). In the maize *Tp 1* mutant, it has been shown that *Tp1* controls the generation and distribution of a diffusible substance which initiates development of juvenile traits (Poethig, 1988).

In addition to genetic regulation, leaf development is strongly influenced by the hormonal status of the leaf. For example, in heterophyllic aquatic species, ABA treatment of the submerged shoot initiates development of aerial leaves, which normally requires exposure to an aerial environment (Mohanram and Rao, 1982). It is proposed that the emergence of the shoot from water results in osmotic stress leading to ABA production and, consequently, aerial leaf development (Goliber, 1989). The young, expanding leaves have higher abscisic acid levels than mature leaves (Raschke and Zeevaart, 1976; Zeevaart, 1980). In woody angiosperms gibberellic acid treatment can induce the formation of juvenile leaves from adult shoots (Rogler and Hackett, 1975).

In several instances hormones have been implicated in regulation of leaf expansion and differentiation. In many dicots the application of cytokinin initiates expansion of cotyledons/leaf (Scolt and Liverman, 1957), which

normally requires exposure to light to trigger leaf expansion (Sangeetha and Sharma, 1988; van Volkenburgh and Cleland, 1979, 1986). In grasses, the unrolling of leaf in seedlings is initiated by light and accompanied by a distinct hormonal change like an increase in gibberellic acid level (Virgin, 1989).

Higher cytokinin contents have been found in immature leaves and apical buds than in mature leaves. Application of cytokinins could promote leaf unfolding and expansion in intact plants (Leech, 1985). It has been reported that the young expanding leaves are the richest source of auxin. The highest concentration of auxin has been found at the leaf base (Allen and Baker, 1980). In basal tissue of the 6th leaf from the bottom in 28-day old maize plants, the IAA level was 2 to 3 times more than that in the apical segments. The auxins at high concentrations inhibited the development of the mesophyll without affecting vein extension (Gifford, 1953). In many dicot species evidence has been obtained that GA_3 may function in regulating leaf growth. GA_3 application alters leaf shape in many species (Jones, 1987), and leaf growth is altered in GA-deficient mutants of tomato (Koornneef *et al.*, 1980) and pea (Ross *et al.*, 1993). Ethylene inhibits leaf expansion. The inhibition involves a general reduction in leaf dimensions, rather than just a reduction in mesophyll tissue. The application of ethylene inhibits leaf expansion by inhibiting cell division (Leopold and Kriedemann, 1978, Scott and Possingham, 1982).

The development of the leaf is strongly influenced by light, a phenomenon which is most predominantly seen during seedling development. The dark-grown seedlings of dicots possess a hypocotyl hook and unexpanded leaves or plumules. Exposure to light initiates photomorphogenic development

of these seedlings where light activates plant photoreceptors like the UV-B photoreceptor, UV-A\blue photoreceptor and phytochrome, leading to leaf/cotyledon expansion in dicots, and unrolling of leaves in monocots (Shropshire and Mohr, 1983). While the genotype of the plants determines size and shape of leaf, light strongly influences cellular differentiation of leaves, leading to the formation of chloroplasts and induction of several enzymes (Kendrick and Krorenberg, 1986). While it is known that many of light's effects are mediated by activation of plant photoreceptor phytochrome, the components involved in the signal chain are not yet known.

Recently great emphasis has been laid on identification of components which regulate photomorphogenetic development of leaf/cotyledon using *Arabidopsis* as a model and selecting mutants which in dark possess the phenotype of light-grown plants. In *Arabidopsis,* several loci have been identified such as *det1*,*cop1*, *2,* 3, 4, 5 and 9 (Chory, 1992; Chory *et al.,* 1989, 1991; Deng *et al.,* 1991, 1992) which initiate in dark-grown seedlings with a phenotype characteristic of light-grown plants. Of these mutants *cop2* , 3, 4 show the expanded cotyledon which is characteristic of light-grown plants, but, at the same time, have undifferentiated plastids (Hou *et al.,* 1993). Further, the above *cop* mutations do not affect hypocotyl development but only regulate cotyledon development.

It is apparent from these studies that the process underlying leaf development is controlled by several regulatory factors, which are both interdependent as well as independent of each other and lead to cell differentiation. Sun *et al.,* (1993) have shown that the *detl* mutant lacks a

phosphoprotein which specifically binds to the promoter of *cab 140* gene of *Arabidopsis*. The protein acts as a repressor of the above gene, as mutant seedlings express a high level of *cab* mRNA in darkness and do not respond to brief red light. The gene product of the *cop9* gene encodes a protein with the characters of both G-proteins and Zinc binding proteins (Deng *et al.*, 1992), which may play a role in carrying a signal from photoreceptor to promoter of light-regulated genes.

In addition to the above factors, the cellular position too can determine the cellular differentiation process. The accumulation of photosynthetic gene products in B and M cells is associated with vascular development (Langdale *et al.*, 1987, 1988). The veins limit transport of factors essential for the development of these cell-types. Maize cells that are close to the vein show a C_4 type localization of Rubisco in B cells, whereas cells which are far off show a C_3 type localization of Rubisco, which suggests that veins might produce a signal which is needed for differentiation of B and M cell specific localization of C_4 enzymes. In the monocot leaf a major signal that influences a C_4 type gene expression is light. In dark-grown plants Rubisco is present in both B and M cells in a C_3 pattern, but on exposure to light Rubisco decreases in M cells and increases in B cells.

2.1.3 Chloroplast biogenesis

The development of chloroplast and leaf are two different processes, but chloroplast development is coordinated and regulated by leaf development. Chloroplasts are derived from small undifferentiated proplastids which are

maternally inherited in plants. The proplastid is a small organelle, 0.5-1.0 μm in diameter, without a distinct internal architecture characteristic of the mature chloroplasts and possesses low amounts of nucleic acids and proteins. The meristematic cells of plant possess only proplastid which differentiates into chloroplast during leaf development. In differentiating mesophyll cells, proplastids transform into chloroplast, a process which is light dependent. The development of a fully functional chloroplast involves regulation of both nuclear and plastidic genes (Mullet, 1988; Mayfield, 1990). However, signals triggering chloroplast development are still not known.

Chloroplast development in angiosperms goes to completion only in the presence of light (Thomson and Whatley, 1980). The development of proplastid to etioplast or chloroplast is regulated by differentiation of leaf cells and availability of light. In absence of light, development follows a different strategy leading to an etioplast stage, characterized by the presence of prolamellar bodies (Weier and Brown, 1970) and a small amount of protochlorophyll. The etioplast to chloroplast differentiation requires the phototransformation of the protochlorophyllide to chlorophyllide (Akoyunoglou and Akoyunoglou, 1986). Light-dependent transformation of etioplasts to chloroplasts may proceed without obvious changes in the rate of transcription or the stability of transcripts of plastid genes (Krupinska and Apel, 1989). However, etioplasts do not synthesize a limited set of chloroplast-encoded polypeptides, major constituents of thylakoid membranes (Klein and Mullet, 1987).

Monocot leaves offer a special model to study the process of chloroplast biogenesis since, at a given stage of development, it consists of a gradient of cells of differing maturity. Chloroplast development occurs during the conversion of meristematic cells of the leaf base into mature mesophyll cells of the expanded leaf. The plastid and nuclear gene expression is active in the dividing cell of the meristem perpetuating the proplastid population (Mullet, 1988). Ultrastructural examination of different segments of light-grown barley leaf showed different plastidic forms right from the leaf base, proplastids, amyloplasts, amoeboplasts and protochloroplasts in the base region and chloroplasts in the middle and tip region (Fig. 1). Plastid development in light-grown plants involves an obligatory amyloplast stage although eoplasts themselves do not contain significant quantities of starch. After the amoeboplast and protochloroplast stages of development the sizes and numbers of starch grains fall and rise again when photoreduction, photophosphorylation and CO_2 fixation become operational in the chloroplasts (Fig. 1) (Wellburn *et al.,* 1986). In dicots early amyloplast developmental stage has been observed. The reported amoeboid stage that follows the amyloplast phase has not been observed and starch persists until quite late in the development of the chloroplast (Saito *et al.,* 1990). During maturation of leaf cells a marked increase in levels of chloroplast proteins has been observed (Ougham *et al.,* 1987).

In monocot plants, the developmental strategies of chloroplasts depends on positional localization in cells. In the basal region of light-grown leaves, B and M chloroplasts are indistinguishable, do not possess starch, or grana in B-

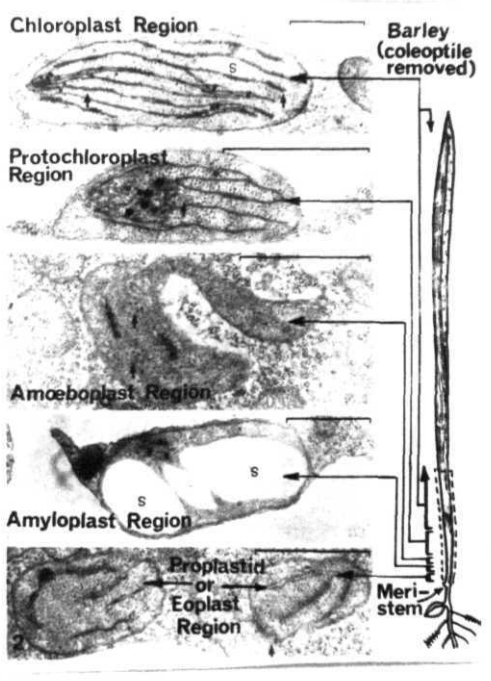

Figure 1. Electron micrograph showing gradient of chloroplast development along the length of barley leaf (From Wellburn et al., 1986).

chloroplast, and 2-4 grana in M-chloroplasts. In the center of the leaves there is a differentiation of chloroplasts, and the M-chloroplasts have 8-10 lamelle but no starch, while B-chloroplasts have starch in some cells but rarely have grana (Perchorowicz and Gibbs, 1980).

2.1.4 Biochemical gradients in monocot leaves

The monocot leaf provides a spectrum of cells at different developmental stages and has therefore been utilized to study various aspects of leaf development in both C_3 plants, e.g, barley (Viro and Kloppstech, 1980) and C_4 plants, e.g, maize (Aoyagi and Bassham, 1986). The biochemical specialization of different cells is evident from possession of a distinct gradient of chloroplast from base to leaf tip with diminutive proplastid at base and fully functional chloroplast at tip (Baker and Leech, 1977).

Monocot leaf possess a distinct gradient of Rubisco accumulation parallel to chloroplast development with maximal Rubisco protein to chloroplast development with maximal Rubisco Protein being in apical region of leaf. However the accumulation of the gene transcript for *SSU* and *LSU* of Rubisco and the polypeptides in maize leaf do not correlate well in the basal region of the leaf. While mRNA for *LSU* and *SSU* can be detected within 1 cm from leaf base, the respective polypeptides accumulate only 2-4 cm from the leaf base (Martineau and Taylor, 1985). In contrast, accumulation of PEP carboxylase mRNA and its polypeptides commences 4-6 cm from the leaf base, and that of LHCP, both mRNA, and polypeptide accumulates progressively from the leaf base (Martineau and Taylor, 1985). It is been hypothesized that appearance of

Rubisco polypeptides is in some way linked to differentiation of M and B cells. In barley leaves, the expression of *LSU* of Rubisco and Rubisco activase transcripts follows a gradient with increasing level towards the tip, but *cab* transcript level peaked at 2 cm from the leaf base and its level declined towards the tip (Zielinski *et al.*, 1989). Remarkably, the mitochondrial gene expression and differentiation shows a gradient with a maxima at the leaf base and a decline towards the tip of the leaf (Topping and Leeve, 1990), with maximal activity in the basal 2-3 cm of the leaf. Obviously, the gradient of mitochondria, and chloroplast development run opposite to each other.

The establishment of the distinct gradient of biochemical specialization mentioned above depends on two factors, viz., cell position and illumination; particularly with respect to the development of chloroplasts and associated proteins. Dark-grown barley leaves possess a distinct gradient of plastid development with diminutive proplastids (1.0 μm) at the base and well-differentiated etioplasts (4.5 μm) at the tip. Moreover, the tip cells have more plastids per cell than the basal region. The illumination of plants stimulates plastid differentiation in all segments of leaf and within 48 h the plastids are more or less of the same size and different cells possess the same number of plastids per cell (Robertson and Laetsch, 1974). Along with plastid differentiation, illumination also increases expression of nuclear and plastidic genes encoding for plastidic proteins in leaf cells (Nelson and Langdale, 1992). The appearance of these mRNA and polypeptides along the leaf length follows a distinct gradient, e.g, light stimulates PEP carboxylase mRNA from the basal level with an increased level of transcript towards the tip (Nelson *et ed.*, 1984, 1989).

The requirement of light is not obligatory for the accumulation of these proteins and a small amount of Rubisco is found in dark-grown maize seedlings, but it is present in both B and M cells (Sheen and Bogorad, 1987; Langdale *et al.,* 1987). Since Rubisco in light-grown leaves is only localized in B cells, it is apparent that in dark-grown maize leaves, the influence of cell position on Rubisco expression is not evident. However, on illumination of maize leaves, there is a suppression of Rubisco in M cells and expression in B cells leading to the appearance of the observed distribution gradient of the plastidic enzymes in B cells alone (Nelson and Langdale, 1992). Moreover, after onset of illumination, Rubisco in M cells is degraded at a faster rate than that in B cells.

Cell position also determines the expression of genes associated with biochemical specialization of Kranz anatomy. It was observed that veins exert an influence on biochemical specialization of nearby cells, and accumulation of C_4 proteins is maximal near veins. Further, as cells are distinct from veins, the level of these proteins declines and as a consequence, even parenchyma cells far from the vein express the gene for Rubisco which is supposed to be restricted to B cells (Langdale *et al.,* 1988). It has been suggested that positional control of B cells on expression of C_4 enzymes is positive and acts locally within a small radius of each vein (Nelson and Langdale, 1992). The influence of light was related to its intensity and low light favored accumulation of Rubisco in M cells while high light favored accumulation of both Rubisco and PEP carboxylase (Usuda *et al.,* 1985). It is evident that light plays a dual role in the monocot C_4 leaf: it stimulates the level of plastidic

enzymes and also suppress the expression of genes (e.g., Rubisco) in incorrect cell types.

Evidently, the expression of genes in the developing leaf occurs after integrating the information about cell types, position and light level. There have been many studies to identify cis-acting elements and trans-acting factors in order to understand how this information is generated and expressed at the molecular /genetic level. While the studies on light regulatory promoter elements are quite advanced and have been extensively reviewed (Gilmartin *et al.,* 1990; Thompson and White, 1991), the information about elements responsible for M or B cell specific expression is very limited. Since many C_4 genes, such as ppc, ppdk, rbcS, can express in dicot C_3 plants like tobacco (Matsuoka and Sanada, 1991), it is evident that the B and M cell's specific expression is dependent on endogenously encoded trans-acting factors (Matsuoka and Numazawa, 1991). It has been suggested that C_4 genes are differently methylated in M and B cells and may help to explain expression pattern of C_4 genes (Ngernprasirtsiri *et al.,* 1989; Langdale and Nelson, 1991). Bansal and Bogorad (1993), using gene bombardment on maize-leaf cells, identified four sequence elements which are involved in differential regulation of *cab*-m-1 gene expression in M and B cells: sequence I (-1026 to - 989) and II (-949 to -937) are needed to repress the gene in B cells, and sequences I, III (-936 to -897) and IV (-896 to -850) are needed to strongly enhanced expression in M cells. The factors determining suppression and enhancement in B and M cells are yet to be identified.

2.2 STARCH MOBILIZATION

In green leaves, the surplus carbohydrates generated during photosynthesis are stored in the form of starch in chloroplasts. Starch content is higher during the day, during which photosynthesis favors starch accumulation in chloroplasts its level declines during the night, when the sugars are generated by its degradation. Starch is mobilized to other plant parts via pholem. In tissues like seeds/tubers, starch is continually present till onset of a new phase of growth and development and is called 'storage' carbohydrate. The photosynthetically generated starch is called 'transitory' starch to signify diurnal oscillation in its level in active photosynthesizing tissues.

The studies on starch degradation in seeds/tubers have revealed that breakdown of starch is mediated mainly by a small number of enzymes, viz., starch debranching enzyme, phosphorylase and amylases, which act on starch to generate sugars. The process of starch biosynthesis and its degradation have been extensively reviewed (Preiss, 1984; Beck and Ziegler, 1989). In the present review, an overview of presence, localization, regulation and molecular properties of amylases and phosphorylase in green leaves is presented, and is compared with properties of enzymes present in storage tissues.

AMYLASES

Amylases are principal starch degrading enzymes and are present in both plants and animals. In plants, amylases can be distinguished into two

principal forms on the basis of their action on starch molecules, which are long linear polymers of glucose with a high degree of branching. The amylase hydrolyzing internal glycosidic bonds of starch leading to fragmentation of molecule is called as ∝-amylase or endoamylase, while the one selectively removing reducing-disaccharide maltose from the non-reducing end of the starch is called as β-amylase. The properties of both enzymes from green leaves are reviewed below.

2.2.1 ∝-amylase

∝-amylase (1,4-∝-D-glucanglucanohydrolase, E.C.3.2.1.1) catalyzes the endohydrolysis of 1,4-∝-D-glucoside linkages of starch and related poly- and oligo-saccharides. On incubation with starch, ∝-amylase action is characteristically seen as a decrease in the viscosity or liquification of starch.

2.2.1.1 Physicochemical properties

∝-amylase is a metalloprotein (Fischer and Stein, 1960), possessing one atom of Ca^{2+} per molecule of enzyme (Bush *et al.*, 1989). The structure of the Ca^{2+} binding domain is nearly similar in all ∝-amylases. The presence of Ca is essential for ∝-amylase activity, as removal of bound Ca^{2+} by incubation with either EDTA or EGTA results in a complete loss of its enzymatic activity (Thoma *et al.*, 1971; Koshiba and Minamikawa, 1983). The activity of ∝-amylase can be restored by removing the chelator and providing Ca^{2+} (Huang and Kao, 1992). The role of Ca^{2+} in maintaining amylase stability is now well recognized and therefore Ca^{2+} is included in the incubation medium along with

∝-amylase to stabilize its activity. It has also been shown that in presence of calcium (10 mM) ∝-amylase can be subjected to heating at 70°C for 5 min to 5 h, without any significant loss of catalytic activity (Stein and Fischer, 1958; Koshiba and Minamikawa, 1983; Beers and Duke, 1990) and this property has been used to distinguish ∝-amylase from other starch hydrolyzing enzymes. However, it is now recognized that ∝-amylases may exist in two sub-groups, Amy1 and Amy2 and one of it possesses lower affinity for Ca^{2+} and is largely insensitive to chelation by EDTA (Bush *et al.,* 1989). For instance, Jacobsen *et al.,* (1986) found that EDTA inactivates Amy2 of barley seed but not Amyl. Likewise, endoamylase from spinach chloroplast too has no apparent requirement for Ca , lacks heat stability, and is sensitive to sulfuhydral oxidizing agents (Okita *et al.,* 1979).

∝-amylase is stable in pH ranges 5.5 - 8 (Beers and Duke 1990), but denatures rapidly at acidic pH, eg., at 3.6 (Thoma *et al.,* 1971). ∝-amylases in many plant species are devoid of cysteine and therefore are not susceptible to damage by SH reagents (Preiss and Levi 1980).

2.2.1.2 Seed ∝-amylase

The molecular properties and regulation of ∝-amylase in plant systems are best characterized in barley, summarized below, where GA-induced ∝-amylase synthesis has been investigated in great detail to decipher molecular mechanisms of hormone action. In essence, in barley, ∝-amylase is encoded by 2 multigene families, located on chromosome 1 and chromosome 6 respectively (Knox *et al.,* 1987). The gene family located on chromosome 6 consists of four

genes which encode polypeptides for ∝-amylase whose isoelectric point is about 5 and are called low pI amylases (Muthukrishnan *et al.,* 1983). The gene family located on chromosome 1 is more complex and consists of at least 7 genes, which encode for polypeptides of ∝-amylase bearing higher isoelectric point of about 6 and are therefore called high pI amylases (Khursheed and Rogers, 1988). Both groups of amylases are characteristically different in terms of their regulation by hormones, and requirement of Ca^{2+} for stability and secretion. It is pertinent to note that ∝-amylase is a secretary protein and after synthesis it is translocated to the cell exterior via the endoplasmic reticulumgolgi body pathway (Jones and Jacobsen, 1991). The role of gibberellins in inducing ∝-amylase synthesis and secretion in barley seed is well known and has been extensively reviewed (Beck and Ziegler, 1989; Fincher, 1989).

2.2.1.3 Leaf ∝-amylases

There have been relatively few studies concerning ∝-amylases in leaf. In comparison to seed amylases, only a little information is available regarding the physicochemical properties and regulation of leaf amylases. Basically, ∝-amylase isolated from leaf/cotyledons possesses similar physicochemical properties as seed amylase; however knowledge about them is fragmentary. The presence of ∝-amylase in green leaves has been detected in many plant species (Gates and Simpson, 1968) such as spinach (Okita and Preiss, 1980), pea (Ziegler, 1988), barley (Jacobsen *et al.,* 1986), *Arabidopsis* (Lin *et al.,* 1988), maize (Echeverria and Boyer, 1986) to name but a few. However, in view of its low activity in leaves, its purification and molecular characterization have been

done only in pea (Ziegler, 1988), spinach (Okita and Preiss, 1980) and *Arabidopsis* (Lin *et al* , 1988).

The properties of pea leaves ∝-amylase is summarized below. The molecular weight of purified pea ∝-amylase is 45 kD, which is also close to the molecular weight of seed amylases, which range between 40-50 kD. The enzyme activity depends on the presence of Ca^{2+} ion in incubation media, as inclusion of 10 mM EDTA results in a rapid loss of activity pointing out the Ca^{2+} metalloprotein nature of the leaf enzyme. As is the case with cereal seed oc-amylases, excess calcium stabilizes purified ∝-amylase against denaturation, effect of heat and low pH. There is no inhibition of amylolytic activity of the above amylase by ∝-, β- or y-cyclodextrins but heavy metal ions, particularly mercury, strongly inhibits ∝-amylase activity. Similarly, maltose also inhibits oc-amylase activity. On other hand, the activity of the enzyme is unaffected by the presence of sulfuhydryl reagents like DTT, and sulfhydryl oxidizing or alkylating reagents lead to only a moderate loss of activity. The substrate specificity and activity patterns of pea oc-amylase on various substrates is akin to seed ∝-amylase. The pH maxima of amylase is at 6.0 in Na-acetate buffer. It is clearly evident that physicochemical properties of ∝-amylase purified from pea leaves are very similar to seed amylase and it possesses almost all the characteristic properties of oc-amylases. The molecular properties of ∝-amylase isolated from shoots and cotyledons of pea (Swain and Dekker, 1966; Beers and Duke, 1990) are identical to pea leaf amylase (Ziegler, 1988), as the peptide maps and molecular weights of these amylases are the same.

It is now known that within the oc-amylase enzyme family, two kinds of amylase can be recognized: type B which are EDTA sensitive but insensitive to -SH reagents, and type A which are insensitive to EDTA but sensitive to -SH reagents (Jacobsen *et al.,* 1986). It has been reported that while pea ∝-amylase belongs to type B, in barley (Jacobsen *et al.,* 1986) and spinach leaves (Okita and Preiss, 1980), ∝-amylases are of the A type. In spinach leaves, though ∝-amylases have almost all the typical properties of oc-amylases, such as substrate specificity and a typical action pattern on amylose. But unlike the typical ∝-amylase, it is resistant to EDTA or EGTA, it is completely inactivated on heating at 65°C even in the presence of Ca^{2+}, and -SH modifying reagents also reduces its activity (Okita and Preiss, 1980). Similarly, oc-amylases from *Arabidopsis* leaves lose its activity on heating at 60°C even in the presence of 20 mM Ca (Lin *et al* , 1988). In *Arabidopsis* leaf, while ∝-amylase was detected on the basis of its capacity to hydrolyze β-limit dextrin, analysis of its products revealed generation of only maltose (Lin *et al* , 1988). It is evident that depending on the species, leaf amylases may basically constitute 2 groups which can be distinguished as type A and B.

In green leaves, in view of generation and localization of starch in the chloroplast, it is expected that the oc-amylase of the leaf is a plastidic enzyme. However, the localization of oc-amylase in plastids has still not been unequivocally demonstrated: e.g., while the presence of an oc-amylase in chloroplasts has been reported for sugar cane (Bourne *et al.,* 1970), pea (Ziegler, 1988), other reports are equivocal about its presence (Beers and Duke, 1990). In barley, no oc-amylase could be detected in chloroplast (Jacobsen *et al.,*

1986). Most reports favor the view that a part of a-amylase activity of green leaves may be plastidic in nature, and this plastidic enzyme may possess properties of either type-A or type-B ∝-amylases. In spinach leaves, Okita and Preiss (1980) detected both chloroplastic and extrachloroplastic ∝-amylases which had characteristics of type-B amylases, and about 5% of a-amylase was in chloroplasts. In pea leaves, while a major amount of a-amylase is present in the extracellular compartment, chloroplast possesses about 5% of total ∝-amylase activity (Ziegler, 1988). The extracellular a-amylase is predominantly present in apoplasts in the cell walls of pea leaves and shoots, but plastidic ∝-amylase has been envisaged as a contamination (Beers and Duke, 1990). In Vicia fab a leaves, about 40% of a-amylase activity is likely to be associated with chloroplasts while the rest is localized outside plastids (Ghiena *et al.*, 1993). The presence of ∝-amylase in chloroplasts in many species is still doubtful due to lack of convincing experiments.

The location of extraplastidic a-amylase is presumed to be cytosol. However, Ziegler (1988), on isolating protoplasts from pea leaves observed that in comparison to leaf, protoplast contained much lower ∝-amylase activity, suggesting that a significant amount of a-amylase may be located in extracellular compartments. The infiltration experiments conducted on pea stem indicate that about 87% of a-amylase activity is located in the apoplast in cell walls (Beers and Duke, 1990).

The regulation of a-amylase activity by GA in barley seeds, now a classic observation, signifies hormone-mediated gene expression of a-amylase in aleurone layers. In comparison, the role of hormones in induction of a-amylase

in green leaves is not evident. In the same barley leaves, water stress rather than GA stimulated accumulation of ∝-amylase in leaves (Jacobsen *et al.*, 1986). The above accumulation results via stress-mediated induction of ∝-amylase mRNA which lead to *de novo* synthesis of ∝-amylase protein, which belongs to only type-A ∝-amylase. It is interesting to note that while barley seeds have low pI and high pI amylases, in leaves only low pI amylase is present, and it is not translocated to the chloroplast but rather is present in the extraplastidic compartment. The question whether the signal peptide of ∝-amylase, which directs its secretion in aleurone layer cells, is redundant in leaf cells still needs to be examined. In pea leaves, the level of ∝-amylase, which is principally located in the apoplast, is in some way determined by chloroplast density and function (Saeed and Duke, 1990b). In fact, the loss of functional chloroplast by Norflurazon treatment increased the ∝-amylase level in the apoplast by about 80-fold (Saeed and Duke, 1990a). It has been postulated that chloroplast produces a negative signal for regulation of oc-amylase activity in pea, and in some organs, e.g., senescening leaves, increase in ∝-amylase activity may result due to loss of chloroplasts (Saeed and Duke, 1990a,b). Since ∝-amylase purified from different organ of pea such as cotyledon/stem/leaves appears to be the same (Ziegler, 1988; Beers and Duke, 1990), the putative signal directing secretion of ∝-amylase to the apoplast is also not known.

While hormonal involvement in regulation of ∝-amylase activity in green leaves is not seen, hormones have been implicated in the regulation of ∝-amylase activity in hypogeal cotyledons of pea seedling, which serves as a storage organ, where the axis induces *de novo* synthesis of ∝-amylase in pea

cotyledons (Hirasawa, 1989; Hirasawa and Yamamoto, 1991). In contrast to barley where water stress promotes accumulation of a-amylase, in deep- water rice submergence of shoot promotes an increase in a-amylase activity at the internodes (Smith *et al.,* 1987), which can also be induced by GA_3 or ethylene treatments to excised internodes. In bean stem, the modulation of a-amylase level correlates with cellular disassembly (Davis, 1984). In mung bean cotyledons, a-amylase development is blocked by an endogenous inhibitor whose action can be blocked by auxins, or imbibition of the cotyledon in water (Morohashi *et al.,* 1989). In tobacco leaves too, activity of two apoplastic ∝-amylases greatly increases on infection with tobacco mosaic virus (Heitz *et al.,* 1991) and the a-amylase induction is characteristically similar to other pathogenesis-related proteins.

One important factor which may influence the ∝-amylase activity in shoot/green tissue is light. Light may have a two-fold effect on amylase activity, first, by promoting photosynthetic generation of starch, and second, by stimulating chloroplast biogenesis, a principal site of a-amylase localization. In spinach chloroplast, amylolytic activity oscillates in a diurnal fashion in light/dark phase, the activity being twice as high in the dark phase. It has been presumed that diurnal oscillation of stromal pH may modulate the amylolytic activity of chloroplasts. In leaves of developing maize seedlings, very little influence of light has been observed on the activity of ∝-amylase (Subbarao, 1992). However, a detailed analysis of the a-amylase level along the axis shows that in maize leaves a-amylase activity is photostimulated particularly at the base of the leaf (Datta, 1992) and is present in both B and

M cells (Echeverria and Boyer, 1986). In contrast, in maize coleoptile and radicle on transfer to light an induction of isozyme band is observed, which has been interpreted as photoinduction of an amylase isozyme which could be a β-amylase (Segundo *et al.,* 1990). However, the interrelationship between chloroplast biogenesis and ∝-amylase induction is yet to be investigated.

2.2.2 β-Amylase

β-amylase (1,4-D-glucanmaltohydrolase, E.C. 3.2.1.2), was named after the product β-maltose, by Kuhn (1925) and Ohlsson (1930). It is present in a few species of higher plants and microbes, but is absent in animals (Thoma *et al.,* 1971). It hydrolyzes amylose from its non-reducing end, releasing β-maltose, and leading to a complete hydrolysis of amylose. Since, it can not bypass ∝-1,6-glucoside linkages; thereby, the hydrolysis of amylopectin results in β-limit dextrin. β-amylase is unable to hydrolyze native starch grains from pea and glucans smaller than maltotetraose (Lizotte *et al.,* 1990).

2.2.2.1 Physicochemical properties

β-amylase has a broad pH optima of 4.0-5.5, and requires free sulfhydryl groups for activity. It is believed that the active center of β-amylase contains a -SH group, because on incubation with SH reagents like *p*-chloromercurybenzoate, N-ethylmaleimide, β-amylase activity is inhibited (Thoma *et al.,* 1971). However, it has also been suggested that there is no direct involvement of -SH groups in the enzyme reaction (Mikami and Morita, 1983). p-amylase has no disulfide bridges and 2 -SH groups were deeply buried

inside the enzyme. Heavy metals as well as other thiol binding reagents inhibit β-amylase activity (Thoma *et al.,* 1971).

2.2.2.2 Seed β-amylase

As with ∝-amylase, the molecular properties of β-amylase summarized below, have been best studied from the storage organs particularly from barley seeds. β-amylase in barley is encoded by 2 genes, one located on chromosome 4 (Jonassen *et al.,* 1981) and a second locus on the short arm on chromosome 4 (Kreis *et al.,* 1988). The MW of barley β-amylase, predicted from its cDNA sequence from barley is 63 kD, which is also close to MW of purified β-amylase protein. However, in the presence of reducing agents 4 forms can be purified from seeds having MW 59.7 kD, 58 kD, 56 kD and 54 kD with corresponding isoelectric points 5.2, 5.3, 5.5 and 5.7 respectively. These multiple forms of β-amylase result from C-terminal processing of a single gene product of β-amylase by proteases (Lundgard and Sevensson, 1987). Unlike ∝-amylase, which is induced de novo during barley seed germination, p-amylase in barley endosperm is synthesized during seed development along with storage proteins, and is stored in a latent form which is activated during germination by post-translational modification (Lundgard and Sevensson, 1987). The majority of β-amylase in barley endosperm exists in a bound form which is considered to be latent or inactive. The proteolysis or reducing agents releases the enzyme from bound form and also increases its activity (Sandergren and Klang, 1950). The notion that bound p-amylase is latent and free p-amylase is active has been questioned recently as it has been shown that reduced activity of bound β-amylase is due to steric hindrances (Sopanen and Lauriere, 1989).

2.2.2.3 Leaf β-amylases

In barley, the developing endosperm possesses 2 β-amylase isoforms. One appears early in endosperm development and is followed by the other which is the major enzyme of barley endosperm. Both enzymes are encoded by different population of mRNA whose levels correspond to development of two respective β-amylase proteins (Shewry *et al.,* 1988). It has been found that the β-amylase encoded by the locus on chromosome 4 is the major seed form of β-amylase while other enzyme encoded by chromosome 2 constitutes the protein expressed in the leaves and shoots (Shewry *et al* . 1988; MacGregor and Dushickn, 1989). Similarly, two distinct β-amylases have also been reported in wheat and rye, one which was specific to starchy endosperm, and another present in root, leaves or green tissue (Daussant and Lauriere, 1990; Daussant *et al.,* 1991). It is found that while one β-amylase has an endosperm-specific promoter and is expressed only during seed development, the other β-amylase is ubiquitously expressed and therefore is also present in other organs of plants.

A perusal of cDNA sequence of the ubiquitous and endosperm-specific β-amylase sequence of rye reveals that ubiquitous β-amylase is only 77% homologus with endosperm β-amylase (Sadowski *et al.,* 1993; Rorat *et al.,* 1991). It is also distinct from dicot β-amylases and on comparison with *Arabidopsis* leaf β-amylase, it shows only 61% homology (Monroe and Preiss, 1990) and shows 62% homology with sweet potato tubers β-amylase.

In contrast to cereals however, sweet potato p-amylase gene is encoded by only one gene (Yoshida *et al.,* 1991, 1992). Recently, Ishiguro *et al.,* (1993) detected a nuclear factor which binds 5' upstream sequence of p-amylase gene in sweet potato and is a member of bZIP family.

The cDNA clones of the ubiquitous p-amylase of rye have been obtained and its properties have been compared with endosperm-specific p-amylase (Sadowski *et al.,* 1993). It codes for 503 amino acids and has a deduced MW of 56,700 daltons. It differs characteristically from endosperm specific p-amylase of cereals as it lacks gly-rich repeat sequences in the C-terminal of p-amylase. In contrast to endosperm specific p-amylase which undergoes as C-terminal specific proteolytic processing, ubiquitous p-amylase (lacks C-terminal repeat region) does not undergo this processing (Daussant *et al.,* 1991).

In green tissue, p-amylase has been purified from Vicia faba leaves (Chapman et al.. 1972), mustard cotyledons (Subbaramaiah and Sharma, 1987a, 1987b, 1988), *Arabidopsis* (Lin *et al.,* 1988), pea epitocyl (Lizotte *et al.,* 1990) etc. The leaf p-amylase basically possesses molecular properties similar to the p-amylase of storage tissue, but differs in a few aspects. The pH optima of mustard p-amylase is 5.8-6.2 which is more towards neutral pH then that of potato or barley which range between pH 4 to 5 (Subbaramaiah and Sharma, 1990; Lin *et al* ,1988; Greenwood and Milne, 1968). Also mustard p-amylase is not susceptible to inhibition by cyclodextrins which are competitive inhibitors of p-amylase (Thoma and Koshland, 1960), while pea p-amylase is slightly inhibited (Lizotte *et al* , 1990). The specific activities of leaf p-amylase is also lower than that of seed p-amylase (Lin *et al.,* 1988).

β-amylases from leaf constitute a heterogenous group with molecular weights in range of 50 - 65 kD (Subbaramaiah and Sharma, 1988; Lizotte *et al.,* 1990), with Vicia faba p-amylase being an exception with a MW of 27 kD: in contrast to other p-amylases which exist as monomer, it is present as a tetramer in leaves. p-amylase from mustard cotyledon (Subbaramaiah, 1987), and pea shoot (Lizotte *et al.,* 1990), do not bind to concanvalin A and are not glycoproteins. p-amylase from mustard (Subbaramaiah and Sharma, 1987b), and pea (Lizotte *et al.,* 1990), also have isoelectric points more towards the acidic side, than that of p-amylase storage tissues. Both mustard and pea p-amylase do not require SH-groups for catalytic activity of enzyme.

Analogous to ∝-amylase, in the majority of plant species, p-amylase in leaves is located in extraplastidic fractions. In a few cases, the presence of β-amylase has been detected in chloroplasts, e.g., in *Arabidopsis* (Lin *et al.,* 1988), pea (Kakefuda, *et al.,* 1986; Levi and Preiss, 1978), but a cytoplasmic contamination contributing to presence of p-amylase in chloroplast can not be ruled out (Beers and Duke, 1990). Moreover others have failed to detect p-amylase activity in pea chloroplasts (Ziegler, 1988). In mustard cotyledons, p-amylase activity is localized exclusively in cytosolic fraction; no p-amylase activity has been detected in chloroplast (Manga and Sharma, 1990). While chloroplastic localization of p-amylase is uncertain, vacuoles isolated from protoplasts of pea, wheat and *Arabidopsis* (Monore and Preiss, 1990), showed high activity of p-amylase (Ziegler and Beck, 1986). However, in spinach and *Chenopodium*, p-amylase is cytosolic in nature (Ziegler and Beck, 1986). The distribution of p-amylase activity in different tissue has not been analyzed in

detail. In sweet potato roots p-amylase was present throughout the root (Hagenimana *et ed.,* 1992), but in broad bean leaves, p-amylase is localized specifically in the epidermal cell layers (Chapman *et ed.,* 1972).

In general, p-amylase in most species is found in extraplastidic compartments, but in view of its localization in vacuoles of pea, *Arabidopsis* and wheat, the possible vocuolar localization in other species needs to be examined. The signal directing p-amylase to the vacuole is, however, not known. Though p-amylase of *Arabidopsis* is located in vacuoles, its sequence is also very similar to N-terminal of soybean and sweet potato (Monroe and Preiss, 1990).

The information on regulation of p-amylase activity in leaf is scanty and most studies have been concerned only with its detection and localization. Further, most available information on p-amylase pertains only to cereal seeds (Pan *et al.*, 1988). In mustard cotyledons involvement of GA has been ruled out in photoregulated increase in amylase activity in leaves. The photoregulated P-amylase activity results from phytochrome-mediated enhancement of p-amylase synthesis (Sharma and Schopfer, 1982, 1987). Unlike in cereal seeds, no inactive form of p-amylase, could be immunochemically detected in mustard cotyledons, and increase in activity of the enzyme strictly correlated with the increase in its protein level (Subbaramaiah and Sharma, 1989).

The photoregulation of p-amylase seems to be a characteristic feature of monocot seedlings too, as it has also been detected in maize seedlings (Subbarao, 1992). In barley leaves, though water stress enhanced α-amylase

activity, there was no induction of 6-amylase activity (Jacobsen *et al.,* 1986). In pea seedlings, chloroplast destruction which specifically elevated ∝-amylase activity, showed only a slight stimulation of 6-amylase (Saeed and Duke, 1990b). The most significant elevation of 6-amylase activity has been noticed in *Arabidopsis* mutants having altered starch metabolism. Activity upto 40-fold higher than in wild types has been noticed in mutants, only when it was grown under 12 h photoperiod, but not under continuous light (Casper *et al.,* 1985). Interestingly, both starchless and starch-overproducing mutants possessed the elevated 6-amylase activity. Casper *et al.,* (1989) suggest that sucrose acts as an inducer of 6-amylase activity in the *Arabidopsis* mutant. The role of sucrose on 6-amylase induction is evident in sweet potato petiole cuttings, where sucrose induces an accumulation of 6-amylase by *de novo* synthesis of enzymes (Nakamura *et al.,* 1991). In addition to sugar, a slight induction of 6-amylase has also been noticed with respect to light (Nakamura *et al.,* 1991).

The functional role of extraplastidic 6-amylase in shoots is not yet known. It is likely that 6-amylase located in the extraplastidic fraction may have a defense related function (Ohto *et al.,* 1992), as chitosan and galactosan fragments can induce 6-amylase synthesis in leaf petiole cuttings of sweet potato (Ryan and Farmer, 1991). Moreover, expression of 6-amylase gene can also be induced by ABA and induction by all of above promoters can be suppressed by GA (Ohto *et al.,* 1992). However, more information is needed to establish a clear role of extraplastidic 6-amylase.

2.2.3 Phosphorylase

Phosphorylases (1,4-∝-D-Glucan:orthophosphate D-glucosyltransferase, E.C. 2.4.1.1.) are transglucosylases that catalyze the reversible transfer of glucose residues between (1 >4) ∝-D glucan and inorganic phosphate. Phosphorylase activity can be detected in all starch-containing plant tissues. Phosphorylase can act both as glucan degrading and glucan-synthesizing enzyme (Beck, 1985; Tsai and Nelson, 1968, 1969), depending on relative concentrations of glucose-1-phosphate and iP. But primarily, it is a degradative enzyme (Steup, 1988, 1990). It degrades linear chains of (1 >4) ∝-linked glucose residues in the presence of inorganic phosphate, with the formation of glucose-1-phosphate. Like ∝-amylase, phosphorylase is also present in animals and plants, and the most characterized phosphorylase is the one purified from rabbit muscle. In plants most information about molecular properties of phosphorylase, summarized below, has been obtained from potato tuber phosphorylase.

2.2.3.1 Tuber phosphorylase

Potato phosphorylase (type I) is a large molecule containing 916 amino acids with a MW of about 103916 daltons, and *in vivo,* it exists as a dimer (Nakano *et al.*, 1989; Lee, 1960a). Phosphorylase also contains one molecule of pyridoxal phosphate per monomer as a cofactor (Lee, 1960b). Potato phosphorylase can be distinguished from rabbit muscle phosphorylase by lack of allosteric regulation; and its activity is also unaffected by AMP (Lee, 1960a). It also has no phosphate and is not phosphorylated by phosphorylase kinase

from rabbit muscle (Lee, 1960a). It acts on maltose, dextrin, amylose, amylopectin, but poorly on glycogen (Smith, 1977). Potato tuber also contains another type of phosphorylase called type II which has a MW of 90,000 daltons. Unlike type I phosphorylase, it has high activity for glycogen. The type II phosphorylase is a minor phosphorylase of potato tubers and its level is 100-fold lower than type I phosphorylase (Gerbrandy and Verleur, 1971; Shimamura *et al.,* 1982).

The cDNA of potato phosphorylase type I is cloned, it encodes for 966 amino acids, of which 50 amino acids constitute signal peptides directing its translocation to chloroplast/amyloplasts (Nakano *et al.,* 1989). It is pertinent to note that 51% and 40% of the amino acid sequence of the above phosphorylase is identical with rabbit and E.coli phsphorylase, respectively. However, plant phosphorylase is unique in having an amino acid sequence consisting of 78 amino acids mostly hydrophobic, near the central portion of protein sequence (Nakano *et al.,* 1989).

2.2.3.2 Leaf phosphorylase

Leaf phosphorylase has been purified from a number of plant species such as maize (Mateyka and Schnarrenberger, 1984, 1988), spinach and potato (Steup and Schachtele, 1981). In potato leaf, both type I and type II phosphorylase are detectable and are located in cytosol and plastid respectively (Conrads *et al.,* 1986). In leaf, platidic phosphorylase exists as a dimer, has a subunit of 104 kD, and immunologically cross-reacts to type I tuber phosphorylase. The minor, type II phosphorylase of tuber cross-reacts with

cytosolic phosphorylase of potato leaves and has a molecular weight of 94 kD. The leaf plastidic and cytosolic phosphorylase represent two antigenically distinct enzymes as they do not cross-react with each other (Conrads *et al.*, 1986).

The properties of cytoplasmic and plastidic phosphorylase purified from spinach leaves have been compared and found similar in many respects such as activity towards inorganic phosphate during phosphorolysis, and pH optima of glucan synthesizing and degrading activities (Steup and Schachtele, 1981; Shimamura *et ed.,* 1982). However, their activity towards glucans varies considerably whereas chloroplastic phosphorylase has affinity for linear low molecular weight maltodextrins and very low affinity for branched polyglucans glycogen, cytoplasmic phosphorylase possesses high affinity for branched polyglucans and has low affinity for maltodextrins (Steup *et al.*, 1980, Steup **and** Schachtele, 1981). Unlike plastidic phosphorylase, the cytosolic phosphorylase is effectively inhibited by maltotetrose on cyclodextrins, both acting as competetive inhibitors (Steup and Schachtele, 1981; Shimamura *et al.,* 1982). The two phosphorylases are not interconvertible proteins; possess different primary structure as is evident from the difference in immunological properties and peptide patterns (Conrads *et al.,* 1986).

The regulation of phosphorylase activity in plant leaves has not been investigated in detail. In pea cotyledons both cytosolic and plastidic phosphorylases have been detected and plastidic phosphorylase has been detected in both **proplastids** and amyloplasts. The amount of either enzyme depends on the developmental state of the organ. During seed development,

cytosolic enzyme is a minor enzyme but plastidic phosphorylase is a major enzyme. However, during germination, the level of plastidic enzyme remains constant but the level of cytosolic enzyme increases significantly (Berkel *et al.*, 1991). The plastidic phosphorylase possesses a distinct N-terminal transit peptide which is processed during its translocation to chloroplast, as is evident from the fact the MW of precursor and mature polypeptide is 116 kD and 105 kD respectively. In pea, chloroplasts possesses two types of plastidic phosphorylases, one of which is present in etioplasts and the other appears during photo-induced in chloroplast biogenesis (Berkel *et ed.,* 1991). Plastidic phosphorylase in pea cotyledon is localized in the stromal space of the chloroplast (Berkel *et al.,* 1991). In potato tuber, the location of plastidic phosphorylase depends on tuber age. In the young tuber, it is present in the stroma of amyloplasts, and in mature tubers, it is localized outside the amyloplasts near the membrane of the amyloplasts (Brisson *et al.,* 1989).

In maize leaves, phosphorylase enzyme is present in two distinct locations, i.e., mesophyll and bundle sheath cells, the cytosolic one being confined to mesophyll, and plastidic one is located in bundle sheath chloroplasts (Mateyka and Schnarrenberger, 1984; 1988). Both enzymes have a pH optima around pH 7 and their affinity for substrate is similar to spinach phosphorylases and akin to cytosolic and plastidic phosphorylase, respectively (Mateyka and Schnarrenberger, 1988). However, there is no information about the regulation of phosphorylase in both monocot and dicot leaves during leaf development. In the only study done, it was observed that, in spinach leaves, the activity of cytosolic phosphorylase increased after 35 days of sowing by 4-8

fold, which declined back to initial level by 45th day from sowing. On the other hand, the level of plastidic phosphorylase remained nearly constant (Hammond and Preiss, 1983).

Functional role of Starch degrading enzymes

The multiplicity of starch degrading enzymes viz ∝-amylase, p-amylase and starch phosphorylase have engendered the question regarding relative importance and role of these enzymes in the process of starch degradation in plant tissues. A clear role for ∝-amylase in degradation of starch is evident in cereal seeds germination, where *de novo* synthesized ∝-amylase after secretion to endosperm is responsible for the degradation of starch stored in endosperm (Beck and Ziegler, 1989). The degradation of starch in endosperm is initiated by ∝-amylase although other enzymes also participates in this response. The role of p-amylase in cereal seeds germination is less clear and has been speculated that due to presence of an excess amount of p-amylase, it may have a nutritive role as a storage protein (Shewry *et* a/., 1988). In potato tuber phosphorylase plays a major role in starch mobilization (Steup, 1988; Steup, 1990).

The close association of p-amylase and starch grain in cereal seeds indicates its logical role in starch degradation during seed germination. Even dry cereal seeds consist of a low level of free p-amylase which may participate in the initial degradation of starch during seed imbibition (Pan *et al.*, 1988). Although p-amylase can not degrade intact starch grains, it can act on gelatinized starch after boiling (Lizotte *et al.*, 1990). However, p-amylase has

been demonstrated to attack native starch granules that have not been partly degraded by other enzymes or solubilized by boiling (Nakamura *et al.*, 1991; Sun and Henson, 1991).

Enzyme extracted from resting barley seeds is able to convert the entire starch content of grain into maltose in less than half an hour at 20°C. Therefore, it appears that the enzyme present in grain is in large excess with regards to its enzymatic function. β-amylase activity in cereal seeds is 500-fold more than needed. A 100-fold reduction would still have enough β-amylase for the mobilization of endosperm starch (Sopanen and Lauriere, 1989).

The functional role of these enzymes is less clear in photosynthetic tissues such as leaves. Since a major portion of amylolytic enzymes both α-amylase and β-amylase is localized in extraplastidic compartment, which does not contain a suitable carbohydrate polymer, there have been doubts about their importance in mobilization of photosynthetic starch (Dunn, 1974). In green leaves, β-amylase is reported to be present predominantly in cytosol (Manga and Sharma, 1990), in few cases in the vacuole (Ziegler and Beck, 1986) and in chloroplasts (Kakefuda *et al.*, 1986; Okita *et al.*, 1979). Due to the location of this enzyme outside the chloroplasts, its function is unclear (Monroe and Preiss, 1990).

Moreover, in most species a clear demonstration of localization of α-amylase in chloroplasts has not been shown (Beers and Duke, 1988). In case of β-amylase, it is now firmly established that above enzyme in green leaves is extraplastidic in nature (Manga and Sharma, 1990) and the reports

describing its localization in chloroplastic may result from contamination of cytosolic β-amylase. Moreover precursor to β-amylase lack a N-terminal transit peptide which is needed to decrease its import to chloroplasts (Kreis *et al.*, 1988, Mikami and Morita, 1983). Similar to amylases *in vivo* function of cytosolic phosphorylase is also unclear (Yang and Steup, 1990). Not with standing these reports, it is now assumed that ∝-amylase by virtue of its capacity to hydrolyze native starch granule, is the primary enzyme responsible for initiating starch degradation in chloroplasts, on which other starch degrading enzyme act. Therefore, it has been proposed that phosphorylase rather than amylase present in chloroplast is important for mobilization for photosynthetic starch.

MATERIALS AND METHODS

CHAPTER 3

MATERIALS AND METHODS

3.1 GENERAL METHODS

Pearl millet (*Pennisetum americanum* var WCG-75) seeds obtained from the Andhra Pradesh State Seed Corporation, Hyderabad, were used for the experiments.

3.1.1 Seed Storage and Seedling Growth

Seeds were stored at 4°C in closed polythene bags and were germinated on four layers of Krepe Kraft paper (Jayshree Traders, New Delhi) which were presoaked in distilled water (DW) for 4 h. Papers were cut slightly shorter than the size of the plastic box or tray so that after soaking, the size of the sheets was nearly equal to the interior bottom of boxes or trays. Seeds were first extensively washed with DW and were soaked in DW for 8 h at 25°C before sowing on papers. The time of washing of the seeds was considered as the time of sowing.

Pearl millet seeds were sown either in transparent plastic boxes (9.5 cm / X 9.5 cm *b* X 5 cm *h)* or in plastic trays (40 cm Z X 30 cm *b* X 7 cm *h),* as per the requirement of experimental material. In plastic boxes 25 seeds were sown in 5 rows (5 x 5) and in plastic trays 375 seeds were sown in 25 rows (15 x 25). After sowing, 5 ml DW was added to plastic boxes and 90 ml DW was added

to plastic trays. The top of the boxes and trays were covered with plastic lids and glass plates, respectively, and were kept under red light or in darkness at 25 ± 1°C. After 4 days from sowing, 5 ml and 50 ml DW was added daily to the boxes and trays respectively. Seedlings were normally grown in plastic boxes for most experiments. Seedlings were grown in trays when a large amount of plant material was needed, e.g., during chloroplast isolation. The temperature was maintained at 25°C ± 1°C throughout the growth of the seedlings. Since after 5 days of growth, the height of the seedling is nearly equal to box/tray height and seedlings start touching the lids, the covering lids were removed and seedlings were grown in open boxes/trays.

3.1.2 Light Sources

The red light source consisted of two 47" long cool-white fluorescent tubelights (40 W x 2), whose output was filtered through 2 layers of 6 mm thick red plexiglass sheets (λ_{max} 650 nm) (Manga and Sharma, 1988). The distance between plants and light source was about 53 cm, and the intensity of red light at the top of the plants was 0.67 Wm . The ends of the tubelights were wrapped in black paper to prevent far-red light leakage. Long wavelength far-red light was obtained by filtering the output of a 300 W projector through Schott RG-9 interference filters (λ_{max} 756 nm). At the top of the seedlings, far-red light intensity was 6.0 Wm^{-2}. Blue light (λ_{max} 450 nm) was obtained using a setup similar to obtaining red light except that red plexiglass sheets were replaced by blue plexiglass sheets (λ_{max} 450 nm). Blue light intensity was 0.13 Wm^{-2} at the top of seedlings. For dark controls, after sowing

of seeds, plastic boxes or plastic trays were wrapped in black cloth and were kept in a black cardboard box at 25° ± 1°C.

All manipulations of seedlings were done under a dim-green safe light, obtained by filtering the output of a cool-white fluorescent tubelight (40 W) through six layers of green cellophane paper (λ_{max} 530 nm). The ends of the tubelights were covered with black paper. The intensity of the green light was not greater than 0.01 Wm^{-2} and light exposure did not last longer than 2 min at any given time.

3.1.3 Herbicide Treatment

For herbicide treatment, the seeds were soaked in Norflurazon (0.4 mM) solution, 12 h prior to sowing and then were germinated on Krepe Kraft papers (papers were presoaked with Norflurazon solution for 4 h). Control seedlings were treated and grown similarly with DW, in place of NF solution.

3.2 ENZYME ASSAYS

3.2.1 Amylase

Plant organs 1 g or organelle consisting of 500 mg protein were homogenized in a precooled mortar and pestle on ice along with 500 mg sea-sand (2:1, tissue/sea sand ratio) in 60 mM sodium acetate buffer pH 6.1, (5 ml buffer/gm.FW) containing 10 mM $CaCl_2$, 5 mM β-mercaptoethanol and 1 mM phenylmethylsulfonyl fluoride. The homogenate was clarified by centrifugation at 7,600*g* for 30 min. Unless otherwise mentioned, all steps were carried out at 4°C. Amylase activity was assayed in a 4 ml reaction mixture containing 30

mM Na-acetate buffer, pH 4.6, 8 mg amylose, 0.1 mM NaF and an aliquot of supernatant. The enzyme assay was carried out at 35°C for 60 min, and at 30 min. intervals, 500 µl aliquots were withdrawn. The amount of maltose liberated in the aliquots was measured by using dinitrosalicylic acid as a reducing agent (Bernfeld, 1955). The increase in reducing sugars was determined by measuring absorbance at 540 nm using maltose as the standard (Fig. 2).

α-amylase activity was measured by using its specific substrate β-limit dextrin (4 mg/ml) in place of amylose in the above assay mixture. β-limit dextrin was prepared as per the procedure described by Whelan (1964). The α-amylase assay was carried out after thermal inactivation of β-amylase activity in extract by heating the supernatant for 10 min in the presence of 10 mM $CaCl_2$ at 70°C.

3.2.1.1 Optimization of Amylase Assay

3.2.1.1.1 Optimum pH

The pH optima for amylases was determined by assaying amylase activity in different buffers containing 4 mg/ml amylose at 30°C. The buffers used were: sodium-citrate, 50 mM (pH 4 - 6.3), sodium-acetate, 50 mM (pH 4 - 5.8) and Tris-HCl, 50 mM (pH 7.2-9).

3.2.1.1.2 Optimum Temperature

The optimum temperature for amylase assay was determined by assaying amylase activity in 50 mM Na-acetate buffer, pH *4.6,* containing 5

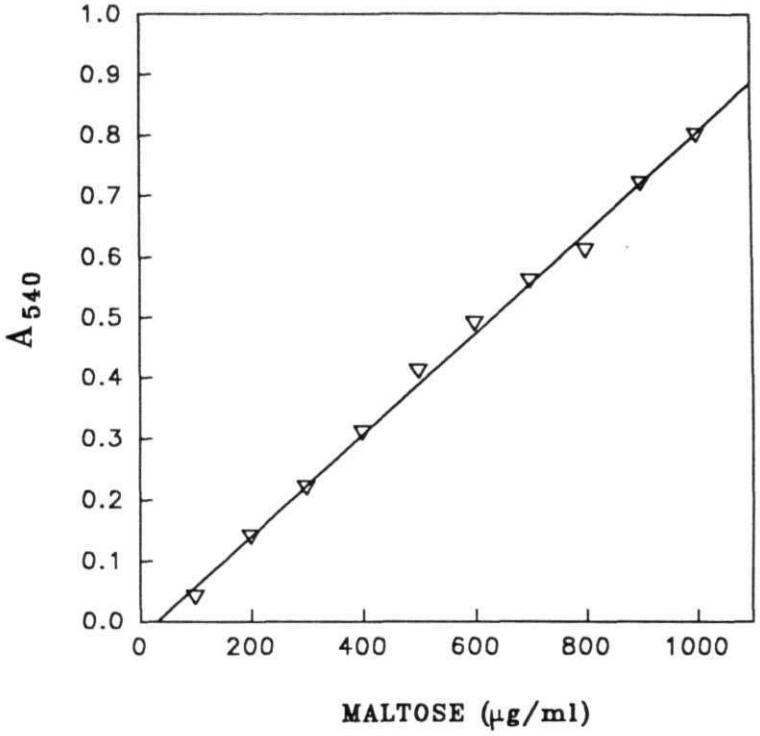

Figure 2. The standard curve of maltose estimation.
Maltose was estimated by the method of Bernfeld (1955).

mM $CaCl_2$, 4 mg/ml amylose, 1.5 mM NaF at different temperatures for 30 min in a water bath. The constancy of temperature was continuously monitored with a thermometer.

3.2.1.1.3 Stability of Amylase Activity

The stability of amylase during prolonged storage was investigated by storing 15 nkat amylase at 4°C and at 35°C for 5 days. Amylase activity was assayed daily using the standard assay protocol.

3.2.1.1.4 Effect of Calcium

20 nkat of amylase in 60 mM Na-acetate buffer, pH 4.6, was incubated at 70°C for 15 min in the presence or absence of 10 mM $CaCl_2$. The solution was cooled to 30°C and amylase activity was assayed using standard assay protocol.

3.2.1.1.5 Effect of EDTA

20 nkat of amylase was dialyzed against 5 mM EDTA for 2 h at 4°C. Thereafter, amylase activity was assayed using the standard protocol.

3.2.2 PHOSPHORYLASE

3.2.2.1 Biosynthetic Pathway

The biosynthetic assay of phosphorylase was based on phosphorylase-mediated polymerization of substrate glucose-1 -phosphate on primer (n-Glucose), leading to amylose synthesis and liberation of inorganic phosphate.

The orthophosphate set free during amylose synthesis was measured colorimetrically using the standard protocols. The phosphorylase assay was carried out essentially as per Whelan's (1955) procedure. The leaves were homogenized in a precooled mortar and pestle on ice with an equal amount of sea-sand in 50 mM Tris-HCl buffer, pH 8 (3 ml buffer/gm.FW). The homogenate was clarified by centrifugation at 10,000 g for 30 min at 4°C. Phosphorylase was assayed in a reaction mixture containing 25 mM glucose-1-phosphate, 15 mg amylose, 60 mM Na-citrate pH 5.0, 20 mM NaF, 0.3 mM $HgCl_2$, and 0.1 mM ammonium molybdate in a final volume of 3.5 ml, along with an aliquot of supernatant not exceeding 1 mg protein, or 5 units of phosphorylase activity. A 1 ml aliquot was withdrawn immediately after the addition of supernatants, to determine zero time value, thereafter 1 ml aliquots were withdrawn at 15 and 30 min. After withdrawing, the aliquot was quickly mixed with 1 ml 10% TCA, to inactivate phosphorylase and the mixture was centrifuged at 8000*g* for 15 min at 4°C. The amount of released inorganic phosphate into the clear supernatant was determined using the procedure described by Le Bel *et ed.,* (1978).

3.2.2.2 Degradative Pathway

Phosphorylase activity was also measured using a coupled photometric enzyme assay following the procedure described by Steup and Latzko (1979) with a few modifications. The seeds or vegetative tissue (leaf, coleoptile, root), or cells or cell organelle were homogenized in a mortar and pestle on ice along with an equal amount of sea sand in 5 ml of 50 mM K-phosphate buffer, pH

7.5. The homogenate was centrifuged for 30 min at 25,000*g* at 4°C, and an aliquot from clear supernatant was used for the phosphorylase assay.

The assay mixture contained, in a final volume of 5 ml, 100 mM HEPES pH 7, 50 mM K-phosphate pH 7, and 15 mg amylose, and assay was carried out for 15 min at 30°C. The aliquots were withdrawn at the beginning and at the end of the assay and were boiled at 100°C for 4 min. After cooling, denatured protein was removed by centrifugation at 1000*g* for 30 sec and, thereafter, an aliquot was withdrawn from the supernatant to determine the amount of glucose-1-phosphate formed by coupled enzyme assay.

The aliquot (0.1 ml) was assayed in 1 ml assay mixture, containing 30 mM Tris-HCl, pH 7.5, 10 mM $MgCl_2$, 1.8 mM NADP, 1.45 units of phosphoglucomutase (sigma) and 0.15 units of Glucose-6-phosphate dehydrogenase (sigma). The reaction was initiated by addition of NADP and, thereafter, the increase in absorbance due to NADPH formation was measured at 340 nm. The phosphorylase activity was calculated by using the NADPH molar extinction coefficient: E = 6.2 mM^{-1} cm^{-1}.

3.2.2.3 Optimization of Phosphorylase Assay

3.2.2.3.1 Optimum pH

The optimum pH for phosphorylase activity was determined by homogenizing pearl millet leaves in Tris-buffer, 50 mM (pH 6 to 9). The pH optimum for phosphorylase activity was determined by assaying in different

buffers at 30°C. The buffers used were Na-acetate, 50 mM (pH 3.5 to 6), Na-Citrate, 50 mM (pH 3.5 to 6) and Tris-HCl, 50 mM (pH 7 to 10).

3.2.2.3.2 Optimum Temperature

Optimum temperature for phosphorylase assay was determined by assaying phosphorylase activity in Tris-HCl buffer, 50 mM (pH 7.5 for degradative pathway, pH 8 for biosynthetic pathway) at different temperatures.

3.2.3 PHOSPHATASES

The phosphatase activity was assayed after homogenizing 2 g leaves in 6 ml, 50 mM MES-Tris buffer, pH 6.5, along with an equal amount of sea sand in a precooled mortar and pestle. The homogenate was centrifuged for 30 min at 25,000*g* at 4°C. The phosphatase assay was conducted with using 5 mM β-glycerophosphate as substrate in a 500 µl reaction mixture at 30°C for 30 min. The 50 µl aliquots were withdrawn at the zero time and at 30 min, and phosphatase activity was terminated by mixing with an equal amount of 10% cold TCA, thereafter the volume was made upto 1 ml with DW. The amount of phosphate released was estimated using the method described by Le Bel *et al.*, (1978).

3.2.4 PEP carboxylase

Phosphoenolpyruvate carboxylase (PEP) activity was estimated following the procedure described by Nott and Osmand (1982). PEP carboxylase activity

was assayed by a coupled enzyme assay using malate dehydrogenase and measuring NADH oxidation at 340 nm. The reaction mixture (1 ml) contained 25 mM Tricine-KOH, pH 7.8, 5 mM $MgCl_2$, 10 mM $NaHCO_3$, 2 units malate dehydrogenase (MDH), 0.2 mM NADH, and 2.5 mM phosphoenolpyruvate. The reference cuvette contained the above reaction mixture minus PEP. PEP carboxylase activity was measured using the extinction coefficient of NADH E = 6.2 mM^{-1} cm^{-1}.

3.3 ESTIMATIONS

3.3.1 Protein Estimation

The Bradford (1976) method was used to estimate protein content ranging between 5-40 μg (Fig. 3). The Lowry *et at.,* (1951) method was used to estimate protein, ranging between 10-120μg. Before estimating by the Lowry's method, proteins in the supernatant were precipitated by mixing with an equal amount of 10% TCA and the precipitate was redissolved in 1 N NaOH, to avoid inhibitory compounds in crude extracts (Peterson, 1983). The standard curve was drawn using the bovine serum albumin fraction V as a standard protein (Fig. 3A).

3.3.2 Chlorophyll Estimation

Chlorophyll content was determined by using extension coeffecient derived by Bruinsma (1961). Chlorophylls were extracted from leaf tissue by homogenization in 80% acetone and centrifugation. The chlorophyll content of chloroplast was estimated after diluting the 50 μl chloroplast suspention with

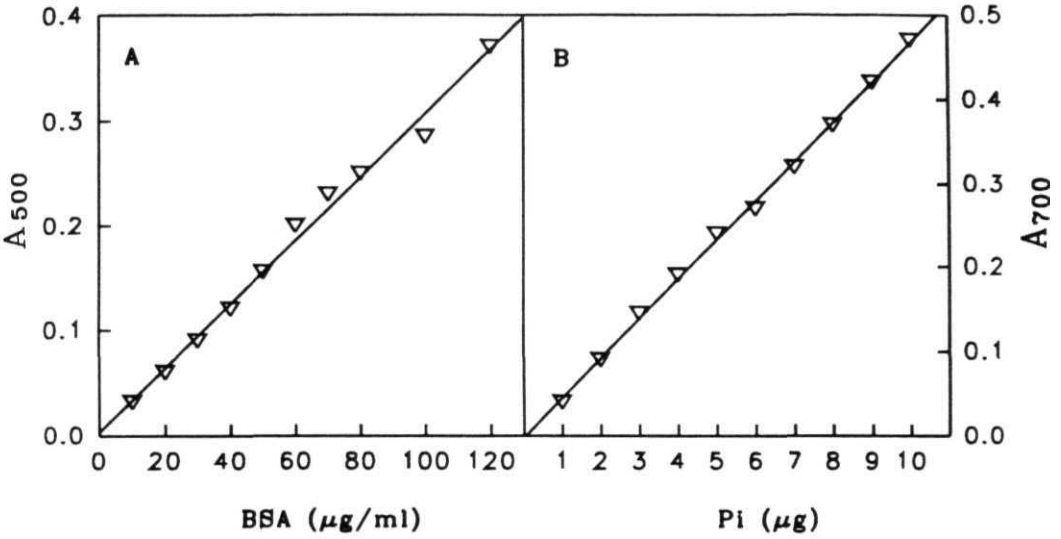

Figure 3. The standard curves of protein and inorganic phosphate estimation.

A. Protein was estimated by the method of Lowry et al., (1951) Bovine serum albumin fraction V (BSA) was used as standard protein.

B. Inorganic phosphate (Pi) was estimated by the method of Le Bel et al., (1978).

5 volumes of 80% acetone. In either sample chlorophyll content was estimated by reading its absorbance at 652 nm and the chlorophyll concentration was calculated by using the formula: A_{652} X 27.8 X Dilution Factor /g FW.

3.3.3 Inorganic Phosphate Estimation

Inorganic phosphate content was estimated using the method described by Le Bel *et al* . (1978). The proteins in aliquots were first precipitated by mixing with an equal volume of 10% TCA and centrifuging the mixture at 4°C for 10 min. The phosphate content of supernatant was estimated, after mixing 1 ml of the supernatant with 3 ml of reagent A [Copper acetate, pH 4, prepared with 0.25% copper sulphate pentahydrate and 4% sodium acetate trihydrate (w/v), in 2 N acetic acid (v/v)], 0.5 ml of reagent B [5% ammonium molybdate (w/v)], and 0.5 ml of reagent C [2% metol or elon in 5% sodium sulfite] with a vortex mixture. The phosphate content was calculated after measuring the absorbance of the mixture at 700 nm after 7 min. The standard curve was prepared by using anhydrous KH_2PO_4 (438 mg/100 ml) in DW (Fig. 3B).

3.4 INTERCELLULAR FRACTION ATI ONS

3.4.1 Isolation of mesophyll and bundle sheath protoplasts

Leaves harvested from 7-10 day old seedlings were used for isolation of mesophyll cells and bundle sheath strands.

3.4.1.1 Enzymatic Isolation of Mesophyll Protoplast and Bundle Sheath Strands

Protoplasts were isolated, after incubating pearl millet tissue in a digestion medium (Day *et al* 1981), containing 2% (w/v) cellulase Onozuka R-10, 0.2% (w/v) macerozyme R-10, 10 mM sodium ascorbate, 0.2% (w/v) BSA, 20 mM MES-KOH pH 5.5, 1 mM $CaCl_2$, 1 mM $MgCl_2$ and 0.6 M sorbitol. 1 gm leaves were chopped to 1 mm segments and washed thrice with 10 ml of digestion medium without enzymes (Medium A). The leaf segments were then incubated in 10 ml digestion medium for 2 h at 25°C without agitation under red light in petri dishes. After 2 h, the digestion medium was replaced with medium B (10 mM MES-KOH, pH 6, 0.6 M sorbitol and 1 mM $CaCl_2$) and the dishes were gently tapped to liberate the protoplasts. The medium containing the protoplasts was filtered successively through 300 μm, 100 μm, and finally through a 80 μm nylon mesh. The filtrate was centrifuged at 100*g* for 5 min, and the pellet was gently resuspended in 6 ml of medium B in which sorbitol was replaced by 0.6 M sucrose. On top of the medium B, containing protoplasts, 2 ml of medium A was layered and the tubes were centrifuged at 300*g* for 5 min. The intact protoplasts present in the interface of the above step gradient were collected. In this procedure bundle sheath strands remained undigested and were retained on 80 μm nylon mesh during filtration. The yield of protoplasts was 3-4 x 10 mesophyll protoplasts/gm.FW.

3.4.1.2 Mechanical Isolation of Bundle Sheath Strands

For large scale preparation, bundle sheath strands were isolated using the mechanical method followed by Chollet and Ogren (1973) with a few modifications. 20 gm of leaves were cut into 5 cm segments and homogenized in a pre-cooled blender at 4°C at low speed for 20 sec in a 100 ml isolation medium containing 50 mM Tris-HCl (pH 8), 0.35 M sorbitol, 10 mM Na-ascorbate, 1 mM $MnCl_2$, 5 mM EDTA, and 0.2% (w/v) BSA. The homogenate was filtered through a 350 μm nylon mesh and the fragments that were retained on the mesh were rehomogenized for 30 sec at full speed in 100 ml of isolation medium. After the filtration, the fragments were processed as described above. The last three filtrates were pooled and passed through a 80 μm nylon mesh. Bundle sheath strands retaining on nylon mesh were washed with a wash buffer containing 50 mM Tris-HCl, pH 8, 0.35 mM sorbitol, 20 mM EDTA, 1 mM $CaCl_2$.

3.4.1.3 Isolation of Bundle Sheath Protoplast

The protoplasts were isolated by incubating the bundle sheath strands obtained by mechanical method for 4 h in a digestion medium. The digestion medium and protocol for isolating protoplasts was essentially similar to the one used for isolation of mesophyll protoplast (see section 3.4.1.1).

3.4.2 Isolation of intact chloroplasts

3.4.2.1 Isolation of Mesophyll Chloroplasts by Mechanical Method

The isolation procedure for chloroplasts was adapted from Palmer (1986). Twenty grams of leaves were homogenized in a pre-cooled Waring blender (5 sec homogenization X 5 times) in a isolation buffer containing 50 mM Tris-HCl buffer, pH 8.0, (6 ml buffer/gm.FW), 0.35 M sorbitol, 5 mM $MgCl_2$, 1 mM $CaCl_2$, 2 mM ethylenediamine tetraaetic acid (EDTA), 5 mM β-mercaptoethanol, 10 mM Na-ascorbate. The homogenate was centrifuged at 1000*g* for 15 min and the pellet was washed 3 times with a wash buffer containing 50 mM Tris-HCl, pH 8.0, 0.35 M sorbitol, 20 mM EDTA, and 0.1% (v/v) β-mercaptoethanol. Thereafter, the pellet was suspended in 4 ml of the wash buffer and layered on top of a step gradient of 31% and 54% (w/v) sucrose. The gradient was centrifuged at 30,000*g* for 40 min at 4°C. The intact chloroplasts obtained at the interface of 31% and 54% sucrose were diluted 5 times with the wash buffer and were pelleted by centrifugation at 1000*g* for 15 min.

The procedure yielded 1.125 X 10^{10} chloroplasts/gm.FW.

3.4.2.2 Isolation of Chloroplasts from Mesophyll and Bundle Sheath Protoplasts

Mesophyll and Bundle Sheath protoplasts were resuspended in a medium containing 50 mM Tris-HCl, pH 8, 0.35 mM sorbitol, 20 mM EDTA, and 1 mM $CaCl_2$ and, the protoplasts were disrupted by repeated filtering

through a 30 μm nylon mesh. The nylon mesh was fitted to the nozzle end of a 1 ml disposable syringe and protoplasts were broken by filling the protoplast suspension two or three times in the syringe. This procedure broke the protoplasts but left chloroplasts intact. The released intact chloroplasts were centrifuged at *250g* for 1 min to obtain a chloroplast pellet largely free of the cytosolic fraction. Chloroplasts pellet were resuspended in 50 mM Tris-HCl buffer, pH 7.5, containing 0.35 M sorbitol, 5 mM $MgCl_2$, 1 mM $CaCl_2$, 2 mM EDTA, and 5 mM β-mercaptoethanol.

The procedure yielded 2.8 X 10^7 bundle sheath chloroplasts from 50 gm of leaves.

3.4.3 CONFIRMATION OF CHLOROPLAST'S INTACTNESS

3.4.3.1 Ferricyanide Reduction Test

The intactness of chloroplasts was confirmed by the ferricyanide reduction test outlined by Lilley *et al*, (1977). Isolated chloroplasts suspended in 50 mM Tris-HCl, pH 8.0, 5 mM $MgCl_2$, 1 mM $CaCl_2$, 1 mM $MnCl_2$, 2 mM EDTA and 0.35 M sorbitol were subjected to the ferricyanide reduction test. K-erricyanide solution (3 mM) was prepared in chloroplast wash buffer. The intact chloroplast suspension (100μl) containing 100μg or less chlorophyll was either mixed with 1 ml of chloroplast suspention buffer (intact chloroplasts) or was lysed by (broken chloroplasts). Thereafter it was supplemented with 1.9 ml of potassium ferricynide solution and was assayed for Hill activity. The reduction of ferricyanide was measured by noting A_{520nm} at zero and after 30 min.

3.4.3.2 Phase Contrast Microscopy

The intactness of chloroplast was also confirmed by phase contrast microscopy. Under a phase contrast microscope, intact chloroplasts appeared highly reflective and surrounded by a bright halo, whereas broken chloroplasts appeared dark and granular. The chloroplast preparation consists largely intact chloroplasts (>90 %).

3.4.3.3 Protoplast and Chloroplast Counting

The number of protoplasts and chloroplasts were counted using Neubauer's chamber. The number of protoplasts and chloroplasts were measured by using the formula:

$$\text{No of cells}/\mu\text{l} = \text{No of cells in 16 large squares X 10 X } \frac{1}{\text{dilution}}$$

3.4.4 ENZYME EXTRACTION FROM PROTOPLAST/CHLOROPLAST

3.4.4.1 Osmotic Shock

The protoplasts were lysed by osmotic shock to yield an intact chloroplasts preparation and a cytosolic fraction. Protoplasts suspended in 0.6 M sorbitol medium were centrifuged at 100*g* for 3 min. The protoplasts were osmotically lysed by resuspending in a medium containing 0.35 M sorbitol, 50 mM Na-acetate, pH 4.6, 1% (w/v) BSA, 10 mM EDTA, and 1 mM $CaCl_2$ for 10 min. and was centrifuged at 250*g* for 2 min. and supernatent was collected. The supernatent so obtained was used for assaying cytosolic enzyme activity.

The pellet containing intact chloroplasts was suspended in 100 μl of above resuspension medium and was used for assaying plastidic enzyme activity.

For isolating amylases, protoplasts were resuspended in the 50 mM Na-acetate buffer, pH 4.6, and for phosphorylases, protoplasts were resuspended in 50 mM Tris-HCl buffer, pH 7.5.

3.4.4.2 Sonication

The protoplast or chloroplasts were also disrupted by sonication, at 4°C. Protoplasts or chloroplasts were suspended in 2 ml 60 mM Na-acetate buffer, pH 4.6 for amylases, or in 50 mM Tris-HCl, pH 7.5 for phosphorylase extraction. The samples were sonicated, in a 3.5 cm wide and 11 cm long test tube surrounded with ice, by eight 20 sec bursts in a MSE 150 Watt sonicater at 40% of its maximum amplitude (60 W). An interval of 30 sec was maintained between each sonication burst. At the end of treatment, samples were centrifuged at 8,000*g* for 5 min and supernatants were collected.

3.5 ELECTROPHORESIS

3.5.1 Native Gel Electrophoresis

Non-denaturing, discontinuous gel electrophoresis was performed in 1.5 mm thick slab gels using the electrophoretic buffer system of Davis (1964). The running gel was prepared with 7% (w/v) acrylamide, 0.375 M Tris-HCl, pH 8.9, 0.07% (w/v) ammonium persulphate, and 0.05% (v/v) N,N,N',N'-tetramethylethylene diamine (TEMED). The running gel was overlaid with stacking gel consisting of 2.5% (w/v) acrylamide, 61.25 mM Tris-HCl, pH 6.7,

0.07% (w/v) ammonium persulphate, and 0.05% (v/v) TEMED. The running buffer was made of 25 mM Tris-HCl, 192 mM Glycine, pH 8.3.

5 nkat of enzyme or 0.2 mg protein in 20% (v/v) glycerol, and 0.005% (w/v) bromophenol blue was loaded in the wells. The electrophoretic run was performed at 4°C for 8 h, with a constant voltage 90 V during migration through the stacking gel and 120 V through the running gel. The voltage was maintained constant till the completion of electrophoresis.

3.5.2 SDS-PAGE

The electrophoresis of denatured protein in polyacrylamide gel in the presence of an ionic detergent sodium dodecyl sulphate (SDS) was essentially carried out by following the procedure of Laemmli (1970).

10% (w/v) Acrylamide was polymerized as 1 mm thick separating gel, in 0.375 M Tris-HCl buffer, pH 8.8, containing 0.1% (w/v) SDS, 0.05% (w/v) ammonium persulphate, and 0.03% (w/v) TEMED. 4% (w/v) stacking gel was made in 0.125 M Tris-HCl, pH 6.8, containing 0.1% (w/v) SDS, 0.05% (w/v) ammonium persulfate, and 0.03% (w/v) TEMED. Samples were prepared in a sample buffer containing 62.5 mM Tris-HCl, pH 6.8, 2% (w/v) SDS, 10% (w/v) Glycerol, and 5% (v/v) β-mercaptoethanol, and were boiled for 4 min at 100°C for uniform coating of detergents. After cooling, the samples were loaded in the wells of gel and overlaid with 0.375 M Tris-HCl, pH 8.8 buffer containing 1% (w/v) SDS.

Electrophoresis was carried out at 37°C for 8 h at 120 V. The running buffer was made of 25 mM Tris, 192 mM glycine, pH 8.3, and 0.1% (w/v) SDS. The following marker proteins were used: bovine serum albumin (MW, 66,000), egg albumin (MW, 45,000), glyceraldehyde-3-phosphate dehydrogenase (MW, 36,000), carboxyanhydrase (MW, 29,000), trypsin inhibitor (MW, 14,000). All the marker proteins were dissolved at 1 mg/ml concentration in the sample buffer and a 10 μl mixture was loaded on SDS-PAGE gel.

3.5.3 Contact Prints

1% (w/v) agar solution containing 5% (w/v) amylose was prepared by boiling it in 60 mM sodium acetate buffer, pH 4.6. The agar solution was uniformly layered on a clean glass plate at 37°C and the plate was kept at 4°C for 30 min to solidify agar. After the electrophoretic run, the polyacrylamide gel was washed with 60 mM Na-acetate buffer, pH 5.2 for 30 min and then the gel was carefully overlaid on agar gel and a thin layer of 60 mM Na-acetate buffer was maintained on the top of the gel. Precaution was taken to avoid trapping of any air bubbles in between two gels. The gels were incubated at room temperature for 3 h in a humid chamber. At the end of the incubation period the polyacrylamide gel was carefully removed from the top of agar gel and thereafter, both the agar and the acrylamide gels were stained for amylase activity as described below.

3.5.4 Enzyme staining

3.5.4.1 Amylase

After PAGE, amylase activity was detected by following the procedure of Work and Work, (1972). The gel was first washed with 100 ml extraction buffer (60 mM Na-acetate, pH 6.1, 10 mM $CaCl_2$, and 5 mM β-mercaptoethanol) for 30 min, with gentle shaking. Thereafter, the gel was transferred to a reaction mixture containing 0.5% (w/v) amylose in 60 mM sodium acetate buffer, pH 4.6, and 0.1 mM NaF. The gel was incubated with the above mixture for about 3 h at the room temperature. At the end of incubation period the gel was washed with distilled water to remove adhering amylose solution and was left in a closed container for 15 min at 35°C. Thereafter, the transparent amylolytic bands against intense blue background were visualized after submerging the gel in iodine solution containing 6 mM I_2, and 50 mM KI in 0.2 M HCl for 1 min (Segundo *et al.*, 1990). The gels were immediately photographed and stored in 5% methanol and 7% acetic acid mixture at 4°C. The above procedure detects both ∝-amylase and β-amylase bands without distinction.

To visualize ∝-amylase bands after PAGE, contact printing was done with agar gel containing 0.5% (w/v) β-limit dextrin in place of amylose. The incubation and staining of the gel was carried as described above. In order to visualize minor ∝-amylase bands the gel was incubated for 9 h.

3.5.4.2 Phosphorylase

Phosphorylase activity was visualized by incubating polyacrylamide gels in a mixture which favored biosynthesis of starch by providing amylose as primer. After electrophresis, the gel was first washed with 50 mM citrate buffer, pH 6, for 30 min and then incubated at 30°C in a mixture containing 28.5 mM glucose-1-phosphate (Di-potassium salt), 0.1% (w/v) amylose, and 71.5 mM Na-citrate, pH 5.5 for 3 h. The incubation medium was also supplemented with 20 mM NaF, 0.3 mM $HgCl_2$ and 0.1 mM ammonium molybdate to inhibit the amylase's and phosphatase's activity present in the gel. At the end of incubation period the gel was washed with DW to remove adhering amylose and was left in DW for 1 h at 37°C. The formation of phosphorylase isoforms were visualized by staining gel with iodine solution as described for amylase (section 3.5.3.1). The phosphorylase isoforms were visualized as deep violet bands against light blue stained gel. The gel was washed overnight with DW leading to nearly transparent gel with deep blue phosphorylase bands.

3.5.5 Renaturation of denatured amylase protein

The protein extracts were first subjected to SDS-PAGE and amylolytic activity was recovered as per the procedure described by Segundo *et al.*, (1990). After SDS-PAGE, the gel was placed in a plastic tray (15 cm x 20 cm) containing 200 ml 1% (v/v) Triton X-100 and SDS was allowed to exchange with Triton X-100 for 2 h at room temperature with 3 changes by fresh Triton X-100 solution at 30 min intervals. The amylase activity was visualized using the procedure described above (section 3.5.3.1).

3.6 IMMUNOLOGICAL STUDIES

3.6.1 Double Diffusion

Double diffusion analysis was carried out following the procedure of Ouchterlony, (1949). 1% (w/v) agar solution was prepared in PBS [10 mM phosphate buffer, pH 7.4, containing 0.9% (w/v) NaCl] buffer by boiling it for 2 min. After cooling, the agar solution was layered on a glass/plastic plate to a thickness of about 2 mm and after solidification at room temperature for 1 h, the plate was kept at 4°C for 3 h. Holes were punched in gel with a steel template giving rise to a central well and 6 peripheral wells. The central well was loaded with antiserum and the antigens to be tested were placed in peripheral wells. After loading the wells, the agar gel was incubated at room temperature, in a closed humid chamber to avoid dehydration of the gel. The precipitin line appeared after an overnight incubation.

3.6.2 Single Radial Immuno-Diffusion

Single radial immunodiffusion was performed using the procedure outlined by Mancini *et al.*, (1965). 1% (w/v) agar solution was prepared in PBS buffer, pH 7.5. After cooling to 40°C the required amount of antiserum 1% (v/v) was mixed with the agar solution and the gel was immediately poured on a glass plate or on a plastic plate for solidification. Uniformly spaced 2 mm diameter wells were punched with a gel puncher and different concentrations of antigen were loaded in the wells. The outward diffusion of antigen leads to the formation of radial ring of precipitin line. The diameter of the ring was used to determine the antigen concentration by using the formula given below.

A calibration curve was plotted using known concentration of the antigen (μg) versus ring diameter. The ring diameter was measured as the diameter in two directions perpendicular to each other and the plotted diameter was calculated using the following relation:

Plotted diameter = (precipitin ring diameter)^2 -(well diameter)^2

The same relationship was used to estimate antigen in unknown samples. Fig 4 shows the standard curve obtained with different concentrations of antigen.

3.6.3 Immunoelectrophoresis

A glass microscopic slide was coated with 1% (w/v) agarose solution, prepared in 10 mM barbital buffer, pH 8.3. The gel was coated with a uniform 3 mm thickness on the slides and wells were punched at one end of the slide. The antigen was loaded in the wells and slides were connected to the buffer tank with 3 mm Whatman paper wicks. Electrophoresis was conducted at 40 volts/cm using 10 mM sodium barbital buffer, pH 8.8, at 4°C for 90 min. After the electrophoretic run, a trough was cut in between the wells and the appropriate concentration of required antiserum was added. The slides were incubated at 37°C in a closed humid chamber till the precipitin arcs were clearly visible.

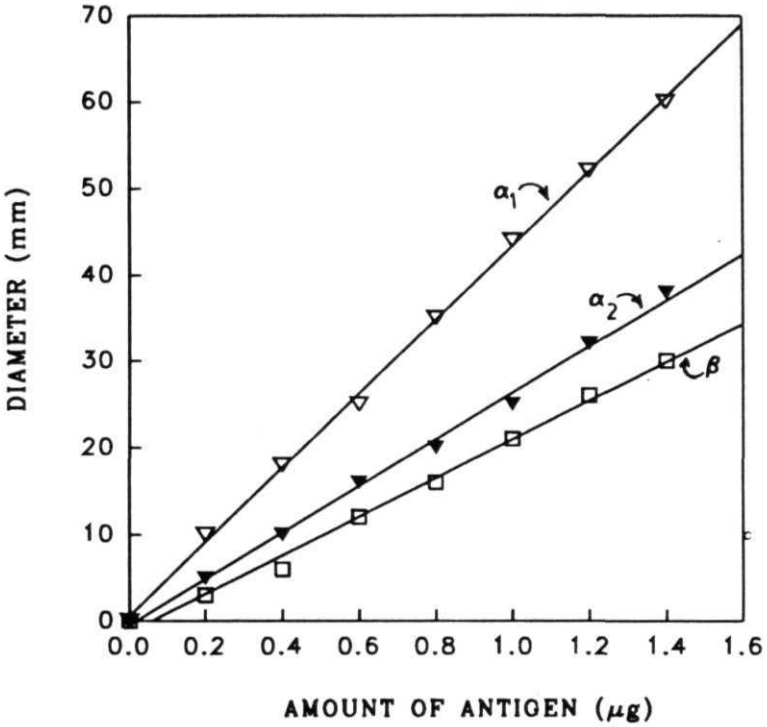

Figure 4. Representative standard curves for the estimation of α_1-, α_2- and β-amylase proteins by single radial immunodiffusion. The standard curves were prepared using α_1-, α_2-, and β-amylase proteins purified from maize seeds.

3.6.4 Western Blotting

Western blotting was done using the procedure of Renart and Sandoval (1984). β-amylase from leaves and ∝-amylase from mesophyll and bundle sheath chloroplasts were subjected to native gel electrophoresis. After PAGE, the gel was soaked in a transfer buffer [Tris 25 mM, glycine 192 mM, 20% (v/v) methanol, and 0.02% (w/v) SDS] for 1 h. The nitrocellulose paper was soaked for 15 min in the transfer buffer before blotting. The electrophoretic transfer was performed in a transblot unit at 30 mA current at 25°C for 8 h. At the end of the blotting, the unreacted sites on the blot were blocked by placing the blot in NET buffer [50 mM Tris, pH 7.5, 5 mM EDTA, 150 mM NaCl, 0.05% (v/v) NP-40, and 0.025% (w/v) gelatin] containing 1% (w/v) BSA for 1 h. The blot was first incubated with its specific antibody (1:100 dilution in NET buffer containing 0.002% Na-azide) for 3 h with gentle agitation. Thereafter, the blot was washed three times with NET buffer. The blot was then incubated with peroxidase coupled anti-rabbit IgG. (1:1000 dilution in NET buffer containing 0.1% BSA) for 1 h. The blot was washed 3 times with NET buffer, and was finally washed with TBS buffer (Tris-HCl, pH 7.4 and 0.9% NaCl).

The bands were visualized by using 0.5 % (w/v) 3'-3' diaminobenzidine as substrate along with 1% (w/v) $CoCl_2$ and 0.01% (v/v) H_2O_2 in PBS buffer, as blue bands on the nitrocellulose paper within 2 min of the incubation period. In case the blot was incubated in a solution of 25 μg of O-diansidine per 1 ml TBS buffer, consisting of fresh 0.01% (v/v) H_2O_2, brown bands were obtained.

3.7 *IN VIVO* SYNTHESIS

3.7.1 *In Vivo* Labeling

To determine the gradient of amylase's synthesis along the length of the leaf, leaves were excised into 1 cm segments numbered from the base. The 7-d old seedlings yielded 6 and 8 segments for dark and light-grown seedlings respectively. Each segment was further chopped to small 2 mm pieces. In case of *in vivo* labeling of bundle sheath, the same protocol as described below for leaf cells was followed by using bundle sheath strands in place of leaf segments. BSS were first isolated either by enzymatic or by mechanical method. Roughly 2.8 X 10^7 BSS were used for labeling.

In vivo labeling was carried out in a 1.5 ml Eppendorf tube containing 50 mg leaf segments suspended in 150 µl of sterile labeling buffer (10 mM Tris-HCl buffer, pH 7.4, 10 mM $CaCl_2$) containing 40 µci of ^{35}S-methionine (> 1000 ci/nmol), with constant shaking for 4 h at 25°C. The labeling was stopped by transferring tubes to ice bath and labeled tissue was washed thrice with ice-cold homogenization buffer containing 25 mM Tris-HCl, pH 7.5, 5 mM EDTA along with 10 mM cold methionine. The final wash was carried out with the same buffer without methionine, and buffer adhering to the tissue was blotted with tissue paper. The tissue was homogenized in 200 µl homogenization buffer in a precooled mortar and pestle. The homogenate was clarified by centrifugation in a microfuge at 14000*g* for 10 min at 4°C. The supernatant was supplemented with SDS (0.8 %, w/v) and was boiled for 4 min. The aliquots were withdrawn to determine total incorporation of radiolabel into proteins after precipitation with 10% TCA.

3.7.2 Immunoprecipitation of Labeled Proteins

The labeled products were immunoprecipitated by using specific antiserum for a given antigen. The supernatants were equalized with respect to the amount of radiolabeled proteins, and different volumes of labeled aliquots were made to 0.5 ml with homogenization buffer. It was then diluted by adding an equal volume of dilution buffer [50 mM Tris-HCl, pH 7.5, 5 mM EDTA, 300 mM NaCl, 1% (w/v) Triton-X 100].

To each test tube 10 μl antiserum was added, and tubes were incubated first for 1 h at 37°C and then overnight at 4°C. At the end of the incubation, 30μl *Staphylococcus* cells were added and the mixture was vigorously agitated for 2 h. The immune-complex absorbed on *Staphylococcus* cells was collected by centrifugation at 14,000*g* for 30 seconds in a microfuge. The cells were washed 4 or 5 times by suspending in 1 ml washing buffer [50 mM Tris-HCl, pH 7.5, 150 mM NaCl, 5 mM EDTA, 0.1% (w/v) Triton-X 100, and 0.2% (w/v) SDS] and recentrifuging it at room temperature. The final wash was carried out by using above buffer without detergents. The cells were suspended in 30 μl of electrophoresis sample buffer [50 mM Tris-HCl buffer, pH 6.8, 4% (w/v) SDS; 10% (v/v) β-mercaptoethanol, and 20% (v/v) glycerol] and boiled for 4 min. After centrifugation the supernatant was subjected to SDS-PAGE.

3.7.3 Fluorography

Fluorography was carried out according to the procedure of Bonner (1983). At the end of PAGE, gel was first fixed in a solution containing 50%

(v/v) methanol and 12% (v/v) acetic acid mixture for 1 h. The gel was dehydrated by soaking it in dimethyl sulfoxide (DMSO) with constant shaking and the DMSO was replaced twice at 30 min. intervals. PPO [2,5-Diphenyloxazole] was impregnated into the gel by submerging it in 25% (w/v) PPO in DMSO solution for 2-3 h. Thereafter, the PPO present in the gel was precipitated by transferring the gel to water for 1 h, and the excess DMSO present in the gel was removed by changing the water 3 times.

The gel was dried at 80°C under vacuum for 1 h in a commercial gel drier and the dried gel was exposed to Kodak X-omat AR film (Bonner 1983) for 30 days at -70°C in a cassette. Radioactivity in the bands was determined by scintillation counting after excision of the area corresponding to the band on X-ray film from the dried gels.

RESULTS

CHAPTER 4

RESULTS

The monocot leaf offers an ideal system to study the influence of light on cell and organelle differentiation. As the leaf possesses cells in a gradient of different maturity states due to a basal meristem, it generates files of cells with a continuous gradient of differentiation with the oldest cells at the tip of the leaf and the youngest cells proximal to the basal meristem. Additionally, the light-mediated biogenesis of chloroplast in leaves also follows a gradient similar to the cellular differentiation. In the C_4 monocot leaf, chloroplast biogenesis is further influenced by spatial influence. In the present study, we have investigated the influence of light on development of the starch-degrading enzymes in pearl millet leaves, and also the interaction between photostimulation of enzyme activity and chloroplast biogenesis.

4.1 MORPHOLOGICAL FEATURES OF THE GERMINATING SEEDLINGS

Pearl millet (*Pennisetum americanum)* seeds are ovoid and about 2 mm in length. The imbibition of seeds with water initiated germination, and radical and shoot tip protruded from seed coat around 24 h from sowing. The leaf remained in coleoptile for 3-4 d from sowing then ruptured the coleoptile. The length of leaf gradually increased from 3-d to 10-d during the period of our investigation. The light and dark-grown seedlings manifested significant morphological differences, characteristic of photomorphogenic and

scotomorphogenic development pathways. The light-grown seedlings had green expanded leaves and a short mesocotyl because of light mediated suppression of mesocotyl elongation. The upper part of the leaf was wider, whereas at the base the lamina was narrow. Similarly, the upper portion of the leaf was dark green while base was pale green. In contrast, dark-grown seedlings possessed a long mesocotyl but the leaf was smaller in size. Moreover, the dark-grown leaf was yellow in color due to lack of chlorophyll. In both light and dark-grown seedlings the basal region of the leaf was tightly rolled. Since pearl millet seedlings were grown in distilled water, in light after 12 d and in dark after 9 d the senescence begin, therefore seedlings were not used beyond this age.

Fig. 5 shows the development of pearl millet seedlings in light and darkness during the course of our study in light and darkness. The effect of light on leaf development was studied by comparing continuous red light-grown seedlings with control seedlings grown in darkness. There was no influence of light on seed germination, which was similar in both light and dark. Upto 2-d the seedling size was equal in both light and dark. A photo-stimulation of leaf growth was visualized 3-d after sowing. In light-grown seedlings, the primary leaf was about 11 cm long on 10-d whereas in dark-grown seedlings, the leaf expansion ceased completely after 8 d, the leaf being about 7 cm.

4.2 AMYLASES

4.2.1 Optimization of amylase assay

The pH optima for amylase was determined by assaying degradation of amylose in different buffers ranging in pH from 3.8 to 9.0. The buffers (50 mM

Figure 5. The morphology of pearl millet seedling under various treatments.
A. The development of shoot 0-3 d and leaf 3-10 day in dark grown and red light grown seedlings.
B. 7d old seedlings grown in presence of Norf lurazon or DW in red light and darkness.
C. The morphology of single seedlings grown as described in B.

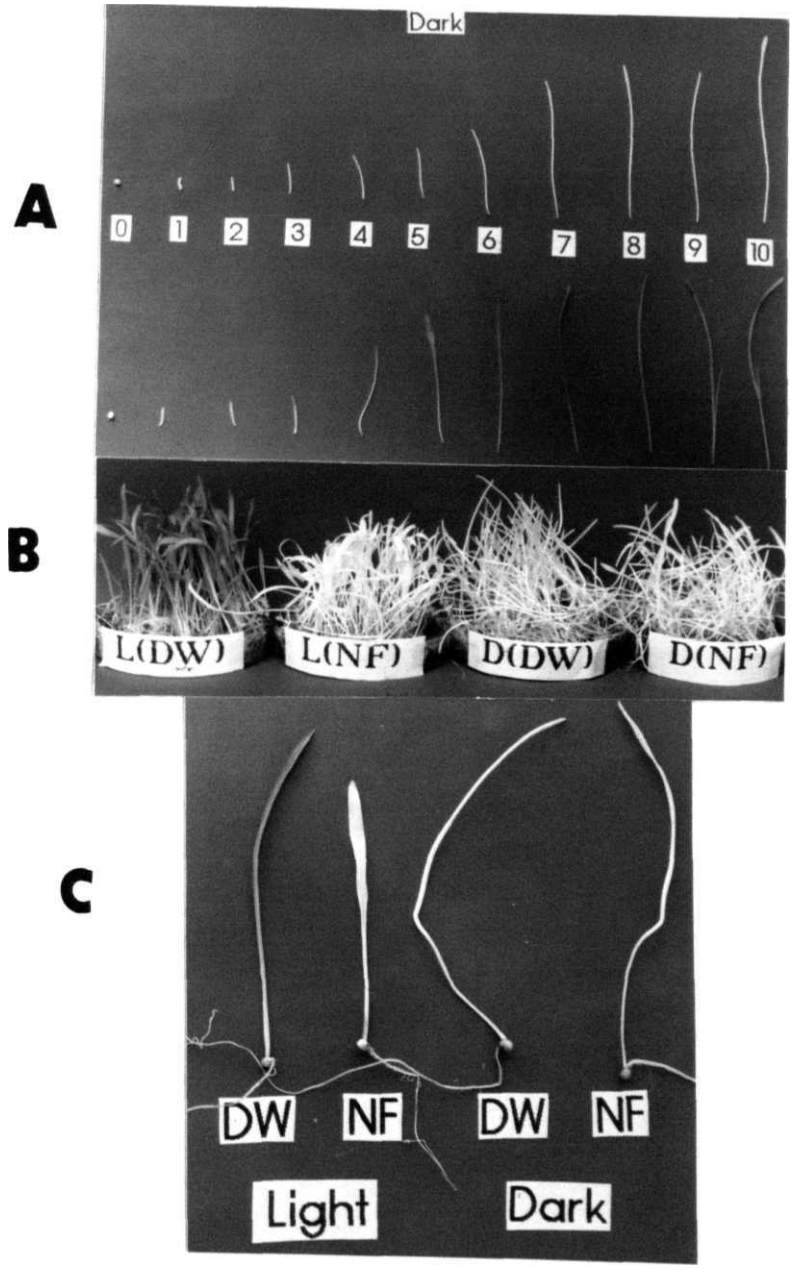
A
Dark
0
1
2
3
4
5
6
7
8
9
10
B
L(DW)
L(NF)
D(DW)
D(NF)
C
DW
NF
DW
NF
Light
Dark

each) used were: Na-acetate (pH 4.0 to 5.8), Na-citrate (pH 4 to 6.3) and Tris-HC1 (pH 7.2 to 9.0). The pH optima of amylase activity depended on the nature of the buffer employed. With the Na-acetate buffer, the pH optima was at pH 4.6, while with the Na-citrate buffer the pH optima was at pH 5.2. The maximal amylase activity was observed in the acetate buffer (Fig. 6A).

The optimal temperature for amylase action was determined by assaying amylase at different temperatures ranging from 20°C to 80°C. The amylase activity gradually increased with the temperature from 20°C to 50°C, thereafter remained at a plateau till 70°C, and then it rapidly declined due to denaturation (Fig. 6B). The temperature optima for amylase was at 50°C.

The amylase activity was quite stable in supernatants stored at low temperature. At 4°C, the amylase activity in supernatant was stable for about 3 d and thereafter it gradually declined. In contrast, in supernatant stored at 37°C such a stability of amylase was not observed and the activity gradually declined (Fig. 6C).

4.2.2 Inter-organ distribution of amylases

The distribution of amylase activity was analyzed in different organs of 7-d old pearl millet seedlings. The amylase activity was present ubiquitously in all organs of the seedlings (Fig. 7). The maximal amylase activity was detected in seeds, and was 30-40 fold higher than in other organs. Although amylase activity was present in leaf, root and coleoptile, the activity-levels were not similar.

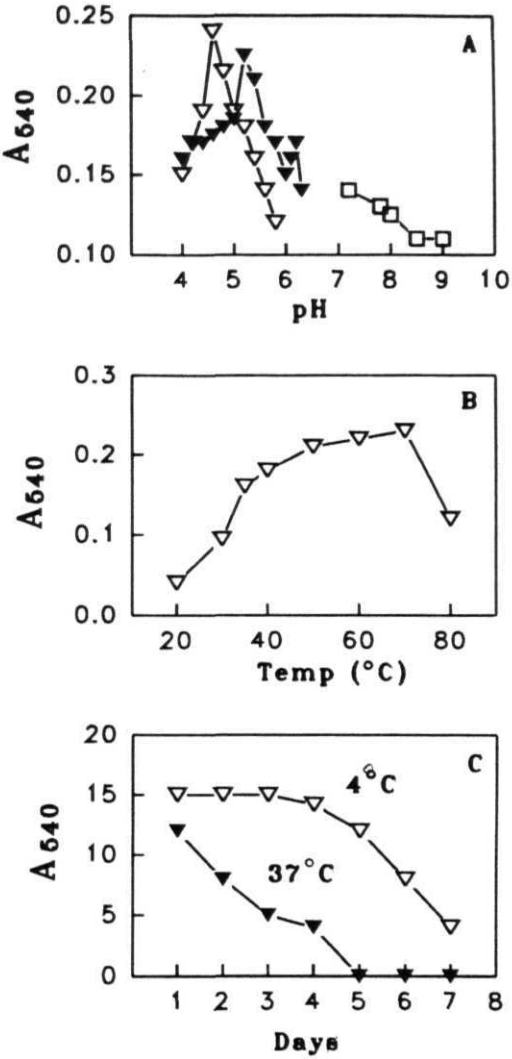

Figure 6. Optimization of amylase assay.

A. pH optima of amylase activity. The buffers used were Na-acetate buffer (v), Na- Citrate buffer (♥), Tris-HCl buffer (D).

B. Temperature optima of amylase activity.

C. Effect of temperature on stability of amylase activity.

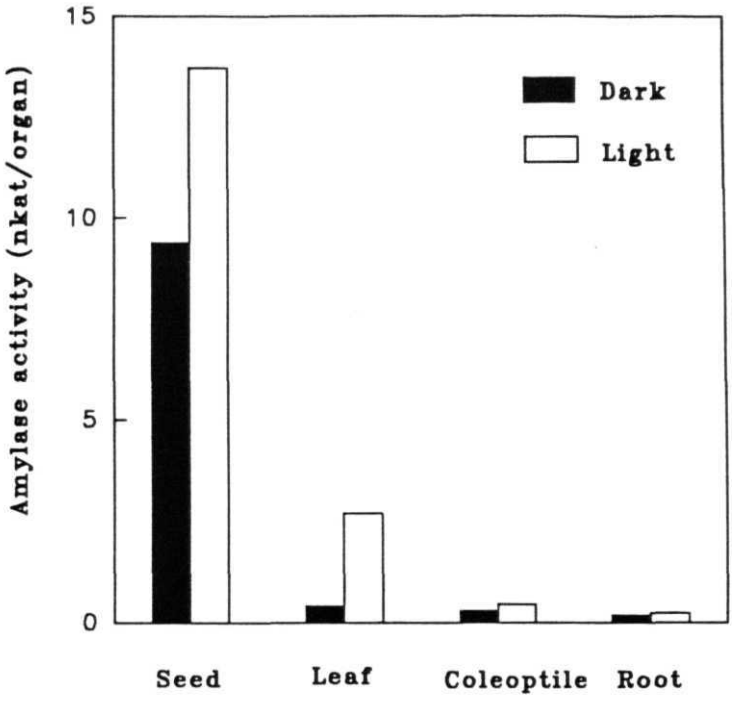

Figure 7. Amylase activity in different organs of pearl millet seedlings.

4.2.3 Effect of rl/fr light

In pearl millet seedlings, the studies on inter-organ distribution of amylase activity revealed that the light-grown leaf possesses a significantly higher amylase activity compared to the respective dark control (Fig. 7). The possibility of light-mediated promotion of amylase activity in leaf was examined by transferring 3-d old etiolated seedlings to continuous RL. The transfer of etiolated seedlings to continuous RL promotes a substantial increase in amylase activity (Fig. 8), as seen after 24 h or 48 h of transfer. The likelihood of phytochrome being the photoreceptor for observed photostimulation of amylase activity was ascertained by exposing 3-d etiolated seedlings to cyclic brief light pulses with 8 h dark intervals. It is evident that brief RL pulses too promote a significant increase in amylase activity in pearl millet leaves, whereas FR pulses are not effective in stimulating amylase activity. Moreover, if a RL pulse is followed by a FR pulse, the inductive effect of the RL pulse is nullified indicating the participation of phytochrome in this photoresponse.

4.2.4 Time course of amylase photostimulation

The time course of photostimulation of amylase activity under continuous RL was studied in leaves of pearl millet seedlings right from the sowing. In germinating seedlings the coleoptile emerges 24 h after sowing. For the first two days, amylase activity was measured in the shoot tip after removing coleoptile. The amylase activity from the time of coleoptile emergence to 3rd d remained at a low basal level (Fig. 9). A steady increase in amylase

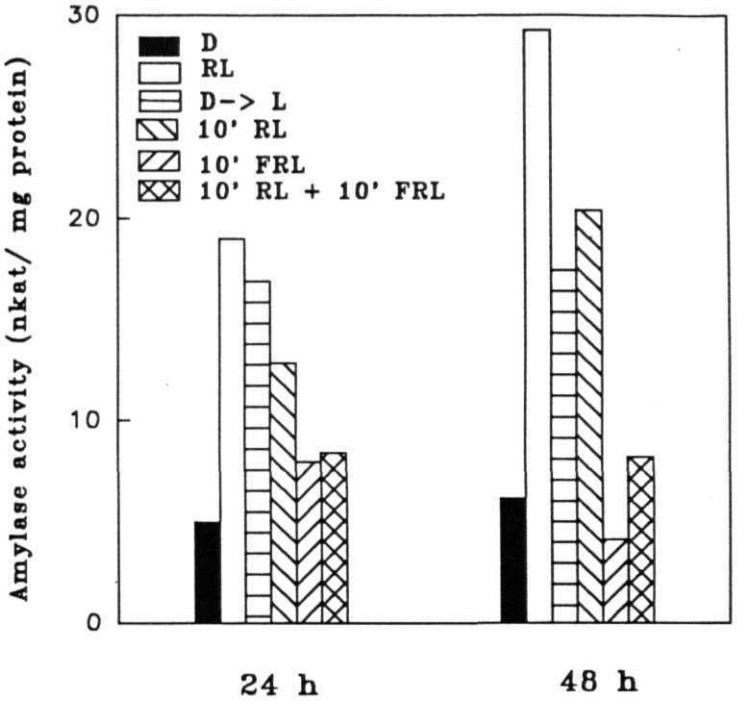

Figure 8. Effect of 10 min red light (RL) and far-red light (FRL) on amylase activity in pearl millet seedlings.
Seedlings were grown in darkness for 3-d after sowing. Thereafter, the seedlings were subjected to 10 min light pulses separated by an interval of 8 h in darkness. The amylase activity was measured at 4-d and 5-d after sowing. The control seedlings were grown in continuous darkness or light.

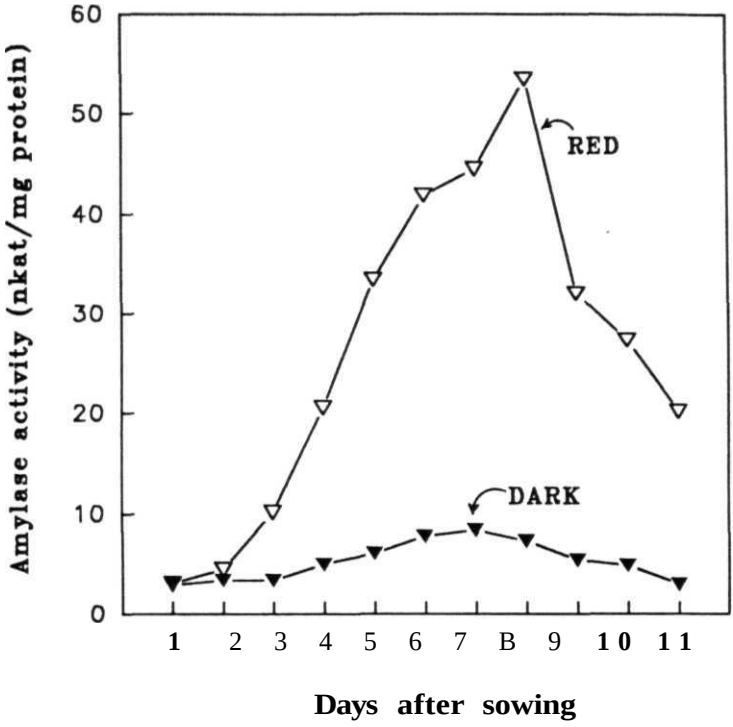

Figure 9. Time course of amylase activity in the leaves of pearl millet seedlings.
Seedlings were grown in continuous red light (▽) or darkness (▼) from the time of sowing.

activity was observed from 3rd d onwards in red light-grown leaf and it reached a peak on 8th d, thereafter, a rapid decline was noticed. In comparison, the dark-grown seedlings showed only a slight increase in amylase activity from 3rd d upto 7th d and then the activity slowly decreased. The possibility that the observed photostimulation of amylase activity may be an artifact of light-mediated change in the parameter (protein) used for calculating amylase activity, was also examined. Amylase activity was calculated on the basis of several parameters such as protein, fresh weight and leaf, to detect any artifactual photostimulation of amylase activity due to light-stimulated change in parameter. Fig 10 shows that irrespective of parameter used, the same qualitative pattern of photostimulation of amylase activity was observed, ruling out the possibility of any artifacts (Fig. 10A,B,C).

4.2.5 Effect of blue light

Fig. 11 shows the time course of amylase activity in seedlings grown under blue light. Blue light also elicited an induction of amylase activity similar to red light. The time course of increase in amylase activity in leaves by blue light was qualitatively similar to red light. However, under blue light, amylase activity increased albeit at a slower rate than that under continuous red light (cf. Fig. 9). Blue-light-mediated stimulation in amylase activity reached maximum on 8th d and thereafter it declined continuously till 10th d.

Since blue-light-mediated amylase induction is qualitatively very similar to that observed with red light, it was investigated whether brief pulses of blue light can also elicit amylase increase like RL pulse. Fig. 12 shows the effect

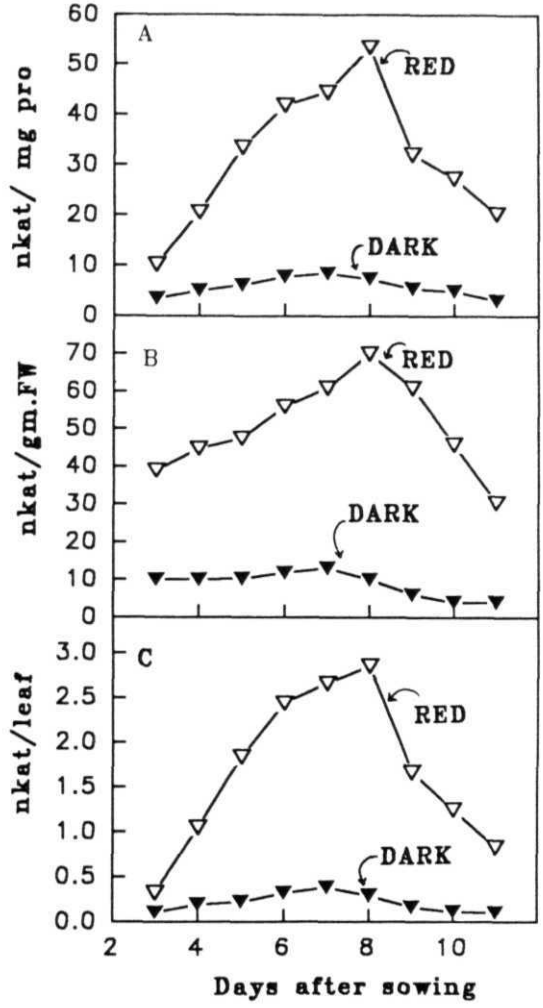

Figure 10. Time course of amylase activity in pearl millet leaves. Seedlings were grown in either continuous red light (▽) or in the darkness (▼) from 3-d onwards. Amylase activity was calculated using different parameters as indicated below.
A. protein basis.
B. gm FW basis.
C. per leaf basis.

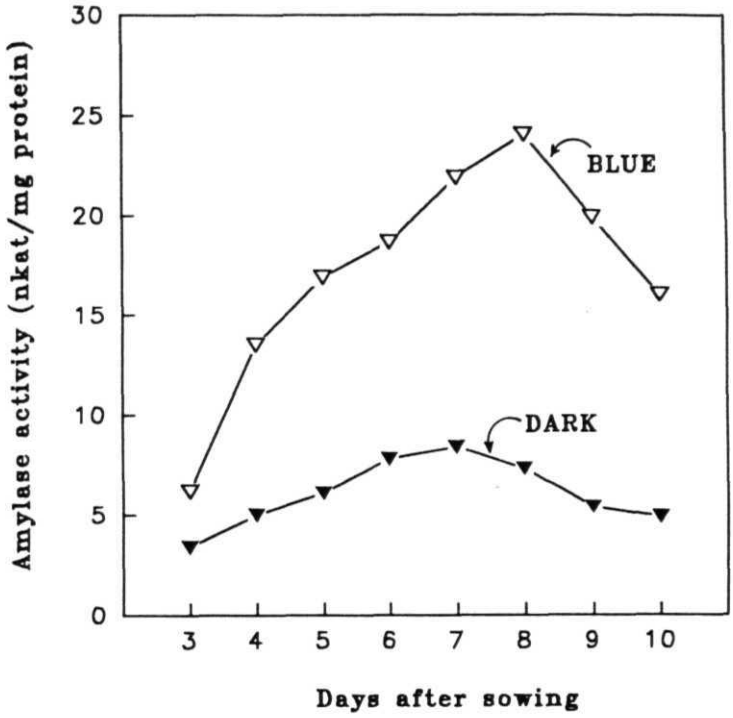

Figure 11. Time course of amylase activity in the leaves of pearl millet seedlings.
Seedlings were grown in continuous blue light (v) or darkness (▼) from the time of sowing.

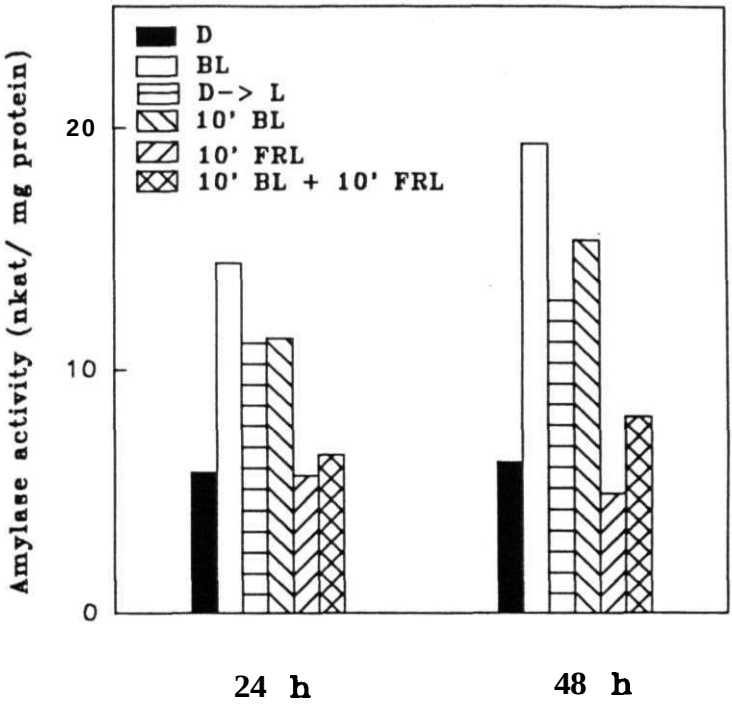

Figure 12. Effect of 10 min blue light (BL) and far-red light (FRL) on amylase activity in pearl millet seedlings.
Seedlings were grown in darkness for 3-d after sowing. Thereafter, the seedlings were subjected to 10 min light pulses separated by an interval of 8 h in darkness. The amylase activity was measured at 4-d and 5-d after sowing. The control seedlings were grown in continuous darkness or light.

of 10 min pulses of blue light, far-red light, and blue light followed by far-red light. It is evident that cyclic exposure of a brief blue light pulse enhanced the amylase activity which could be reversed to a level close to the dark control, if it was followed by a far-red light pulse.

4.2.6 Distinction between ∝- and p-amylase activity

In higher plants amylase activity consist of two distinct enzyme proteins, *viz.*, oc-amylase and p-amylase. Therefore, we examined if light treatment affected both of these enzymes or only one of them. In pearl millet both endo-amylase (∝-amylase) and exo-amylase (p-amylase) activities were detected. The discrimination between ∝-amylase and p-amylase activities present in supernatants was done by using different methods based on the physicochemical properties of the respective enzymes.

It is well established that the presence of 10 mM Ca protects ∝-amylase activity. Moreover, in the presence of calcium (10 mM) oc-amylase can be even subjected to heating at 70°C for 5 min to 5 h without any significant loss of the catalytic activity (Stein and Fischer, 1958; Koshiba and Minamikawa, 1981; Beers and Duke, 1990). In present study, therefore, oc-amylase activity was measured after inhibiting p-amylase activity by heat treatment for 5 min at 70°C in the presence of 10 mM $CaCl_2$.

Since ∝-amylase requires Ca^{2+} for stability (Bush *et al.*, 1989), therefore, inclusion of chelating agent like EDTA (Koshiba and Minamikawa, 1981) inactivates it. In order to measure p-amylase activity, oc-amylase activity was

inhibited by incubating the supernatants with 10 mM EDTA for 2 h at 4°C. However, EDTA treatment is not well suited for estimating β-amylase activity, as presence of EDTA in aliquots creates an artifactual problem in estimation of reducing sugars, as EDTA interfers with the absorbance of the dinitrosalicylic acid reagent. As little as 2 μM EDTA interferes with the measurement of the reducing sugar and a complete inhibition of color development occurres at 45 mM concentration. Therefore, p-amylase activity was usually estimated by subtracting ∝-amylase activity from total amylase activity.

In the course of our study, differentiation between these two amylases was also made by using a specific substrate, β-limit dextrin. While ∝-amylase alone can degrade p-limit dextrin, the amylose can be degraded by both ∝- and P-amylase (Thoma *et al.*, 1971).

4.2.7 Time course of ∝- and β-amylase induction

The time course of red-light-mediated stimulation of amylolytic activity of pearl millet leaves was reanalyzed with respect to relative induction of ∝-amylase and p-amylase. The total amylase activity was determined by using amylose as substrate, and thereafter, after heat inactivation of p-amylase, ∝-amylase activity was detected using β-limit dextrin as substrate. The β-amylase activity was measured by subtracting ∝-amylase activity from total amylase activity.

The red-light-mediated stimulation of amylase activity in pearl millet leaves resulted largely from an increase in the β-amylase activity which constituted 80-90% of total leaf amylolytic activity in light-grown seedlings (Fig. 13). Light strongly promoted β-amylase activity in 3-d old light grown seedlings. The light-mediated β-amylase activity reached a maxima on 8-d and thereafter declined. Interestingly, in dark-grown leaves, β-amylase activity could be detected significantly only after 6th d of sowing (Fig. 13A). In 4-d to 6-d old seedlings, p-amylase activity was found to be below the limit of detection.

The time course of ∝ -amylase stimulation by red light followed a different pattern (Fig. 13B). Though ∝-amylase activity in leaf gradually increased till 5-d, no significant difference could be visualized between dark and light grown seedlings. The promotive effect of light on ∝-amylase activity was visualized only after 5-d from sowing. After attaining a maxima on 6th d, ∝-amylase activity decreased in both cases.

4.2.8 Effect of norflurazon on amylase activity

The interrelationship between light-mediated amylase increase and the chloroplast development was investigated by growing pearl millet seedlings with Norflurazon (NF), a chlorosis- inducing herbicide (Henson, 1985; Burgers and Taylor, 1987; Reiss *et al.*, 1983; Blume and McClure, 1980). The treatment of pearl millet seedlings with NF completely prevented chloroplast development in light and resulted in the development of albino seedlings either under strong white light or continuous red light.

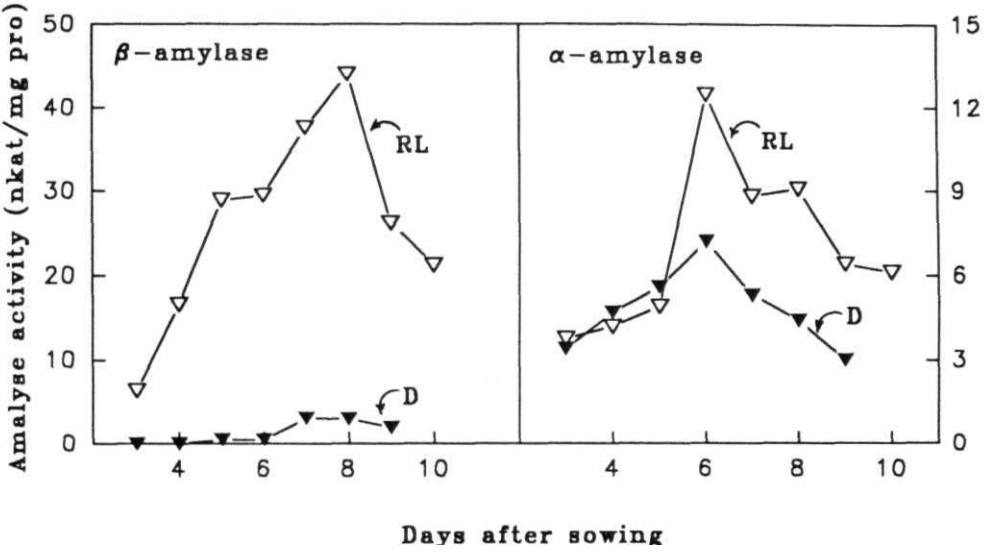

Figure 13. Time course of α- and β-amylase activity in pearl millet leaves. Seedlings were grown in either continuous red light (v) or in darkness (▼) from the time of sowing.
A. β-amylase activity.
B. α-amylase activity.

In NF-treated light-grown seedlings, the fresh weight of the leaves was less than the green leaves, and the profiles of the protein level was similar to that of dark grown seedlings. In 3-d old seedlings, fresh weight as well as protein contents were nearly equal in control and NF-treated samples. Subsequently, difference in fresh weight as well as protein contents gradually became apparent. In dark-grown seedling, NF treatment had no significant effect either on the fresh weight or on protein content (Fig. 14A,B). By contrast, NF treated seedlings grown under RL had a lower protein content than DW grown seedlings (Fig. 14B) and the protein content paralleled to dark control seedlings.

The effect of NF on photostimulation of amylase activity was studied in leaves of pearl millet seedlings. The NF-treatment decreased the photostimulation of amylase level in leaves of pearl millet seedlings (Fig. 15A). In 3-d old pearl millet seedlings, amylase activity in NF-treated seedlings and in control seedlings was equal. The NF-mediated reduction in amylase activity was manifested significantly in 4 to 8 d old seedlings. In NF-treated seedlings too, photostimulated increase in amylase activity was maximal on 8th d and then declined. The application of NF had only a small effect on the amylase level in the dark-grown seedlings and the activity was equal to the control seedlings (Fig. 15).

However, an individual examination of α-amylase and β-amylase activity in 7-d old seedlings revealed that while NF only partially inhibited the photostimulation of β-amylase (Fig. 15B), it completely blocks the

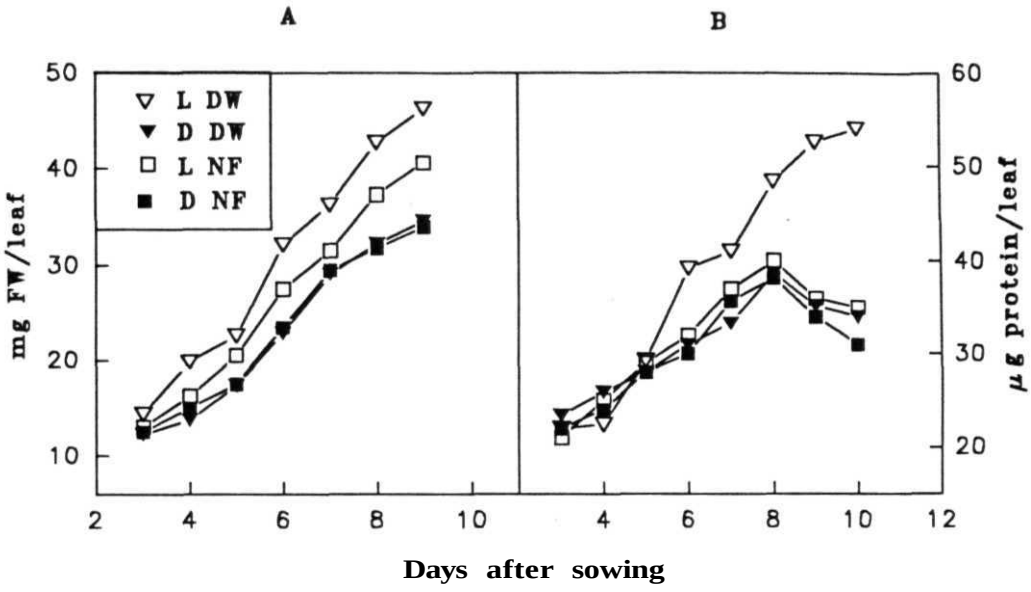

Figure 14. Time course of increase in fresh weight and protein content in pearl millet leaves.
Seedlings were grown in distilled water (DW), (▽ , ▼) or in Norflurazon (NF), (□ , •) from the time of sowing, either in continuous red light (v,o) or in darkness (▼,■).
A. Fresh weight B. Total Protein.

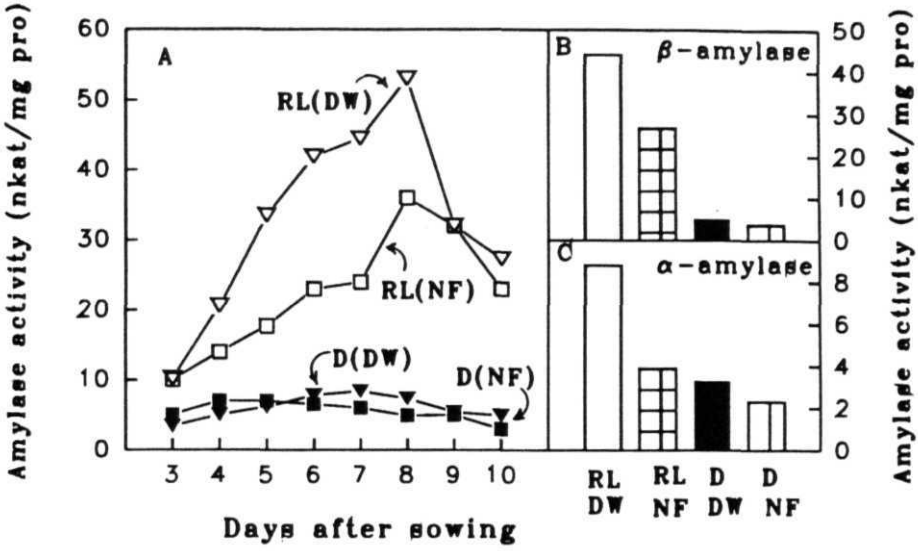

Figure 15. Effect of Norflurazon on the time course of amylase activity in pearl millet leaves.
Seedlings were grown either in continuous red light (D) or in darkness (•) in presence of Norflurazon (NF). The control seedlings were grown in distilled water (DW) in red light (▽), or in darkness (▼).
A. Time course of total amylase activity.
B. β-amylase activity in 7-d old seedlings.
C. ∝-amylase activity in 7-d old seedlings

photostimulation of ∝-amylase activity (Fig. 15C). On the contrary, it did not effect both ∝-amylase and β-amylase activities in dark-control seedlings.

4.2.9 Electrophoresis

In higher plants, both ∝-amylase and β-amylase are encoded by a small multigene family, and therefore, gene products of these enzymes are likely to be resolved in multiple isoforms after electrophoresis in native forms. In the present study, amylase activity from light-grown leaves was resolved into two distinct isoforms after PAGE, a slowly migrating isozyme (Rf 0.21) and a rapidly migrating isozyme group (Rf 0.71). In dark-grown leaves, only the later isozyme group was found, which stained as an intensified single band and probably contained closely migrating multiple amylase species. [In some samples, two weak bands of amylase were also visualized below this major isozyme having Rf value of 0.72 and 0.73 respectively.] In addition to the fast-migrating amylase isozyme, a slow migrating isozyme was also present in light-grown leaves, however, it was less intense in staining (Fig. 16A). Since the dark-grown seedlings lacked the above amylase isozyme (Fig. 16B), the appearance of this specific isozyme in leaves depended on light. The application of NF, which reduced total amylolytic activity in light-grown leaves (Fig. 15), eliminated the slow isoform of amylase (Fig. 16C), but did not qualitatively affect the composition of fast isoform of amylase both in light and darkness (Fig. 16C,D).

Since after PAGE the gels were stained by incubating in amylose which is degraded equally by both ∝- and β-amylase, an identification of molecular

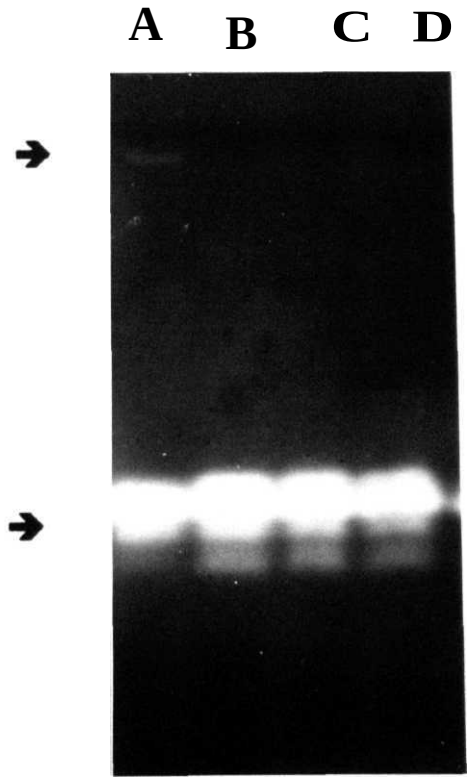

Figure 16. Electrophoretic analysis of amylase isoforms, in leaves of 7-d old seedlings.
Seedlings were grown in continuous red light or in darkness in distilled water (DW) or in 0.4 mM Norflurazon (NF). Amylase activity was visualized using amylose as a substrate (4mg/ml).
Lane A- RL(DW), Lane B- D(DW), Lane C- RL(NF), Lane D- D(NF)

nature of isoforms is not possible. However, the fact that the slow-migrating isoform is eliminated by NF-treatment points out the possible association of this isoform with plastids, which was ascertained by isolating chloroplast from pearl millet leaves.

4.2.10 Isolation of intact chloroplasts

The basic function of amylolytic enzymes in higher plants is the mobilization of starch. In photosynthetically active cells, starch is localized in the chloroplasts, which generates starch during the light period and is metabolized during the dark periods. Since chloroplasts are the site of starch metabolism, experiments were conducted to study the possible localization of starch degrading enzymes in the chloroplast. Since the experiments showed that light triggers the appearance of an additional slow-migrating isozyme of amylase, whose appearance is blocked in NF-treated albino leaves, the likelihood of this amylase isoform being a chloroplastic protein was investigated.

In order to clearly assign a plastidic location to an enzyme, it is essential that intact chloroplasts should be obtained to eliminate cross-contamination of cytosol or adsorption of cytosolic components. A step gradient of sucrose was employed to isolate intact chloroplasts from leaves. It is known that intact chloroplasts do not reduce ferricyanide, but can reduce it only after an osmotic shock which rupturs the envelop membrane (Lilley *et al.*, 1977). In the present study, the isolated chloroplasts failed to reduce ferricyanide via the Hill reaction, but could do so only after an osmotic shock (data not shown), indi-

cates that plastidic preparation consisted of intact chloroplasts. The intactness of isolated chloroplasts was also confirmed by phase-contrast microscopy. Fig. 17 shows that under a phase-contrast microscope broken chloroplasts which appear granular and dark green in color are few in number, whereas intact chloroplasts are highly reflective, round, and bright yellow in color (Fig. 17A).

The contamination of cytosolic enzymes in isolated chloroplast preparation was examined by assaying PEP carboxylase, a marker enzyme for cytosol. Table 1 shows that while PEP carboxylase activity could be detected in cytosolic fraction, it was below the limit of detection in chloroplast preparation. It is evident from the above study that our chloroplast preparation consisted of intact chloroplasts.

4.2.11 Chloroplasts possess only ∝-amylase activity

The isolated intact chloroplasts were subjected to an osmotic shock and homogenization in mortar to rupture the chloroplast envelope membrane for estimating plastidic amylase activity (Table 2). In contrast to the cytosolic fraction, isolated chloroplasts possessed only low amylase activity indicating that most amylase activity is localized in extraplastidic compartment. Moreover, amylase activity could be liberated only after disruption of the intact chloroplasts by sonication, confirming chloroplastic localization of amylase activity (Table 2). A gradual increase in the duration of the sonication period correlated with the released amount of amylase and the total amylase activity can be recovered with 8 x 20 sec bursts with a 1 min time gap.

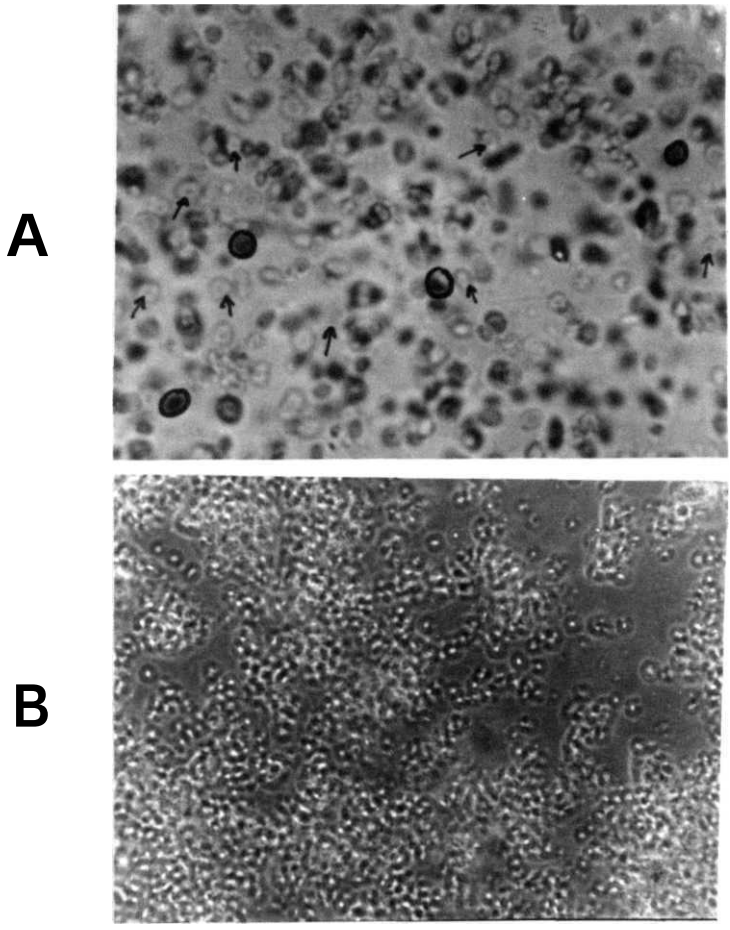

Figure 17. Phase contrast microscopy of isolated chloroplasts. Chloroplasts were isolated from leaves of 10-d old light grown seedlings.
A. Intact chloroplasts (indicated by an arrow) along with broken chloroplasts (marked by circle).
B. Intact chloroplasts.

Table 1. The intracellular distribution of a- and ß-amylase activity in the leaves of 10-d old red light grown pearl millet seedlings. The substrate specificity vas used to distinguish between a- and fi-amylase.

Fraction	Amylase activity (nkat/mg protein)		PEPC activity (µmol/mg chl)
	ß-amylase	α-amylase	
Homogenate	19.4	6.6	·
Cytosol	21.6	0.3	2.03
Chloroplast	0	5.0	0.001

* •-estimation not done.

Table 2. Liberation of amylolytic activity by disruption of isolated intact chloroplasts.

	Total activity (nkat)	
Plastidic pellet (3000g)	61.24	(100 %)
Homogenization in mortor and pestle	60.04	(98.0%)
Osmotic shock	60.80	(99.3%)
Sonication		
10 sec, 6 Bursts	22.80	(37.2%)
2 0 sec, 4 ,,	45.63	(74.5%)
2 0 sec, 8 ,,	**60.80**	(99.3%)
20 sec, 10 ,,	60.80	(99.3%)
30 sec, 3 ,,	45.63	(74.5%)

The absence of PEP carboxylase activity in isolated chloroplast discounted the contamination of a cytosolic amylase in chloroplasts. Unlike the cytosolic amylase isoform, the chloroplastic amylase could degrade both amylose and β-limit dextrin with equal efficiency (Table 1). Since plastidic amylase could degrade both amylose and β-limit dextrin with equal efficiency, it is likely to be an oc-amylase in nature. In etioplasts isolated from dark-grown seedlings, no amylase activity was detected. The elimination of functional chloroplasts by NF-treatment of light-grown seedlings also eliminated plastidic amylase activity (data not shown).

In the present study, amylase isozymes were visualized after PAGE by using amylose as a substrate. Since amylose is degraded both by oc-amylase and β-amylase, it is not possible to distinguish whether an isozyme belongs to ∝-amylase or β-amylase. In view of the above limitation, ∝-amylase bands were distinguished from β-amylase after PAGE by employing β-limit dextrin, which is degraded only by oc-amylase, but not by β-amylase. Since β-limit dextrin solution is viscous and fails to penetrate the polyacrylamide gel, oc-amylase isozymes were visualized by contact printing of polyacrylamide gel on an agar gel containing β-limit dextrin. The difference in isoform patterns obtained using amylose and β-limit dextrin as substrate, was used to distinguish ∝-amylase isozymes from β-amylase (Fig. 18).

The contact printing of gels for 3 h revealed that out of the two isozymes, only the minor isozyme having a low Rf value (0.21), present in leaves of light-grown seedlings (Fig. 18A), could degrade both amylose (Fig. 18A) and β-limit dextrin (Fig. 18C) and this was thereafter identified as ∝-

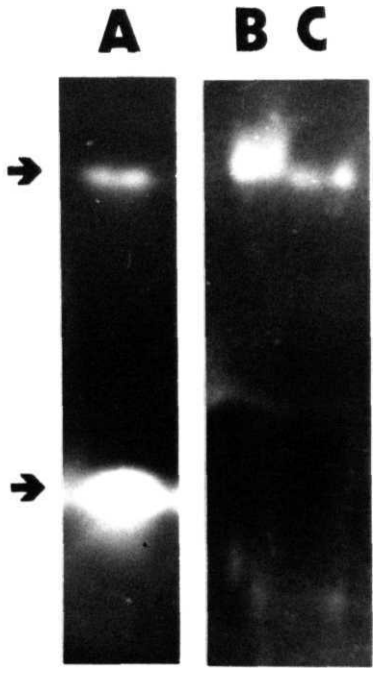

Figure 18. Identification of amylase isozymes as a-amylase and β-amylase on the basis of substrate specificity after native PAGE.

A. a- and β-amylase isoforms were distinguished by using amylose as substrate.
B. The presence of α-amylase isoform in chloroplast extract was detected by contact printing on a β-limit dextrin containing agar gel.
C. The a-amylase isoform in total leaf extract was detected by contact printing on a β-limit dextrin containing agar gel. The band which does not degrade β-limit dextrin was identified as /3-amylase.

amylase. The fast-migrating major isozyme of leaf could not degrade β-limit dextrin but degraded amylose (Fig. 18A); therefore, it was identified as β-amylase (Manners, 1985).

4.2.12 Localization of amylases in mesophyll and bundle sheath cells

In a C_4 plant like Pearl millet, the cellular organization of leaf can be distinguished anatomically into M cells and B strands. The B strands were isolated both from green and etiolated leaves by combining mechanical and enzymatic methods. Although the green and etiolated leaves possessed chloroplasts and etioplasts respectively, the basic arrangement of B morphology, cell wall thickness etc., were essentially similar in both (Fig. 19). The extent of M contamination in B was negligible when checked by assaying PEP carboxylase activity, the cytosolic enzyme localized exclusively in M cells.

The distinction of contaminants was also made using microscopy of isolated cells as a tool, e.g., the B contamination in M cells preparation was ascertained by visualizing the presence of brick shaped B cell wall in M preparation (Horuath *et al*., 1978). On the other hand, contaminating M cells in the B preparation were distinguished by their physical localization, in between B strands. M protoplasts and B strands preparation devoid of contamination were used for the subcellular fractionation studies. Since commercial Onozuka R-10 cellulase was contaminated by a fungal α-amylase,

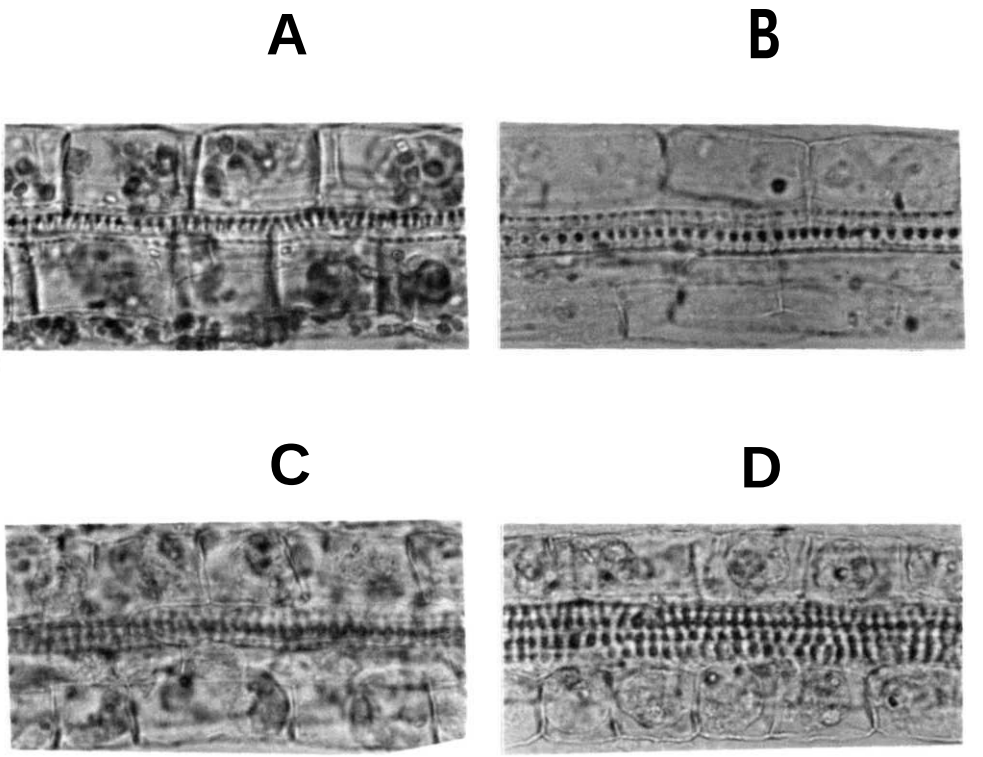

Figure 19. Phase contrast **micrograph** of bundle sheath strands isolated from leaves of **10-d** old seedlings. Seedlings were grown in either light (DW) (A) ; Light (NF) (B); or in darkness (DW) (C), darkness (NF) (D).

after isolation, the protoplasts were extensively washed till contaminating fungal amylase was fully removed.

4.2.13 Amylase activity in mesophyll cells

The isolated M protoplasts were fractionated after a gentle osmotic shock into cytosolic and plastidic fractions. The plastidic fraction obtained from protoplasts consisted of intact chloroplasts which were then disrupted to release internal plastidic proteins. The cytosolic as well as chloroplastic fractions were analyzed individually for the presence of ∝-amylase and B-amylase activities. Table 3 shows relative distribution of ∝-amylase and B-amylase activity in both M and B respectively. In M, about 80-85% of amylase activity was recovered in the cytosol and the remaining activity was found in the chloroplast. The cytosolic amylase of M mainly consisted of B-amylase which is evident by the fact that it degraded B-limit dextrin less efficiently than amylose. In comparison to cytosol, the chloroplastic amylase degraded both B-limit and amylose with an equal efficiency being ∝-amylase in nature (Fig. 20A).

In addition to B-amylase, cytosol had also contained trace amounts of ∝-amylase activity which was observed only after prolonged contact printing of PAGE gels (Fig. 20E). The presence of cytosolic ∝-amylase was demonstrated by contact printing of gels for a prolonged period (9 h) on B-limit dextrin containing agar gels. The staining of the contact prints revealed different isozymes of ∝-amylase, with Rf values of 0.59, 0.68, 0.75, 0.79 and 0.82. These cytosolic isozymes were present in a low amount in leaf cells. Apart from

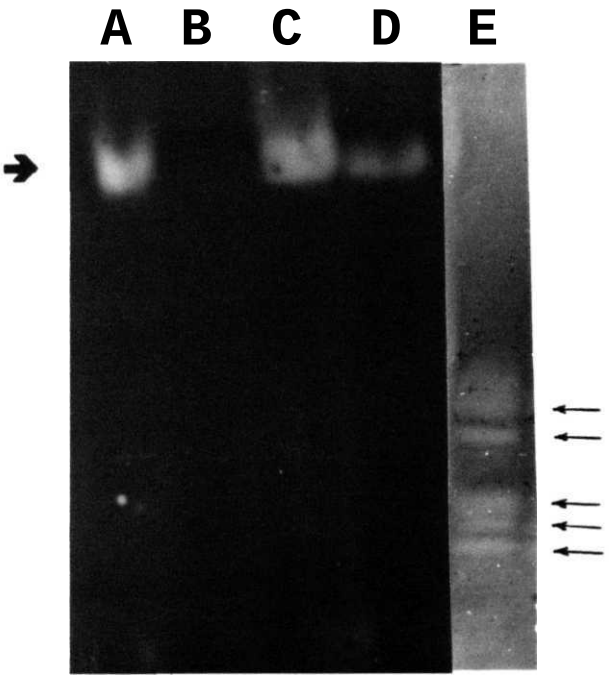

Figure 20. Isozymes of α-amylase in mesophyll and bundle sheath cells.
Seedlings were grown either in continuous red light or in darkness, in DW or in NF (0.4mM) for 8 days. Amylase activity was visualized by contact printing on a β-limit dextrin gel.
Lane A Mesophyll chloroplasts; Lane B Bundle sheath Strands NF; Lane C Bundle sheath Strands DW; Lane D Bundle sheath chloroplasts; Lane E Mesophyll cytosol.

these, 3 other minor isozymes with Rf values of 0.49, 0.52 and 0.54 were also present but could not be photographed due to weak bands. This isozyme pattern was neither influenced by light nor by Norflurazon treatment.

4.2.14 Amylase activity in BSS

In a fashion similar to the one described for M, amylase activity was also estimated in B cells (Table 3). In cytosolic fraction neither β-amylase nor ∝-amylase could be detected and total ∝-amylase activity in B was found to be localized only in chloroplasts. By contrast, ∝-amylase activity was totally absent in the B strands isolated from either NF-treated seedlings or from dark-grown seedlings (Table 3). The level of ∝-amylase activity in M chloroplast was also compared to B chloroplasts. The M chloroplasts lack Rubisco and therefore possess less protein than the B chloroplasts. Similarly, both chloroplast types possess different chlorophyll levels too. Table 4 shows that the level of ∝-amylase activity in chloroplast is clearly influenced by the parameter used to express it. However, it is also evident on the basis of chloroplast as a unit, that B chloroplast possessed 1.76-fold higher ∝-amylase activity than M chloroplasts.

4.2.15 Physicochemical characterization of plastidic amylase

The substrate specificity of plastidic amylase was akin to its molecular nature as «-amylase. Since ∝-amylase activity is stabilized by the presence of Ca^{2+}, the role of Ca^{2+} in sustaining plastidic ∝-amylase activity and its pH optima was also examined. The presence of $CaCl_2$ in chloroplast-disruption

Table 3. The intercellular distribution of a- and fi-amylase activity in the leaves of 10-d old red light grown pearl millet seedlings. The substrate specificity was used to distinguish between a- and fi-amylase.

	Amylase activity (nkat/mg protein)	
	fi-amylase	α-amylase
M cells	21.6	4.8
M cytosol	18.1	0.3
M chloroplast	0	5.0
B strands	0	2.8
B chloroplast	0	2.7
B cytosol	0	0
B (NF)	0	0
B [D (DW)]	0	0

* DW-distilled water; NF-Norflurazon.

Table 4. Specific activity of plastidic α-amylase in mesophyll and bundle sheath chloroplasts. The specific activity was expressed using different parameters.

	α-amylase activity				pkat/10 chloroplasts	
	nkat/mg protein		nkat/mg chl			
Mesophyll chloroplast	5.38	(100%)	25.5	(100%)	75	(100%)
Bundle sheath chloroplasts	2.65	(49.2%)	38.7	(151.8%)	132	(176%)

mixture increased plastidic ∝-amylase activity with maximal activity at 10 mM $CaCl_2$ (Fig. 21A). However, addition of EDTA to the above mixture, even in presence of $CaCl_2$, drastically reduced plastidic ∝-amylase activity (Fig. 21B). Similar results were also obtained when the plastidic fractions were dialyzed against EDTA, which completely inactivated plastidic ∝-amylase. The inclusion of $CaCl_2$ in the medium also protected plastidic ∝-amylases against the denaturation after heat treatment at 70°C (Table 5). The studies of pH optima of plastidic ∝-amylase revealed that pH optima is at 6.2, which is in contrast with cytosolic β-amylase activity localized at 4.6. ∝-amylase isolated from both M and B showed a similar pH optima (Fig. 22).

The presence of ∝-amylase in leaf was also supported by its capacity to renature after SDS-PAGE. The extracts of seed, leaf and B strands were separated by SDS-PAGE and subsequently SDS was exchanged by incubating gel in Triton X-100. On staining the gel for ∝-amylase activity, a clear band was visualized with a Rf value of 0.325 (Fig. 23). Though in leaf as well as in seeds several cytosolic and chloroplastic ∝-amylase isozymes exists after renaturation only a single band of ∝-amylase was visualized. The molecular weight of ∝-amylase polypeptide was 46kD (Fig. 45).

4.3 GRADIENT OF PHOTOSTIMULATION

In monocot leaf, a gradient of cells with differing maturity exists by virtue of a basal meristem. Since these cells may respond differentially to light, we have investigated light-regulated changes in amylase activity along the leaf length. The primary leaf which emerges first, was excised from 7-d old

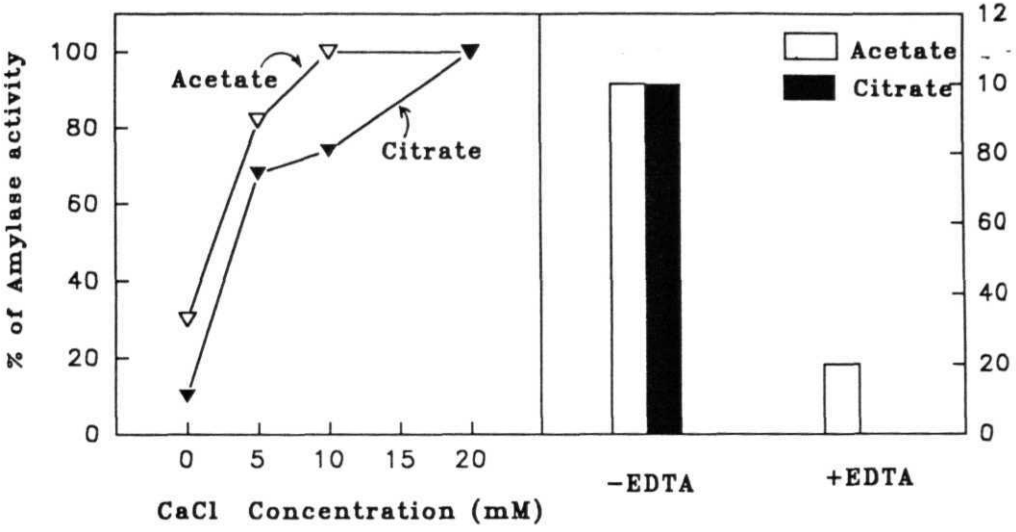

Figure 21. Effect of $CaCl_2$ on plastidic ∝-amylase activity.

A. ∝-amylase activity in acetate and citrate buffer, supplemented with different amounts of $CaCl_2$.

B. Effect of 10 mM EDTA on ∝-amylase se activity.

Table 5. Effect of $CaCl_2$ and EDTA on chloroplastic amylase activity in the leaves of 10-d old red light grown seedlings. The substrate specificity and sensitivity to heat treatment was used to confirm α-amylase activity.

Fraction	α-amylase activity (nKat)
M Chloroplasts	5.0
Chloroplastic fraction + 10 mM $CaCl_2$ + 10 min at 70°C	4.6
Boiled enzyme with out $CaCl_2$	0
After dialysis against 5mM EDTA	
-$CaCl_2$	0
+$CaCl_2$ (M)	0
+$CaCl_2$ (B)	0

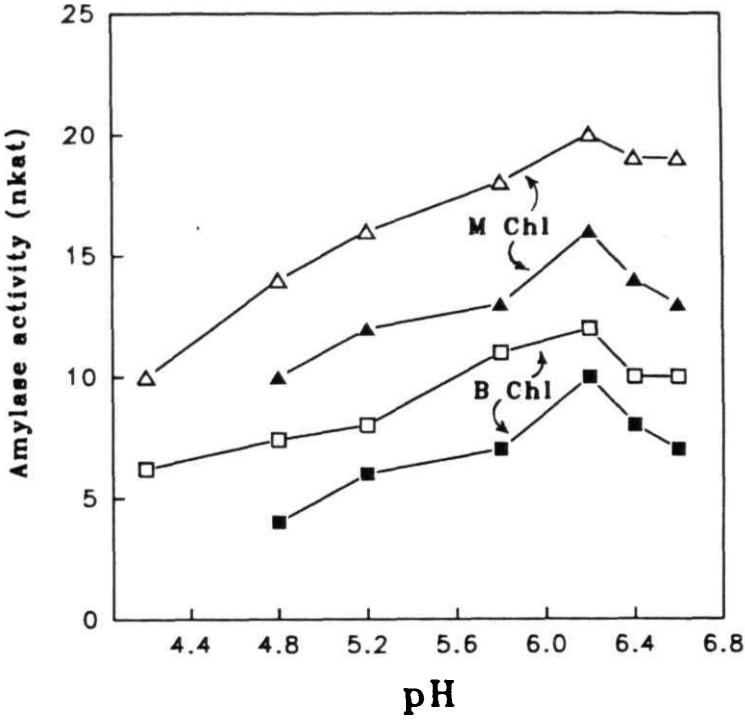

Figure 22. pH optima for plastidic α-amylase in pearl millet leaves.
The buffers used were Na-acetate (pH 4.2 to 6.6, A ; D)/ Na-citrate (pH 4.2 to 6.6, ▲ ; •).
Amylase activity in mesophyll chloroplasts (Δ , ▲) and bundle sheath chloroplast (□ , ■).

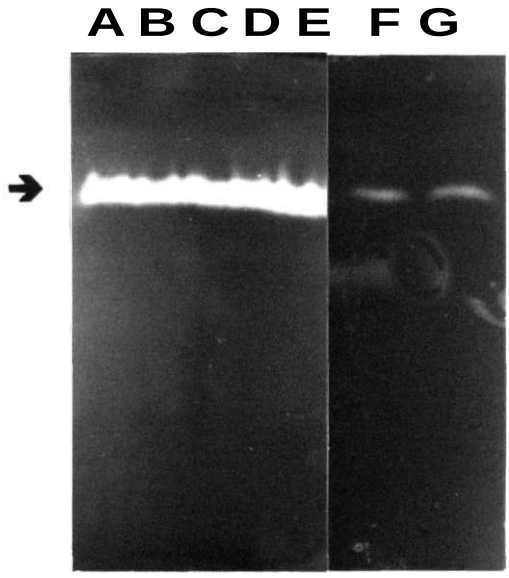

Figure 23. Renaturation of denatured α-amylase after SDS PAGE. Leaf and bundle sheath extracts were subjected to SDS PAGE and after electrophoresis SDS was exchanged with Triton X-100, followed by the detection of amylolytic activity. The amylolytic activity was detected using amylose as a substrate.
A-E. Seed
G. Leaf
H. Bundle sheath

seedlings. The length of the leaf at a given time point was dependent on growth conditions: in 7-d old seedling, the leaf was 8 cm long in light-(DW)-grown seedlings, and 6 cm long in dark-(DW)-grown or NF-treated seedlings. The leaf was dissected into 1 cm segments successively from the base to the tip, and amylase activity was analyzed in these individual segments.

The analysis of chlorophyll in developing pearl millet leaves shows that total chlorophyll increases from base to tip of the leaf (Fig. 24B). Similarly, the protein content also increased from the base to the leaf tip. However, in light-(DW)-grown seedlings, total protein content was more compared to other seedlings as leaf was longer in length (Fig. 24A).

4.3.1 Amylase activity along leaf axis

The analysis of amylase activity along the leaf axis showed that in dark-grown leaves, basal segments possess low amylase activity, which increases towards the leaf tip. On the other hand, in light-grown leaves, the amylase distribution was dependent on the position of the segment in the leaf. The maximal photostimulation of amylase activity was observed in the 2nd segment from the base of the leaf. A comparison of amylase activity in individual segments (Fig. 25) shows that in 2nd segment, light stimulates amylase activity by 15-fold. In subsequent leaf segments, the magnitude of photostimulation of amylase activity declined towards the tip of the leaf (Fig. 25).

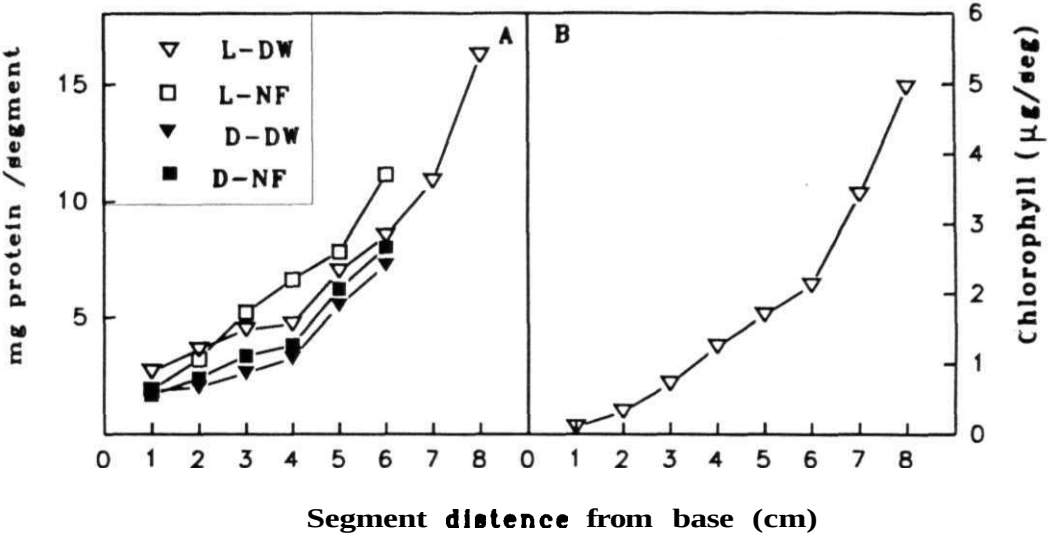

Figure 24. The content of protein and chlorophyll in different segments of 7-d leaf.
Seedlings were grown in distilled water (DW) (v , ▼) or Norflurazon (NF) (□ , ■) from the time of sowing, either in continuous red light (▽, D) or in darkness (▼, ■)•
A. Protein.
B. Total chlorophyll.

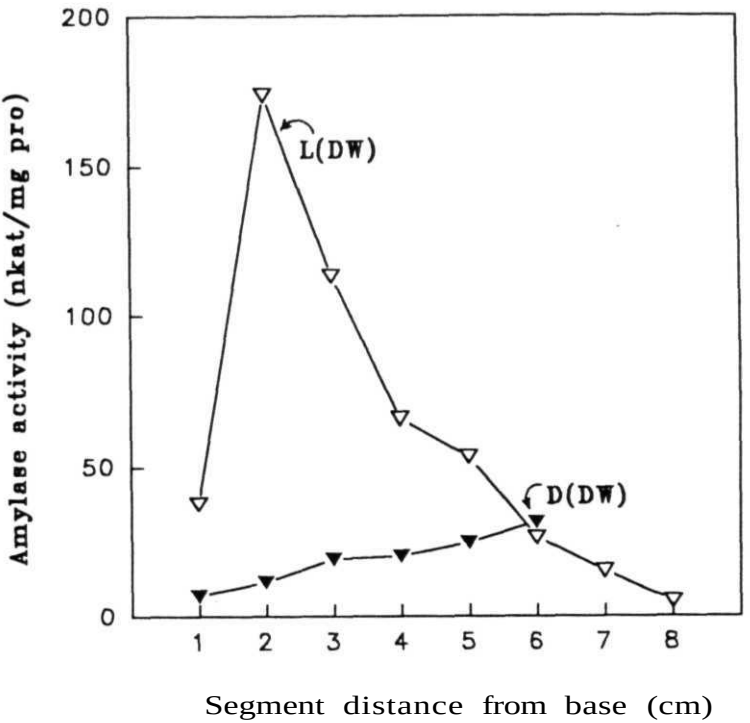

Figure 25. Relative photostimulation of amylase in different segments (1 cm) of leaf.
The light grown leaf of 7-d old seedlings (v) was 8 cm long while the leaf in darkness (▼) was 6 cm long. The segments are numbered from the base (segment 1) to the tip of the leaf.

The hypothesis that the observed photostimulation gradient of amylase activity results because of gradient of photosensitivity in leaf cells in responding to light with respect to amylase induction, was examined by transferring dark-grown seedlings to light (Fig. 26). Similar to the seedlings grown in continuous light, in seedlings, transferred to light photostimulation of amylase is also maximally seen in 2nd segment from base. In other segments, towards the tip, particularly from 3-6, the level of amylase activity was less than in the dark control. It is evident that within a short period of 12 h, the gradient of amylase distribution is altered from a gradual increase towards tip which is typical of dark-grown leaf to a gradient showing maximal amylase activity being in the segments proximal to the leaf base (Fig. 26).

4.3.2 Distribution of ∝- and *ft* -amylase activity along the leaf axis

Since in pearl millet amylase activity comprises of ∝- and β-amylase, the effect of light on photostimulation of ∝- and β-amylase was also examined. Fig. 27 shows that the gradient of photostimulation of amylase activity largely corresponds to the gradient of β-amylase activity. Photostimulation of β-amylase was predominant in the section proximal to the base and it gradually decreased towards the tip. Likewise, in dark-grown seedlings β-amylase activity increased towards the tip (Fig. 27), showing higher β-amylase activity in apical segments.

The level of β-amylase isozyme in different segments of leaf corresponded clearly with β-amylase activity gradient observed under light and darkness. In light-grown seedlings, distribution of P-amylase isozymes shows

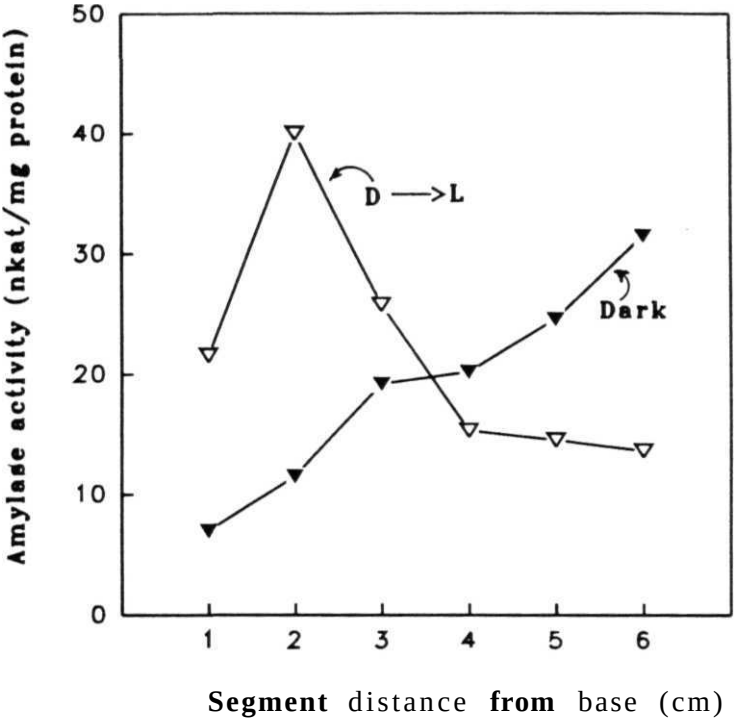

Figure 26. Photostimulation of amylase activity along with leaf length. Seedlings grown 6½ days in continuous darkness were transferred to light for 12 h (v). Control seedlings (7-d) were grown under continuous darkness (♥).

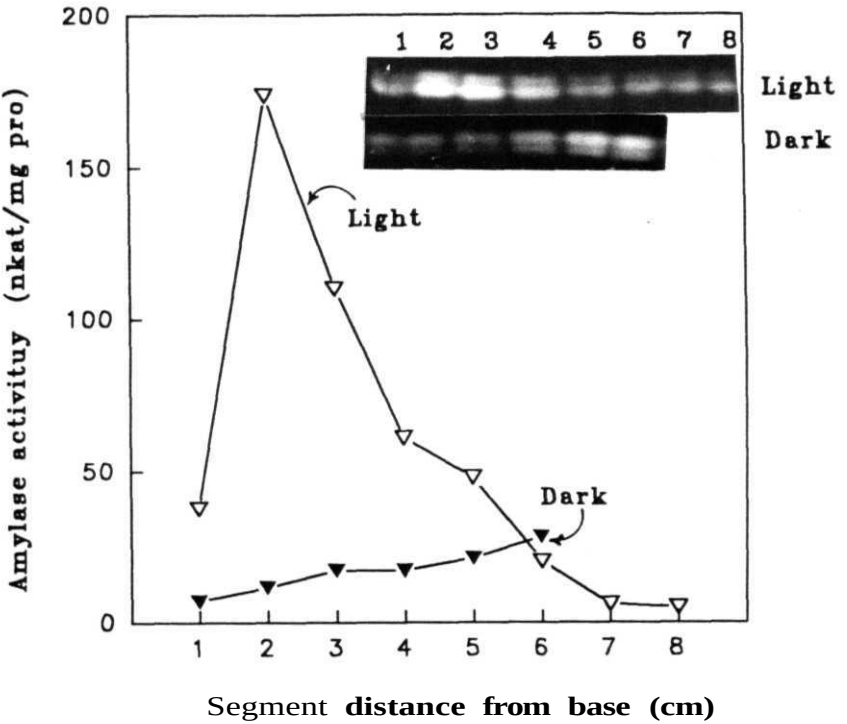

Figure 27. Photostimulation of β-amylase activity in the different sections (1 cm) of first leaf of 7-d old seedlings.
The length of leaf in light and dark grown seedlings was 8 cm and 6 cm respectively. The segments are numbered from the base (segment 1) to the tip of the leaf. The inset shows the level of β-amylase isozymes in different segments of light and in dark grown leaves.

a gradient similar to distribution of β-amylase activity in leaf segments, with the level β-amylase isozyme being maximal in the second segment of the leaf (Fig. 27, inset).

In contrast, in light-grown seedlings, ∝-amylase activity appeared only in the third segment from the base of the leaf and increased gradually towards the tip of the expanding leaf. In dark-grown seedlings too, ∝-amylase activity appeared only in the third segment onwards and slightly increased towards the tip. Photostimulation of ∝-amylase activity in leaf segment was apparent only from 4th segment of light-grown leaves (Fig. 28). Similar to the distribution of ∝-amylase activity of leaf, plastidic ∝-amylase isozyme was detected from the 3rd segment onwards and its level increased towards the tip of the leaf (Fig. 28, inset). Though the cytosolic ∝-amylase was also present in pearl millet leaves, due to its extremely low activity its gradient could not be determined.

Since exposure of seedlings to light also induces chloroplast biogenesis, dependence of photostimulation of amylase on chloroplast biogenesis was investigated by using NF-grown seedlings. Fig. 29A shows that the magnitude of photostimulation in NF-treated seedlings in light is less than that in the controls; however NF-treatment did not affect the qualitative pattern of the gradient. Both activity of amylase as well as isozyme pattern of β-amylase showing maximum photosensitivity in the second segment, subsequently it declined towards tip. Similarly, in dark-grown seedlings too, NF-treatment did not influence the pattern of amylase distribution. It is pertinent to note that in NF-treated seedlings, while the β-amylase isozyme

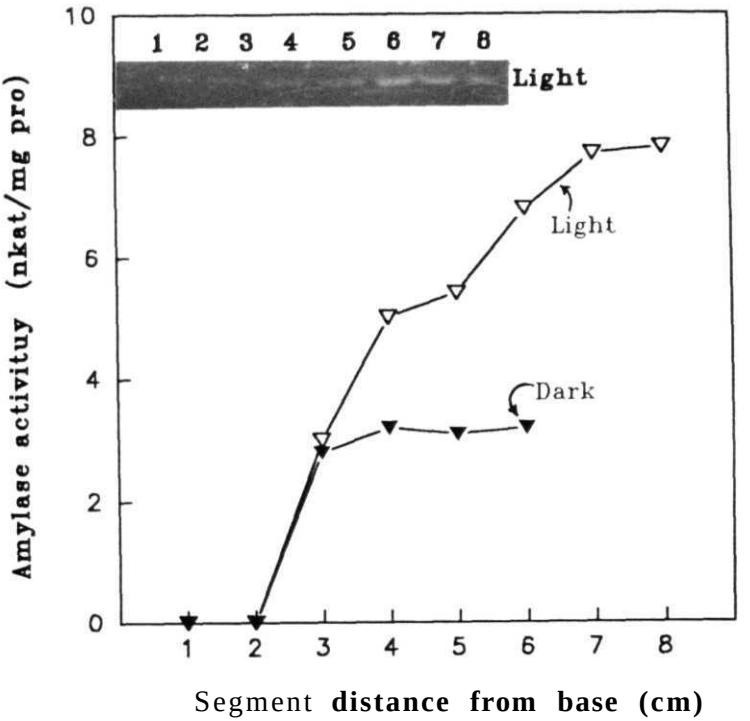

Figure 28. Photostimulation of ∝-amylase activity in the different segments (1 cm) of leaf of 7-d old pearl millet seedlings.
The length of leaf in light and dark grown seedlings was 8 cm and 6 cm respectively. The segments are numbered from the base (segment 1) to the tip of the leaf. The inset shows the plastidic ∝-amylase isoforms in different segments of light grown leaves. The plastidic ∝-amylase activity was totally absent in dark grown seedlings.

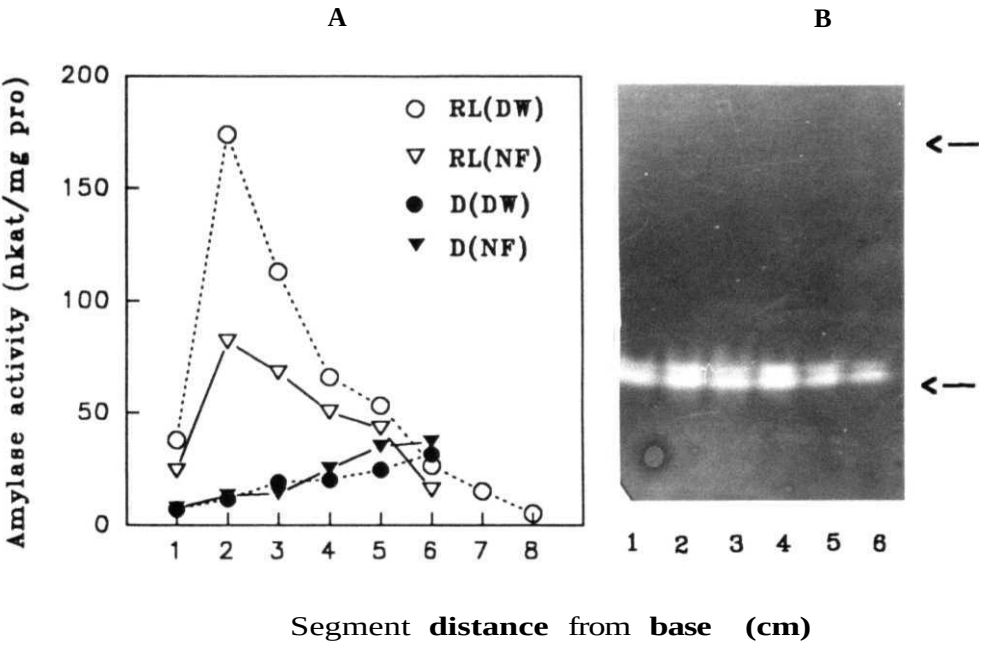

Figure 29. Effect of Norflurazon on the photostimulation of amylase activity in the different sections (1 cm) of leaf of 7-d old pearl millet seedlings.

Seedlings were grown in Norflurazon (NF) from the time of sowing in continuous red light (▽) or in darkness (▼). The control seedlings were grown in distilled water (DW) (Dotted lines) in red light (o) or in darkness (•).

A. NF effect on amylase activity.

B. β-amylase isozymes in different segments of Norflurazon treated leaves. The plastidic ∝-amylase band was totally absent in light (NF) grown seedlings (upper arrow).

profile was similar to that of the control seedlings, the chloroplastic ∝-amylase band was totally absent (Fig. 29B).

4.3.3 Temporal and spatial dependence of photostimulation gradient of β-amylase

The analysis of amylase activity along leaf axis clearly reveals that total amylase activity in pearl millet leaves, i.e., p-amylase activity, shows a gradient of photostimulation which is localized in the segment proximal to the leaf base. Since in the monocot leaf, basal meristems continuously contribute new cells, the position of each cell with reference to the base constantly changes during the course of leaf development. In view of continual changes in cellular position, and increase in amylase photoinduction with age, we examined whether the light sensitivity of 2nd segment near the base is dependent on temporal age of leaf, or on spatial localization of segment by analyzing the pattern of gradient during the period of leaf development. The photostimulation gradient was analyzed in primary leaf every d right from 3-d to 10-d after sowing. The length of pearl millet leaf during the period increased with its age from 3 to 10 cm.

Fig. 30 shows the gradient of p-amylase in light-grown pearl millet leaves of different age. It is evident that during initiation of leaf development, i.e., on of 3rd and 4th d, though p-amylase activity is photostimulated, the activity increases towards the tip. However, from 5th d onwards the maximal pbotostimulation of p-amylase is always noticed in 2nd segment from leaf base irrespective of leaf age, indicating that the photostimulation of p-amylase

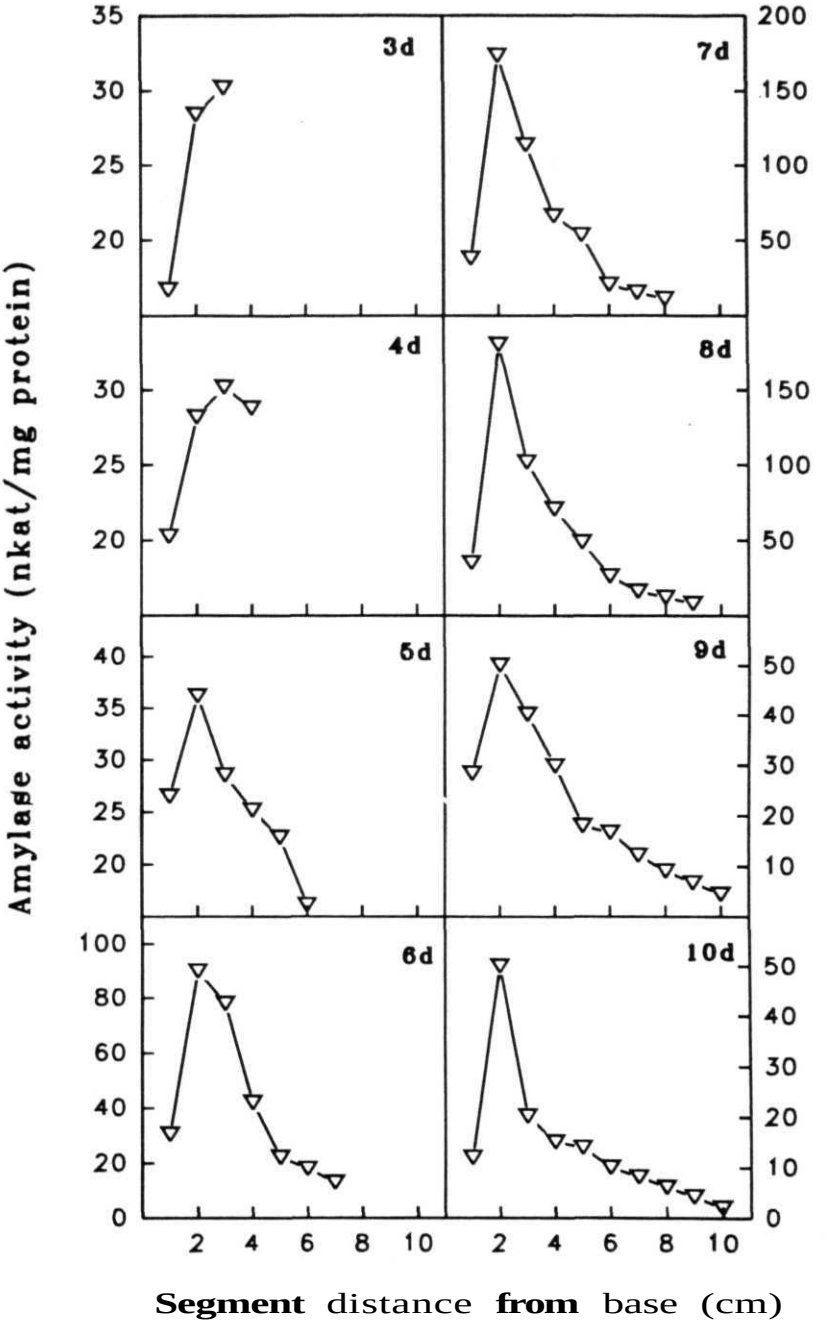

Figure 30. Photostimulation of amylase activity gradient 3d to lOd old light (DW) grown seedlings. Segments are numbered from base (1) to tip of the leaf.

induction is strictly determined by cellular position. Although during 5-10 d amylase activity increases up to 8th d and then it declines irrespective of total β-amylase activity of leaf, after 5th d maximum amylase activity is present in the segment proximal to leaf base (Fig. 30).

The data were also plotted by numbering segments from the tip for comparision (Fig. 31). It is evident that since the photostimulation gradient is determined by proximity to basal meristematic cells, the segment showing maximal photostimulation is continually shifted to right with age, therefore a numbering a segments from base gives a better graphical representation of the data (cf. Fig. 30).

In monocot leaf, the position of the cell is constantly shifted in relation to base, as the cell moves on to a more mature state. It is evident that maximal photostimulation of amylase is seen in the 2nd segment from the base, which, with continued cell division at the base would move up yielding place to new cells. The influence of the above cell movement, which constantly changes cellular position, on acquired amylase activity was analyzed by determining amylase activity in same set of cells in the leaf. It is self-evident that if the tip is used as a reference of position, the cellular position of a given set of cells remain essentially constant as newly generated cells at base acquire a new segment number, with reference to the tip. In this way, the fate of acquired amylase activity in a given segment of leaf could be visualized during the period of the leaf growth. The data presented in Fig. 32 clearly highlight that during the period of photosensitivity, i.e., 5-10 d from sowing, at the time of its appearance, a given segment has low activity of amylase, which is

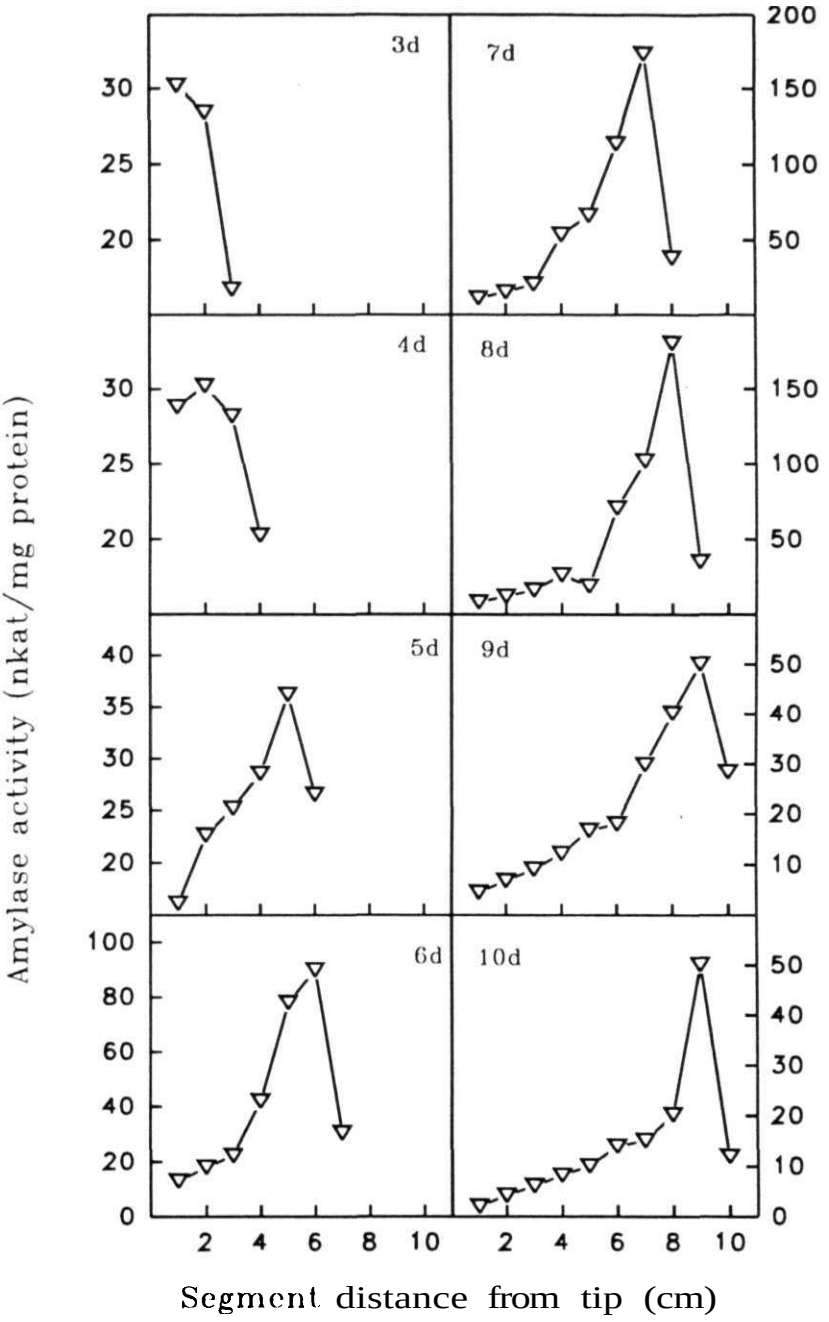

Figure 31. Photostimulation of amylase activity gradient 3d to 10d old 1(DW) grown seedlings. The values at top left or right hand corner of figure refers to the age of seedlings. Segments are numbered from tip (1) to base of the leaf.

Figure 32. Photostimulation of amylase activity in different segments of first leaf of pearl millet seedlings.
Amylase activity was analyzed in segments excised from primary leaves of 3d to lOd old L(DW) grown seedlings. The segments are numbered from tip (1) to base of the leaf. The amylase activity in Fig. shows the activity of the same segment during the leaf development. Values on top right or left corner of each figure refers to the position of segment with respect to top.

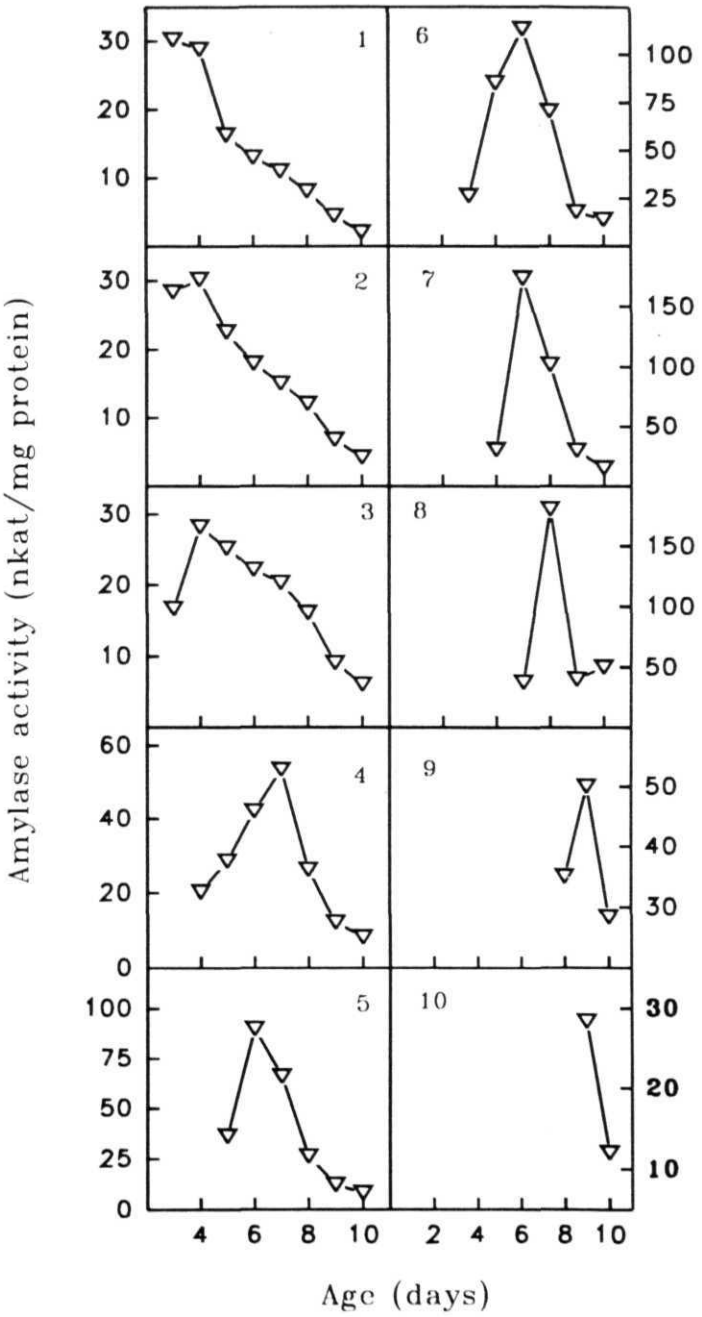
Amylase activity (nkat/mg protein)
1
2
3
4
5
6
7
8
9
10
30
20
10
60
40
0
100
75
50
25
150
4
6
8
10
2
Age (days)

Figure 33. Photostimulation of amylase activity in different segments of first leaf of pearl millet seedlings. Amylase activity was analyzed in segments excised from primary leaves of 3d to 10d old L(DW) grown seedlings. Segments are numbered from base (1) to tip of the leaf. The amylase activity profile in figure shows the enzyme activity at the same position with respect to leaf base. Values on top right or left corner of each figure refers to the position of segment with respect to base.

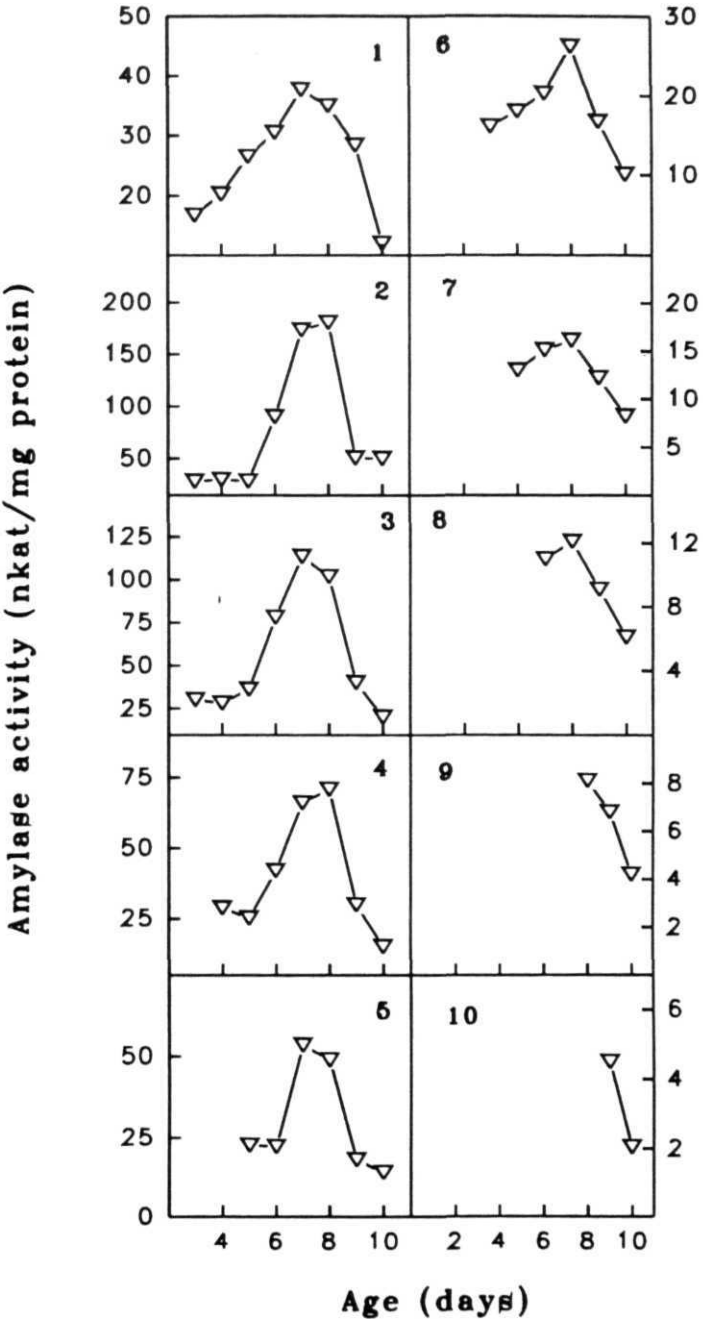
Amylase activity (nkat/mg protein)
Age (days)
1
2
3
4
5
6
7
8
9
10

photostimulated by the time the segment acquires a distance of about 1 cm from the base of leaf. The magnitude of photostimulation however depends on the age of the seedling i.e., 7-8 d old seedlings shows maximal stimulation. Thereafter, on further shift in position with respect to base, the magnitude of photostimulated amylase activity gradually declined as the segment became older and distant from leaf base. Segments 1-3 which are generated during early leaf development also show a decline in amylase activity with increasing age (Fig. 32).

The effect of cellular position (in relation to the base of the leaf) on photostimulation of amylase was examined by plotting the activity of amylase in leaf segments numbered with reference to the base at different ages (Fig. 33). It is evident that with increase in age amylase activity increased in the basal segment which declined after 7 d from sowing. While the segments 2-4 do not show changes during 3-5 d, they show a significant increase in amylase activity from the 6th d onwards, and then the magnitude of photoinduction declines after the 8th d from sowing. Such an increase in amylase activity with age was seen in other (5-8) segments too. In general segments 2-5 were the most photoresponsive. The magnitude of photostimulation increased from the 5th to 8th d and then declined in all segments (Fig. 32).

4.4 IMMUNOLOGICAL ANALYSIS

While it is likely that the photoinduction of α-amylase and β-amylase observed in the present study results via de novo synthesis, it is equally possible that the enzymes are activated from a zymogen form, or that the

observed activity changes arise from changes in the levels of activators/inactivators. Immunochemical methods were therefore used to establish the mode of induction of amylases. Antibodies were used to examine several parameters such as quantification of particular enzyme, contribution of individual enzyme to total activity, whether the abundant enzyme masks the presence of minor enzyme activity, and also to investigate the *in vivo* rates of synthesis of enzyme proteins under influence of light.

4.4.1 Characterization of antiserum

The immune sera used in present investigation were raised against α-amylases (α_1- and α_2-) and β-amylases purified from endosperm of maize seeds (Subbarao, 1992). The polyclonal antibodies were obtained against α_1-amylases, α_2-amylases, and p-amylase from maize, and were demonstrated to be monospecific by a variety of techniques (Subbarao, 1992). The prefix against each antiserum denotes the antigen obtained from maize seed against which that antiserum was obtained. The monospecificity of individual amylase antiserum from maize, namely, α_1-, α_2-, and p-antiserum against pearl millet amylase was first ascertained by Ouchterlony double immunodiffusion reaction. The polyclonal antibodies raised against maize amylase cross-reacted with pearl millet α-amylase and p-amylase with high affinity (Fig. 34). In contrast, pearl millet p-amylase did not cross-react with mustard p-antiserum (data not shown) and, also, mustard p-amylase did not cross-react with maize β-antiserum (Fig. 34C).

Figure 34. Ouchterlony double diffusion analysis of pearl millet **amylases** against maize **antiserums.**
The central wells were filled with respective maize antisera, while peripheral wells were filled with pearl millet sample. The letters in parentheses indicate the position of antigen wells.

A. **Immunodiffusion** against α_1- **antiserum** from maize.
Root (1), Coleoptile (2), **leaf(3)**, Seed (4).

B. **Immunodiffusion** against α_2-antiserum from maize.
Root (1), Coleoptile (2), leaf (3), Seed amylase(4).

C. **Immunodiffusion** against β-antiserum from maize.
Maize β-**amylase** (1), Seed (2), Leaf (3), Coleoptile (4), Root (5), Mustard β-amylase (6).

D. **Immunodiffusion** of different subcellular **fractions/cell** extracts against α_1-**antiserum.**
Mesophyll **chloroplasts** (1)/ Bundle Sheath Strands (2), Bundle Sheath Chloroplasts (3), Mesophyll cytosol (4, 5), Blank well (6).

E. **Immunodiffusion** of denatured pearl millet crude extracts against /3-antiserum.
Native protein (2), Denatured protein (3), Blank wells (1,4).

F. Staining of precipitin line for β-**amylase** activity, after immunodiffusion against /3-antiserum.
Seed (1, 2, 4), Leaf (3).

G. Staining of precipitin line for /3-amylase activity after immunodiffusion against /3-antiserum.
Leaf(l), Chloroplast (2), Bundle sheath strands (3), Blank well (4).

H. Staining of precipitin line for α-**amylase** activity after immunodiffusion against α_1 -antiserum.
Leaf (1), Chloroplasts (3), Seed (2,4).

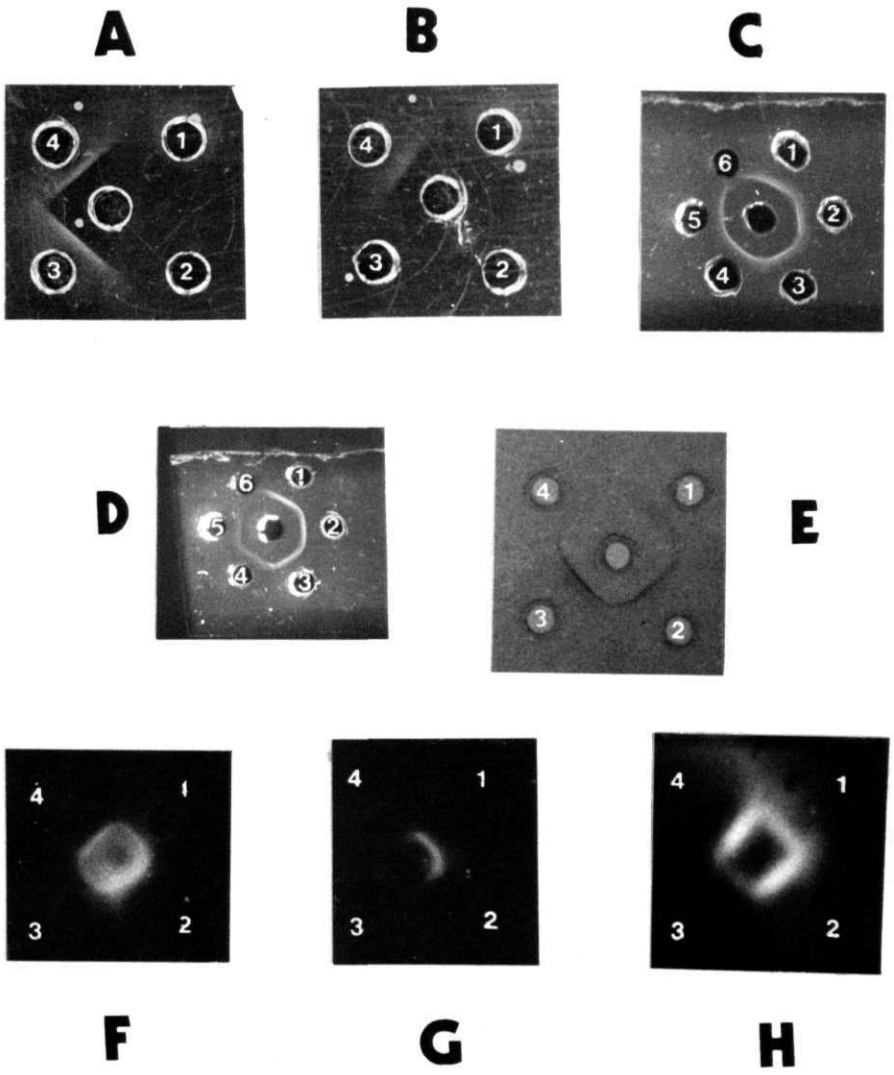
A
B
C
D
E
F
G
H

The double diffusion analysis revealed that like maize, pearl millet seedlings also possess P, α_1 and α_2, the three amylolytic proteins, (Subbarao, 1992) viz., one p-amylase and two α-amylases, which were named as α_1 and α_2 amylases. In pearl millet seedlings, the antigenic activity of α_1-amylase was present in leaf and seed (Fig. 34A), whereas p-amylase protein was present in all parts of seedlings. By contrast, the α_2-amylases antigenic activity was detectable only in the pearl millet seed (Fig. 34B). There was no significant difference in antigenic identity between pure maize amylase and pearl millet amylases (data not shown). The precipitin line against maize p-amylase completely fused with the precipitin line against the p-amylase present in different organs of pearl millet seedling (Fig. 34C). A complete fusion of precipitin line was obtained with maize antigen demonstrating a high degree of antigenic identity between maize and pearl millet amylases.

In pearl millet seedlings, the denatured amylases obtained after boiling the sample in SDS-PAGE buffer, retained its cross-reactivity against p-serum and was antigenically identical to native enzyme. The double diffusion analysis showed a precipitin arc emphasizing full identity between these samples (Fig. 34E).

The precipitin line generated between amylase and the respective antiserum retained its enzymatic activity and could be stained for amylase activity. The p-amylase activity was detected as colorless zones against the dark blue background which intensely stained with iodine (Fig. 34F,G). The α-amylase activity in the immunocomplex was also visualized as the colorless zone on dark blue background with iodine staining (Fig. 34H).

In view of the low amount of antigen cross-reacting with α_1-antiserum, total cytosolic α-amylase from leaf was enriched by immuno-precipitation with α_1-antiserum and subjected to Ouchterlony double diffusion against α_1-antiserum. A single precipitin line was visualized against α_1-anti serum. However, a similar immunoprecipitate with α_2 antiserum did not show any amylase antigen (data not shown). The isolated chloroplastic amylase showed a precipitin line only with α_1 antiserum (Fig. 34D).

4.4.1.1 Western blotting

The existence of antigens in pearl millet seedling cross-reacting with antiserums raised against maize α_1- and β-amylase was also checked by western blotting. The chloroplastic and cytosolic extracts from leaf containing α- and β- amylase, were first electrophoresed under non-denaturing conditions and then were electroblotted on nitrocellulose sheets. The nitrocellulose sheets were then probed with α_1 and β-antiamylase serum. The Rf values of the α- and p-amylase bands on the nitrocellulose sheet after western blotting corresponded with respective isoforms as shown earlier by substrate specific staining of gels (see Fig. 16 and 20). On electrophoresing plastidic amylase, a single band was visualized against α_1-antiserum on a position corresponding with Rf value of plastidic amylase, i.e., 0.21. (Fig. 35A) Similarly, cytosolic amylase too showed a single band of amylase against p-antiserum with Rf value 0.72 (Fig. 35B).

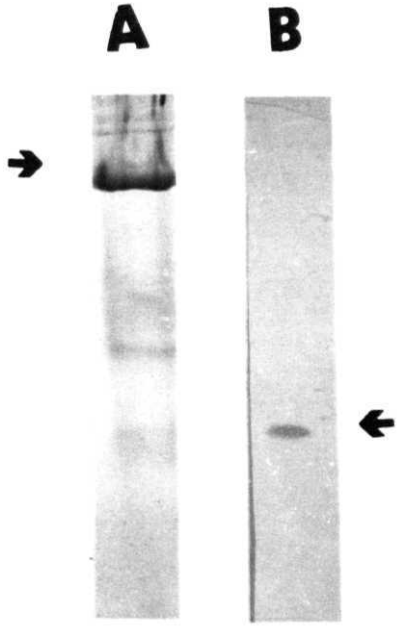

Figure 35. Western blotting of chloroplastic and cytosolic amylases.
A. Chloroplastic α-amylase (probed by α_1-antiserum)
b. Cytosolic β-amylase (probed by β-antiserum) .

4.4.1.2 Immunoelectrophoresis

The specificity of cross-reaction of leaf ∝-amylase with $\propto_1$-antiserum and the possibility of the existence of multiple antigens was analyzed by immunoelectrophoresis. The plastidic ∝-amylase on immunoelectrophoresis revealed a single precipitin arc, after diffusion against $\propto_1$-antiserum confirming that $\propto_1$-antiserum recognized a leaf amylase. Similarly, seed ∝-amylase too showed only single precipitin arc against $\propto_1$-antiserum (Fig. 36).

4.4.2 Quantification of amylase protein level

4.4.2.1 Immunoprecipitation

While the experiments outlined above confirmed the existence of ∝-amylase activity in chloroplasts, at the same time the presence of a low amount of β-amylase activity in chloroplast can not be excluded. In order to ascertain whether plastidic amylase also includes B-amylase, immunoprecipitation of plastidic components was carried out using $\propto_1$,$\propto_2$, and β-antiserum. Table 6 shows that while $\propto_2$ and B-antisera are ineffective to immunoprecipitate plastidic amylase activity, only $\propto_1$-antiserum is able to immunoprecipitate it, both from mesophyll as well as bundle sheath chloroplasts.

4.4.2.2 Immunotitration

In cereals, particularly in barley, it has been shown that increase in B-amylase activity during seed germination results from activation of preformed zymogen, i.e. an inactive β-amylase protein. The existence of inactive ß-

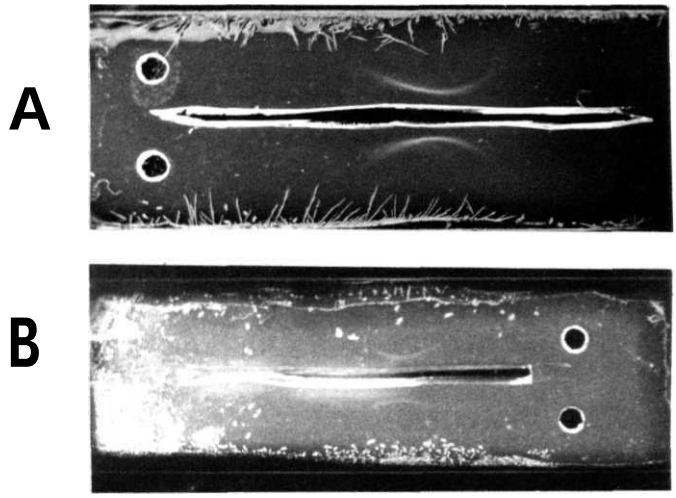

Figure 36. Immunoelectrophoresis of seed and plastidic α-amylase against α_1-antiserum.
A. Seed
B. Mesophyll chloroplasts

Table 6. **Immunoprecipitation** of **chloroplastic α-amylase** with α_1 α_2 and fi-antiserums. Plastidic **amylase** (15 nkat) isolated from 8 d old red light grown seedling was incubated with 15 **µl** of α_1-, α_2-, or fi-antisera. The supernatent was assayed for amylase activity after precipitation of immune complex.

Serum used	Organ	**α-amylase** activity (nkat)
	Mesophyll	
Control		14.80
Non **immune** serum		14.90
α_1**-antiserum**		0
α_2**-antiserum**		14.85
8-antiserum		14.75
	Bundle sheath	
Control		14.60
Non immune serum		14.25
a,-antiserum		0
α_2**-antiserum**		14.20
8-antiserum		14.90

amylase molecules in leaf extract was ascertained by immunotitration of p-amylase from dark-grown and light-grown leaves. The crude supernatants from light and dark-grown pearl millet seedlings were immunotitrated against a constant amount of p-antiserum. The residual p-amylase activity in the supernatant was determined after the removal of antigen-antibody complex. Fig. 37 shows that though varying amounts of p-amylase activity were incubated with a fixed amount of antisera, the immuno-inhibition magnitude was constant. Since the profile of immunoinhibition and the subsequent escape of p-amylase activity of both dark and light-grown seedlings were similar, this indicates that equal p-amylase activity present in the dark/light-grown leaves represents equal amounts of p-amylase protein.

4.4.2.3 Single radial immunodiffusion

4.4.2.3.1 Chloroplastic amylase

Single radial immunodiffusion is often employed to quantify the amount of an antigen from a crude supernatant as the amount of an unknown antigen can be calculated after obtaining a standard curve against purified antigen (Fig. 4). It was demonstrated by using SR1D that irrespective of light treatment, equal amylase activity in different samples shows precipitin rings of equal diameters (Fig. 38C). The plastidic ∝-amylase from mesophyll and bundle sheath, with equal amylolytic activity on SRID revealed precipitin rings of the same diameter (Fig. 38B). However, at the same time, loading equal amounts of total protein on SRID, the diameter of rings were proportional to the amount of p-amylase activity in respective extracts (Fig. 38D).

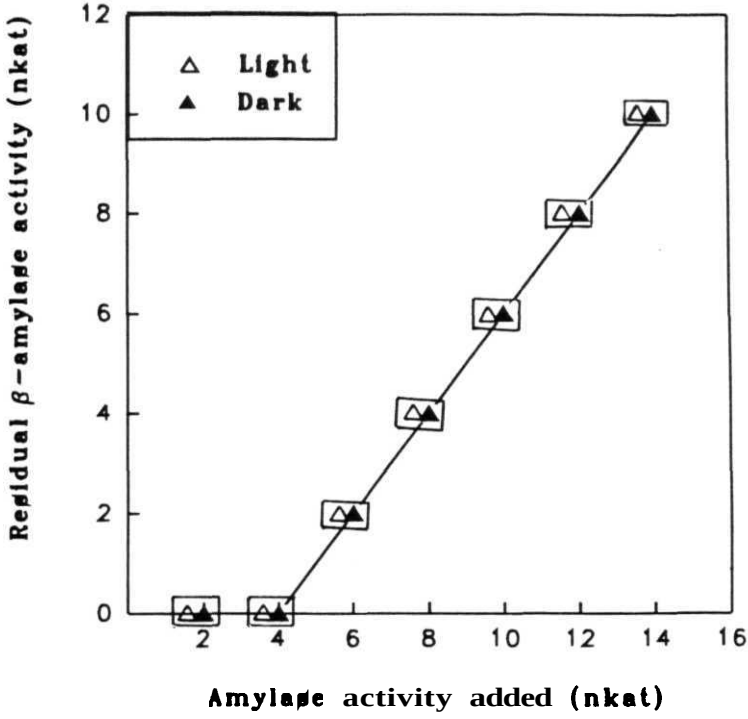

Figure 37. Immunotitration of β-amylase in crude extracts isolated from pearl millet seedlings.
A fixed volume of antiserum (1/32 dilution) was mixed with increasing amount of amylase enzyme (2-14 nkat) prepared from the pearl millet leaves grown either in light (△) or in darkness (A). The resultant mixture was incubated at 4 C for 12 h and immunocomplex was separated by centrifugation at 10,000*g* after absorption on *Staphylococcus aureus* cell walls. The supernatant was assayed for β-amylase activity.

Figure 38. Single radial immunodiffusion.

A. Quantification of /3-amylase protein at different time points by SRID.
The supernatants obtained from leaves of 2-10 day old RL grown seedlings were concentrated and aliquots containing equal amount of proteins were loaded in the wells, punched on agar gel containing 1% (v/v) maize /3-antiserum. The numbers on the top of wells indicate the age of seedlings. The absolute amount of /3-amylase protein was quantified by using a standard curve presented in Fig 3.

B. Detection of α-amylase in pearl millet chloroplasts.
Pearl millet mesophyll and bundle sheath chloroplastic extracts were subjected to SRID. Equal amylase activity was loaded in wells in agar gel containing 1%(v/v) α_1-anti serum.
a. Mesophyll chloroplast, b. Bundle sheath chloroplasts.

C. On loading equal /3-amylase activity from light and dark grown leaves, resulted in rings of equal diameter against /3-antiserum, showing equivalence in /3-amylase protein level.
(a) 7-d L (b) 7-d D.

D. Detection of /3-amylase in light and dark grown leaves.
Concentrated crude extract from 7-d and 8-d old pearl millet seedlings was subjected to SRID in agar gel containing /3-antiserum. Equal protein from 8-d old pearl millet seedlings was loaded in the serial wells made in agarose gel
(a) 8-d dark; (b) 7½-d dark —> 12h light;
(c) 7-d dark —> 24h light; (d) 8-d light.

A

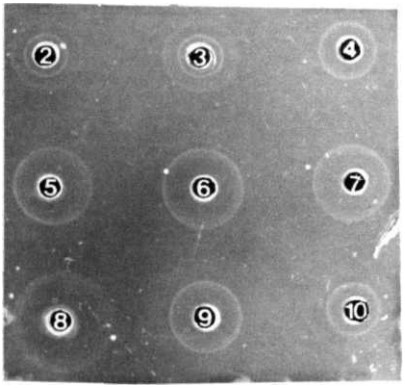

B

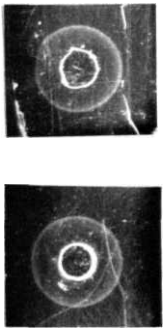

C

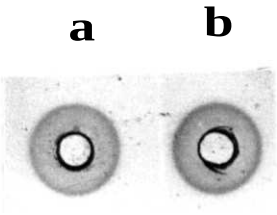

D

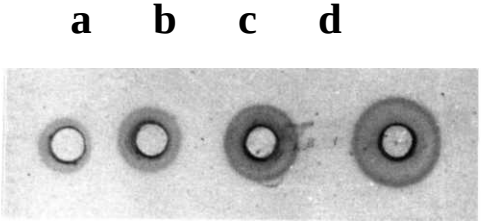

The increase in β-amylase activity in pearl millet leaves directly correlated with a corresponding increase in the amount of β-amylase protein (Fig. 38A). In an analogous fashion to β-amylase activity, β-amylase antigen could not be detected in leaves of 3-d light-grown leaves, but appeared in dark-grown leaves only on the 7th d from sowing (Fig. 39A). The peak of β-amylase protein level and subsequent decline in light-grown seedlings were identical with β-amylase activity profile.

The light-mediated increase in ∝-amylase activity and the increase in protein level of ∝-amylase were parallel at all time points from sowing. The level of ∝-amylase declined in darkness after the 8th d, but in light it remained at a constant level after the 8th d (Fig. 39B).

The observed effect of brief RL and FR on β-amylase activity is also reflected a change in the level of antigenic protein (Fig. 40). The red-light-induced increase in β-amylase activity (Fig. 8) was paralleled by an increase in level of β-amylase protein. Moreover, reversal of RL effect by FR, bringing about a change in level of β-amylase activity, also decreased β-amylase protein (Fig. 40).

4.4.2.3.2 Distribution of amylase along leaf length

The distribution of β-amylase as well as ∝-amylase proteins was measured along the leaf length in 7-d old leaves. The primary leaf was dissected into one cm segments, numbered sequentially from base, and the amounts of ∝- and β-amylase protein were determined by SRID. In light-grown

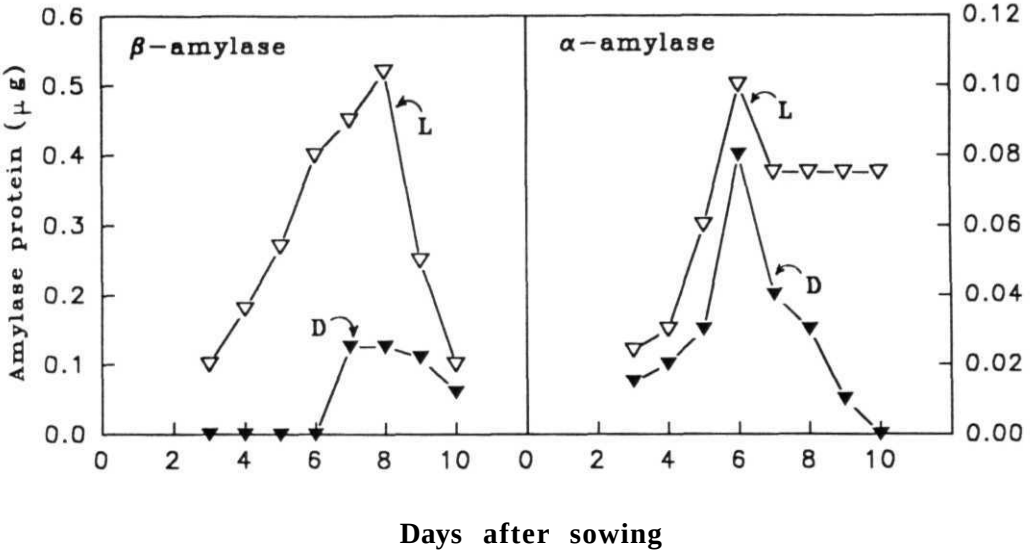

Figure 39. Quantitative estimation of ∝-amylase and β-amylase protein amount by SRID in pearl millet leaves.
Seedlings were grown either in continuous red light (▽) or in darkness (▼) from the time of sowing.
A. β-amylase B. ∝-amylase.

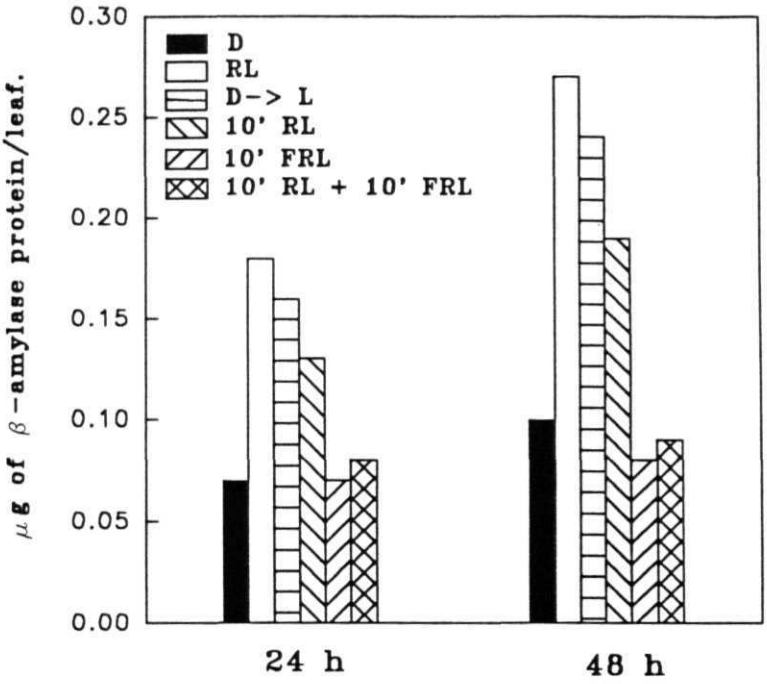

Figure 40. Effect of 10 min red light (RL) and far-red light (FRL) on β-amylase protein in pearl millet seedlings. Seedlings grown in darkness for 3-d were subjected to 10 min light pulses separated by an interval of 8 h in darkness. The amylase activity was measured at 4-d and 5-d after sowing. The control seedlings were grown in continuous darkness or light.

leaves, the amount of β-amylase protein was higher in the second segment of the leaf and thereafter it declined from 3rd to 8th segment, whereas in dark-grown leaves β-amylase protein level increased towards the tip (Fig. 41A). Similarly ∝-amylase protein too gradually increased from 3rd to 8th segment in light and dark leaves and could not be detected in the first two segments. The level of ∝-amylase protein was much lower in dark-grown leaves than in light-grown leaves (Fig. 41B).

4.5 *IN VIVO* LABELLING OF AMYLASES

The distribution of amylase along the leaf axis clearly shows that both ∝- and β-amylase protein levels distinctly vary along the leaf length, and the amount of respective protein at a given position is determined by light and darkness. The *in vivo* level of a protein is however a sum total of its turnover which includes a relationship between its synthesis and degradation. Since increase in protein level as assayed by SRID may arise by increased rates of de novo synthesis and/or by decrease in degradation, the distinction between these two processes was made by determining the rate of in *vivo* labelling of respective enzymes in leaf segments. The rate of *in vivo* synthesis of ∝- and β-amylase was determined by incubating leaf segments/cells in S-methionine and immunoprecipitating radiolabelled amylases.

Incorporation of ^{35}S-methionine in each segment was followed by loading equal amounts of radioactivity in proteins to gel for electrophoresis. The separation of radiolabelled proteins on gel yielded a pattern with respect to the spatial position of the segment of the leaf from where the segment was derived.

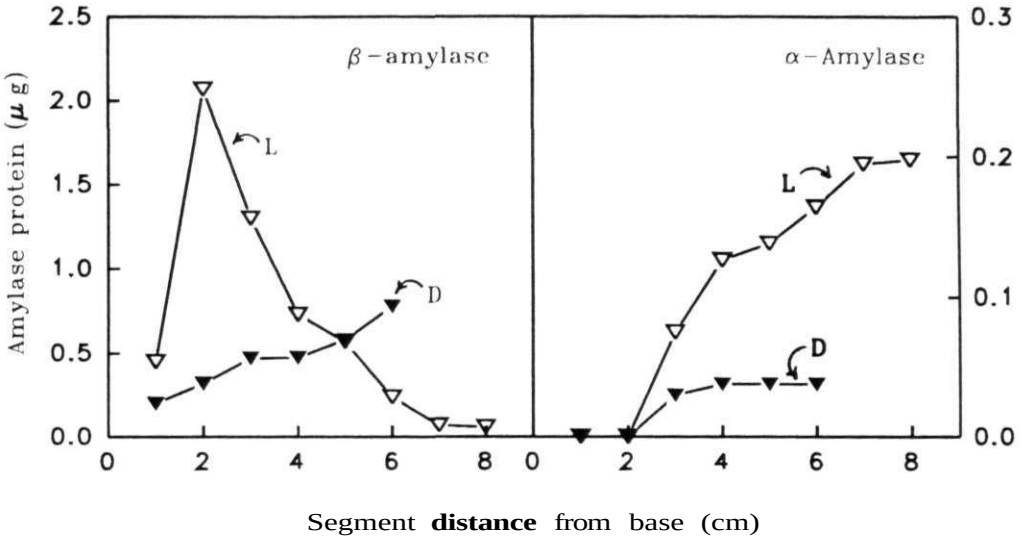

Figure 41. Relative photostimulation of β-amylase and ∝-amylase protein in the different segments (1 cm) of leaf of 7-d old seedlings. The segment are numbered from base (1) to tip of the leaf. A. β-amylase ; B. ∝-amylase.

4.5.1 β-Amylase synthesis

In light-grown seedlings, p-amylase synthesis was largely restricted to the basal 2 segments and declined in the successive segments. The fluorogram after immunoprcipitation of newly synthesized p-amylase revealed a high level of p-amylase synthesis only in first two segments with a low level in third segment. Probably in other segments also, p-amylase synthesis could be visualized, by increasing the amount of radioactivity loaded on the gel. Maximum synthesis of p-amylase was observed in the first segment (Fig. 42). In comparison to light-grown leaves the rate of synthesis was low in dark-grown leaves, however in dark too, the rates of p-amylase synthesis declined towards the tip of leaf. It is evident that the high level of synthesis in basal segment in leaf contributes to observed photostimulation of p-amylase which contributes to the obtained profile of p-amylase protein level.

4.5.2 ∝-Amylase synthesis

The ***in*** *vivo* labelling revealed a gradient of ∝-amylase synthesis that was similar to p-amylase, where ∝-amylase synthesis was most prominently localized in basal segments of leaf and it progressively declined towards the tip (Fig. 43). The effect of light in ∝-amylase synthesis was discernible in the basal segment, but in other segments, the rate of synthesis of ∝-amylase in light was slightly less than that in dark-grown seedlings. The profile of ∝-amylase synthesis was dramatically opposite to ∝-amylase activity distribution in leaf both in light and darkness, as in basal segments actively synthesizing ∝-amylase, no ∝-amylase protein level could be detected by SRID (Fig. 40).

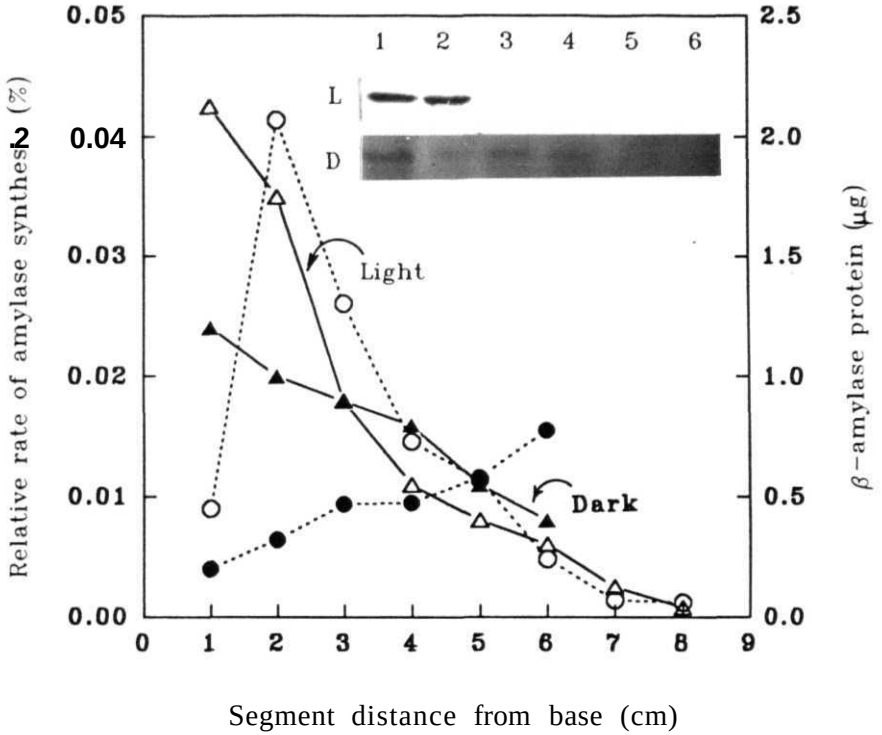

Figure 42. Rate of β-amylase synthesis (solid line) in different segment of 7-d old seedling leaf.
The individual segments from light (△) and dark (▲) grown leaves were pulse labeled with ^{35}S methionine and rate of synthesis was determined as described in materials and methods. The dotted line shows β-amylase protein level in segments. The fluorogram for light and dark grown leaves are exposed for 30 and 45 days respectively. The inset shows the level of β-amylase synthesis in different segments of light and dark grown leaves.

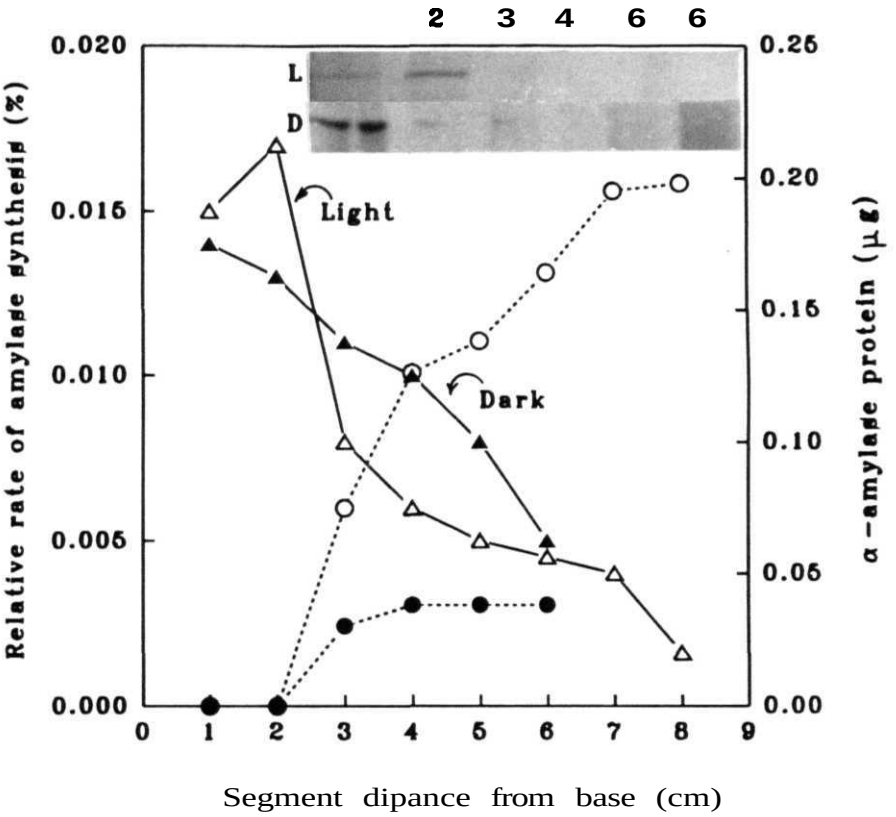

Figure 43. Rate of ∝-amylase synthesis (solid line) in different segment of 7-d old seedling leaf.

The individual segments from light (a) and dark (A) grown leaves were pulse labeled with S methionine and rate of synthesis was determined as described in materials and methods. The dotted line shows ∝-amylase protein level in segment. The fluorogram for light and dark grown leaves are exposed for 30 and 45 days respectively. The inset shows the level of ∝-amylase synthesis in different segments of light and dark grown leaves.

Figure 44 . **Demonstration** of **α-amylase** synthesis in bundle sheath strands by **immunoprecipitation** with **α_1-antiserum.**

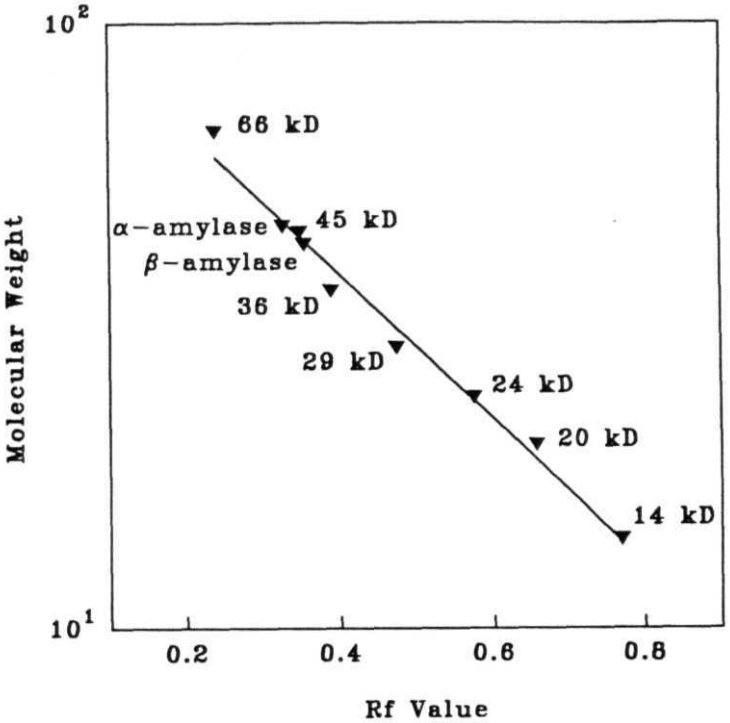

Figure 45. Determination of molecular weight of oc-amylase and β-amylase by SDS-PAGE.
The labeled samples were immunoprecipitated with B- and α_1-antiserum respectively and were separated on SDS-PAGE. The molecular weights were determined against a standard curve obtained by running standards of known molecular weight under identical conditions. The molecular weight of the standards used were a) α-lactalbumin (14.2 kD); b) Trypsin inhibitor (20.1 kD); c) Trypsinogen (24 kD); d) Carbonic anhydrase from bovine erythrocytes (29 kD); e) Glyceraldehyde-3-phosphate dehydrogenase from rabbit muscle (36 kD); Egg albumin (45 kD); Albumin bovine (66 kD).

4.5.3 ∝-Amylase synthesis in bundle sheath strands

In view of presence of a plastidic ∝-amylase in bundle sheath strands, isolated bundle sheath strands were radiolabeLled with ^{35}S-methionine for 3 h. The radiolabelled proteins were immunoprecipitated with $\propto_1$- and β-antiserums. In B strands, pulse labelling and subsequent immunoprecipitation with $\propto_1$-antiserum showed only a single immunoprecipitated band (Fig. 44). However, using β- and $\propto_2$-amylase antisera no synthesis of β-amylase or $\propto_2$-amylase proteins could be seen in B cells.

4.5.4 Molecular weight determination

The molecular weight of radiolabelled peptide of ∝- and also β-amylase was determined by SDS-PAGE with protein molecular weight markers. The molecular weights of p-amylase and ∝-amylase are 43 kD and 46 kD respectively (Fig. 45). The molecular weight from BSS had similar molecular weight to total ∝-amylase, i.e., 46 kD.

4.6 PHOSPHORYLASES

Phosphorylase activity of pearl millet leaf was measured by both biosynthetic and degradative pathways. In the biosynthetic pathway, glucose-1-phosphate is polymerized by coupling to amylose, releasing inorganic phosphate leading to starch formation. Phosphorylase activity was measured either by estimating the formation of starch or by estimating the amount of inorganic phosphate released in the biosynthetic pathway. In the degradative pathway, in the presence of inorganic phosphate, starch was sequentially

degraded to release glucose-1-phosphate whose level was enzymatically estimated.

4.6.1 Optimization of biosynthetic assay

The optimum pH at which phosphorylase activity could be maximally extracted was estimated by homogenizing pearl millet leaves in 50 mM Tris-HC1 buffer (pH 6-9). Fig. 46A shows that maximum extraction of phosphorylase activity was obtained at pH 8. The extraction of phosphorylase was dependent on molarity of homogenization buffer. On using Tris-HCl buffer of different concentration (30-150 mM) to extract the phosphorylase activity, maximal activity was obtained with a 50 mM buffer (Fig. 46B).

The temperature optimum for assaying phosphorylase was determined by conducting assays at different temperatures ranging from 20°C to 60°C; the maximal activity was detected at 30°C (Fig. 46C). Similarly, the optimum pH for estimation of phosphorylase activity was measured by assaying it in different buffers at various pH and maximal activity was obtained in Na-citrate buffer at pH 5 (Fig. 46D).

4.6.1.1 Inhibitors

In view of the presence of amylase and phosphatase in crude supernatants which could influence the employed biosynthetic assay for phosphorylase activity, where amylase can influence substrate level by degrading starch and phosphatase may release phosphate from glucose-1-Phosphate. Therefore the activity of phosphorylase was estimated in presence

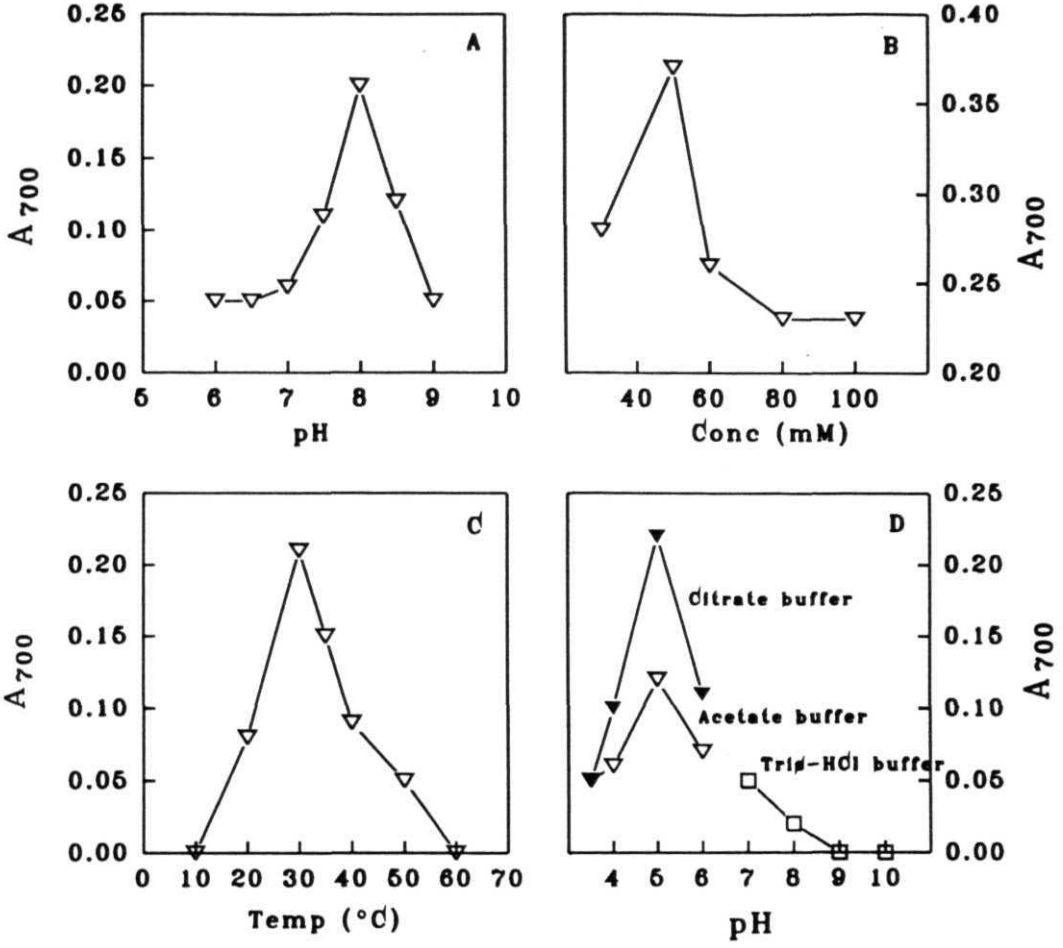

Figure 46. Optimization of phosphorylase extraction and assay in biosynthetic pathway.
A- Extraction of phosphorylase activity in Tris-HCl (50 mM) buffer of varying pH.
B- Effect of varying concentration of Tris-HCl pH 8.0 on assay of phosphorylase.
C- Temperature optima of phosphorylase activity.
D- pH optima of phosphorylase activity assay. Buffer used were Na-citrate (▼), Na-acetate (▽), Tris-HCl (D).

of appropriate inhibitors to block interference of these enzymes. In this investigation $HgCl_2$, ammonium molybdate and NaF (Porter, 1953; Pan *et al.*, 1988) were used to inhibit phosphatases and amylase activity in the assay mixture. The effectiveness of these inhibitors in their respective action was estimated by establishing proper controls.

The data presented in Table 7 and Fig. 47 show that the phosphorylase activity as measured by release of inorganic phosphate can be optimized by including inhibitors of amylase and phosphatase action. It is evident from the absence of glucose-1-phosphate from the assay mixture that no phosphate is released; however in the presence of glucose-1-phosphate, but absence of starch, a slight release of phosphate is evident indicating a possible action of phosphatases. It is also evident that on inclusion of NaF, $Hgcl_2$ and molybdate, the release of phosphate via phosphorylase action is maximal.

4.6.2 Optimization of degradative assay

In the degradative pathway, in the presence of inorganic phosphate and amylose, phosphorylase catalyzes the breakdown of starch to yield glucose-1-phosphate. The increase in the amount of glucose-1-phosphate was measured by using a coupled assay with phosphoglucomutase and glucose-6-phosphate dehydrogenase enzymes where reduction of NADP is measured at 340 nm. The pH optima for extraction of phosphorylase activity from leaves was determined as described earlier by homogenizing leaves in 50 mM Tris-Hcl buffer, with pH ranging from 6 to 9 and it was found that optimum pH for extraction was 7.5 (Fig. 48A). Similarly, temperature optima of phosphorylase activity was

Table 7. Estimation of **phosphorylase** activity estimation in biosynthetic pathway. NaF, **$HgCl_2$** and ammonium molybdate were used as inhibitors to inhibit **α-amylase** and phosphatases activity.

	Starch	G-1-P	Inhibitors	A_{700}
a	+	+	-inhibitors	0.19
b	+		-do-	0
c	-	+	-do-	0.05
d	+	+	-NaF	0.32
e	+	+	**-$HgCl_2$**	**0.23**
f	+	+	-Ammonium molybdate	0.21
g	+	+	+Inhibitors	0.28

* G-l-P - Glucose 1 phosphate; NaF- 20 mM; $HgCl_2$- 0.2 mM; $(NH_4)_6Mo_7O_{24}.4H_2O$- 0.1 mM.

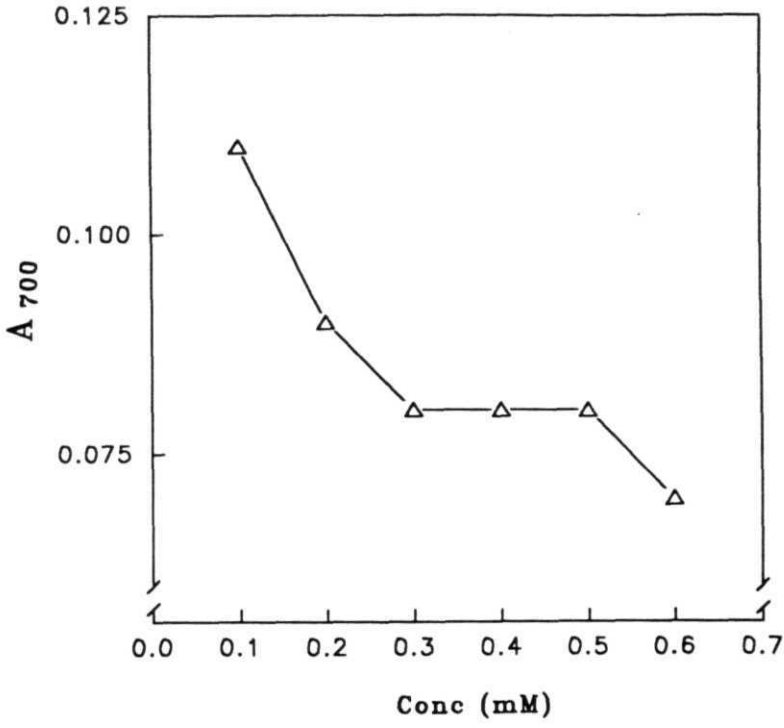

Figure 47. Effect of ammonium molybdate on phosphorylase activity. Phosphorylase activity was measured in presence of varying concentration of ammonium molybdate (0.1-0.6mM) in assay mixture.

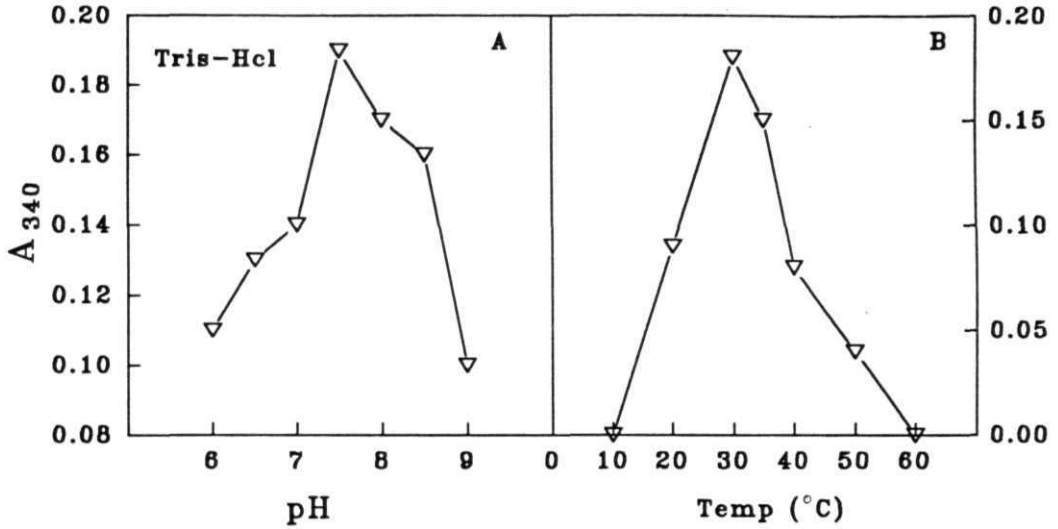

Figure 48. Optimization of phosphorylase activity in pH.
B- Temperature optima of phosphorylase activity.

estimated by assaying in different temperatures, and was found to be 30°C (Fig. 48B).

4.6.3 Distribution of phosphorylase activity in seedlings

The distribution of phosphorylase activity was measured in different organs of 7-d old pearl millet seedlings. The enzyme activity did not significantly deviate between light and dark grown seedlings. The maximal phosphorylase activity was detected in the primary leaf of seedlings, while the coleoptile too possessed nearly equal activity. In comparison to the above organs the activity in seeds and roots was nearly 3 times less (Fig. 49).

4.6.4 Time course of phosphorylase increase

In pearl millet seedlings grown under continuous red light and darkness, phosphorylase activity was measured in the biosynthetic pathway. Fig. 50A shows that both in light and darkness, phosphorylase activity in leaf increased with age attaining a peak at the 8 d after sowing. At all time points phosphorylase activity in light-grown seedlings was less than that in the dark controls (Fig. 50A).

The estimation of phosphorylase activity in the biosynthetic pathway however, was besieged with insensitivity and fluctuations, as the above assay essentially determines release of inorganic phosphate, the precise measurement of which is difficult due to contamination arising from extraneous sources. Moreover, phosphorylase primarily functions **as a** degradative enzyme *in vivo*. In view of this, in further experiments,

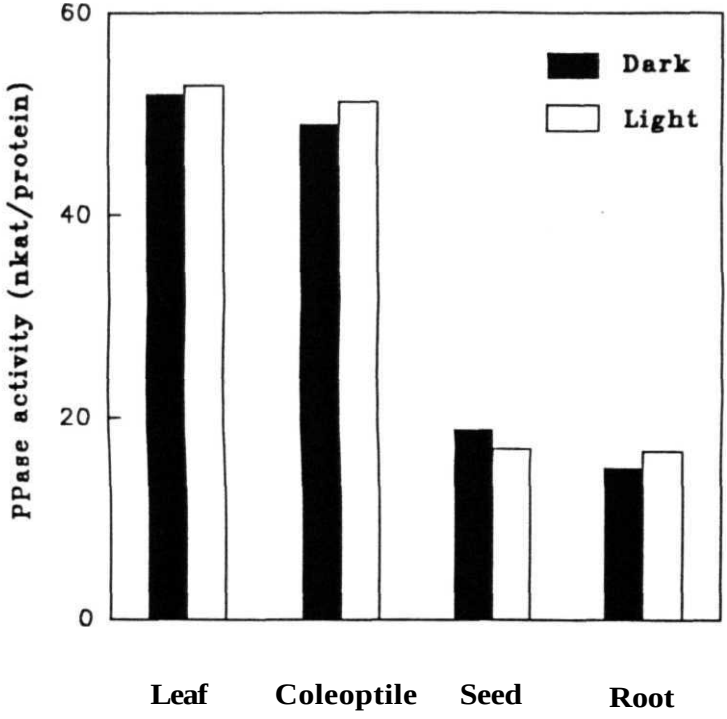

Figure 49. Phosphorylase activity in different organs of pearl millet seedlings.

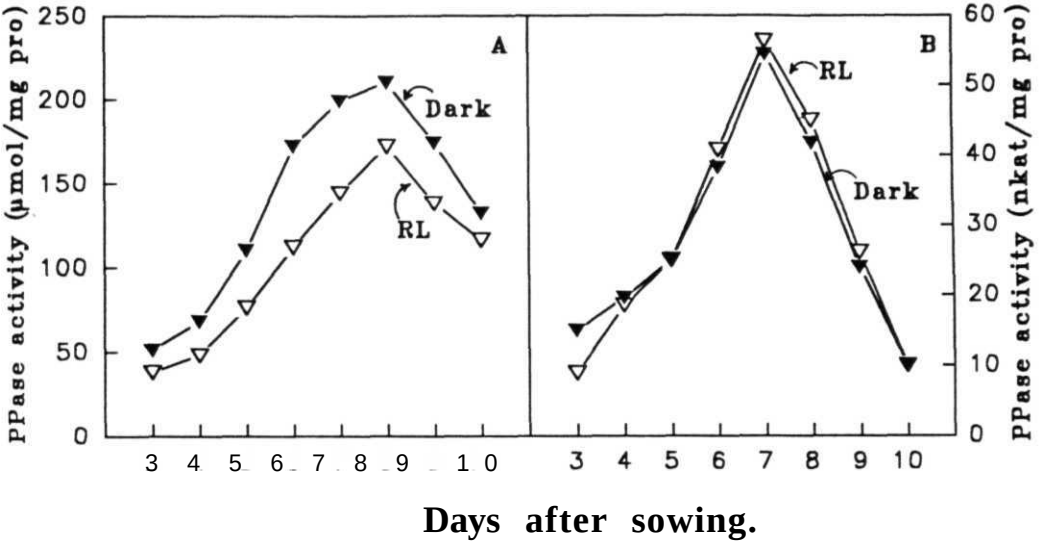

Figure 50. Time course of phosphorylase activity in the leaves of pearl millet seedlings.

Seedlings were grown in continuous red light (v) or in continuous dark (▼). Phosphorylase activity was assayed in biosynthetic pathway (A), and in degradative pathway (B).

phosphorylase activity was assayed by the degradative pathway, and the biosynthetic pathway was used only to visualize isoforms of phosphorylase after PAGE.

Fig. 50B, shows the time course of change in phosphorylase activity measured by a degradative assay at different time points in light and darkness. It is evident that in pearl millet leaves there is no apparent photostimulation of phosphorylase activity. No significant difference in phosphorylase activity was observed between light and dark-grown seedlings. In either case phosphorylase activity increased with age reaching a peak at the 7 d after sowing and then it declined.

4.6.5 Effect of norflurazon on time course of phosphorylase activity

Since phosphorylase is reported to exist as both plastidic and cytosolic isoforms, the interrelationship of chloroplast biogenesis with phosphorylase activity in light and dark-grown seedlings was determined by treating seedlings with Norflurazon. The application of NF to pearl millet seedlings led to an overall reduction in phosphorylase activity at all time points. Nevertheless, the time course of phosphorylase increase was qualitatively similar to DW-grown seedlings. There was no apparent difference in phosphorylase activity of NF-treated seedlings grown in light and darkness (Fig. 51).

4.6.6 Intercellular distribution of phosphorylase activity

In view of pearl millet being a C_4 plant, intercellular distribution of phosphorylase activity was probed in isolated mesophyll and B cells. Table 8

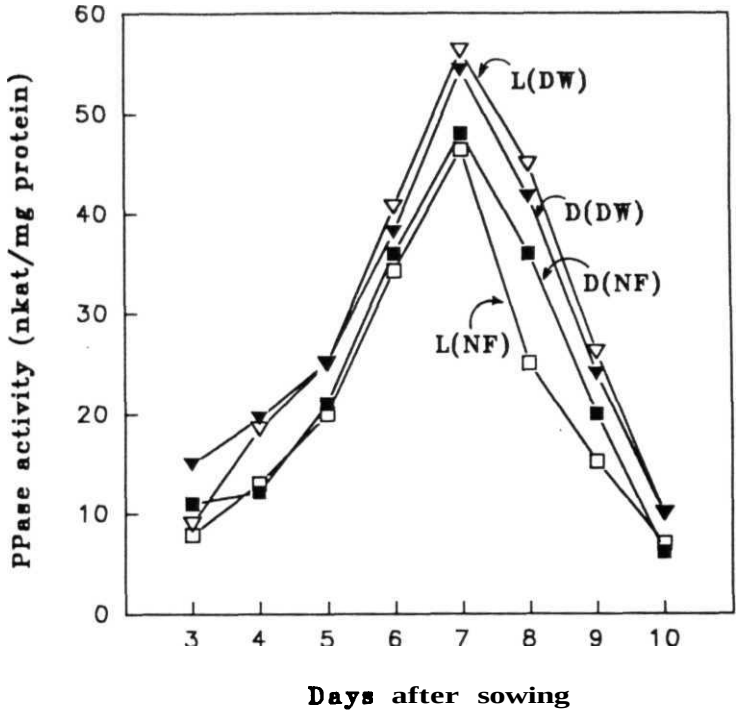

Figure 51. Time course of phosphorylase activity in leaves.
Seedlings were grown in presence of NF in continuous red light (□) or in darkness (•). The control seedlings were grown in distilled water (DW) in red light (▽) or in darkness (▼). Phosphorylase activity was measured via degradative pathway.

shows that in light-grown seedlings phosphorylase activity can be detected in both mesophyll and B cells.

The cell fractionation studies revealed that the phosphorylase activity present in the mesophyll cells is exclusively localized in cytosol. In isolated plastids from mesophyll, phosphorylase activity was nearly absent (Table 8). In contrast, in B cells, the entire phosphorylase activity was exclusively located in the chloroplasts (Table 8).

The estimation of phosphorylase activity in isolated B from DW and NF grown seedlings revealed that B strands possessed an equal amount of phosphorylase activity in both light and dark samples as well as NF-treated dark samples, but it was totally absent in L(NF)-grown seedlings (Table 9). The B phosphorylase activity did not depend on chloroplast biogenesis, as etioplasts isolated from B cells also possessed phosphorylase activity. It is apparent from this observation that unlike other plastidic proteins such as Rubisco and *cab*, the biosynthesis of plastidic phosphorylase is independent of differentiation of etioplasts and chloroplasts.

4.6.6.1 **Isozymes of phosphorylases**

The isozyme composition of phosphorylase was analyzed by non-denaturing polyacrylamide gel electrophoresis. The phosphorylase from light-grown leaves consists of two isozymes, migrating at Rf 0.24 and 0.28 respectively (Fig. 52A). These isozymes were also seen in leaves of seedlings

Table 8. Intercellular distribution of ohloroplastio and non chloroplastic **phosphorylase activity in the leaves of 8 day old red light grown pearl millet seedlings.**

Fraction	Phosphorylase activity nkat/mg protein
Homogenate	4 8.80
M Cytosol	31.80
M Chloroplasts	00.18
B **Homogenate**	2 0.50
B Chloroplasts	19.90

Table 9. Phosphorylase **activity in bundle sheath strands of 8 day old pearl millet seedlings.**

Fraction	Phosphorylase activity (nkat/mg protein)
L(DW)	20.50
L(NF)	0
D(NF)	19.82
D(DW)	21.00

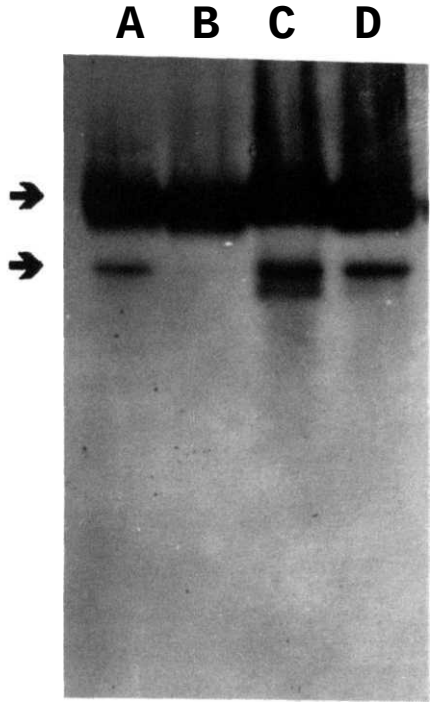

Figure 52. Isozymes of phosphorylase present in leaves of 7-d old seedlings.
Seedlings were grown in light or in darkness in presence of either DW or 0.4 mM NF. The crude extracts from leaves were electrophorsed in native PAGE. Phosphorylase isozymes were visualized by incubating gel in 1 % amylose solution and glucose-1-phosphate for 3 h at 35°C. At the end of incubation gel was stained with KI-I_2 solution. Starch synthesized by phosphorylases stained as clue band against light blue back ground, of the soluble starch permeated gel.
(A) RL (DW), (B) RL (NF), (C) D (DW), (D) D (NF).

grown under darkness; therefore the appearance of these isozymes was independent of light or darkness (Fig. 52A,C).

The possible localization of the above isozymes in the plastidic compartment was studied by growing seedlings in presence of NF (Fig. 52B,D). In dark-grown seedlings, Norflurazon had no effect on phosphorylase and both the isozymes of phosphorylase were expressed similarly to control (Fig. 52D). However, in light-grown seedlings NF treatment eliminated fast-migrating isozyme of phosphorylase (Fig. 52B). Since NF treatment of light-grown seedlings lead to degeneration of plastids, it is likely that phosphorylase isozyme which disappeared, having Rf 0.28, is localized in the chloroplast (Fig. 52B), and therefore the other isozyme (Rf 0.24) is likely to be located in the cytosol.

It has been shown that in pearl millet leaves both M and B possess phosphorylase activity, and both cell types were therefore analyzed for isozyme associated with them. The PAGE of M cells showed that phosphorylase activity consisted only of cytosolic phosphorylase (Fig. 53D,E) and no phosphorylase activity was detected in M chloroplast (Fig. 53B), whereas in B cells, the phosphorylase activity was reported only by fast-migrating plastidic isozyme (Fig. 53A,C). In B strands isolated from NF-treated light-grown fast-migrating plastidic isozyme was totally absent (Fig. 54D). This chloroplastic isozyme is specifically localized only in leaves and is absent in other organs of the seedling, like coleoptile, seed (Fig. 55) and root (data not shown).

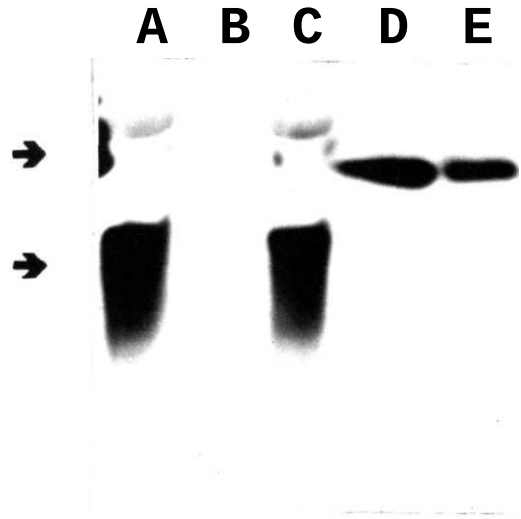

Figure 53. Distinction of chloroplastic and cytosolic phosphorylases in pearl millet seedlings.
Chloroplasts were isolated from mesophyll and bundle sheath strands. Purified intact chloroplasts were ruptured by osmotic shock, and after centrifugation, supernatants were subjected to native PAGE.
(A) Bundle sheath homogenate; (B) mesophyll chloroplasts; (C) Bundle sheath chloroplasts; (D) Mesophyll homogenate; (E) Mesophyll cytosol.

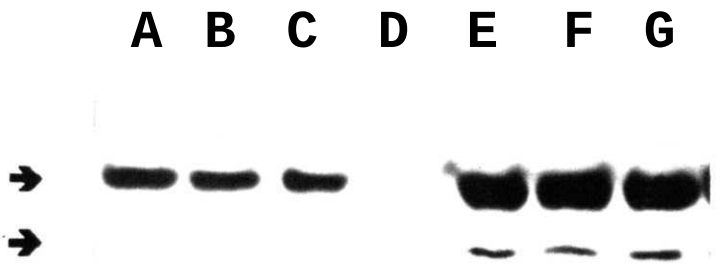

Figure 54. Electrophoretic analysis of phosphorylase isozymes, in different subcellular fractions.
Seedlings were grown either in dark or in red light with DW or Norflurazon solution. Different cell fractions were loaded on the gel.
Track (A) RL (DW) Mesophyll extract; Track (B) RL (NF) mesophyll extract; Track (C) RL (NF) Total extract; Track (D) RL (NF) Bundle sheath extract; Track (E) D (DW) Total extract; Track (F) D (NF) Total extract; Track (G) RL (DW) total extract.

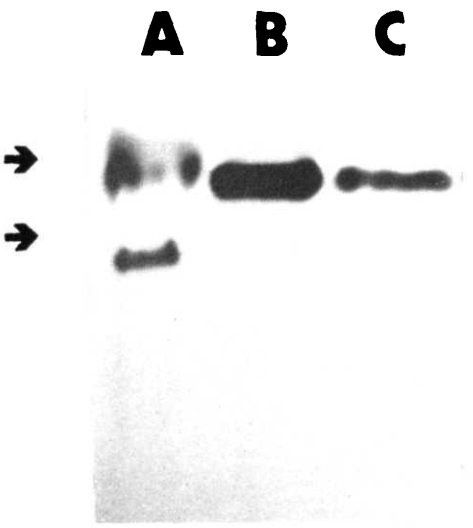

Figure 55. Phosphorylase isozymes in different organs of pearl millet seedlings.
Extracts from different organs were subjected to electrophoresis. Track (A) leaf extract, (B) coleoptile, (C) seed.

4.6.7 Phosphorylase gradient in leaves

In view of the distinctive localization of phosphorylase in two subcellular compartments, i.e., cytosol and chloroplast, and moreover, the cytosolic isozyme being in M cells and plastidic isozyme in the B, it is imperative that regulation of both phosphorylase forms may takes place via distinct pathways. Since earlier experiment have shown that plastidic ∝-amylase and cytosolic β-amylase in the same leaf show different distribution patterns in light-grown leaves, the distribution of phosphorylase in leaves was analyzed by excising leaf segments in a similar fashion as described earlier for amylases.

Fig. 56 shows distribution of total phosphorylase activity in light and dark-grown seedlings. It is evident that in dark-grown seedlings, phosphorylase activity is low in basal segments and it progressively increases towards the tip. By contrast in seedlings grown in light, while the basal segment possessed nearly equal phosphorylase activity to dark-grown seedlings, in the 2nd and 3rd segments it is significantly higher than dark grown seedlings. Furthermore, from the 4th segment onwards the activity was significantly less than in the dark controls. The above result was obtained irrespective of base unit used for the expression of phosphorylase activity, either segment or protein (Fig. 56A,B).

It is important to note that if the phosphorylase activity of all segments (Fig. 56A) is pooled up to obtain the total phosphorylase activity it is 3.31 nkat and 3.02 nkat in light and dark respectively. It is evident that though *in vivo* light and dark grown leaves have a different distribution of phosphorylase

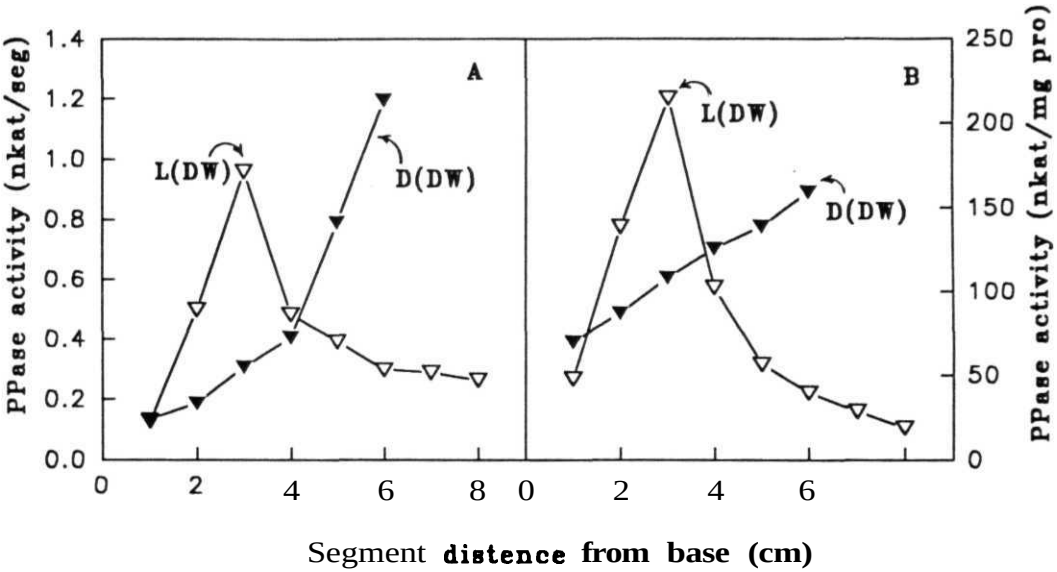

Figure 56. Phosphorylase activity in the different sections (1 cm) of 7-d old leaf.
The segments (1 cm) are numbered from base (1) to the tip of leaf.
(A) phosphorylase activity is calculated on per segment basis
(B) phosphorylase activity is calculated on mg protein basis.

activity along the leaf axis, on estimating the total phosphorylase activity of the whole leaf, nearly equal activity is obtained in light and darkness masking the effect of light on phosphorylase stimulation. The profile of phosphorylase distribution activity in 7 d and 8 d old seedlings is closely similar indicating that light affects the distribution of phosphorylase activity along the axis of the leaf (Fig. 57).

4.6.7.1 Phosphorylase gradient in light and dark grown leaves

The electrophoresis of phosphorylase isozymes revealed that the relative proportion of plastidic and cytosolic enzymes in light and dark-grown leaves was clearly influenced by the location of the segment position along the axis of the leaf. In light-grown seedlings (within limits of our phosphorylase activity assay), in basal segments, the activity of plastidic isozyme of phosphorylase could not be seen in the first three segments, but could be seen in segments 4-8 from the base. In terms of relative preponderance, in the basal segment, plastidic isoform was absent up to the 3rd segment whereas cytosolic isoform was prominently present. The level of plastidic isozyme gradually increased towards the tip from the 4th segment onwards to a maximal activity at the tip of the leaf. On the other hand the cytosolic phosphorylase was more intense in basal segments, and from segment 4 onwards the level declined towards the tip of leaf (Fig. 58). In fact, in regions close to the leaf tip, i.e., segment 7-8, cytosolic phosphorylase was nearly absent. Interestingly, in the same leaf while plastidic phosphorylase was absent in 1-3 segments, cytosolic phosphorylase was completely absent at the tip (Fig. 58, inset).

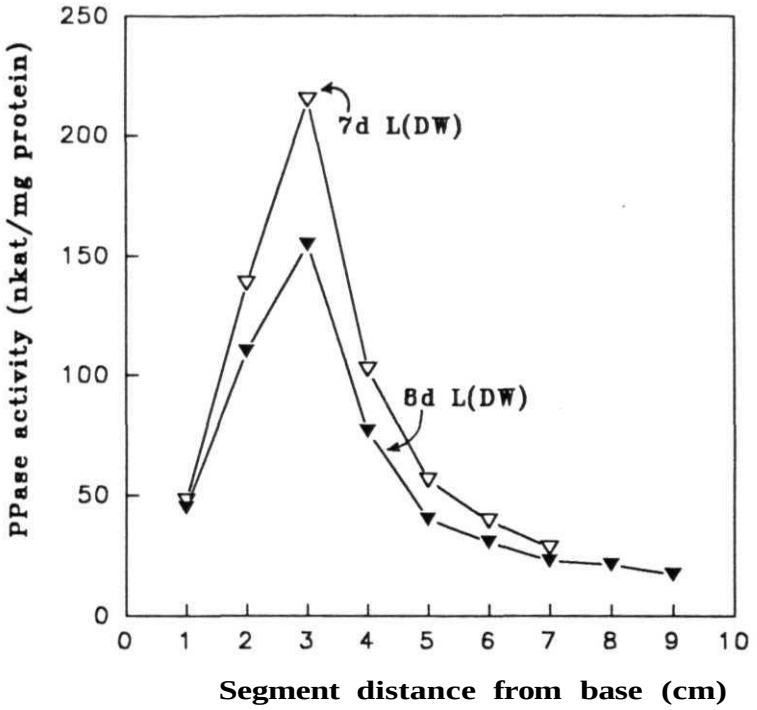

Figure 57. Distribution of phosphorylase activity in leaves of 7-d and 8-d old light grown seedlings. The segments are numbered from the base (1) to the tip of the leaf.

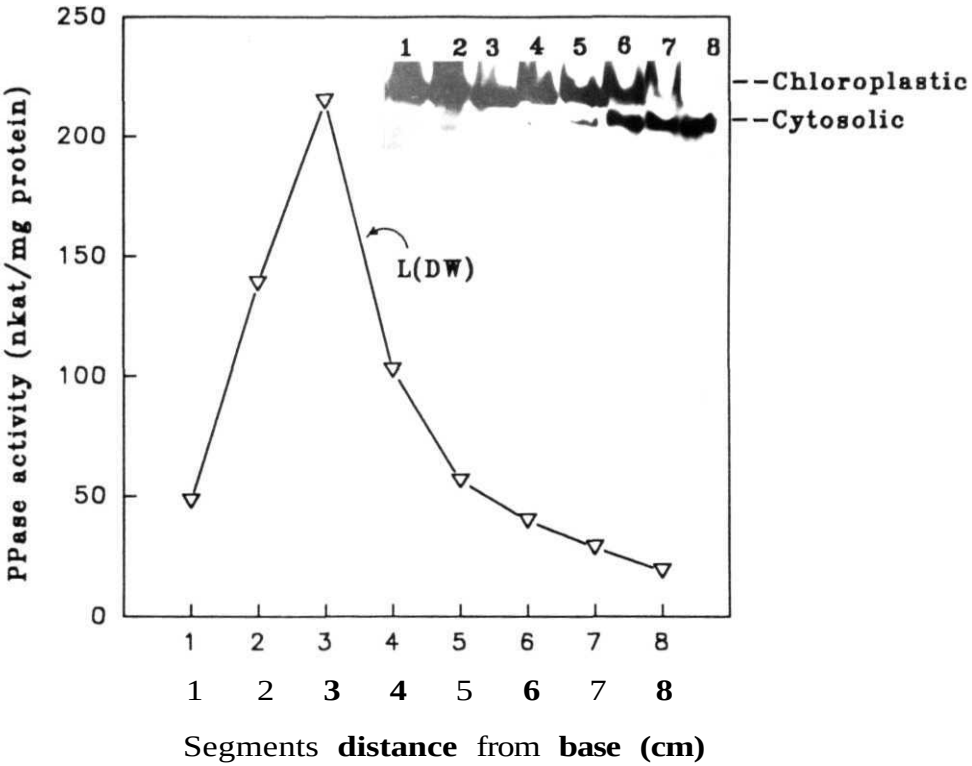

Figure 58. Phosphorylase activity in different sections of 7-d old light grown leaves. Inset shows the gradient of cytosolic and plastidic isozymes along with the leaf length.

In dark-grown leaves, total phosphorylase activity increased towards the tip, with the tip having a nearly two-fold higher activity than the base. In contrast to light-grown leaves, in basal segments as well as in the tip of the leaf, both cytosolic and plastidic isoforms can be detected. However, in the base, while cytosolic isoform is more dominant, in tip the activity of plastidic isoform is close to cytosolic isoform. The relative preponderance of isoforms reveals that in dark the level of plastidic phosphorylase isoform increases from the base to the tip of the leaf. On the other hand, the level of cytosolic isoforms which is higher in segment 1-4 declines in the tip region in segment 5-6 (Fig. 59).

4.6.7.2 Effect of norflurazon on phosphorylase distribution

Earlier experiments revealed that Norflurazon treatment reduces phosphorylase activity of leaf, eliminating plastidic isozyme localized in B cells. Fig. 60 shows the analysis of phosphorylase distribution in the NF-treated leaves. It is evident that distribution of phosphorylase in the NF-treated leaf is akin to distribution of phosphorylase in light-grown seedlings with maximal activity present in the third segment of the leaf. However, electrophoresis of phosphorylase showed that only cytosolic isozyme was present in NF-treated seedlings and its level declined towards the leaf tip (Fig. 60, inset).

In no segment was any activity of plastidic isozyme detected. Assuming that NF treatment does not affect the cytosolic phosphorylase activity, the subtraction of total phosphorylase activity of light-grown NF-treatment

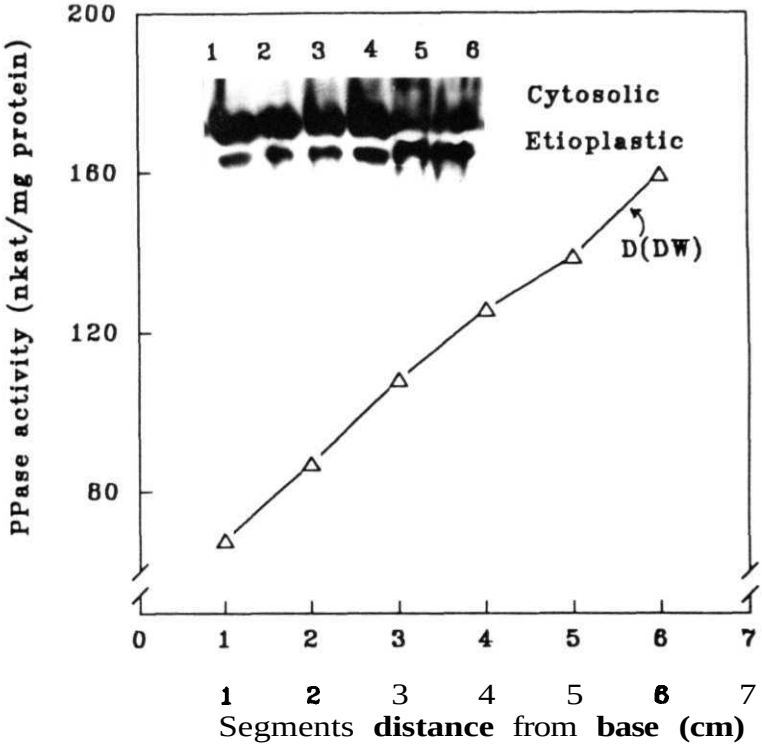

Figure 59. Phosphorylase activity in different sections of 7-d old dark grown leaves.
Inset shows the gradient of cytosolic and etioplastic isozymes along the leaf length.

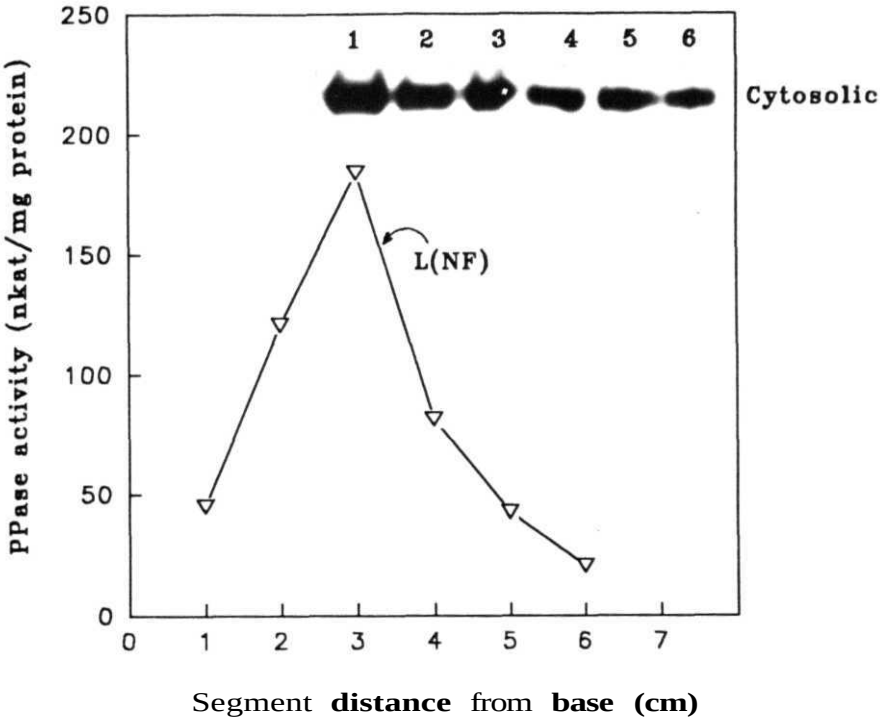

Figure 60. Distribution of cytosolic phosphorylase activity in Norflurazon-treated light grown leaves (7-d). Inset shows the gradient of cytosolic isozyme along the leaf length. The plastidic phosphorylase is absent in NF treated seedlings.

seedling from light-grown seedlings showed that plastidic phosphorylase comprise 20% of phosphorylase activity.

4.6.7.3 Gradient in isolated bundle sheath and mesophyll cells

In view of spatial separation of phosphorylase in two compartments, we took advantage of it and assayed phosphorylase activity after separating mesophyll and B cells from individual segments from 7-d old pearl millet leaves. The result obtained clearly supports the earlier observation.

In light-grown plants, plastidic isozyme is not seen in B in the first two segments. Thereafter, its activity increased towards the tip of the leaf. On other hand, mesophyll cells showed only cytosolic phosphorylase and had a gradient as observed in intact leaves. The basal segments were more enriched in cytosolic phosphorylase which declined towards the the tip from segment 3 onwards (Fig. 61).

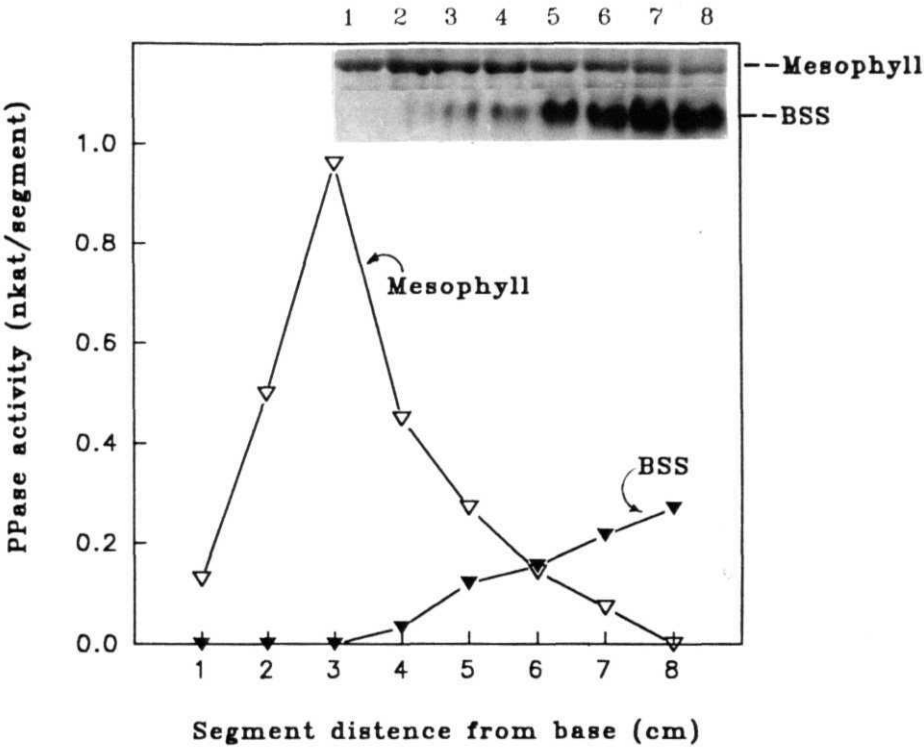

Figure 61. Distribution of phosphorylase activity in bundle sheath and mesophyll cells isolated from different segments of leaf (7 d). Inset shows the gradient of isozymes in mesophyll cells and bundle sheath strands along the leaf length.

DISCUSSION

CHAPTER 5

DISCUSSION

The morphology of plants is optimized in order to survive in a given set of environmental conditions, and also to make the best use of environmental factors, such as light. Basically, light drives the photosynthetic reaction in chloroplasts localized in green leaf cells. Leaves, in addition to acting as an organ responsible for in photosynthetic generation of starch, also perceive the photoperiodic duration of light. Furthermore, in higher plants, development of the leaf strongly depends on the availability of light. Despite a surge of studies in recent years, the molecular basis of leaf development is still not fully understood. Moreover, development of the leaf follows different strategies in dicotyledons and monocotyledons due to the determinate and indeterminate nature respectively, of their meristems. In the present investigation, the photoregulation of starch degrading enzymes in pearl millet leaf has been studied in relation to leaf development and chloroplast biogenesis in pearl millet seedlings.

5.1 AMYLASES

5.1.1 Phytochrome regulates amylase activity in leaves:

In pearl millet seedlings, maximal amylase activity was present in seeds and in other parts of the seedlings also amylase activity was detected (Fig. 7). Such ubiquitous distribution of amylases has also been observed in other monocot seedlings such as maize (Subbarao, 1992) and barley (Jacobson *et al.*,

1986). In general, the level of amylase activity was higher in light-grown-seedlings, barring root, indicating that amylase is a photoregulated enzyme.

It was observed that in continuous light-grown seedlings, the onset of photostimulation of amylase activity, in some way is associated with leaf expansion, and amylase photostimulation is seen from the 3rd d onwards along with the initiation of leaf expansion, culminating in a peak on the 8 d (Fig. 9). The responsiveness of leaf to photostimulate amylase activity between 3-8 d is temporally determined. Subsequently even though seedlings are still under continuous light, the loss of responsiveness triggers a decline in amylase activity after the 8 d. The mechanism underlying amylase decline is not known, but could result from; inhibition of amylase synthesis; stimulation of amylase degradation or a combination of both. The observed time course of amylase activity in pearl millet leaves is also similar to photoregulation of amylase in mustard cotyledons (Sharma and Schopfer, 1982) and in maize leaves (Subbarao, 1992), where too after attaining a peak, amylase level eventually declines.

Since, in pearl millet leaves, amylase activity is photostimulated by continuous red light (Fig. 9), it is likely that this photoresponse is mediated by a photoreceptor, such as phytochrome or protochlorophyllide, or both of them may be involved. A clear distinction between the participation of these two photoreceptors in a photoresponse can be made by exploiting the photoreversible nature of the phytochrome molecule, where photoresponse triggered by active Pfr form of phytochrome 'which is generated by a brief pulse of red light (660 nm)' can be reversed, if it is followed by a terminal far-red light

pulse (730 nm). Such RL/FR reversible responses have been termed as low-fluence response and are characteristically attributed to phytochrome (Shropshire and Mohr, 1983). Cyclic red light (10 min) treatments of pearl millet seedlings separated by dark intervals of 8 h, significantly stimulated amylase activity in leaves (Fig. 8). While FR light alone was largely ineffective, it reversed the effect of a preceding RL pulse. This experiment showing reversibility of RL-mediated response by FR clearly established the identity of the photoreceptor regulating amylase activity as phytochrome (Fig. 8).

It is now well recognized that phytochrome exists as a small multigene family (Sharrock *et al.,* 1986; Quail, 1991) consisting of several phytochrome species, of which phytochrome A is present predominantly in etiolated seedlings and serves as a signal to perceive response under continuous FR light. Under continuous RL used in this study, phytochrome A level rapidly declines due to suppression of transcription (Quail, 1991), destabilization of its mRNA (Colbert *et al.,* 1983), and proteolytic degradation (Vierstra, 1993). On the other hand the level of other phytochrome species does not change so severely under continuous light (Wang *et al.,* 1993). In view of multiplicity of phytochrome species it is logical to ask which of the phytochrome species is involved in regulation of amylase activity in seedlings. While no direct data on accumulation kinetics of different phytochrome species are available in pearl millet, in oat, a monocot species, it has been shown that in continuous light-grown plants there is no accumulation of phytochrome A, but other light-stable phytochromes accumulate in the seedlings (Wang *et al.,* 1993). It is therefore conceivable from these data that the light-grown seedlings used in this study

would possess phytochrome species other than phytochrome A in greater quantity. While these findings do not directly implicate a role of a particular phytochrome species in the observed photoresponses, it is likely that the sustainment of photoregulated amylase increase in continuous light-grown seedlings is via the action of light-stable phytochrome.

Although photoregulation of several enzymes have been reported in cereal leaves (Downton and Hawker, 1973), the specific involvement of phytochrome has been investigated only in a few cases. Reports on photoregulation of leaf amylases are few, and detailed inspection of the role of photoreceptor in controlling the response has been done in this laboratory (Subbaramaiah and Sharma, 1989). In chick pea cotyledon, RL stimulated α-amylase activity, and could also substitute for axis (Casado *et al.*, 1991). The photoinduction of amylase may depend on other factors too, e.g., in a *Arabidopsis* mutant lacking starch, β-amylase level is elevated by 40-fold only when plants are grown under 12 h photoperiod, whereas in continuous light the level of β-amylase is equal in mutant and wild types. It was ascribed that such elevation of β-amylase activity results from fluctuation in photosynthetic carbon fluxes during photosynthesis (Casper *et al.*, 1989).

In cereal seeds, particularly in barley, it has been reported that amylase induction is strongly influenced by plant hormones, regulating amylase gene expression (Fincher, 1989). In leaves, although photoregulation of amylase has been reported in mustard cotyledons (Sharma and Schopfer, 1987; Subbaramaiah and Sharma, 1989), and maize (Subbarao, 1992), there is no evidence in favour of hormone mediated amylase induction. In barley seedlings,

where amylase induction in seed is characteristically triggered by gibberellic acid, there is no evidence for such a role of GA in regulation of leaf amylases (Jacobsen *et al.,* 1986). In barley, since amylase regulation in seed is regulated by hormone, and in leaf the same enzyme is regulated by water stress, it is evident that regulation of an enzyme in two different organs may be governed by two distinct mechanisms. In fact, a hormonal participation of GA in photoinduction of amylase was ruled out in mustard cotyledons (Drumm *et al.*, 1971).

5.1.2 Blue light effect is mediated via phytochrome

The blue light effect on amylase induction was demonstrated as a consequence of action of phytochrome. The similarity between blue and red light action is apparent at many levels. The time course of amylase induction in blue light is very similar to red light, albeit the magnitude of photostimulation was less in blue light (Fig. 11). Although RL and BL elicit the same qualitative response, quantitatively the magnitude of response in BL is one-third of the RL. The photoregulation of amylase activity is also observed on replacing brief red light pulses with blue light. The reversal of blue light effect by far-red light clearly shows the role of phytochrome in blue photoresponse (Fig. 12). Evidently, though blue light pulse also elevated amylase activity, it operated via phytochrome rather than via a separate blue light receptor. The results obtained do not suggest role of any photoreceptor other than phytochrome on amylase induction and are in agreement with our previous results in mustard cotyledon (Manga and Sharma, 1988), where too,

blue light effect on amylase induction was demonstrated to be a consequence of activation of phytochrome.

5.1.3 Amylolytic activity consists of α-amylase and β-amylase

Since, in many higher plants, amylolytic activity consists of both α-amylase and β-amylase, the specific presence and contribution of both enzymes in photostimulation of amylase activity was ascertained. The distinction between α- and β-amylase activity was made by heat stability of α-amylase in the presence of Ca^{2+}, and also by its capacity to degrade β-limit dextrin. In accordance with other reports, in light-grown leaves, β-amylase contributed 80-90% of total amylolytic activity, and the remainder was α-amylase activity (Fig. 13A,B). In several systems amylase activity in leaf predominantly consists of β-amylase, e.g., in mustard, amylolytic activity of cotyledons constituted only of β-amylase and no α-amylase activity could be detected (Subbaramaiah and Sharma, 1989). Similarly in Vicia fab a (Chapman *et al.*, 1972; Ghiena *et al.*, 1993) and in maize (Subbarao, 1992) leaves also, among the two amylases, β-amylase activity was most prominent.

The existence of both α-amylase and p-amylase in pearl millet leaf is further confirmed by immunological detection of antigens reacting with monospecific maize α_1- and p-antiserum. The monospecificity of α_1- and β-antiserum were ascertained by a variety of techniques such as double diffusion, immunoelectrophoresis and western blotting (Fig. 34-36). Moreover, the identity of antigens as amylases was also confirmed by retention of amylase activity in immuno-complex after double diffusion (Fig. 34F-H). The detection

of both α-amylase and β-amylase antigens in the leaf validated the use of heat inactivation and β-limit dextrin as a tool to detect α-amylase activity in the present study.

The specificity of maize α_1-, α_2- and β-antiserum against pearl millet amylases was established in several ways. First, the precipitin lines generated against respective α_1-, α_2-, β-amylase antigen of maize completely fused with pearl millet leaves, showing existence of antigenically identical proteins in both plants (Fig. 34A-C). Second, the precipitin line could be stained for amylolytic activity after removal of all unbound proteins from gel (Fig. 34F-H). Third, both immunoelectrophoresis (Fig. 36) and western blotting (Fig. 35) showed presence of a single antigen band against respective antiserum after the native gel, whose Rf value corresponded with the position of α- and β-amylase isozymes on the gel. Fourth, the distribution of antigens of α_1-, α_2- and β-amylase proteins in different parts of the seedling was similar to that observed for maize (Subbarao, 1992). In pearl millet too, like maize (Subbarao, 1992), two α-amylases, namely α_1- and α_2,- and one β-amylase were present in seeds, but in other parts α_2-amylase could not be detected, and only α_1-amylase and β-amylase were present in all organs of seedlings (Fig. 34A-C). The existence of these three amylases appears to be a common feature in cereals as these have also been detected in sorghum and barley (Mundy, 1982).

5.1.4 **Phytochrome** stimulates de novo synthesis of **∝-amylase and β-amylase** in leaves

In cereals, the regulation of amylolytic activity has been best studied during seed germination, during which **∝-amylase** is de novo synthesized and secreted from scutellum and aleurone layers to endosperm, and **β-amylase** is activated from a latent form (Fincher, 1989). It is therefore likely that a similar mechanism may operate the photostimulation of amylolytic activity in pearl millet leaves. An analysis of time course of photostimulation of **∝-amylase** and **β-amylase** revealed many distinctive features. Since **β-amylase** is the predominant amylolytic enzyme in leaves, photostimulation of **β-amylase** activity closely paralleled the total amylolytic activity of leaf, with a peak at the 8th d from sowing. In contrast, in dark-grown leaves, a little amount of **β-amylase** activity could be detected only after 5 days from sowing (Fig. 13A). Although the time course study shows that light stimulates **β-amylase** activity in a highly regulated manner, the mode of **β-amylase** modulation is not known.

The possibility of activation of **β-amylase** contributing to observed photostimulated increase was assessed by **immunotitration** of varying amount of **β-amylase** activity against a fixed amount of **β-antiserum**. The observation that on immunotitrating varying amounts **of β-amylase** activity from dark and light-grown leaves against a fixed amount of **β-antiserum,** the release from inhibition and subsequent escape curve follow similar profile (Fig. 37), ruled out any possible contribution of inactivation/activation as a mechanism to **photoregulate β-amylase** activity in leaves.

These results indicated that photostimulation of p-amylase increase results via increase in the level of p-amylase protein under the influence of light, which was ascertained by analyzing the time course of changes in β-amylase level in light and darkness by SRID. The time course of level of p-amylase antigen clearly paralleled the increase in p-amylase activity (Fig. 39A) and supported the view that it is the increase in β-amylase protein level which contributes to observed photostimulation of p-amylase in leaves, rather than an activation which takes place in cereal endosperm.

An increase in p-amylase protein is also seen when seedlings were transferred from darkness to light (Fig. 38D). On the other hand, equal levels of p-amylase activity from dark and light-grown leaves always generated an equal diameter ring on SRID (Fig. 38B). In general, various experiments conducted using SRID broadly confirmed that in pearl millet leaves there is a strict correlation between p-amylase protein and p-amylase activity at the time of points tested, and observed changes in p-amylase activity closely parallels change in p-amylase protein levels (Fig. 38A).

The results also ruled out the possibility of changes in level of inhibitors/activators by light, which might have regulated p-amylase level indirectly. It is, therefore, clearly evident that the influence of light on β-amylase increase is solely exercised by modulating p-amylase protein level. While the observed results are indicative of light-stimulated de novo synthesis of protein, alternatively it is possible that the observed increase in p-amylase protein level may result from light-mediated inhibition of p-amylase degradation. This possibility seems to be however remote, as in mustard

cotyledon photostimulated p-amylase increase exclusively resulted from an increase in p-amylase mRNA level leading to de novo synthesis and the rate of p-amylase degradation was not influenced by light. (Sharma and Schopfer, 1987; Subbaramaiah and Sharma, 1989). Therefore it can be assumed that phytochrome increases p-amylase activity by stimulation of de novo synthesis in pearl millet leaves.

Although we have not investigated if there is an activation of p-amylase in pearl millet endosperm at all, activation of p-amylase is a general feature in most cereals seeds such as barley (Nishimura *et al.,* 1986), wheat and rye (Bureau *et al.,* 1989) etc. It is evident that the same enzyme in different organs may be regulated by different mechanisms. Recent evidence has indicated that there may be two different β-amylases in cereals, one specifically localized, in endosperm, and other present in all parts of seedlings (Daussant and Lauriere, 1990; Daussant *et al.,* 1991). The possibility that one located in endosperms is regulated by activation during germination, and another p-amylase located in other organs being regulated by other factors like light, due to difference in the gene organization remains an attractive possibility. Though, in our study, we have not distinguished whether endosperm and leaf p-amylase are identical or dissimilar, an investigation on these lines would be most useful to understand the dual regulation of the enzyme in different organs.

In addition to stimulating p-amylase activity, light also stimulated increase in ∝-amylase activity in leaf. The ∝-amylase activity could be detected in leaves right from the 3rd d, both in light and darkness, which increased gradually. A distinct effect of light on induction of ∝-amylase activity is

apparent only from the 6th d onwards and thereafter oc-amylase activity declined in both light and darkness, but light-grown leaves possessed more ∝-amylase activity (Fig. 13B). Though ∝- and β-amylases were both photoinducible in pearl millet leaves, the time course of their increase was different and perhaps both were stimulated using independent signal pathways.

In both light and dark-grown seedlings, maximum oc-amylase antigen was obtained on the 6th d and after a little decline it remained constant in light-grown seedlings, whereas in dark-grown seedlings it gradually decreased (Fig. 39B). The stabilization of oc-amylase in light-grown seedlings and decline in dark-grown seedlings after a temporal point of 6 d may arise as a consequence of different subcellular localization of this enzyme in dark and light-grown leaves. Since in dark-grown leaves, ∝-amylase is in extraplastidic compartment and in light-grown leaves it is also located in chloroplast (see below for details), and chloroplast stabilizes its level, the sustainment of a constant level of oc-amylase in 6 d old seedlings onwards may reflect the activity of chloroplastic oc-amylase. The import of oc-amylase protein in chloroplast stabilizes its level while the cytosolic amylase is susceptible to degradation. The kinetics of oc-amylase level indicates that in light-grown leaves, the plastidic amylase is stabilized at a constant level by virtue of chloroplast localization, whereas in dark-grown leaves, it continuously declines, due to lack of protection of cytosolic amylases.

5.1.5 Compartmentalization of ∝-amylase and β-amylase in leaves

The logical site of localization of starch degrading enzymes in green leaves is chloroplast, because it is the site of synthesis and deposition of starch, the substrate for starch degrading enzymes. The reports on compartmentalization of starch degrading enzymes are contrary to the above notion. As most studies have indicated, both ∝-amylase and β-amylase are located in extraplastidic compartments (Ziegler, 1988) and in instances where an amylolytic activity is detected in chloroplasts, the possibility of contamination by extraplastidic amylases has often been invoked (Beers and Duke, 1990). The demonstration of localization of an enzyme in chloroplast requires isolation of intact chloroplasts free of cytosolic contamination, and showing association of the enzyme with it. Alternatively, many plastidic enzymes are synthesized only during light-induced transformation of etio-plasts/proplastid to chloroplasts and therefore are absent in etioplasts/proplastids, and consequently can not be detected in dark-grown-tissues. While it is difficult to distinguish in crude extract prepared from light/dark-grown tissues, the contribution of different cytosolic and plastidic enzymes, to measure amylolytic activity, as on disruption of leaf, all components of cellular constituents are merged. In these cases too, appearance or disappearance of a specific enzyme activity can be seen by native PAGE, as several enzymes exist as isoforms, and if a new isoform appears or one isoform disappears, depending on its level, relative mobility and other factors, most times it can be visualized on native PAGE (Scandalios, 1974).

In the present study, amylolytic activity from light-grown seedlings on native PAGE was resolved in two groups of bands (Fig. 16A), namely, a slowly migrating minor isozyme, and a major broad band, which in some samples consisted of 2-3 closely migrating isozymes. Since the minor band was absent in dark-grown seedlings, which nevertheless possessed a major band (Fig. 16B), the role of light in inducing the appearance of the above isozyme was self-evident. Since light also triggered the chloroplast biogenesis, it is likely that this band is associated with chloroplast differentiation. The identity of amylase isoform separated on native PAGE as α-amylase and p-amylase was ascertained by western blotting (Fig. 35), and enzyme activity assays (Fig. 34F-H). Both minor and major bands were visualized on the gels with amylose, whereas only minor band was visualized with β-limit dextrin gels (Fig. 18B,C), and, was therefore identified as α-amylase. The identity of the major band as P-amylase is implied by its failure to degrade p-limit dextrin. A final confirmation of the above isozymes as α-amylase and p-amylase was made by blotting the gel on nitrocellulose papers and using monospecific antiserum for α_1- and p-amylase. The p-antiserum recognized the major band (Fig. 35B) and α_1-antiserum recognized the minor band (Fig. 35A), which closely corresponded with Rf value reported for α-amylase and p-amylase. It is evident from the foregoing that the available evidence clearly indicates that light induces a new amylase band, which is α-amylase in nature and is likely to be localized in chloroplasts.

Norflurazon is a powerful inhibitor of carotenoid synthesis, and lack of carotenoids causes photo-oxidation of various plastid components including

chlorophyll, membranes and proteins in plants grown under light, leading to degeneration of chloroplasts and loss of plastidic proteins (Oelmüller, 1989). Since, in light, NF treatment functionally destroyed the chloroplasts (Mayfield and Taylor, 1987; Batschauer *et al.*, 1986), in the present study NF was used as a tool to distinguish the plastidic localization of amylase. It has been observed that in NF-grown plants, chloroplastic enzymes are reduced, whereas cytoplasmic, glyoxisomal and mitochondrial enzymes are maintained at normal levels (Blume and McClure, 1980; Reiss *et al.*, 1983).

Norflurazon treatment rendered leaf of pearl millet seedlings photosynthetically inactive in light, due to degeneration of plastids resulting in albino leaves (Fig. 5B,C). While NF application did not affect amylase activity in dark- grown seedlings (Fig. 15B), in light-grown seedlings it reduced amylase activity by 30-50%. Nevertheless, the profile of photostimulation of total amylase followed a qualitatively similar pattern to control seedlings (Fig. 15A).

The enzymatic analysis of NF-grown seedlings revealed that in light-grown seedlings, while NF slightly suppressed β-amylase photostimulation, it completely blocked the photoinduced rise in oc-amylase level. Since the light induced ∝-amylase band was totally absent in NF-treated seedlings (Fig. 16C), which lacks functional chloroplasts, it is evident that light-induced ∝-amylase is localized in plastids. Since NF grown seedlings still have a residual oc-amylase activity it is evident that oc-amylase is also present in extraplastidic compartments too (Fig. 15C).

5.1.6 ∝-amylase is present in plastids

Since the light-induced appearance of an ∝-amylase isozyme was interlinked with chloroplast development, the presence of amylase in chloroplast was confirmed by studying amylolytic activity of isolated plastids. Generally, the studies demonstrating plastidic localization of enzymes, are impeded by the presence of cytosolic contaminants in plastid preparations or else isolated plastids are broken which may have lost its contents to cytosol, or may be contaminated by cytosolic components. In this context, a demonstration of plastidic integrity and purity is an essential step before a plastidic localization of an enzyme can be inferred, and it is all the more essential in a case where the same enzyme is present in cytosol too. In the present study, the intactness of plastids were established by several methods (Hall, 1972). First, the intactness of chloroplast was confirmed by phase-contrast microscopy, where only a small number of chloroplasts were seen without plastidic envelop, and most were intact (Fig. 17). Second, the absence of ferricyanide reduction by plastid preparation, which could be seen only after rupturing chloroplasts by osmotic shock, unequivocally shows that plastid preparation contained mainly intact chloroplasts. Third, the absence of PEP carboxylase activity in isolated chloroplasts ruled out contamination of cytosolic proteins in isolated chloroplast preparation (Table 1).

In isolated chloroplasts amylolytic activity could be detected only after rupturing the envelope membranes by osmotic shock or sonication (Table 2). The molecular identity of a plastidic enzyme like ∝-amylase was established by its capacity to hydrolyze β-limit dextrin and by western blotting. Since no

∝-amylase activity could be detected in etioplasts, it is evident that light-mediated chloroplast development is necessary for photostimulation of ∝-amylase. The dependence of photoinduction of ∝-amylase on chloroplast development is also apparent from the observation, that NF-treatment which eliminated functional chloroplasts, also suppressed the formation of plastidic ∝-amylase. No β-amylase activity could be detected in plastidic preparation. In most plants, among the two amylases only ∝-amylase has been detected in plastids, and the presence of any β-amylase is attributed to a cytosolic contamination.

The plastidic ∝-amylase from pearl millet leaf cross-reacted only with $\propto_1$-antiserum (Fig. 34D), but not with β- or $\propto_2$-antiserum. Moreover, the $\propto_1$-antiserum employed for detection of plastidic enzyme cross-reacted with both cytosolic and plastidic ∝-amylases and also with one ∝-amylase species from seed (Fig. 34D). Since, in seeds, ∝-amylase after synthesis is secreted to endosperm (Subbarao, 1992), and plastidic ∝-amylase after synthesis in cytosol needs to be translocated across the envelope membrane, these two may not be the same amylase. However, the wider cross-reactivity of $\propto_1$-antiserum may arise because being a polyclonal antibody, it recognizes certain commonly present epitopes on the surface of antigens constituting the gene family of $\propto_1$-amylase proteins. Inspite of having different sequences, these amylase species, i.e., $\propto_1$-amylase of seed, cytosolic and plastidic amylase of leaf are likely to belong to the same multigene family, whereas $\propto_2$-amylase belongs to the other family which expresses only in seed.

The localization of ∝-amylase in chloroplast has been debated in many cases. ∝-amylase was detected in chloroplasts of spinach (Okita *et al.,* 1979; Okita and Preiss, 1980), but several studies with pea and barley indicate that ∝-amylase is either absent or displays very low activity in the chloroplasts (Stitt, 1984; Stitt *et al.,* 1978; Kakefuda *et al.,* 1986). Ziegler and Beck (1986) found that one-fourth of the amylolytic activity of wheat was associated primarily with the chloroplasts, and slightly higher amylolytic activity in pea.

Okita *et al.,* (1979) found both ∝-amylase and β-amylase activity in plastids, but these were only 5% of total amylolytic activity of leaf. Okita and Preiss, (1980) also showed that plastidic and extraplastidic amylase differed in their substrate specificity. Though, Ziegler (1988) found an endoamylase in pea chloroplast which was similar to cereal ∝-amylase, Beers and Duke, (1990) doubt its presence in the same system. Li *et al.,* (1992) have also reported localization of plastidic ∝-amylase in leaf of sugar beet.

5.1.7 Molecular properties of plastidic ∝ -amylase

The amylolytic activity associated with plastids was specifically identified as an ∝-amylase. A general property of ∝-amylase is that it requires Ca^{2+} to maintain the structure of the active site and also stability of the enzyme (Bush *et al.,* 1989; Fischer and Stein, 1960), therefore a chelating agent like EDTA, inactivates ∝-amylase activity (Koshiba and Minamikawa, 1981). In contrast, β-amylase (Lizotte *et al.,* 1990) and starch - debranching enzyme (Swain and Dekker, 1966) do not require Ca^{2+} for their activity. The plastidic amylase possessed several properties which are characteristics of ∝-

amylase. For instance, its activity was remarkably dependent on presence of Ca $^{+}$ in solution (Fig. 21A). Moreover, on dialyzing plastidic extracts against EDTA, which chelates Ca^{2+}, activity was irreversibly lost (Fig. 21B). The chloroplastic amylase was also resistant to heat in the presence of 10 mM $CaCl_2$ (Table 5). A final proof of it being ∝-amylase was obtained by its renaturation by Triton X-100 after SDS-PAGE (Segundo *et al.*, 1990), which was also demonstrated for maize ∝-amylase (Segundo *et al.*, 1990). In the present study denatured ∝-amylase from seed, leaf, B strands was renatured after SDS-PAGE, by exchange with Triton X-100 (Fig. 23). Lin *et al.*, (1988) though, detected four endoamylases $\propto_2$, $\propto_3$, $\propto_4$ and $\propto_5$, likely to be associated with chloroplast in *Arabidopsis* but did not study the molecular properties of these enzymes, Nevertheless, these results further confirms the existences of ∝-amylases in plastids.

The profile of pH optima was not sharp and showed more shallow increase towards optimal pH, which was different from cytosolic β-amylase, and was localized at pH 6.2 (Fig. 22). The molecular weight of pearl millet ∝-amylase (46 kD) falls within the range reported for higher plant ∝-amylases. The MW of wheat and sorghum isozymes ranges between 42 to 42.5 kD and 41.5 to 42.7 kD, respectively. The four ∝-amylase isozymes of barley have approximately the same molecular weights of 44,000 daltons (Jacobsen and Higgins, 1982). In pearl millet, like maize (Subbarao, 1992), $\propto_1$-amylase molecular weight is 46,000 daltons. The pearl millet β-amylase molecular weight is 43,000 daltons. In most cases plant β-amylases MW is higher than

the a-amylase MW, whereas in pearl millet it is less than the a-amylase MW (Fig. 45).

5.1.8 a-amylase is also present in extraplastidic compartments

The fact that plastidic a-amylase could be detected only in light-grown leaves while a significant a-amylase activity could be detected even in dark-grown leaves raises a question about its subcellular localization. Since induction of plastidic amylase is obligatorily dependent on light and presence of chloroplasts, it is evident that in dark-grown leaves a-amylase activity comprises of extraplastidic amylases. Since NF treatment eliminates chloroplast, in NF-grown seedlings the residual a-amylase activity would essentially consist of extraplastidic a-amylase (Fig. 15C). In pearl millet leaves cytosolic α-amylase is present at extremely low level, and after PAGE, cytosolic a-amylase can be resolved into 7 isozymes on prolonged incubation on a β-limit dextrin gel (Fig. 20, lane E). Interestingly, whereas the plastidic a-amylase is homogenous and is visualized after native PAGE as a single band, the cytosolic α-amylases are a heterogenous group consisting of multiple a-amylase isoforms. The precise subcellular localization of a-amylase in extraplastidic fraction was not investigated. In pea it was found that, most of extraplastidic a-amylase activity, upto 87% of the total, was found to be localized in the apoplast of stem and leaves (Beers and Duke, 1988; Saeed and Duke, 1990a). Though in other systems it is not known whether a-amylase is present or absent in chloroplast, it appears that the largest amount of the total a-amylase activity in leaf tissue is extrachloroplastic (Kakefuda *et al.*, 1986; Ziegler and Beck, 1986).

In pea seedlings, Saeed and Duke, (1990b) observed that Norflurazon stimulated ∝-amylase activity by > 80-fold, which was largely localized in the apoplasts. Lincomycin and chloromphenical increased ∝-amylase activity in light-grown seedlings to the same magnitude as Norflurazon, indicating that the effect of Norflurazon was probably through the destruction of plastid ribosomes. It was proposed that chloroplasts produce a negative signal for the regulation of the apoplastic ∝-amylase in pea (Saeed and Duke, 1990a). In this study, in NF-grown seedlings, there was suppression of plastidic ∝-amylase activity and no enhancement of cytosolic amylase could be detected (Fig. 15B,C).

5.1.9 In bundle sheath cells only plastidic ∝-amylase is present

Pearl millet being a C_4 plant has a typical kranz leaf anatomy with distinct M and B cells and within these cells more amylase activity was present in M cells than in B cells (Table 3). In pearl millet leaves, chloroplastic a-amylase was present both in M and B chloroplasts. However, B chloroplast possessed higher amylolytic activity than the M chloroplast when expressed on either number of chloroplasts basis or on chlorophyll basis (Table 4). The higher amylase activity in M chloroplasts on mg protein basis, was however due to the lack of Rubisco in M chloroplasts. The exclusive localization of ∝-amylase in B cells was confirmed by light-induced appearance of ∝-amylase isozyme in B cells, which could be eliminated by a NF-treatment (Fig. 20B).

No ∝ -amylase activity could be detected in dark-grown B cells (Table 3). Unlike M cells, where both ∝- and β-amylases are present, B cells possess only

plastidic ∝-amylase activity, and cytosolic ∝-amylase was also absent (Table 3). A specific localization of ∝-amylase in B cells is akin to its principal function to generate starch during photosynthesis and the presence of a photoinduced plastidic ∝-amylase is an essential requirement for its mobilization to sugars. While in maize B cells, both nonplastidic and plastidic starch degrading enzymes were detected (Echeverria and Boyer, 1986), in pearl millet, only plastidic phosphorylase and ∝-amylase were detected in B cells. Cytosolic β-amylase, ∝-amylase and cytosolic phosphorylase were absent in these cells.

5.1.10 p-amylase is a extraplastidic protein

In pearl millet leaves, β-amylase activity was mainly restricted to the extraplastidic compartment and no p-amylase activity could be detected in isolated plastids (Table 3). In a few isolated studies it has been shown that β-amylase too is present in chloroplast (Lin *et al.*, 1988; Beers and Duke, 1988; Kakefuda *et al.*, 1986), but contaminants are a likely explanation (Beer and Duke, 1990). On the other hand, in our study at no stage we could detect any P-amylase activity in chloroplasts of pearl millet (Table 3, Fig. 20) and mustard (Manga and Sharma, 1990). Both enzymatically (Table 3, Fig. 20) and antigenically (Fig. 34G, Table 6), using p-amylase specific antiserum, no p-amylase protein was detected in chloroplasts. Since specific p-antiserum in this study can detect protein levels upto 10 pg, it is evident that the p-amylase is not present in pearl millet chloroplasts. p-amylase was also restricted to M cells and no extraplastidic p-amylase could be observed in B cells. Interestingly, in dark-grown leaves, p-amylase was nearly absent for above 5 days from sowing, while in light it was detectable right from initiation of leaf

expansion (Fig. 39A). Though, there is little information available regarding gene sequence of p-amylase, in barley (Kreis *et ed.*, 1988), mustard (Subbaramaiah and Sharma, 1989) and sweet potato (Nakamura *et ed.*, 1991) P-amylase has no N-terminal transport peptide that can lead its import to plastids. The p-amylase photostimulation was independent of chloroplast biogenesis, although NF lowered the magnitude of photostimulation of β-amylase (Fig. 15B).

In some species such as pea and wheat, p-amylase is localized in vacuole (Ziegler and Beck, 1986), and in mustard (Manga and Sharma, 1990), maize (Subba rao, 1992) pea, wheat, Spinach, (Ziegler and Beck, 1986) p-amylase is extraplastidic in nature. The physiological function of extraplastidic p-amylase is questionable (Monroe and Preiss, 1990). It has been observed that *Arabidopsis* mutants, which overproduces starch (Casper *et al.*, 1989; Monroe and Preiss, 1990), or are starchless, have highly elevated level of p-amylase in leaves. However, the elevation of p-amylase level was seen only in mutants exposed to 12 h photoperiod but not in the one grown under continuous light.

The reasons why absence as well as over-production of starch, both increase the level of p-amylase protein is not yet known. Since in *Arabidopsis* leaves, p-amylase activity is light regulated, it should have an important function, but in the absence of starch in cytosol, it is illogical to have an enzyme in an compartment with no substrate. One suggestion has been that perhaps the enzyme acts as a synthetic enzyme *in vivo* (Manners, 1985). There have been a few reports of the presence of soluble glucans in cytosols of a few species (Steup, 1988; Yamada *et al.*, 1986), which may perhaps be substrates

for β-amylase and other extraplastidic starch degrading enzymes. Moreover, in species where β-amylase is located in the vacuole of leaves, a new role for it will have to be looked for. Lizotte *et al.*, (1990) have speculated that vacuolar β-amylase may participate in hydrolysis of maltodextrins stored in vacuole. Since the mutants deficient in β-amylase like soybean (Adams et al., 1981), and rye (Daussant *et al.*, 1981), do germinate normally, it has been taken as evidence for the nonessential role of β-amylase in plants. However, this view is negated by the observation that, since in storage tissues β-amylase, being a storage protein, accumulates 100-500 fold excess amounts, even after a great reduction in its level, the residual level is sufficient for degradation of starch in mutant leaves (Sopanen and Laurière, 1989).

5.1.11 Photostimulation of ∝-amylase and β-amylase in leaf follows different gradients

Cereal leaves are an ideal system for studying the developmental gradients because each leaf contains a full spectrum of development by virtue of basal meristem. Since different cells of cereal leaves are developmentally distinct, the observed increase in amylolytic activity of pearl millet leaves is in reality a total of differential alteration in amylase level in the whole leaf. Strictly speaking, the analysis of photostimulation of amylase activity in whole leaf extract does not distinguish if a particular cell type or cells of a particular region respond more or less to RL exposure. Moreover, ∝-amylase being a plastidic enzyme, its photostimulation may be dependent on development of chloroplast, which itself follows a distinct gradient of development from base to tip. The electron micrograph of plastids from cereal leaves shows a

progressive chloroplast development from base to the tip of leaf (Wellburn *et al.,* 1986), where at base only proplastids are present which in dark-grown leaves differentiate to etioplast, whereas in light-grown leaves the plastids develops to chloroplast (Rebeiz and Rebeiz, 1986). Additionally, pearl millet leaves possess dimorphic chloroplasts and the chloroplasts of the B are structurally and functionally different from M chloroplasts.

In pearl millet leaves, the extent of photostimulation of amylase in leaf is determined by cellular position; in dark the amylolytic activity gradually increases from base to the tip of leaf, whereas in contrast in light a maximal amylase activity is in the 2nd segment from base and then activity declines towards the tip (Fig. 25). Evidently, the observed photostimulation gradient arises as a consequence of cellular sensitivity gradient to respond to the light signal and a similar gradient has been observed, e.g., the gradient of photostimulation of chlorophyll a/b binding protein synthesis in barley leaves (Zielinski *et al.,* 1989).

5.1.12 β-amylase Gradient

Since amylolytic activity of pearl millet leaf comprises ∝-amylase and β-amylase, the effect of light on gradient of β-amylase activity was independently analyzed. The identity between profiles of β-amylase and total amylase gradient indicates that the observed photostimulation gradient of total amylase activity basically represents photostimulation of β-amylase activity, which is in conformity with β-amylase being the major amylase in pearl millet (Fig. 27). Determination of gradient of β-amylase induction by cellular position is further

confirmed by the observation that in leaves transferred from dark to light, the photostimulation gradient is similar to light-grown leaves (Fig. 26).

Quantification of p-amylase protein along the length of the light-grown leaf correlated with the observed gradient in p-amylase activity and a maximal level of p-amylase protein was detected in the 2nd segment from base. In subsequent segments, a gradual decrease in p-amylase protein content also correlated with the decrease in p-amylase activity. In dark-grown leaves a different pattern was obtained, wherein p-amylase protein gradually increased towards the tip of the leaf (Fig. 41 A). It is evident that the distribution pattern of p-amylase in pearl millet leaf is strongly influenced by light, and unlike ∝-amylase gradient (see below), where light only quantitatively stimulated ∝-amylase activity but did not alter the gradient, light changed the p-amylase gradient pattern in leaf. Like pearl millet, in barley leaves also, p-amylase was also concentrated in the basal half of the leaf and was localized in the extrachloroplastic compartments.

The effect of light on p-amylase induction was also investigated by studying the rates of *in vivo* synthesis of p-amylase in different segments. In light-grown seedlings, p-amylase synthesis was very high in the first two basal segments of the leaf and then sharply declined in subsequent segments towards the tip. In contrast, the rate of p-amylase synthesis was quite low in leaf segments of dark-grown seedlings (Fig. 42). Evidently, the observed photostimulated increase in p-amylase protein level in basal segments results from light-mediated increase in de novo synthesis of p-amylase. A similar correlation between increase in p-amylase activity and in *vivo* synthesis rates

was also observed in mustard cotyledons (Sharma and Schopfer, 1987; Subbaramaiah and Sharma, 1989). The possible mechanisms determining β-amylase gradient are discussed in a later section.

5.1.13 ∝-amylase Gradient

Pearl millet leaf possess a continuous gradient of plastids in different stages of development right from proplastid at base to mature dimorphic chloroplasts to the tip of the leaf. Analysis of ∝-amylase distribution in leaf segments revealed a clear association between the development of chloroplasts and plastidic ∝-amylase. Basal segments, where chloroplast is still undifferentiated, lack ∝-amylase activity and ∝-amylase activity can be conclusively detected only from the 3rd segment from leaf base, with a continual increase towards the leaf tip (Fig. 28). Though the ∝-amylase gradient is similar in light and dark grown leaves, in light the ∝-amylase increase was more pronounced than the corresponding dark control. Like β-amylase, the distribution of ∝-amylase activity in leaf segments was also identical to distribution of its protein (Fig. 41B). Moreover, the observed appearance and the increase in the level of plastidic isoform in light-grown leaves from the 3rd segment closely correlated with the increase in the level of ∝-amylase protein. Both in dark and light-grown leaves no ∝-amylase protein could be detected in the first two segments of leaf.

Surprisingly, the gradient of ∝-amylase synthesis was very different from the observed gradient of ∝-amylase protein in the leaf. While the ∝-amylase protein could not be detected in basal segments (Fig. **41B),** *in vivo*

labelling (Fig. 43) showed that the basal two segments are most actively engaged in oc-amylase synthesis. Furthermore, whereas oc-amylase synthesis declined towards the leaf tip, the accumulation of oc-amylase protein level was more towards the tip of the leaf.

This discrepancy between gradient of ∝-amylase synthesis and accumulation of ∝-amylase protein may arise via several possible ways. It is possible that the level of ∝-amylase protein in apical segment is elevated by either increased synthesis or decreased turnover. However, the possibility of increased synthesis of ∝-amylase in apical segment is clearly ruled out, as ∝-amylase synthesis is higher in basal segments, therefore it is more likely that in the apical segments, reduced degradation of oc-amylase causes increase in oc-amylase protein level. Therefore, in apical segments, though the rate of oc-amylase synthesis is low, but due to lack of enzyme turnover its level increases. While the mechanism responsible for reduced turnover of cytosolic oc-amylase is not known, the plastidic amylase may be protected from turnover by virtue of this import in chloroplast. In pearl millet, appearance of plastidic oc-amylase intimately depends on chloroplast's differentiation, and though basal segments actively produce oc-amylase protein, in the absence of functional chloroplast it is degraded (Fig. 29B). The possibility of accumulation of latent oc-amylase protein in basal segments is however ruled out, as using SRID, no oc-amylase protein was detected in these segments.

A role of chloroplast in determining accumulation of plastidic oc-amylase is clearly apparent in pearl millet as NF-mediated loss of plastid also destroys plastidic oc-amylase. Although light can stimulate ∝-amylase synthesis, it

cannot accumulate without chloroplasts. It is likely that the lack of differentiated chloroplasts in basal segments causes failure of ∝-amylase protein accumulation in basal segments. Interestingly, the appearance of ∝-amylase in leaf correlates well with acquisition of Rubisco and the capability of chloroplasts to generate starch in chloroplast. The dissimilarity between the gradient of plastidic ∝-amylase and cytosolic p-amylase activity, clearly indicates that though both enzymes are regulated by phytochrome, the signal chain regulating their increase operates independently. In monocot leaves, such a dissimilar gradient is also observed in barley leaves, where gradient of chl a/b binding protein accumulation followed a gradient similar to p-amylase; the Rubisco gradient was similar to ∝-amylase, although both proteins are localized in plastids (Zielinski *et al.*, 1989).

5.1.14 Cellular position determines photosensitivity to light

The presence of a distinct gradient of p-amylase photoinduction in light-grown leaves, where leaf cells in proximity to basal meristem respond maximally to light by stimulating p-amylase activity by several folds, and sluggish response of cells towards the tip to light, implied that the observed gradient results due to a predetermined photosensitivity gradient in the leaf. The existence of the above gradient is internally regulated via developmental homeostasis, which is evident by the fact that leaves transferred from darkness to light also show a photostimulation pattern, similar to the leaves grown under continuous light (Fig. 26). It was observed that pearl millet leaves are maximally photosensitive to p-amylase induction between 3-8 days (Fig. 30), before a decline starts, and it is likely that during this period observed changes

in β-amylase level may result due to increase/decrease in cellular sensitivity of leaf cells with respect to β-amylase photoinduction.

The analysis of photostimulation gradient of β-amylase activity revealed that in the young leaf for first 2 d, i.e., 3rd and 4th day from sowing, the photosensitive gradient is acropetal with maximal sensitivity at or near the tip of the leaf (Fig. 30). The observed photosensitivity gradient is established at the 5 d with the 2nd segment close to base being the most photosensitive, and with age the magnitude of photoinduction in this segment increases with a maximal stimulation on the 8th day. Interestingly, after 8 days, though decline in β-amylase starts, there is no alteration of photosensitivity gradient, except that the magnitude of photoinduction in the 2nd segment is considerably lower. It is evident that a cellular positional signal determines this photosensitivity gradient in pearl millet leaves. The molecular nature of factors controlling this positional determination is still not known (Fig. 30).

Since the position of a cell once formed in pearl millet leaf continually shifts away from the base due to cell division at base, the alteration of cellular position has a distinct influence on β-amylase enzyme in a given leaf segment. In leaf segments 1-3 (from the tip) which are present from the 3rd day, p-amylase activity continually declines, with the shift in the position of segment in relation to base (Fig. 31). In segments 5-9, the photosensitivity of a segment became maximal when it was 2nd segment from base, but thereafter with further shift there is a gradual decline in β-amylase activity (Fig. 32). The overriding influence of cellular position on photostimulation of β-amylase is evident from the fact that as segments become distant from the base, β-

amylase activity also declines. In pearl millet, a given segment of leaf accumulates a maximal level of β-amylase protein in the basal segment where its synthesis is more intense (segment 1-3) (Fig. 41), and thereafter its level declines, due to a continuous turnover of protein, as the segment is shifting away from the base. Additionally, the positional effect of the basal segments on photostimulation of p-amylase is temporally determined and, in general, the basal segments, of leaf are most sensitive during 5-9 days (Fig. 30).

It is likely that in the 2nd segment, where an intensive cell differentiation takes place, cell differentiation may itself be the determinant of observed photosensitivity to p-amylase induction. In wheat leaves, the level of a homologoue of cell cycle control protein p^{34cdc2} controlling cell division was maximal at 1 cm from the leaf base and its level declined gradually to a low level. After 4 cm from base of leaf its level was the same in all segments, whereas in the same leaf Rubisco appeared only after a distance of 28 mm from leaf base (John *et al.*, 1990). The similarity between p-amylase photoinduction and gradient of cell cycle regulating proteins is indicative of a probable role of cell division and differentiation in determining observed photosensitivity gradient of p-amylase. This view is also supported by the observation that the responsiveness to hormone-promoted cell division in wheat leaf is similarly determined by cellular position, and the cell, increasingly distinct from meristem, is unable to resume cell division even after administration of auxins even though all cells of the leaf possess equal rates of uptake and metabolism of auxins (Wernicke and Milkovitz, 1987a,b). The basal segment of the monocot leaf is also metabolically highly active due to the

ongoing process of cell division and differentiation. Analogous to cell cycle proteins, maximal transcription of mitochondrial genes are also localized at the base of wheat leaf and decline sharply within 2 cm from leaf base. Interestingly, mitochondrial transcripts, follow a dramatically opposite gradient from rbcL transcript in the same leaf which encodes a plastidic protein (Topping and Leeve, 1990).

The use of illumination to express positional information has been studied in dark-grown maize leaves, where in leaf cells Rubisco is present in both M and B cells but after exposure to light, Rubisco protein is turned over in M cells and is restricted only to B cells (Sheen and Bogorad, 1987). It is evident that illumination is an essential component in expression of positional information, which is needed to suppress Rubisco in M cells of C_4 plants, and likewise in this study, illumination is needed to express positional influence of basal segment on photostimulation of β-amylase. It is of interest to note that such a expression may be dependent on light intensity, because in monocot leaf developed under low light accumulated C_3 enzymes and Rubisco, while leaves grown under high light intensity showed typical gradients of Rubisco and PEP carboxylase (Usuda *et al.*, 1985; Langdale *et al.*, 1988). Additionally, cell specific expression of C_4 enzymes is also determined by the proximities to the vein (Langdale et al.. 1989).

In summary, it is evident that though the molecular mechanism regulating positional effect on β-amylase photostimulation is not known, similarity of its photoinduction to another cytosolic starch degrading enzyme, phosphorylase (which is discussed in a later section) indicates that the same

mechanism may be operating to determine the gradient of several cytosolic proteins.

5.2 PHOSPHORYLASES

In higher plants, phosphorylase acts as a major enzyme participating in degradation of starch, particularly in photosynthetic tissue. Though phosphorylase acts both as a glucan-degrading as well as a glucan-synthesizing enzyme (Beck, 1985), in plants *in vivo* it primarily acts as a degradative enzyme. (Stitt *et al.*, 1978; Stitt and Heldt, 1981; Stitt and Steup, 1985). In this study the relationship between level of phosphorylase with the photomorphogenic development of leaves was analyzed in detail.

5.2.1 No apparent photoinduction of phosphorylase was observed in leaves

In pearl millet, nearly equal phosphorylase activity was present in different organs of both light and dark-grown seedlings. In general, leaf and coleoptile possessed nearly 3 times higher activity in comparison to roots or seeds (Fig. 49). Since, in seeds, amylolytic activity is about 5-fold higher than in leaves, and in leaf, phosphorylase activity is higher than amylase, it is possible that phosphorylase may have a greater role to play in degradation of transitory starch in leaf.

The profile of time course of phosphorylase activity during leaf development was qualitatively similar to that of amylases, showing a steady rise in phosphorylase activity with a peak on the 7th day and with a

subsequent decline (Fig. 50B). Unlike amylases there was no photostimulation of phosphorylase activity, and both in dark and light, phosphorylase activity profiles were identical. Since pearl millet leaves develop from continuous cell division of a basal meristem, the observed increase in phosphorylase level is likely to be due to a de novo synthesis of enzyme, and after the 7 d, either the process of degradation predominates over the constant rate of synthesis, or new synthesis may be inhibited.

The role of light in phosphorylase induction has not been much investigated. It is observed that light modulates phosphorylase activity by altering the ratio of inorganic phosphate availability during day and night leading to diurnal fluctuations in the activity (Preiss, 1984). Pongratz and Beck (1978) showed that in the chloroplast no diurnal oscillations of phosphorylase was observed, when enzyme was assayed in the presence of saturating inorganic phosphate alone. In maize, continuous illumination of leaf triggered a significant increase in phosphorylase activity (Downton and Hawker, 1973). Although in this study no photostimulation of phosphorylase was observed, it is plausible that since phosphorylase consists of 2 isozymes which may respond to light differentially, the estimation of total phosphorylase activity is not suitable to judge the relative contribution of these 2 phosphorylases.

5.2.2 Cytosolic and plastidic phosphorylases are located in different cellular compartments

In pearl millet seedlings, while leaves possessed 2 phosphorylase isozymes, in other organs such as seed, root, mesocotyl only one isozyme was

present (Fig. 55). The existence of 2 phosphorylase isozymes in leaf, out of which one was common to other organs, indicated that the leaf-specific isozyme may be plastidic in nature. Two phosphorylase isoforms have been observed in roots and etiolated shoots of spinach (Steup *et al.*, 1987; Steup and Latzko, 1979), and it has been shown that plastidic phosphorylase is associated even with amyloplasts (in developing seeds) and with proplastids (in germinating seeds) of pea seedlings (Berkel *et al.*, 1991). Plastidic localization of phosphorylase has also been reported in spinach (Schachtele and Steup, 1986), pea (Berkel et al 1991), and corn (Mateyka and Schnarrenberger, 1988).

The plastidic localization of the above enzyme was confirmed by Norflurazon treatment, which in light-grown seedlings, totally eliminates the leaf-specific form of phosphorylase (Fig. 52B). Since the above isozyme is also present in etioplasts of dark-grown plants (Fig. 52C,D), the synthesis and plastidic localization of this phosphorylase isozyme is independent of chloroplast biogenesis. However, the functional integrity of chloroplast is needed to maintain the activity of the above enzyme inside the chloroplast. Therefore, NF-mediated photooxidation of chloroplast, which extensively damages the thylakoid and destroys the internal architecture of chloroplast (Oelmuller, 1989), also causes irreversible loss of plastidic phosphorylase activity. Whether the above loss of chloroplastic phosphorylase is caused by suppression of its synthesis or import into chloroplast is not known.

Pearl millet, being a C_4 plant, is endowed with compartmentalization of carbon fixation during photosynthesis, with carbon flow from mesophyll to bundle sheath cells. The studies on intercellular distribution of phosphorylase

in pearl millet leaves revealed that phosphorylase activity was present in both bundle sheath cells and mesophyll cells (Table 8). Electrophoresis of phosphorylase from bundle sheath and mosophyll cells showed that each of these cellular types possessed a specific isozyme of phosphorylase. The cytosolic phosphorylase was clearly associated with mesophyll (Fig. 53D) and the plastidic one was associated with the bundle sheath (Fig. 53A). It was further confirmed by isolating chloroplasts from BS cells (Fig. 53C), which showed only the fast-migrating isozyme of phosphorylase which was totally absent in mesophyll chloroplasts (Fig. 53, lane B).

Similarly, in corn too, fast-migrating phosphorylase isozyme was associated with bundle sheath chloroplasts, and slow-migrating phosphorylase isozyme was present in mesophyll cytosol (Mateyka and Schnarrenberger, 1984; 1988). Since plastid and cytosolic phosphorylase are located in different cellular compartments and follow different photoregulation gradients, it is self evident that the cytoplasmic enzyme is not a precursor of the chloroplast enzyme and the two enzymes are not derived from a single gene.

5.2.3 Light alters distribution of phosphorylase in leaves

Pearl millet leaf possess a gradient of cells of different maturity, with an associated gradient of chloroplast maturity towards the tip. Since phosphorylase is localized both in plastid and in cytosol, its distribution was analyzed along the leaf axis. Interestingly, while the time course of phosphorylase activity in dark and light-grown leaves was similar, the distribution of phosphorylase along leaf axis was significantly different. The

distribution of total phosphorylase activity in dark-grown leaf was somewhat similar to amylase distribution which also increased towards the leaf tip. In contrast, in light-grown leaves, phosphorylase activity increased from base and peaked at the third segment from the base and then in the subsequent section, declined to a level lower than that in the dark control (Fig. 56). Since the distinctive pattern of phosphorylase distribution was the same in light and dark-grown leaves, on segment or on total protein basis, it is evident (Fig. 56A,B) that the decline of phosphorylase activity towards the leaf tip in light-grown leaves is not due to an elevated level of plastid proteins in the tip.

It is a coincidence that while the total phosphorylase activity in dark and light-grown leaf is nearly equal, the influence of light on phosphorylase activity is clearly evident in individual segments. However, if phosphorylase activity of each segment is combined, the total phosphorylase activity of the dark-grown leaf is nearly equal to that of light-grown leaves, generating an impression that light does not influence the phosphorylase activity in pearl millet leaves (Fig. 56A). Evidently, the effect of light on phosphorylase activity is masked by using whole leaf for enzyme extraction, even though different segments of leaf do respond differently to photostimulation of phosphorylase.

5.2.4 Cytosolic and plastidic phosphorylase show a distinct gradient of distribution in dark grown leaves

The pattern of phosphorylase distribution however has also to take in account the relative distribution of plastidic/cytosolic phosphorylase in bundle sheath and mesophyll cells. In dark-grown leaves, the isoform belonging to

both cytosolic and plastidic phosphorylases could be detected in all segments of the leaf. The relative level of these isoforms depended on their positional localization, the cytosolic isoform decreased in relative abundance in the last two segments near the tip, whereas in the same segments, plastidic isoform was more abundant (Fig. 59, inset). The suppression of cytosolic isoform and increase of plastidic isoform in the tip indicated that the relative level of cytosolic/plastidic phosphorylase isoform even in darkness is independently determined by positional location.

The accumulation of etioplastic phosphorylase towards the tip may result from a lack of any active turnover mechanism to degrade phosphorylase in plastids. In contrast, the cytosolic phosphorylase may have higher rates of synthesis near the basal segments with its degradation predominating towards the tip, which would account for its observed gradient in the leaf. Essentially, the positional influence of both cytosolic and plastidic phosphorylase is also determined by their location in different intercellular and subcellular compartments. Interestingly, although plastidic phosphorylase is located in BS cells, it accumulates even in the basal segment of dark-grown leaves, where differentiation into kranz anatomy and chloroplast is not yet complete.

5.2.5 Light promotes cytosolic phosphorylase and inhibits plastidic phosphorylase in basal segments of leaves

The distribution of phosphorylase isoforms in light-grown leaves was different than in dark grown-leaves. A distinct suppression of plastidic isoform by light is seen in the basal segments of leaf, where it is well below the limit

of detection by electrophoresis. No isoform of plastidic phosphorylase could be detected in the first three segments of light-grown leaves, and it appeared only in the 4th segment, and then its level increased towards the tip of the leaf. In contrast, the level of cytosolic phosphorylase is quite high in the basal segments, showing a maximal activity in the 3rd segment, and then its level gradually declined towards the tip. In the tip of light-grown leaves, plastidic phosphorylase is more dominant than the cytosolic one (Fig. 58, inset). A comparison of the relative levels of phosphorylase isoform and its activity, clearly indicates that the observed pattern of total phosphorylase activity in pearl millet leaves is strikingly similar to distribution of cytosolic isoform, because cytosolic isoform contributes to about 80% to total phosphorylase activity in light-grown leaves. It is evident that in pearl millet leaves, light plays a dual role, in the basal segments it suppresses the plastidic form and promotes an induction of the cytosolic form, in segments close to the tip, it suppresses the cytosolic form but is ineffective in suppressing chloroplastic phosphorylase activity.

The mechanism by which the above pattern of phosphorylase distribution is generated is at the moment unknown, but it is likely that light-stimulated cytosolic phosphorylase induction is restricted to the first three segments, and in subsequent segments perhaps the degradation or turnover of cytosolic enzyme predominates over its synthesis. On the other hand, plastidic phosphorylase induction is either suppressed in the first three segments, or in the presence of light, a certain state of chloroplast

differentiation is required before light can act on its synthesis or import in plastids.

The distribution of distinct phosphorylase in isolated mesophyll and bundle sheath cells highlights the effect of light on phosphorylase activity in the leaves. No plastidic phosphorylase activity was present in bundle sheath cells isolated from the first three basal segments of leaves, it appeared only in subsequent sections. By contrast, the total activity of cytosolic phosphorylase closely followed phosphorylase activity of mesophyll cells and subsequently declined (Fig. 61). These results too are indicative of a requirement of plastid differentiation to import plastiduc phosphorylase into BS chloroplasts.

It has been reported that in pea, plastidic phosphorylase may consist of 2 isoforms, one associated with etioplasts, and another one with chloroplasts (Berkel *et al.*, 1991). It is likely that in pearl millet too such etioplastic and chloroplastic may exist, and a suppression of the etioplastic and stimulation of the chloroplastic phosphorylase alter phosphorylase activity; but existence of such specific phosphorylase in pearl millet leaves is yet to be confirmed. The effect of light on phosphorylase like amylase, is also determined by the cellular position, that is, the suppression of plastidic phosphorylase and induction of cytosolic enzyme in the basal segments illustrates that it is the cellular position which is a primary determinant of phosphorylase expression in a particular cells, and light simply acts as a modulating agent. The relative amount of phosphorylase in plastid and cytosol fraction has been studied only in the case of pea cotyledon, where, during germination, plastidic enzyme

remained at a constant level, while the level of cytosolic enzyme increased several-fold (Berkel *et ai.,* 1991).

In general, the results obtained above for plastidic phosphorylase are typical of plastidic enzymes in monocot leaves which show a gradient of accumulation of plastidic proteins towards the tip of the leaf (Rubisco). On the other hand, restriction of photoinduction of cytosolic phosphorylase to the base of the leaf, is clearly akin to β-amylase gradients which also show a maximal induction near the base of the leaf.

5.3 FUNCTIONAL ROLE OF STARCH DEGRADING ENZYMES IN LEAVES

5.3.1 Extraplastidic enzymes

The logic behind the existence of starch degrading enzymes in extraplastidic compartments has so far not been understood. In this study, ∝-amylase, β-amylase and phosphorylase were observed in extraplastidic compartments of pearl millet leaves. In general, these enzymes were present only in M cells, and in B cells, the level of these extraplastidic enzymes was below the limit of detection. In literature there are reports showing localization of ∝-amylase in apoplast (Beers and Duke, 1988), and β-amylase in vacuole (Ziegler and Beck, 1986). In pearl millet these enzymes are extraplastidic but their association with a particular subcellular fraction has not been determined. Since the photoregulation gradients of cytosolic β-amylase and phosphorylase along the axis of leaf in light-grown plants are distinctively similar, it may have some hitherto unknown function. In general, while several

functions have been ascribed to cytosolic enzymes in other systems (see review), evidence is rather fragmentary, and more work still needs to be done to understand the function of cytosolic starch degrading enzymes in leaves.

5.3.2 Plastidic enzymes

In C_4 plants transitory starch is generated and stored in the B chloroplasts, therefore the exclusive presence of phosphorylase in B chloroplast, clearly indicates that it plays an important role in starch degradation in a C_4 plant like pearl millet. Hammond and Preiss (1983) suggested that the chloroplastic phosphorylase contributes a major part in degradation of photosynthetic starch. However, in spinach under optimal conditions, assimilatory starch is a very poor substrate for the chloroplastic phosphorylase (Beck, 1985). However, the same can be hydrolyzed efficiently by the action of ∝-amylase (Chang, 1982). Therefore it has been suggested that phosphorolysis rather than amylolysis plays a major role, but the initial steps of degradation are mediated by ∝-amylase (Okita and Preiss, 1980; Steup et al, 1983). Ghiena et al (1993), on the basis of the presence of a 5-fold higher phosphorylase activity than amylase in Vicia fab a chloroplast, suggested that phosphorylase is involved in amylose degradation. Since, in pearl millet, both ∝-amylase and phosphorylase activities are present in B chloroplasts, it is evident that these enzymes may combinedly participate in the degradation of transitory starch. In general, *in vivo* metabolic state of chloroplasts is more favorable for phosphorylase action on starch (Beck, 1985) and its activity may be modulated by Pi concentration in the chloroplast (Kaiser and Urbach, 1977; Lilley *et al.*, 1977). Such a view is supported by the observation that in sugar beet, glucose-1-

phosphate level was high, during the period of active starch degradation (Servaites *et al.,* 1989). In spinach too, starch is likely to mobilize via phosphorolytic pathway in chloroplast, as breakdown products of starch constitute of glucose-1-phosphate, maltose and glucose (Levi and Gibbs, 1976; Stitt and Heldt, 1981). While a significant amount of phosphorylase products was found in pea chloroplasts (Levi and Priss, 1978; Stitt and Heldt, 1981). Ziegler and Beck (1986) reported that the ∝-amylase contribution was more in pea chloroplasts. However, amylolysis of starch results in the formation of degradation products, on which phosphorylases act four times more effectively than on the starting material (Steup *et al.,* 1983; Chang, 1982).

It is generally assumed that the ∝-amylase initiates, or at least plays a key role, in transitory starch degradation (Beck, 1985; Preiss and Levi, 1980). The presence of a-amylase in chloroplast suggests that it plays an important role in starch mobilization. The localization of higher oc-amylase activity in B chloroplasts might be linked to the fact that in C_4 plants, starch is located in B chloroplast. Therefore B chloroplasts need to possess more a-amylase activity than M chloroplasts. This localization of plastidic a-amylase in chloroplast is also consistent with the model for starch breakdown in higher plants proposed by Dunn (1974). According to this model, a-amylase is the only enzyme capable of initiating the digestion of starch granule *in vivo* which is then digested by other enzymes.

The mechanism by which starch degrading enzyme activity in B chloroplasts may be regulated is not known and can be only speculated. Amylolytic starch degradation is regulated by means of pH shifts in the stroma

(Werdan *et al.*, 1975). Amylases exhibit acidic pH optima (Chapman *et al.*, 1972; Thoma *et al.,* 1971). At pH 8, which is the stromal pH upon illumination (Werdan *et al.,* 1975), amylase activity was inhibited roughly by 80%. At pH 7 which is stromal pH of darkened chloroplasts, inhibition was found to be only 50%. Pongratz and Beck, (1978) reported that amylolytic activity was almost twice as high in chloroplasts prepared during the dark phase and only low amylolytic activity was observed in chloroplasts isolated during the light phase. Since plastidic ∝-amylase has a pH optima of about 6.2, it may be possible that the observed pH shift in chloroplast may control the diurnal oscillation of plastidic ∝-amylase activity by controlling plastidic starch mobilization (Pongratz and Beck, 1978).

The notion that only oc-amylase is capable of hydrolyzing native starch granules, is been recently challanged. Sun and Henson (1991) reported that ∝-glucosidase is also capable of initiating degradation of native starch granules. A combination of ∝-glucosidase and ∝-amylase acts synergistically and degrades starch granules 8-11 times further than the sum of these enzymes alone (Sun and Henson, 1991). The role of oc-amylase in degradation of photosynthetic starch has also been questioned by Casper *et al.,* (1989), who isolated a *Arabidopsis* mutant which, lacked the capacity to degrade starch even though it had oc-amylase activity equal to the wild type. They suggested that an unknown factor other than oc-amylase is involved in starch degradation. Similarly, in pea chloroplasts, the presence of oc-amylase is equivocal (Beers and Duke, 1990) notwithstanding earlier reports of Kakefuda *et al.,* (1986) and Ziegler, (1988) who could detect oc-amylase in pea

chloroplasts. Moreover, starch is not essential for growth and development of plant as starchless mutants of *Arabidopsis* (Casper *et al.*, 1985; Lin *et al.*, 1988) survive and complete their life cycle normally if grown under controlled conditions.

In summary, in pearl millet leaves, both ∝-amylase and phosphorylase together play a role in degradation of photosynthetic starch. The coexistence of ∝-amylase and phosphorylase in B cell's chloroplasts is an indication of the cooperative function of these enzymes in transitory starch degradation in leaves. The exclusive localization of phosphorylase in B plastids also emphasizes the importance of phosphorylase in mobilization of photosynthetic starch produced in B chloroplasts.

The similarities in gradients of plastidic phosphorylase activity and ∝-amylase activity in light-grown leaves, which also correlates with appearance functional differentiation of chloroplasts and their capacities to fix CO_2, is a clear proof of the role of these enzymes in degradation of transitory starch. Interestingly, while in etioplasts no ∝-amylase was present, phosphorylase activity in etioplasts could be clearly detected, which may be associated with the presence of starch in the plastids of dark-grown leaves in basal segments (Wellburn *et al.*, 1986).

While in different system the relative importance of phosphorylase or amylase on starch degradation (Levi and Preiss, 1978, Beck, 1985) have been emphasized, in the present study, it has not been possible to distinguish between the relative importance of these two enzymes. However, since ∝-

amylase activity is in general lower than that of plastidic phosphorylase, it is likely that after an initial degradation of starch granules by ∝-amylase, phosphorylase plays a major role in starch metabolism.

5.4 CONCLUSIONS

In pearl millet leaf the distribution of both amylase and phosphorylase is strongly dependent on three factors in the following hierarchical order, cell position, organelle development and light. In dark grown leaf, extraplastidic β-amylase gradient existed with an increase from base to tip and light altered it with a maxima close to basal segment, by stimulating the rate of p-amylase synthesis in basal segments. The development of plastidic ∝-amylase activity depended on chloroplast biogenesis, which was evident by the fact that though at the leaf base rate of ∝-amylase synthesis was quite high, the accumulation of ∝-amylase protein took place only in those cells where chloroplast differentiation had taken place. Similar to β-amylase, light also enhanced activity of cytosolic phosphorylase and this photostimulation was restricted to the leaf base. In contrast, light suppressed accumulation of plastidic phosphorylase in etioplasts in the basal region of leaf and plastidic phosphorylase was present only in bundle sheath chloroplasts from middle of leaf to leaf tip.

SUMMARY

CHAPTER 6

SUMMARY

In the present study, attempts have been made to decipher the interaction between chloroplast development and photoregulation of starch degrading enzymes in pearl millet (Pennisetum americanum) leaves, a NADP-ME type C_4 plant. Since the morphogenetic development of leaf and chloroplast biogenesis both intimately depend on the availability of light, the interrelationship between leaf development, chloroplast biogenesis and photoregulation of cytosolic and plastidic starch degrading enzymes viz., amylases and phosphorylases was investigated, during development of pearl millet seedlings.

In pearl millet (Pennisetum americanum) seedlings light acting via phytochrome stimulated amylase activity in the leaves. This photostimulation mainly results from an enhancement in β-amylase activity, which constituted 80-90% of leaf amylase activity. The native PAGE followed by specific staining for ∝- and β-amylase, by contact printing on amylose or β-limit dextrin containing gel, revealed that these enzymes had different Rf values of 0.21 and 0.71 respectively. Isolated chloroplasts possessed only ∝-amylase and appearance of plastidic ∝-amylase was obligatorily dependent on chloroplast biogenesis. The subcellular and intercellular fractionation studies revealed that, while β-amylase was localized only in the extraplastidic compartment, ∝-amylase was localized both inside the chloroplasts and in the extraplastidic compartment. The mesophy 11 cells contained both ∝- and p-amylase activities but only ∝-amylase activity was detected in the bundle sheath cells.

Norflurazon mediated photooxidation of chloroplasts during leaf development also eliminated plastidic ∝-amylase activity confirming dependence of its photoregulation on the chloroplast biogenesis.

An analysis of photostimulation of amylase along the leaf axis revealed that the segment proximal to the leaf base shows the maximum photostimulation of cytosolic p-amylase. In contrast, photoinduction of plastidic ∝-amylase was intimately dependent on chloroplast biogenesis and followed a gradient akin to the light dependent chloroplast development. The gradient of ∝- and p-amylase activity in leaf also paralleled with respective isozyme gradients in both light and dark grown seedlings.

The effect of light on stimulating amylase synthesis was monitored by using polyclonal $\propto_1$-, $\propto_2$- and p-antiseras raised against maize amylases. Monospecificity of $\propto_1$-antiserum and p-antiserum antibodies was ascertained by double diffusion, western blotting and immunoelectrophoresis. The usage of these antibodies confirmed the localization of p-amylase in mesophyll cytosol and of ∝-amylase in chloroplasts of both mesophyll and bundle sheath cells. Quantification of amylase protein by single radial immunodiffusion showed that the phytochrome mediated increase in p-amylase and ∝-amylase activity results from an increase in the level of the respective proteins.

The *in vivo* labelling of amylases with [S]-methionine and subsequent immunoprecipitation revealed that the increase in amylase activity resulted from an increase in the rate of de novo synthesis of amylase protein. *In vivo* radiolabelling and immunoprecipitation of p-amylase protein revealed that photostimulated increase in p-amylase synthesis was maximal in basal segments of leaf and correlated with changes in p-amylase protein level and

activity. In contrast, while the basal segment possessed high rates of ∝-amylase synthesis, significant level of ∝-amylase protein could not be detected in basal segments of leaf. It was assumed that in absence of functional chloroplasts newly synthesized ∝-amylase protein is rapidly turned over.

In pearl millet seedlings, no specific influence of light on the induction of phosphorylase activity in leaves was apparent. The electrophoresis of extracts from 7-d old leaves revealed the presence of two phosphorylase isozymes migrating at Rf value 0.24 and 0.28 respectively. The mesophyll cells possessed only slow migrating enzyme of phosphorylase which was localized in cytosol, whereas the bundle sheath cells possessed fast migrating isozyme of phosphorylase located in plastids. The appearance of plastidic phosphorylase was independent of chloroplast biogenesis and it was also present in proplastid and etioplast. The sustainment of plastidic phosphorylase activity needed functional integrity of chloroplast, as in Norflurazon treated seedlings, the photooxidation of chloroplast eliminated the plastidic phosphorylase activity. The correlation between phosphorylase and starch localization in bundle sheath chloroplasts indicates that phosphorylase plays a role in starch mobilization.

The distribution of plastidic and cytosolic phosphorylase along the axis of leaf was influenced by light. In dark grown seedlings, phosphorylase activity increased from base to tip of leaf, however, exposure to light altered the phosphorylase gradient in leaf, with maximal phosphorylase activity being in the third segment (3 cm) from the base. Light initiated a photoinduction of cytosolic phosphorylase in the base and middle of the leaf but caused a suppression towards the tip. Dark grown leaves possessed high levels of

plastidic phosphorylase activity with a gradient increasing from base to tip. In contrast, light repressed appearance of plastidic phosphorylase in the first three segments close to the base but was ineffective towards the tip of leaf.

In summary, this study highlights that the cell position is the primary determinant, and the organelle development is the secondary determinant regulating the activity of starch degrading enzymes, while light only acts as a modulating agent on activity of starch degrading enzymes in pearl millet leaves.

REFERENCES

Adams, C.A., Broman, T.H., Rinne, R.W. (1981) Starch metabolism in developing and germinating soyabean seeds is independent of β-amylase activity. Ann. Bot. **48:** 433-439

Akoyunoglou, G.A., Akoyunoglou, J.A. (1986). Post-translational regulation of chloroplast differentiation. In 'Regulation of chloroplast differentiation' (Eds.Akoyunoglu, G., H.Senger) pp. 571-582, Alan R. Liss, Inc.

Allen, J.R.F., Baker, DA. (1980) Free tryptophan and Indole-3-acetic acid levels in the leaves and vascular pathways of *Ricinus communis* L. Planta. **148:** 69-74

Aoyagi, K. Bassham, J.A. (1986) Appearence and accumulation of C_4 carbon pathway enzymes in developing maize leaves and differentiating maize A188 callus. Plant Physrol. 80: 322-33

Baker, N.R., Leech, R.M. (1977) Development of photosystem I and photosystem II activities in leaves of light grown maize (*Zea mays).* Plant Physiol. 60: 640-644

Bansal, K.C., Bogorad, L. (1993) Cell type preferred expression of maize Cab m-1: repression in bundle sheath cells and enhancement in mesophyll cells. Proc. Natl. Acad.Sci. USA **90:** 4057-4061

Bassiri, **A., Irish, E.E., Poethlg, R.S.** (1992) Heterochronic effects of Teopod 2 on the growth and photosensitivity of the maize shoot. Plant Cell. 4: 497-504

Batschauer, A., Mösinger, E., Kreuz, K., D6rr, I., Apel, K. (1986) The implication of a plastid-derived factor in the transcriptional control of nuclear genes encoding the light-harvesting chlorophyll a/b binding protein. Eur J Biochem. **154:** 625-634

Beck, E. (1985). The degradation of transitory starch granules in chloroplasts. In "Regulation of carbon partitioning in photosynthetic tissue". (Eds. R. Heath, J.Preiss), American society of plant physiologist, Rockville, pp. 27-44.

Beck, E., Ziegler, P. (1989) Biosynthesis and degradation of starch in higher plants. Ann. Rev. Plant Physiol. Plant Mol.Biol. **40:** 95-117

Beers, E.P., Duke, S.H. (1988) Localization of ∝-amylase in the apoplast of pea (*Pisum sativum* L.) stems. Plant Physiol. 87: 799-802

Beers, E.P., Duke, S.H. (1990) Characterization of ∝-amylase from shoots and cotyledons of pea *(Pisum sativum* L.) seedling. Plant Physiol. 92: 1154-1163

Berkel, V.J., Candras-Strauch, J., Steup, M. (1991) Glucan-phosphorylase forms in cotyledons of *Pisum sativum* L. Localization, developmental change ***in*** *vitro* translation and processing. Planta. **185:** 432-439

Bernfeld, P. (1955) Enzymes of carbohydrates metabolisms. Amylases ∝- and β-. Methods in Enzymology. 1: 149-158

Blume, D. E., McClure, J.W. (1980) Developmental effects of Sandoz 6706 on activities of enzymes of phenolic and general metabolism in barley shoots grown in the dark or under low or high intensity light. Plant Physiol. **65:** 238-244

Bonner, W. M. (1983) Use of fluorography for sensitive isotope detection in polyacrylamide gel electrophoresis and related technique. Method Enzymol. 96: 215-223

Bourne, E.J., Davis, D.E., Pridham, J.B. (1970) ∝-amylase activity in sugar cane *(Saccharum officinarum* L.) chloroplasts. Phytochem. 9: 345-348

Bradford, M.M. (1976) A rapid and sensitive method for the quantitation of microgram quantities of protein using the principal of protein dye binding. Anal.Biochem. 72: 248-254

Brisson, N., **Giroux, H., Zollinger, M., Camirand, A., Simard, C.** (1989) Maturation and subcellular compartmentation of potato starch phosphorylase. Plant Cell. 1: 559-566

Bruinsma, J. (1961) A comment on the spectrophotometric determination of chlorophyll. Biochem. Biophys. Acta. **52:** 576-578

Bureau, D., Lauriere, C, **Mayer, C, Sadowski, J.,** Daussant, J. (1989) Post translational modifications of β-amylase during germination of wheat and Rye seeds. J. Plant Physiol. **134:** 678-684

Burgers, D.G., Taylor, W.C. (1987) Chloroplast photooxidation affects the accumulation of cytosolic mRNAs encoding chloroplast proteins in maize. Planta **170:** 520-527

Bush, D.S., Sticher, L., van Huystee, R., Wagner. D., Jones, R.L. (1989) The calcium requirement for stability and enzymatic activity of two isoforms of barley aleurone a-amylase. J. Biol. Chem. **264:** 19392-19398

Casado, M., Martin, L., Nicolas, G., Villalobos, N. (1991) Regulatory role of phytochrome in the induction of ∝-amylase activity in excised chick-pea cotyledons. Plant Sci. **78:** 207-215

Casper, T., Huber, S.C., Somerville, C. R. (1985) Alterations in growth, photosynthesis, and respiration in a starchless mutants of *Arabidopsis thaliana* (L.) deficient in chloroplast phosphoglucomutase activity. Plant Physiol. 79: 11-17

Caspar, T., Lin, T-P., Monroe, J., Bernhard, W., Spilatro, S., Preiss, J. Somerville, C. (1989) Altered regulation of β-amylase activity in mutants of *Arabidopsis* with lensions in starch metabolism. Proc. Natl. Acad. Sci. USA **86:** 5830-5833

Chang, C.W. (1982) Enzymic degradation of starch in cotton leaves. Phytochemistry. **21:** 1263-1269

Chapman, G.W.Jr., Pallas, J.E. Jr., Mendicino, J. (1972) The hydrolysis of maltodextrins by β-amylase isolated from leaves of *Vicia faba*. Biochem. Biophy. Acta. **276:** 491-507

Chollet, R., Orgen, W.L. (1973) Photosynthetic carbon metabolism in isolated maize bundle sheath strands. Plant. Physiol. **51:** 787-792

Chory, J., Feinbaum, P.C., Pratt, L., Ausubel, F. (1989) *Arabidopsis thaliana* mutant that develops as a light-grown plant in the absence of light. Cell. **58:** 991-999

Chory, J. (1992) A genetic model for light-regulated seedling development in *Arabidopsis.* Development. **115:** 337-354

Chory, J., Nagpal, P., Peto, C.A. (1991) Phenotypic and genetic analysis of det 2, a new mutant that affects light-regulated seedling development in *Arabidopsis.* Plant Cell. 3: 445-459

Colbert, J.T.H., Hershey, H.P., Quail, P.H. (1983) Autoregulatory control of translatable phytochrome mRNA levels. Proc. Natl. Acad. Sci. USA. 80: 2248-2252

Conrads, J., van Berkel, J., Schchtele, C, Steup, M. (1986) Non chloroplast ∝-1,4-glucan phosphorylase from pea leavaes: Characterization and in situ localization by indirect immu-nofluorescence. Biochem. Biophys. Acta **882:** 452-463

Dale, J.E. (1992) How do leaves grow? Biosicence. 42: 423-432

Datta, R. (1992) M.Phil dissertation.

Daussant, J., Sbaszyniak, B., Sadowski, J., Wiatroszak, I. (1981) Cereal β-amylase immunochemical study on two enzyme deficient inbread lines of Rye. Planta. **151:** 176-179

Daussant, J., Laurière, C. (1990) Detection and partial characterization of two antigenically distinct β-amylases in developing kernels of wheat. Planta. **181:** 505-511

Daussant, J., Sadowski, J., Rorat, T., Mayer, C, Laurire, C. (1991) Independent regulatory aspects and post-translational modifications of two β-amylases of rye. use of a mutant inbred line. Plant Physiol. 96: 84-90

Davis, B. (1964) Disc electrophoresis. II Method and application to human serum proteins. Ann. N.Y. Acad. Sci. **121:** 404-427

Davis, B.D. (1984) Regulation of ∝-amylase activity in bean stem tissues. Plant Physiol. 74: 841-845

Day, D. A., Jenkins, C.L.D., Hatch, M.D. (1981) Isolation and properties of functional mesophyll protoplasts and chloroplasts from *Zea mays.* Aust. J. Plant Physiol. 8: 21-29

Deng, X-W., Casper, T., Quail, P.H. (1991) Copl: a regulatory locus involved in light controlled development and gene expression in *Arabidopsis.* Genes Dev. 5: 1172-1182

Deng, X-W., Matsui, M., Wei, N., Wagner, D., Chu, A.M., Feldmann, K A, Quail, P.H. (1992) Cop 1, an *Arabidopsis* regulatory gene, encodes a novel protein with both a Zn-binding motif and Gβ-protein homologous domain. Cell. 71: 791-801

Dengler, N.G., Dengler, R.E., Grenville, D.J. (1990) Comparison of photosynthetic carbon reduction (kranz) cells having different ontogenetic origins in the C_4 NADP malic enzyme grass *Arundinella hirta.* Can J Bot. 68: 1222-32

Dengler, N.G., Dengler, R.E., Hattersley, P.W. (1985) Differing ontogenetic origins of PCR (Kranz) sheaths in leaf blades of C_4 grasses (Poaceae). Am. J. Bot. 72: 284-302

Downton, **W.J.S., Hawker, J.** (1973) Enzymes of starch and sucrose metabolism in *Zea mays* leaves. Photochemistry. **12:** 1551-1556

Drumm, H., Elchinger, I., Moller, J., Peter, K., Mohr, H. (1971) Induction of amylase in mustard seedlings by phytochrome. Planta. 99: 264-274

Dunn, G. (1974) A model for starch breakdown in higher plants. Phytochem. 13: 1341-1346

Echeverria, E., Boyer, CD. (1986) Localization of Btarch biosynthetic and degradative enzymes in maize leaves. Amer. J. Bot. **73** (2):167-171

Esau, K. (1943) Ontogeny of the vascular bundle in *Zea mays.* Hilgardia. 15:327-368

Fincher, G.B. (1989) Molecular and cellular biology associated with endosperm mobilization in germinating cereal grains. Ann. Rev. Pl. Physiol. Pl. Mol. Biol. 40: 305-346

Fischer, E.H., Stein, E.A. (1960) "The Enzymes" (Eds. P.D. Boyers, A. Lardy, K. Mybrback) Academic Press New York, **Vol. 4A,** pp. 313-343.

Freeling, M. (1992) A conceptual frame work for maize leaf development. Dev. Biol. 44-88

Freeling, ML, Bongard-Pierce, D.K., Harberd, N., Lane, B., Hake, S. (1988) Genes involved in the patterns of maize leaf cell division. In "Temporal and Spatial regulation of plant Genes' (Eds. R B Goldberg) Springer-Verlag wien New York. pp. 41-62

Freeling, M., Bertrand-Garcia R., Sinha, N. (1992) Maize mutants and variants altering develpmental time and their heterochronic interactions. Bioessays. **14:227-236**

Gates, J.W., Simpson, G. M. (1968) The presence of starch and ∝-amylase in leaves of plants. Can J Bot. 46:1459-1462

Gerbrandy, S.J., Verleur, J.D. (1971) Phosphorylase isoenzymes: Localization and occurrence in different plant organs in relation to starch metabolism. Phytochemistry. 10:261-266

Ghiena, C, Schulz, M., Schnabl. H. (1993) Starch degradation and distribution of the starch degrading enzymes in Vicia faba leaves. Plant Physiol. **101:73-79**

Gifford, E.M. (1953) Effects of 2,4 D upon the development of the cotton leaf. Hilgardia. 21:607-644

Gilmartin, P.M., Sarokin, L., Memelinmk, J., Chua, N.-H. (1990) Molecular light switches for plant genes. Plant Cell. 2:369-78

Goliber, T.E. (1989) Regulation of leaf development in heterophyllous aquatic plants. Curr. Top. Plant Biochem. Physiol. 8:184-206

Greenwood, C.T., Milne, E.A. (1968) Starch degrading and synthesising enzymes. A discussion of their properties and action pattern. In Advance of carbohydrate chemistry. 23:281-366

Hagenimana, V., Vezina, L.P., Simard, R.E. (1992) Distribution of amylases within sweet potato *(Ipomea batatas* L.) root tissue. J. Agri. Food Chem. 40:1777-1783

Hall, D.O. (1972) Nomenclature for isolated chloroplasts. Nature New Biol 235:125-126

Hammond, J.B.W., Preiss, J. (1983) Spinach leaf intra and extra chloroplast phosphorylase activities during growth. Plant Physiol. 73:709-712

Heitz, T., Geoffroy, P., Fritig, B., Legrand, M (1991) Two apoplastic ∝-amylases are induced in tobacco by virus infection. Plant Physiol. 97: 651-656

Henson, I.E. (1985) Modification of leaf size in rice (*Oryza sativa* L) and its effects on water stress induced abscisic acid accumulation. Annal of Bot. 56:481-487

Hirasawa, E. (1989) Auxins induce ∝-amylase activity in pea cotyledons. Plant Physiol. 91:484-486

Hirasawa, E., Yamamoto, S. (1991) Properties and synthesis de novo of auxin-induced ∝-amylase in pea cotyledons. Planta 184:438-442

Hoober, K.V. ((1984) Chloroplast. Plenum, New York.

Horuath, G., Droppa, M., Mustardy, L.A., Faludi-Daniel, A. (1978) Functional charactreristics of intact chloroplasts isolated from mesophyll protoplasts and bundle sheath cells of maize. Planta. 141:239-244

Hou, Y., Arnim, A.G.V., Deng, X-W. (1993) A new class of *Arabidopsis* constitutive photomorphogenic genes involved in regulating cotyledon development. The Plant Cell. 5:329-339

Huang, Y., Kao, C.H. (1992) Calcium in the regulation of corn leaf senescence by light. Bot. Bull. Academia Sinica. 33:161-165

Ishigura, S., Tanaka, **M., Kojimoto, A., Kato,** M., **Iwabuchi,** M., **Nakamura, K.** (1993) A nuclear factor that binds to a dyad-symmetric sequence with a CGTCA motif in the 5'-upstream region of the sweet potato β-amylase gene. Plant Cell Physiol.34:567-576

Jacobsen, J.V., Higgins, T.J.V. (1982) Characterization of the ∝-amylases synthesized by aleurone layers of *Himalaya barley* in response to gibberelic acid. Plant Physiol. 70:1647-1653

Jacobsen, J.V., Hanson, A.D., Chandler, P.C. (1986) Water stress enhances expression of an ∝-amylase gene in barley leaves. Plant Physiol. 80:350-359

Jonassen, I.Y., Inguersen, J., Brandt, A. (1981) Synthesis of SP II albumin, β-amylase and chymotrypsin inhibitor C1-1 on poly somes from the endoplasmic reticulum of barley endosperm. Carlsberg Res. Commun.46:175-181

John, P.C.L., Sek, F.J., Caromichael, J.P., McCurdy, D.W. (1990) P34cdc2 homologue level, cell division, phytohormone responsiveness and cell differentiation in wheat leaves. J Cell Science. 97:627-630

Jones, M.G. (1987) Gibberellins and procera mutants of tomato. Planta. 172:280-284

Jones, R.L., Jacobsen, J.V. (1991) Regulation of synthesis and transport of secreted proteins in cereal aleurone. Int. Rev. Cytol. 126:49-88

Kaiser, W., Urbach, W. (1977) The effect of dihydroxy acetone phsophate and 3-phosphoglycerate on O_2 evolution and on the leaves of ATP, and Pi in isolated intact chloroplants. Biochem. Biophys. Acta. 459:337-346

Kakefuda, G., Duke, S.H., Hostak, M.S. (1986) Chloroplast and extrachloroplastic starch degrading enzymes in *Pisum satiuum* L. Planta. 168:175-182

Kendrick, R.E., Krorenberg, G.H.M. (1986) Photomorphogenesis in plants. Martinus Nijhoff/Dordrecht/W.Junk Publishers.

Khursheed, B., Rogers, J.C. (1988) Barley ∝-amylase genes quantitative comparison of steady state mRNA levels from individual members of the two different families expressed in aleurone cells. J. Biol. Chem. 263:18953-18960

Klein, R.R., Mullet, J.E. (1987) Control of gene expression during higher plant chloroplast biogenesis. J. Biol. Chem. 262:4341-4348

Knox, C.A. P., Sonthayanon, B., Chandra, G.R., Muthukrishnana, S. (1987) Structure and organization of two divergent ∝-amylase genes from barley. Plant Mol. Biol. 9:3-17

Koornneef, M., Rolff, E., Spruit, C.J.P. (1980) Genetic control of light-inhibited hypocotyl elongation in *Arabidopsis thaliana* (L) Heynh. Z. Pflanzen Physiol. 100:147-160

Koshiba, T., **Minamikawa,** T. (1981) Purification by affinity chromatography of ∝-amylase-a main amylase in cotyledons of germinating *Vigna mungo* seeds. Plant Cell Physiol. 22:979-987

Koshiba, T., Minamikawa, T. (1983) In vivo synthesis and turnover of ∝-amylase in attached and detached cotyledons of *Vigna mungo* seeds. Plant Physiol. **71:173-176**

Kreis, M., Williamson, M.S., Shewry, P.R., Sharp, P., Gale, M. (1988) Identification of second locus encoding β-amylase on chromosome 2 of barley. Genet. Res. Comb. 51:13-16

Krupinska, K., Apel, A. (1989) Light induced transformation of etioplast to chloroplasts of barley without transcriptional control of plastid gene expression. Mol. Gen. Gene. 467-73

Kuhn, R. (1925) Action of carbohydrate-splitting and glucose-splitting enzymes. Ann.Chem. **443:1**

Kumagai, A., Dunphy, W.G. (1991) THe cdc25 protein controls tyrosine dephosphorylation of the cdc2 protein in a cell-free system. Cell. **64:903-**914

Laemmli, U.K. (1970) Cleavage of structural proteins during the assembly of the head of bacteriophage T4. Nature. 227:680-685

Langdale, J.A., Lane, B., Freeling, M., Nelson, T. (1989) Cell lineage analysis of maize bundle sheath and mesophyll cells. Devl. Biol. 133:128-139

Langdale, J.A., Metzler, M.C., Nelson, T. (1987) The argentia mutation delays normal development of photosynthetic cell types in *Zea mays.* Dev. Biol. 122:243-255

Langdale, J.A., Rothermel, B.A., Nelson, T. (1988) Cellular pattern of photosynthetic gene expression in developing maize leaves. Genes Devl. 2:106-115

Langdale, J.A., Zelitch, I., Miller, E., Nelson, T. (1988) Cell position and light influence C_4 versus C3 patterns of photosynthetic gene expression in maize. EMBO J. 7:3643-3651

Langdale, J.A., Nelson, T. (1991) Spatial regulation of photosynthetic development in C_4 plants. Trends In Gent. 7:191-196

Le Bel, D., Poirier, G.G., Beaudoin, A.R. (1978) A convenient method for the ATPase assay. Anal. Biochem. 85: 86-89

Lee, Y.P. (1960a) Potato phosphorylase purification. Physico-chemical properties and catalytic activity. Biochem. Biophys. Acta. 43:18-24

Lee, Y.P. (1960b) Potato phosphorylase II phosphate and sulfhydryl groups. Biochem. Biophys. Acta. 43:25-30

Leech, R.M., Baker, N.R. (1983) The development of photosynthetic capacity in leaves. In 'The growth and functioning of leaves'. eds J.E. Dale and Milthorpe F.L. Cambridge University Press, Cambridge. pp. 271-308

Leech, R.M. (1985). The synthesis of cellular components in leaves, In 'Control of leaf growth' (Eds. Baker, N.R., Davices, W.J. and Ong, C.K.) Cambridge University Press. pp.93-113.

Leopold, A.C., Kriedemann, P.E. (1978) Plant growth and development. pp. 169-181

Levi, C, Gibbs, M. (1976) Starch degradation in isolated spinach chloroplasts. Plant Physiol. 57:933-935

Levi, C, Preiss, J. (1978) Amylopectin degradation in pea chloroplast extracts. Plant Physiol. 61:218-220

Li, B., **Servaites,** J.C., **Geiger,** D.R. (1992) Characterization and subcellular localization of debranching enzyme and endoamylase from leaves of suger beet. Plant Physiol. 98:1277-1284

Lilley, R.M., Chen. C.J., Mosbach, A., Heldt, H.W. (1977) The distribution of metabolites between spinach chloroplasts and medium during photosynthesis in vitro. Biochem. Biophys. Acta. 460:259-272

Lin, T.P., Spilatro, S.R., Preiss, J. (1988) Subcellular localization and characterization of amylases in *Arabidopsis* leaf. Plant Physiol. 86:0251-0259

Lizotte, P.A., Henson, C.A., Duke, S.H. (1990) Purification and characterization of pea epicotyl β-amylase. Plant Physiol. 92:615-621

Lowry, O.H., Rosebrough, N.J., Farr, A.H., Randall, R.J (1951) Protein measurement with the folin phenol reagent. J. Biol. Chem. **193:** 256-275

Lundgard, R., Sevensson, B. (1987) The four major forms of barley β-amylase purification, characterization and structural relationships. Carlsberg Res. Commun. 52:313-326

MacGreger, A.W., Dushickn, L. (1989) ∝-amylase in developing barley kernals. J.Inst. Brew. 95:29-33

Mancini, G., Carbonara, **Ace., Heremans,** J.F. (1965) Immuno-chemical quantitation of antigens by SRID. Immunochem. 12:235-254

Manga, V.A., Sharma, R. (1988) Blue light mediated regulation of β-amylase activity in mustard (*Sinapis alba* Dcotyledons. Plant Cell Physiol. 29:673-676

Manga, V. A., Sharma, R. (1990) Lack of functional interrelationship between β-amylase photoregulation and chloroplast development in mustard (*Sinapis Alba* L.) cotyledons. Plant Cell Physiol. 31:167-172

Manners, D.J. (1985). Starch. In "Biochemistry of Storage Carbohydrates in Green Plants"(Eds. P.M.Dey, R.A.Dixon), Academic Press, London, pp. 149-203.

Martineau, B., Taylor, W.C. (1985) Photosynthetic gene expression and cellular differentiation in developing maize leaves. Plant Physiol. 78:399-404

Mateyka, C, Schnarrenberger, C. (1984) Starch phosphorylase isozymes in mesophyll and bundle sheath leaves. Plant Sci. Lett. 36:119-123

Mateyka, C, **Schnarrenberger,** C. (1988) Purification and properties of mesophyll and bundle sheath cell ∝-glucan phosphorylase from *Zea mays.* L. Plant Physiol. 86:417-422

Matsuoka, M., Numazawa. (1991) *cis* acting elements in the pyruvate orthophosphatedikinase gene from maize. Mol. Gen. Genet. 228:143-152.

Matsuoka, M., Sanada, Y. (1991) Expression of photosynthetic genes from the C_4 plant, maize in Tobacco. Mol Gen Genet. 225:411-419.

Mayfield, S.P., Taylor W.C. (1987) Chloroplast photooxidation inhibits the expression of a set of nuclear genes. Mol. Gen. Genet. **208:** 309-314.

Mayfleld, S.P. (1990) Chloroplast gene regulation:Interaction of the nuclear and chloroplast genomes in the expression of photosynthetic proteins. Curr Opinion Cell Biol. 2:509-513.

Medford, J.I. (1992) Vegetative apical meristem. Plant Cell. 4:1029-1039.

Mikami, B., Morita, Y. (1983) Location of -SH groups along the polypeptide chain of soyabean p-amylase. Agric. Biol. Chem. 93:777-786.

M oh anra m, H.Y., **Rao,** S. (1982) *In vitro* induction of aerial leaves and of precocious flowering in submerged shoots of *Limnophila indica* by abscisic acid. Planta. 155:521-523.

Monroe, J.D., Preiss, J. (1990) Purification of a p-amylase that accumulate in *Arabidopsis thaliana* mutants defective in starch metabolism. Plant Physiol. 94:1033-1039.

Morohashi., Yukio Katoh, H., Kaneko. Y., Matsushima, H,. (1989) Control of ∝-amylase development in cotyledons during and following germination of mung bean seeds. Plant Physiol. 91:253-258.

Mullet, J.E. (1988) Chloroplast development and gene expression. Ann. Rev. Plant. Physiol. 39:475-502.

Mundy, J. (1982) Isolation and characterization of two immunologically distinct forms of ∝-amylase and a p-amylase from seeds of germinated *Sorghum bioclor* (L). Moench. Carlsberg Res. Commun. 47:263-274.

Muthukrishnan, **S., Chandra, G.R., Maxwell, E.S.** (1983) Hormonal control of ∝-amylase gene expression in barley studies using a cloned cDNA probe. J. Biol. Chem. 258:2370-2375.

Nakamura, K., Otito, M.A., Yoshida, N., **Nakamura,** K. (1991) Sucrose induced accumulation of p-amylase occurs conconmitant with the accumulation of starch and sporamin in leaf petiol cutting of sweet potato. Plant Physiol. **96:**902-909.

Nakano, K., Mori, H., Fukui, T. (1989) Molecular cloning of cDNA encoding potato amyloplast, ∝-glucan phosphorylase and the structure of its transit peptide. J.Biochem. 106:691-695.

Nelson, T., Harpster, M.H., Mayfield, S.P., Taylar, W.C. (1984) Light-regulated gene expression during maize leaf development. J.Cell Biol. 98:558-564.

Nelson, T., Langadale, J.A. (1989) Pattern of leaf development in C_4 plants. The Plant Cell. 1:3-13.

Nelson, T., Langdale, J.A. (1992) Developmental genetics of C_4 photosynthesis. Ann. Rev. Plant Physiol. Plant Mol. Biol. 43:25-47.

Ngernprasirtsiri, J., Chollet, R., Kobayashi, H., **Sugiyama, T., Akazawa, T.** (1989) DNA methylation and the differential expression of C_4 photosynthesis genes in mesophyll and bundle sheath cells of greening maize leaves. J. Biol. Chem. 264:8241-48.

Nishimura, I. H., Nishimura, M., Daussant, J. (1986) Conversion of free a-amylase to bound a-amylase on starch granules in the barley endosperm during dessication phase of seed development. Protoplasma. 134:149-153.

Nott, D.L., Osmand, C.B. (1982) Purification and protperties of phosphoenolpyruvate carboxylase from plants with crcussulaceun acid metabolism. Aust. J. Plant Physiol. 9:409-422.

Oelmuller, R. (1989) Photooxidative destruction of chloroplasts and its effect on nuclear gene expression and extraplastidic enzyme levels. Photochem. Photobiol. 49:229-239.

Ohlsson, E. (1930) Components of malt diastase. Z Physiol Chem. **189:17.**

Ohto, M-a., Nakamurakito, K-K., Nakamura, K. (1992) Induction of expression of genes coding for sporamin and beta-amylase by polygalacturomic acid in leaf-petiole cuttings of sweet potato. Plant Physiol. 99:422-427.

Okita, T.W., Preiss, J. (1980) Starch degradation in spinach leaves. Isolation and characterization of amylase and R-enzyme of spinach leaves. Plant Physiol. 66:870-876.

Okita, T.W., Greenberg, E., **Khun, D.N., Preiss, J.** (1979) Subcullular localization of the starch degradative and biosynthetic enzymes of spinach leaves. Plant Physiol. 64:187-192.

Ouchterlony, O. (1949) Antigen-antiloody reaction in gels. Acta. Pathol. Microbiol. Scand. 26:507-515.

Ougham, H.J., Jones, T.W.A., Evans, M.L. (1987) Leaf development in *Lolium temulentum* L. progressive changes in soluble polypeptide complement and isozymes. J. Exp. Bot. 38:1689-1696.

Palmer, J.D. (1986) Isolation and structural analysis of chloroplast DNA. Methods enzymol. 118:167-169.

Pan, S.M., Chang, T.C., Juang, R.H., Su. J.C. (1988) Starch phosphorylase inhibitor is β-amylase. Plant Physiol. 88:1154-1156.

Perchorowicz, J.T., Gibbs, M. (1980) Carbon dioxide fixation and related properties in sections of the developing green maize leaf. Plant Physiol. 65:802-809.

Peterson, G. L. (1983) Determination of total protein. Methods in enzymol. 91:95-119.

Poethig, R.S. (1987) Clonal analysis of cell lineage patterns in plant development. Am. J. Bot. 74:581-594.

Poethlg, R.S. (1990) Phase change and the regulation of shoot morphogenesis in plants. Science. 250:923-930.

Poethlg, R.S. (1988) Heterochronic mutations affecting shoot development in maize. Genetics. 119:959-973.

Poethlg, R.S. (1989) Genetic mosaics and cell lineage analysis in plants. Trends Genet. 5:273-277

Pongratz, P., Beck, E. (1978) Diurnal oscillation of amylolytic activity in spinach chloroplasts. Plant Physiol. 62:687-689.

Porter, H.K. (1953) The inhibition of ∝-amylase and phosphatase contamination of potato phosphorylase preparation. J. Expt. Bot. **4:44-**52.

Preiss, J., Levi, C. (1980). Starch biosynthesis and degradation. In Proceedings of the fifth International Congress on photosynthesis. (Eds. G. Akoyunoglou) pp.271-320.

Preiss, J. (1984) Starch, sucrose biosynthesis and partition of carbon in plants are regulated by orthophosphate and triose phosphates. Trends in Biochem. Science. 9:24-27.

Quail, P.H. (1991) Phytochrome: a light-activated molecular switch that regulates plant gene expression. Annu. Rev. Genet. 25:389-409.

Raschke, K., Zeevaart, J.A.D. (1976) Absisic acid content transpiration and stomatal conductance as related to leaf age in plants of *Xanthium strumarium*.Plant Physiol. 58:169-174.

Rebeiz, C.C., Rebeiz, C.A (1986). Chloroplast biogenesis 53. Ultrastructural study of chloroplast development during photoperiodic greening, In 'Regulation of Chloroplast differentiation'.pp. 389-396, (Eds.Akoyunoglu, G., H.Senger) pp. 571-582, Alan R. Liss, Inc.

Reiss, T., Bergfeld, R., Link, G., Thien, W., Mohr, H. (1983) Photooxidative destruction of chloroplasts and its consequences for cytosolic enzyme leaves and plant development. Planta. **159:**518-528.

Renart, J., Sandoval, J.V. (1984) Western Blots. Methods in Enzymol. 104:455-460.

Robertson, D., Laetsch, W.M. (1974) Structure and function of developing barley plastids. Plant Physiol. 54:148-159.

Rogler, C.E., Hackett, W.P. (1975) Phase change in *Hedera* fceZix:induction of the mature to juvenile phase change by gibberellin A3. Physiol Plant. 34:141-147.

Rorat, T., Sadausk, J., Grellet, F., Daussant, J., Delseny, M. (1991) Characterization of cDNA clones for rye endosperm specific β-amylase and analysis of β-amylase deficiency in mutant leaves. Ther. Appl. Gen. 83:257-263.

Ross, J.J., Murfet, I.C., James, B.R (1993) Distribution of gibberellins in *Lathyrus odoratus* L.and their role in leaf growth. **102:** 603-608.

Russell, S.H., Evert, R. F. (1985) Leaf vasculature in *Zea mays* L. Planta. 164:448-458.

Ryan, C.A., Fanner, E.E. (1991) Oligosaccharide signals in plants; A current assessment. Ann. Rev. Plant Physiol. Plant Mol. Biol. 42: 651-674.

Sadowski, J., Rorat, T., Cooke, R., Delseny, M. (1993) Nucleotide sequence of a cDNA clone encoding ubiquitous β-amylase in Rye (*Secale cereale* L). Plant physiol. 102:315-216.

Saeed, M., Duke, S.H. (1990a) Chloroplastic regulation of apoplastic α-amylase activity in pea seedlings. Plant Physiol. **93:131-140.**

Saeed, M., Duke, S.H. (1990b) Amylases in pea tissues with reduced chloroplast density and/or function. Plant Physiol. 94:1813-1819.

Saito, G.Y., Chang, Y.C., Walling, L.L., Thomson, W.W. (1990) Chloroplast development and nuclear gene expression in cotyledons of soybean seedlings. New Phytol. **114:547-54.**

Sandergren, E., Klang, N. (1950) On barley amylase and proteinase. J. Inst. Brew. 56: 313-318.

Sangeetha, B., Sharma, R. (1988) Phytochrome-regulated expansion of mustard (*Sinapis alba* L) cotyledons. J. Expt. Bot. 39:1355-1366.

Scandalios, J.G. (1974) Isozymes in development and differentiation. Ann Rev Plant Physiol. 25:225-228.

Schachtele, C, **Steup,** M. (1986) α-1,4-glucan phosphorylase forms from leaves of spinach (*Spinacia oleracea* L.) I in situ localization by direct immunoflurescence. Planta. **167:444-451.**

Scolt, R.A., Liverman, J.L. (1957) Control of etiolated bean leaf disk expansion by gibberellin and adenine. Science. 126:122-123.

Scott, N.S., Possingham, J.V. (1982) Leaf development. In The molecular biology of plant development'. (Eds, H. Smith and D. Grierson) pp. 223-255, Berkeley, University of California Press.

Segundo, B.S., Casacuberta, J.Ma., **Puigdomenech, P.** (1990) Hormonal and light regulation of the multiple amylase isozymes during seed germination and in vegetative tissues of *Zea mays.* Plant Sci. **69:167-**177.

Servaites, J.C., Griger, D.R., Tucci, M.A., Fondy, B.R. (1989) Leaf carbon metabolism and metabolite levels during a period of sinusoidal light. Plant Physiol. 89:403-8.

Sharma, R., Schopfer, P. (1982) Sequential control of phytochrome-mediated synthesis *de novo* of β-amylase in the cotyledons of mustard (*Sinapis alba* L) seedling. Planta. 155:183-189.

Sharma, R., Schopfer, P. (1987) Phytochrome-mediated regulation of β-amylase mRNA level in mustard *(Sinapsis alba* L.) cotyledon. Planta. 171:313-320.

Sharman, B.C. (1942) Developmental anatomy of the shoot *of Zea mays* L. Ann. Rev. Plant Physiol. 6:245-284.

Sharrock, R.A., Lissemore, J.L., Quail, P.H. (1986) Nucleotide and amino acid sequence of a Cucurbita phytochrome cDNA clone: identification of conserved features by comparison with Avena phytochrome. Gene. 47:287-95.

Sheen, J.-Y., Bogorad, L. (1987) Differential expression of C_4 pathway genes in mesophyll and bundle sheath cells of greening maize leaves. J. Biol. Chem. 262:11726-11730.

Shewry, P.R., Parmar, S., Buxton, B., Gale, M.D., Liu, C.J., Hejgaard, J., Kreis, M.(1988) Multiple molecular forms of β-amylase in seeds and vegetative tissues of barley. Planta. 176:127-134.

Shimamura, S., Nagai, M., Fukui, T. (1982) Comparative glucan specificiies of two types of spinach leaf phosphorylase. J. Biochem. **91:703-717.**

Shropshire, W. Jr, Mohr, H. (1983) Photomorphogenesis. In Encyclopaedia of plant physiol. **Vol 16A.** Springer Verlag, Berlin.

Smith, L.G., Green, B., Hake. S. (1992) A dominant mutation in maize homeobox gene knotted-1 cause its ecotopic expression in leaf cells with altered fate. Development. **116:**

Smith, L.G., Hake, S. (1992) The initiation and determination of leaves. The Plant Cell. 4:1017-1027.

Smith, M.A., John, V., Jacobsen, J.V., Kende, H. (1987) Amylase activity and growth in internodes of deep water rice. Planta. **172:114-120.**

Smith, H. (1977). Regulation of enzyme synthesis and activity in higher plants. Proc. Photo. Soc. Symp. Acad. Press, London.

Sopanen, T., Laurlère, C. (1989) Release and activity of bound β-amylase in germinating barley grains. Plant Physiol. 89:244-249.

Steeves, T.A., Sussex, **I.M.** (1989). Patterns in plant development. 2nd Edition Cambridge University Press, London.

Stein, E.A., Fischer, E.H. (1958) The resistance of ∝-amylase towards proteolytic attack. J. Biol. Chem. 232:867-871.

Steup. M. (1988) Starch degradation. Biochem. Plants 14:255-295.

Steup, M. (1990) Starch degrading enzymes. Methods Plant Biochem. 3:103-128.

Steup, M.C., Conrads, J., Van Berkel, J. (1987). Compartment specific phosphorylase forms from higher plants in progress. In Photosynthesis Research. (Eds. J.Biggins) **Vol.3,** pp. 479-482, Dordrecht, Martinus Nijhoff.

Steup, M., Latzko, E. (1979) Intracellular localization of phosphorylase in spinach and pea leaves. Planta. 145:69-75.

Steup, M., Robenek, H., Melkonian, M. (1983) *In vitro* degradation of starch granules isolated from spinach chloroplasts. Planta. 158:428-436.

Steup, M., Schächtele, C. (1981) Mode of gucan degradation by purified phosphorylase forms from spinach leaves. Planta. 153:351-361.

Steup, M., **Schächtele,** C, **Latzko. E.** (1980) Purification of a non-chloroplastic ∝-glucan phosphorylase from spinach leaves. Planta. 148:168-173.

Stitt, M. (1984). Degradation of Starch in chloroplasts: a buffer to sucrose metabolism. In 'Storage carbohydrates in vascular plants' (Eds. Lewis, D.H.) pp. 205-229, Cambridge University Press, New York.

Stitt, M., Bulpin, P.V., ap Rees, T. (1978) Pathway of starch breakdown in photosynthetic tissues of *Pisumsativum*.Biochem Biophy Acta. 544:200-214.

Stitt, M., Heldt, H.W. (1981) Simultaneous synthesis and degradation of starch spinach chloroplasts in the light. Biochem. Biophy. Acta.**638:**1-11.

Stitt, M., Steup M. (1985). Starch and Sucrose degradation. Encyclopaedia of Plant Physiology **Vol.18** Higer Plant Cell Respiration (Eds. Douce, R, Day, D.A.), pp. 347-389, Berlin, New York, Springer Verlag.

Subbaramaiah, K., Sharma, R.P. (1988) Affinity binding of higher plant p-amylases to starch. Starch. 40:182-185.

Subbaramaiah, K., Sharma, R.P. (1987a) Imuunoaffinity purification of β-amylase from mustard *(Sinapis alba* L.) cotyledons. J. Chromatography. 408:385-387.

Subbaramaiah, K., Sharma, R.P. (1987b) Purification of β-amylase from mustard *(Sinapis alba* L.) to homogeneity by chromatofocusing and gel permeation chromatography. J. Chromato. **390:**463-467.

Subbaramaiah, K., Sharma, R.P. (1989) β-amylase from mustard *(Sinapis alba* L) cotyledons. Immunochemical evidence for synthesis *de novo* during photoregulated seedling development. Plant Physiol. 89:860-866.

Subbaramaiah, K., Sharma, R.P. (1990) Characterization of β-amylase from *Sinapis alba* cotyledons. Phytochemistry 29:1417-1419.

Subbaramaiah, K. (1987) PhD dissertation.

Subbarao, K. (1992) PhD dissertation.

Sun, L., Doxsee, R.A., Arel, E., tobin. E.M. (1993) CA-1, a novel phosphoprotein, interacts with the promoter of the cab 140 gene in *Arabidopsis* and is undetectable in det 1 mutant seedlings. Plant Cell. 5:109-121.

Sun, Z., **Henson,** C.A. (1991) A quantitative assessment of the importance of barley seed α-amylase, β-amylase, debranching enzyme and α-glucosidse in starch degradation. Arch. Biochem. Biophys. 284:298-305.

Swain, R.R., Dekker, E.E. (1966) Seed germination studies. II Pathways for starch degradation in germinating pea seedlings. Biochem. Biophy. Acta. 122:87-100.

Thoma, J.A., Koshland, D.E.Jr. (1960) Competitive inhibition by substrate during enzyme action. Evidence for the induced by substrate during enzyme action.Evidence for induce fit theory. J. Amer.Chem.Soc. 82:3329-3333.

Thoma, J A, Spradlin, J.E., Dygert, S. (1971) PLant and animal amylases. In "The Enzymes" (Eds. Boyer, P.D) Academic Press, New York. pp. 115-189.

Thompson, W.F., White, M.J. (1991) Physiological and molecular studies of light regulated nuclear genes in higher plants. Ann.Rev.Plant Physiol.Plant Mol.Biol. 42:423-466.

Thomson, W.W., Whatley, J.M. (1980) Development of non green plastids. Ann. Rev. Plant Physiol. 31:375-394.

Topping J.F., Leeve C. J. (1990) Mitochondria gene expression during wheat leaf development. Planta. 182:399-407.

Tsai, C.Y., Nelson, O.E. (1968) Phosophorylase I and II of maize endosperm. Plant Physiol. 43:103-112.

Tsai, C.Y., Nelson, O.E. (1969) Two additional phosophorylases in developing maize seeds. Plant Physiol. 44:159-167.

Usuda, H., Ku, M.S.B., Edwards, G.E. (1985) Influence of light intensity during growth on photosynthesis and activity of several key photosynthetic enzymes in a C_4 plant (*Zea mays).* Physiol. Plant. 63: 65-70.

van Volkenburgh, E., Cleland R.E. (1979) Separation of cell enlargement and division in bean leaves. Planta. **146:245-247.**

van Volkenburgh, E., Cleland R, E. (1986) Wall yield threshold and effective turgor in growing bean leaves. Planta. 167:37-43

Vierstra, R.D. (1993) Protein degradation in plants. Ann. Rev. Plant Physiol. Plant Mol. Biol. 44: 385-410.

Virgin, H. I. (1989) An analysis of the light induced unrolling of the grass leaf. Physiol. Plantarum. 75:295-298.

Viro, M., Kloppstech, K. (1980) Differential expression of the genes for ribulose 1, 5-bisphosphate carboxylase and light harvesting chlorophyll a/b protein in the developing barley leaf. Planta. **150:41-45.**

Vollbrecht, E., Veit, B., Sinha, N., Hake, S. (1991) The developmental gene knotted-1 is a member of maize homeobox gene family. Nature. **350:241-**243.

Wang, J.-L., Turgeon, R., Carr, J.P., Berry, J.O. (1993) Carbon sink to source. Transition is coordinated with establishment of cell-specific gene expression in a C_4 plant. The Plant Cell. 5:289-296.

Weier, T.E., Brown D.L. (1970) Formation of the prolamellar body in 8-day dark-grown seedlings. Amer J Bot. 57:267-275.

Wellburn, A.R., Gounaris, I., Owen, J.H., Laybourn-Parry, J.E.M., Wellburn, F.A.M. (1986). In 'Regulation of chloroplast differentiation'. pp. 371-381, (Eds.Akoyunoglu, G., H.Senger) pp. 571-582, Alan R. Liss, Inc.

Werdan, K., Heldt, H.W., Milovancev, M. (1975) The role of pH in the regulation of carbon fixation in the chloroplast stroma. Studies on CO_2 fixation in the light and dark. Biochem. Biophysic. Acta. 396:276-292.

Wernicke, W., Milkovitz, L. (1987a) Effect of auxins on the mitotic cell cycle in development in wheat. Physiol. Plant. 69:16-22.

Wernicke, W., Milkovitz, L. (1987b) Roles of uptake and metabolism of indol-3-acetic acid and 2-4 di-chloro phenoxy acetic acid in cultured leaf segments at different stages of development in wheat. Physiol. Plant. 69:23-28.

Whelan, W.J. (1964) Hydrolysis with β-amylase and preparation of the β-amylase limit dextrin of amylopectin. In RL whistler. Meth. Carbo. Chem. pp. 261-266, Academic Press, New York.

Whelan, W.J. (1955) Phosphorylases from plants. Meth. in Enzym. 1:192-200.

Work, T.S., Work, E. (1972) Laboratory techniques in biochemistry and molecular biology. 1: 385-389.

Yamada, H., Yanahira, S., Kiyohana, H., Cyong, J-C., Otsuka, Y. (1986) Water soluble glucans from the seed *Coix lacrymajobi* var. ma-yuen. Phytochem. 25:129-132.

Yang, Y., Steup, M. (1990) Polysaccharide fraction from higher plants which strongly interacts with the cytosolic phosphorylase isozyme. **94**: 960-969.

Yoshida, N., Nakamura, K. (1991) Molecular cloning and expression in Escherichia coli of cDNA encoding the subunit of sweet potato p-amylase. J. Biochem. 110:196-201.

Yoshida, N., Hayashi, N., Nakamura, K. (1992) A nuclear gene encoding β-amylase of sweet potato. Gene. 120:255-259.

Zeevaart, J.A.D. (1980) Changes in the levels of abscisic acid and its metabolities in excised leaf blades of *Xanthiumstrumanium* during and after water stress. Plant Physiol. 66:672-678.

Ziegler, P., Beck. (1986) Exoamylase activity in vacuoles isolated from pea and wheat leaf protoplasts. Plant Physiol. 82:1119-1121.

Ziegler, P. (1988) Partial purification and characterization of the major endo amylase of mature pea leaves. Plant Physiol. 86:659-666.

Zielinski, R.E., Jefferey, W.M., Jenkins, M.E. (1989) Coordinate expression of Rubisco activase and Rubisco during barley leaf cell development. Plant Physiol. 90:516-521.

Photochemistry and Photobiology Vol. 54, No. 4, pp. 651-657, 1991
Printed in Great Britain

0031-8655/91 $03.00 + 0.00

INTERACTION BETWEEN CHLOROPLAST BIOGENESIS AND PHOTOREGULATION OF AMYLASES IN *Pennisetum americanum* LEAVES*

K. J. M. VALLY and R. SHARMA†
School of Life Sciences, University of Hyderabad, Hyderabad-500134, India

(*Received* 7 *December* 1990; *accepted* 4 *March* 1991)

Abstract—In pearl millet *(Pennisetum americanum)* seedlings, light acting *via* phytochrome stimulates amylase activity in the leaves. The maximum photostimulation of amylase is observed in the segment proximal to the leaf base. This photostimulation mainly results from an enhancement in β-amylase activity (EC 3.2.1.2), which constitutes 80–90% of leaf amylase activity. The subcellular fractionation studies revealed that while β-amylase is localized only in the extraplastidic compartment, α-amylase (EC 3.2.1.1.) is localized both in the cytosol and in the chloroplasts. The mesophyll cells contained both a- and β-amylase activity, but only a-amylase activity was present in the bundle sheath cells. The Norflurazon-mediated photooxidation of chloroplasts during leaf development also eliminated plastidic α-amylase activity, confirming dependence of its photoregulation on the chloroplast biogenesis.

INTRODUCTION

In higher plants, chloroplast biogenesis obligatorily depends on the environmental availability of light. In the absence of light, the proplastid in leaf cells develops into an **etioplast.** The exposure to light rapidly transforms etioplasts to chloroplasts **(Hoober,** 1984). Additionally, light triggers a large number of photomorphogenetic responses in plants, many of which are realized by photoregulation of gene expression in the nucleus as well as in the plastids (Shropshire and Mohr, 1983; Kendrick and Kronenberg, 1986). It has been acknowledged that the nucleus plays a major role in chloroplast function and development (Kobayashi *et al.*; 1987). Nevertheless, it is now apparent that the chloroplast can also influence, in a feedback fashion, the expression of specific nuclear genes encoding plastidic proteins (Oelmüller, 1989). The studies on developmental mutants of chloroplasts or studies where chloroplasts are experimentally destroyed clearly demonstrate that the loss of chloroplast is accompanied by a concomitant decrease in the rate of gene expression of nuclear encoded plastidic proteins (Oelmiiller, 1989). Hitherto the molecular nature of the putative plastidic factor, which may be involved in the above nuclear-plastidic interactions, is **not** known.

We initiated this study to decipher the extent of feedback influence of chloroplast biogenesis on the **photoregulated** increase of amylase activity in pearl millet *(Pennisetum americanum)* seedlings. A monocotyledon, pearl millet has leaves which are well suited for this study. The cell division is localized at a basal meristem, which offers a gradient of plastids and leaf cells at different developmental stages along the leaf axis from the base to the tip. In addition, *Pennisetum americanum* [a C_4 plant (Hoober, 1984)] has dimorphic chloroplasts *viz.* bundle sheath chloroplasts, in which thylakoids are not differentiated into grana and mesophyll chloroplasts which contain grana and are morphologically similar to chloroplasts of C_3 plants. In C_4 plants bundle sheath chloroplasts carry out the process of carbon fixation leading to the formation of starch (Hoober, 1984). It is observed that in C_4 plants, e.g. *Zea mays*, the enzymes involved in starch biosynthesis, ADP glucose pyrophosphorylase, starch synthase and branching enzymes are predominantly localized in the bundle sheath cells, whereas the starch degrading enzymes like amylases and phosphorylases are predominantly present in the mesophyll cells (Spilatro and Preiss, 1987; Downton and Hawker, 1974).

In recent years the subcellular and intracellular distribution of starch degrading enzymes, particularly amylases in leaf cells, have been investigated intensively to decipher their role in starch mobilization (Ziegler, 1988; Manga and Sharma, 1990). The amylases have been reported to occur in cytosol (Manga and Sharma, 1990), vacuoles (Zieglar and Beck. 1986), plastids (Zieglar, 1988) and also in cell walls (Saeed and Duke, 1990). Because in many species most amylolytic activity is present in extraplastidic compartments of cells, there have been many doubts regarding the role of amylases in the mobilization of photosynthetically generated starch (Beck and Zieglar, 1989). In this study we have used Norflurazon-induced photooxidation of chloroplasts in pearl millet seedlings (Henson, 1984) as a tool to investigate plastidic localization of amylase and the

*This paper is dedicated to Professor Masaki Furuya on the occasion of his 65th birthday. One of the authors (RS) appreciates having the opportunity to work in his laboratory as a visiting scientist.

†To whom correspondence should be addressed.

interrelationship between **photoregulation of** amylase and **chloroplast** biogenesis.

MATERIALS AND METHODS

Pearl millet (*Pennisetum americanum*) var. **WCG.75** seeds were obtained from State Seed Corporation, Hyderabad, India The **seedlings** were grown **at 25°C** in transparent plastic boxes on germination paper pie-soaked (12 h) with either distilled water or Norflurazon solution (0.4 m*M*). Seedlings were grown under continuous red light (λ_{max} 650 nm, **fluence** rate, 0.67 W m^{-2}), or blue light (λ_{max} 450 nm. fluence rate 0.13 W m^{-2})(Manga and Sharma. 1988) or in darkness. The long wavelength **far** red light was obtained by using Schott interference filters and two 300 W projectors (λ_{max} 756 nm. fluence rate 6 W m^{-2}) (Manga and Sharma, 1988).

Enzyme assay. The primary leaves were homogenized in a pre-cooled mortar and pestle with sea-sand in an extraction buffer containing 60 mM Na-citrate, pH 6.1, 10 m*M* mercaptoethanol and 10 mM $CaCl_2$. The homogenate was clarified by centrifugation at 7600 *g* for 30 min at 4°C. Amylase activity was measured as described **earlier** (Manga and Sharma, 1988). α-Amylase activity was **measured** by using a specific substrate β-limit dextrin (2 mg/mL) after inactivating β-amylase activity by incubating supernatant at 70°C for 10 min in the presence of 10 m*M* $CaCl_2$. The protein and chlorophyll estimations were done by using the procedure of Lowry *et al.*. (1951) and Arnon (1949) respectively.

Isolation of intact chloroplasts. The **procedure** for chloroplast isolation was adapted from Palmer (1986). Twenty grams of leaf material were homogenized in a pre-cooled Waring blender (5 s homogenization x 5 times) in a 50 m*M* Tris–HCl buffer, pH 8.0. (6 mL/g fresh weight) containing 0.35 M sorbitol. 5 m*M* $MgCl_2$, 1 m*M* $CaCl_2$, 2 m*M* ethylene diamine **tetraacetic** acid (EDTA), 5 m*M* mercaptoethanol. 10 m*M* Na-ascorbate. The homogenate was centrifuged at 1000 *g* for 15 min and the pellet was washed 3 times with a wash buffer containing 50 m*M* Tris-HCl (pH 8.0). 0.35M sorbitol. 20 m*M* EDTA, **0.1%** (vol/vol) mercaptoethanol Thereafter the pellet was suspended in 4 mL of the above buffer and layered on top of a 31% and 54% sucrose (wt/vol) step gradient. The gradient was centrifuged at 30000 *g* for 40 min at 4°C. The intact chloroplasts obtained at the interface **of** 31% and 54% sucrose were diluted 5 times with wash buffer and were pelleted by centrifugation at 1000 *g* for 15 min. The intactness **of** chloroplasts was confirmed by the ferricyanide reduction test (Lilley *et al.*, 1975) and phase contrast microscopy. Chloroplasts were disrupted by sonication to obtain plastidic enzymes. The purity of the plastidic preparation was confirmed by estimating phosphoenol pyruvate (PEP) carboxylase as a marker enzyme of the cytosol (Nott and Osmond. 1982):

Isolation of mesophyll and bundle sheath cells. Mesophyll and bundle sheath cells were isolated with the enzymatic method of Day *et al.* (1981). with few modifications. Bundle sheath strands were also isolated by using the mechanical method of Chollet and Ogren (1973) with some changes in the isolation buffer, which contained 50 m*M* Tris–HCl (pH 8.0), 0.35 M sorbitol, 10 m*M* Na-ascorbate, 1 m*M* $CaCl_2$, 1 m*M* $MnCl_2$, 5 m*M* EDTA, 0.2% BSA (wt/vol). Bundle sheath strands which were retained **on** 80 μm nylon mesh were finally washed with wash buffer (**50** m*M* Tris–HCl, pH 8.0, **0.35** M sorbitol, 20 mM EDTA, 1 m*M* $CaCl_2$). The bundle sheath protoplasts were isolated by the enzymatic method by incubating the strands in the protoplast isolation medium. The bundle sheath chloroplasts were obtained after passing the above protoplasts through a **30** μm nylon mesh.

Electrophoresis. The polyacrylamide slab gel electrophoresis was performed according to Davis (1964). **To** visualize **amylase** isozymes, the gel was washed with extraction buffer **for** 15 min and incubated in a reaction mixture containing 0.5% amylose in 60 mM Na-acetate buffer, pH 4.6, for 3 h at room temperature. The transparent amylolytic bands were visualized after submerging the gel in iodine solution containing 5.7 m*M* I_2, 43.3 mM KI in 0.2 M HCl for 1 min. The contact prints for amylase **isoforms** were obtained by layering the polyacrylamide gel after electrophoresis on a 1% agar gel containing 0.5% (wt/vol) amylose in 60 mM Na-acetate buffer, pH 4.6, for 3 h. **To** differentiate the α-amylase band, amylose in the above agar gel was replaced by 0.5% (wt/vol) β-limit dextrin. Staining of the agar gels was carried out as described above for the polyacrylamide gels. To visualize **cytOSOlic** α-amylases, contact printing was conducted for 9 h, as these isozymes were present in a very low amount

The level of amylase in the leaves of pearl millet seedlings grown in darkness or in continuous red/blue light was determined at different time points from sowing onward. Figure 1 shows that red light stimulates amylase activity right from the time of emergence of pearl millet leaves, and by the 8th day it is 7-fold higher than the amylase level of dark grown seedlings. In contrast blue light, although it does stimulate amylase activity, is less effective than red light. Under both blue and red light the amylase activity declines after the 8th day from sowing. Table 1 shows that blue or red light pulses of 10 min duration with 8 h intervals also induce amylase activity. Moreover, the inductive effect of these light pulses can be significantly reversed by following them every time with a 10 min far red light pulse, a treatment which reverses phytochrome mediated photoresponses (Shropshire and Mohr, 1983).

In higher plants amylase activity consists of two distinct enzyme proteins *viz.* α-amylase and β-amylase (Manners, 1985); therefore, the relative extent of **photoregulation** of these enzymes in the above

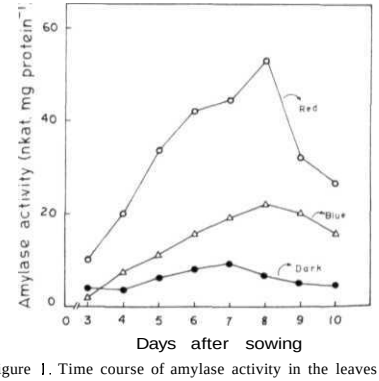

Figure 1. Time course of amylase activity in the leaves of pearl millet seedlings. Seedlings were grown in continuous red light (○), blue light (A), or in darkness (•) from the time of sowing.

Table 1. **Effect** of brief red/blue and far red light on the amylase activity in pearl millet leaves

Treatment*	Amylase activity (nkat/mg protein)	
	Red light	Blue light
5 d cont. dark (control)	06.20 ± 1.01	06.20 ± 1.01
5 d cont. light	29.25 ± 1.08	19.34 ± 0.70
3 d D + 2 d L	17.40 ± 1.10	12.80 ± 0.36
3 d D + 6 × (10 min L + 8 h D)	20.42 ± 1.47	15.33 ± 1.80
3 d D + 6 × (10 min FRL + 8 h D)	04.10 ± 0.40	04.90 ± 1.09
3 d D + 6 × (10 min L + 10 min FRL + 8 h d)	10.20 ± 0.54	08.03 ± 1.03

Seedlings were grown in continuous darkness for 3 d after sowing. Thereafter, the seedlings were subjected to six 10 min light pulses separated by an **interval** of 8 h in darkness. The enzyme activity was measured 5 d (120 h) after sowing. The control seedlings were grown in continuous darkness or light for 5 d (120 h).

*L—either red or blue light; D—dark; d—day; FRL—Far red light; h—hour.

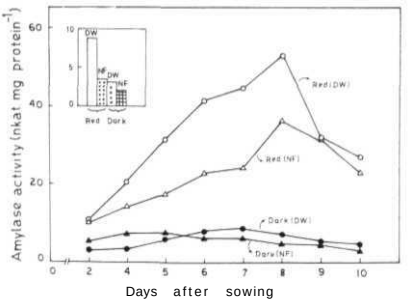

Figure 3. Effect of Norflurazon on the time course of amylase activity in pearl millet leaves. Seedlings were grown in Norflurazon (NF) from the time of sowing in continuous red light (A) or in darkness (A). The control seedlings were grown in distilled water (DW) in red light (○), or in darkness (●). The inset shows the a-amylase activity in NF treated 7 day-old pearl millet seedings.

photoresponse was also ascertained. The distinction between these two amylases was made by using a specific substrate. (3-limit dextrin. While α-amylase alone can degrade [3-limit dextrin, the amylose can be degraded by both a-amylase and β-amylase. The red light mediated stimulation of amylase activity in pearl millet leaves resulted largely from an increase in the β-amylase activity, which constituted 80–90% of total leaf amylolytic activity in light grown seedlings (Fig. 2). In darkness β-amlyase activity could be significantly detected only after the 6th day from sowing. The photoregulation of α-amylase activity in leaves followed a different kinetic pattern than (3-amylase (Fig. 2).

The interrelationship between light mediated amylase increase and **chloroplast** development was investigated by growing pearl millet seedlings with Norflurazon, a chlorosis-inducing herbicide (Henson, 1984). Treating pearl millet seedlings with Norflurazon completely prevents chloroplast development in light and also decreases the level of photostimulation of amylase in leaves (Fig. 3). At the same time application of Norflurazon had almost no effect on the amylase level in the dark grown seedlings. The inset in Fig. 3 shows that in the presence of Norflurazon. u-amylase photostimulation is significantly lowered.

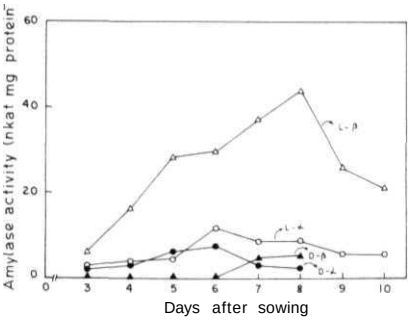

Figure 2. Time course of development of α-amylase (○, •) and (i-amylase (A, A) activity in pearl millet leaves. Seedlings were grown in either continuous red light (○, A) or in darkness (•, •) from the time of sowing. L—red light; D—dark; α—α-amlyase;β—β-amylase.

The amylolytic activity of the pearl millet leaves was analyzed by electrophoresis to study the effect of light and Norflurazon on the isozymes of amylases in leaves. The analysis of amylase isozymes from pearl millet leaves (Fig. 4, lanes 1–4) shows that in dark grown seedlings only a fast migrating amylase isozyme group was present (R_f 0.71). The exposure of seedlings to continuous light induces the appearance of an additional slowly migrating amylase isozyme (R_f 0.21). The treatment of seedlings with Norflurazon abolishes the appearance of a light induced amylase isozyme with a low R_f value (Fig. 4).

The distinction between the above amylase isoforms as a-amylase and p-amylase was made by contact printing of polvacrylamide gels on an agar gel containing (3-limit dextrin (data not shown). The contact printing of the above gels for 3 h on agar gel containing (3-limit dextrin as a substrate revealed only one isozyme having a low R_f value (0.21). In contrast, the fast migrating major isozyme {R, 0.71) of leaf could not degrade (3-limit dextrin, and therefore is p-amylase in nature (Manners, 1985). Evidently light, in addition to stimulating total amylolytic activity of leaf, also induces a new isozyme of amylase (R, 0.21), which can be identified as α-amylase on the basis of its substrate specificity. The

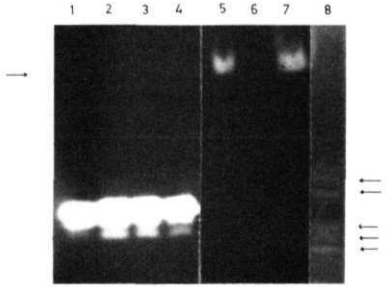

Figure 4. The **electrophoretic** analysis **of** amylase **isoforms** in leaves of 7 day **old** pearl millet seedlings. The seedlings were grown in **continuous** red light and darkness in distilled water (DW) or in 0.4 m*M* Norflurazon (NF). The gel was stained by submerging it in an amylose-containing solution (lanes 1-4). The gel for **isolated chloroplasts** (lane 5) and supernatant **from** mesophyl cells (lane 8) and extract from bundle sheath strands (lanes 6–7) was contact printed on **a** β-limit dextrin **containing agarosc** gel. Lane 1—red light DW; lane 2—dark DW; lane 3—red light NF; lane 4—dark DW; lane 5—mesophyll **chloroplasts;** Lane 6—bundle sheath strands NF; lane 7 bundle sheath strands DW; lane 8—dark DW.

contact printing of gels for a prolonged period (9 h) on β-limit dextrin gels revealed five additional isozymes of a-amylase having higher R_f values (0.59, 0.68, 0.75. 0.79, 0.82), which were present in a low amount in leaf cells (Fig. 4, lane 8). The pattern of these isozymes was not influenced by either light or Norflurazon treatment (data not shown).

The subcellular **fractionation** of pearl millet leaves into **cytosolic** and **plastidic** fractions revealed that 80–90% of amylase activity is present in the cytosolic fraction, with the balance present in chloroplasts (Table 2). The substrate specificity (Table 2) and electrophoretic analysis (Fig. 4) of the chloroplastic fraction revealed that the chloroplast had a minor isozyme (R_f 0.21) of amylase representing a-amylase activity (Fig. 4, lane 5). On the other hand, the cytosolic fraction mainly consists of β-amylase, as shown by its inability to degrade β-limit dextrin (Table 2). Pearl millet leaves, in addition to β-amylase, also contain *ca* 5 α-amylase isozymes (Fig. 4, lane 8) in the cytosol, but their contribution towards the a-amylase activity of leaves is quite low (Table 2). The estimation (Table 2) and electrophoretic analysis of amylase in isolated bundle sheath strands showed the presence of only plastidic a-amlyase isozyme (Fig 4, lane 7), while cytosolic β-amylase activity was totally absent. Furthermore, in bundle sheath strands isolated from Norflurazon-treated seedlings plastidic a-amylase was also absent, confirming its plastidic localization (Fig. 4, lane 6). The purity of the isolated chloroplast preparation was checked by using PEP carboxylase, a cytosolic enzyme which was absent in the chloroplastic fraction (Table 2).

Figure 5 shows the spatial gradient of photostimulation **of** amylase activity along the axis of pearl millet leaves beginning from basal meristem. It is evident that in dark grown seedlings there is a gradual increase in amylase activity towards the tip of the leaf, whereas in light grown seedlings the maximum photostimulation **of** amylase activity is observed in the 2nd segment from the base of the leaf; in subsequent leaf segments, the magnitude of photostimulation of amylase activity declines towards the tip of the leaf. The above increase in the amylase activity in pearl millet leaves closely corresponds with the gradient **of** β-amylase activity. The inset of Fig. 5 showing the p-amylase isozymes clearly reveals that in light p-amylase activity follows the same pattern as the photostimulation of total amylase activity in pearl millet leaves. On the other hand, in light, plastidic a-amylase activity shows a gradual increase towards the tip of the leaf (Fig. 5, inset).

DISCUSSION

In higher plants, the studies on ***in vivo*** regulation of amylases have been largely confined to seeds, where hormonal regulation of amylase induction

Table 2. The inlracellular distribution of a- and β-amylase activity in the leaves of 10 day old red light grown pearl millet seedlings. The substrate specificity and sensitivity to heat **treatment** was used to distinguish between α- and p-amylase

Fraction	Amylase activity (nkat/mg protein) Amylose	β-limit dextrin	PEP carboxylase activity (μmol/mg Chl)
Homogenate	25.0 (100%)	6.6 (100%)	*
Cytosol	21.9 (88%)	0.3 (4.6%)	2.03
Chloroplast	4.5 (18%)	5.0 (76%)	n.d.
Chloroplastic fraction, +10 mM $CaCl_2$ +10 min at 70°C	5.0 (20%)	4.4 (67%)	*
Bundle sheath strands	2.876	2.65	*

n.d.—not detected
•Estimation not done.

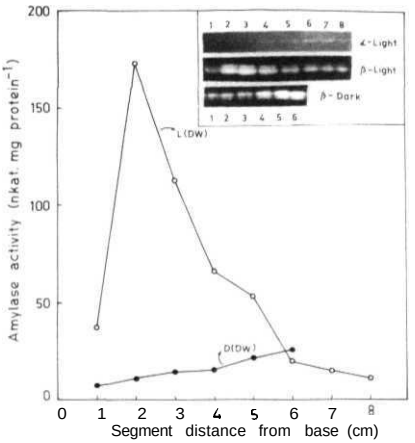

Figure 5. The relative photostimulation **of** amylase in the **different** sections (1 cm) of first leaf **of** 7 day old pearl millet seedlings. The segments are numbered from the base (segment 1| **to** the tip **of** the leaf. The light grown leaf (○) was 8 em long while the **leaf** in darkness (●) was 6 cm in length. The inset shows the gradient **of** β-amylase activity in light and in darkness and **of** plastidic α-amylase activity in light along the axis **of** leaf. The plastidie α-amylase activity was totally absent in dark grown seedlings. In order to clearly visualize β-amylase isozyme in dark grown leaves a concentrated extract was applied to gel.

and secretion have been investigated in detail **(Akazawa** *et al.,* 1988). In contrast, in leaves there is not much evidence **for** hormonal regulation of the amylase level (Drumm *el al.*, 1971). In pearl millet leaves red light acting ***via*** phytochrome leads to a significant induction of amylolytie activity during the course of seedling **development** (Fig. 1). The photoreversibility of red and also of blue light pulses by a far-red light pulse (Table 1) confirms the involvement of phytochrome in mediating the above photoresponse (Shropshire and Mohr, 1983). The greater effectiveness of brief pulses of light than continuous light points to participation of phytochrome. Under continuous red light Pfr destruction leads to a stationary state, which is likely to be lower than the Pfr level maintained by brief light pulses. Likewise, less effectiveness of blue light in stimulating amylase activity, in comparison to red light may also be a consequence of the lower photostationary state of phytochrome under blue light (Sponga *et al.,* 1986). The close similarities in these results obtained in a monocot seedling with our earlier studies on a dicot seedling, indicate that photoregulation of amylase is an intregral part of intracellular photomorphogenesis in developing leaves of higher plants (Manga and Sharma, 1988; Subbaramiah and Sharma, 1989). The photostimulation of amylase level in pearl millet leaves is largely brought about by enhancement of the β-amylase level (Fig. 2). Although a-amylase also shows a photostimulation of its activity, its total contribution to the amylolytie activity of leaves is much less.

In green leaves the principle function of amylase is to mobilize starch generated during photosynthesis, therefore, it is logical to assume that amylase is also localized in the chloroplasts. Moreover, we also expected that the increase in amylase level should be correlated with ehloroplast development and acquisition of photosynthetic competence. In this study, we used Norflurazon-mediated chlorosis of leaves (Henson, 1984) to study the interrelationship between ehloroplast biogenesis and amylase photoregulation. In pearl millet leaves the light-mediated stimulation of plastidie a-amylase is clearly associated with the light-mediated ehloroplast development. In seedlings grown in light in the presence of Norflurazon, which blocks the ehloroplast biogenesis, the plastidie a-amylase induction (as seen by the appearance of a new isozyme (R_f 0.21)] is totally suppressed (Fig. 4). These results clearly indicate that the photostimulation of plastidie a-amylase, like other plastidie proteins, is dependent on the availability of functional chloroplasts (Oelmüller, 1989). It is likely that, although a signal chain triggered by phytochrome may operate in Norflurazon-treated seedlings, in the absence of ehloroplast active plastidie a-amylase, molecules cannot accumulate. At the same time β-amylase photostimulation could take place even in the absence of chloroplasts, albeit Norflurazon lowered the level of β-amylase in light grown leaves. On the contrary, Saeed and Duke (1990) observed a Norflurazon-mediated stimulation of a-amylase activity in pea seedlings, which is localized in the apoplast, while it had no influence on the cytosolic (i-amylase activity. A similar Norflurazon-mediated decrease in the level of non-plastidic enzymes is observed in mustard seedlings where Norflurazon treatment lowered the level of glycollate oxidase and **hydrooxypyruvate** reductase, but at the same time enhanced the level of isocitrate lyase and malate synthase (Bajracharya *et al.*, 1987).

These results point out that while in mesophyll cells a-amyiase is localised in both plastidie and cytosolic fraction respectively, β-amylase is localized exclusively in the cytosolic fraction. The subcellular fractionation studies (Table 2) also confirmed the spatial localization of a- and β-amylase activity in plastidie and cytosolic compartments. Furthermore the intracellular fractionation revealed that only plastidie a- amylase is present in bundle sheath strands. Moreover, the finding that in Norflurazon-grown leaves, bundle sheath strands are totally devoid of a-amylase activity, confirms the plastidie localization of a-amylase in bundle sheath cells.

The localization and the role of a-amylase in the chloroplasts have been doubted in many studies

(Kakefuda *et al.*, 1986; Jacobson *et al.*, 1986). In C_4 plants CO_2 fixation into starch occurs in bundle sheath chloroplasts (Hoober, 1984), so the localization of α-amylase in bundle sheath chloroplasts of pearl millet leaves is positively correlated with its role in starch degradation. Although in mesophyll cells both α- and β-amylases are present, most α-amylase is localized in plastid while β-amylase is cytosolic in nature.

Monocot leaves, by virtue of having a basal leaf meristem, maintain a natural gradient of cells and organelles of increasing maturity from the base to the tip. The analysis of photostimulation of amylase along the gradient shows that the segment next to the meristematic base of pearl millet leaf shows the maximum increase in amylase activity. In contrast, in dark this gradient of amylase level is not apparent. The gradient of photostimulation of amylase activity in pearl millet leaf is closely akin to the gradient of photostimulation of chlorophyll *alb* binding protein synthesis in barley leaves (Zielinski *et al.*, 1989). This gradient of photostimulation of amylase activity results from a stimulation of β-amylase activity. In contrast plastidic α-amylase shows a gradient with increasing activity towards the tip of the leaf, similar to a gradient of RUBP carboxylase level in barley leaves (Zielinski *et al.*, 1989). The dissimilarity of gradients of plastidic α-amylase and cytosolic β-amylase activity, dependence of α-amylase photoregulation on chloroplast biogenesis, and their distinct spatial localization clearly indicate that though both enzymes are regulated by phytochrome, the signal chains regulating their increase operate independently of each other.

Acknowledgements—The authors are thankful to Dr E. Mösinger, Sandoz, Basel for providing us with a sample of Norflurazon. The authors wish to thank the Dean, School of Life Sciences for his support. This work was supported by University Grants Commission (F-3-115/86-SR II) and Council of Scientific and Industrial Research (38(674)/87-EMR-II) grants.

REFERENCES

Akazawa, T., T. Mitsui and M. Hayashi (1988) Recent progress in α-amylase biosynthesis. *The Biochemistry of Plants* (Edited by P. K. Stumpf, and E. E. Conn), Vol. 14, pp. 465-492. Academic Press, New York.

Arnon, D. I. (1949) Copper enzymes in isolated chloroplast polyphenoloxidase in *Beta vulgaris*. *Plant Physiol.* **24,** 1-15.

Bajracharya, D., R. Bergfeld, W. D. Hatzfeld, S. Klein and P. Schopfer (1987) Regulatory involvement of plastids in the development of peroxisomal enzymes in the cotyledons of mustard *{Sinapis alba* L.) seedlings. *J. Plant Physiol* **126**, 421-436.

Beck. E. and P. Ziegler (1989) Biosynthesis and degradation of starch in higher plants. *Ann. Rev. Plant Physiol. Plant Mot. Biol.* **40,** 95–117.

Chollet, R. and **W. L. Ogren** (1973) **Photosynthetic** carbon **metabolism** in isolated maize bundle sheath strands. *Plant Physiol.* **51.** 787-792.

Davis. B. J. (1964) Disc electrophoresis. Method and application to human serum proteins. *Ann. N.Y. Acad. Sci.* **121.** 404-427.

Day. D. A., C. I D. Jenkins and M. D. Hatch (1981) Isolation and properties of functional mesophyll protoplast and chloroplasts from *Zea mays. Aust. J. Plant Physiol.* 8, 21–29.

Downton, W. J. S. and S I Hawker (1973) Enzymes of starch and sucrose metabolism in *Zea mays* leaves. *Phytochem.* **12.** 1551-1556.

Drumm, H., 1. Elichinger, K. Peter, 1. Mollcr and H. Mohr (1971) **Interaction** of amylase in mustard seedlings **by** phytochrome. *Planta* **99,** 265-274.

Hcnson. I E. (1984) Inhibition of abscisic acid accumulation in seedling shoots of pearl millet (*Pennisetum americanum*) following **induction** of chlorosis by Norflurazon, Z. *Pflanzenphysiol* **114,** 35-44.

Hoober, K. V. (1984) *Chloroplast.* Plenum, New York.

Jacobsen, J V . A D. Hanson and P. C. Chandler (1986) Water Stress enhances expression of an a-amylase gene **in barley** leaves. *Plant Physiol* **80,** 350–359.

Kakefuda, G., S. H. Duke and M. S. Hostak (1986) **Chloroplast** and **extrachlorplastic** starch-degrading enzymes in *Pisum sativum* L. *Planta* **168,** 175-182.

Kendrick. R. E. and Ci. **11.** M. Kronenberg (1986) ***Photomorphogenesis in Plants.*** Martinus Nijhoff/W. Junk, **Dodrecht,** The Netherlands.

Kobayashi, H., L. Bogorad and C. D. Miles (1987) Nuclear generegulated expression of chloroplast genes for **coupling** factor one in maize. *Plant Physiol.* **85,** 757-767.

Lilley, R. McC.M. P. Fitzgerald, K. G. Rienits and D. A. Walker (1975) Criteria of intactness and photosynthetic activity of spinach chloroplast preparation. *New Phytol.* 75. 1-10.

Lowry, O. H., N J. Rosebrough. A H. Farr and R. J. Randall (1951) Protein measurement with the folin phenol reagent *J Biol. Chem.* **193**, 256–275.

Manga, V. A. and R. Sharma (1988) Blue light mediated regulation of p-amylase activity in mustard ***(Sinapis*** *alba* L.) cotyledons. ***Plant*** *Cell Physiol.* **29**, 673-676.

Manga, V, A. and R. Sharma (1990) Lack of functional interrelationship between β-amylase photoregulation and chloroplast development in mustard (*Sinapis alba* L.) cotyledons *Plant Cell Physiol.* **31.** 167-172.

Manners, D. J. (1985) Starch. In *Biochemistry of Storage Carbohydrates in Green Plants* (Edited by Dey P. M. and R A. Dixon), pp. 149–203. Academic Press, London

Nott, D. L. and C B. Osmond (1982) Purification and properties of PEP Carboxylase from plants with CAM metabolism. *Aust J. Plant Physiol.* 9, 409-422.

Oelmüller, R. (1989) Photooxidative destruction of chloroplasts and its effect on nuclear gene expression and extraplastidic enzyme levels. *Photochem. Photobiol.* **49,** 229-239.

Palmer, J. D. (1986) Isolation and structural analysis of chloroplast DNA. *Methods Enzymol.* **118,** 167-169.

Saeed, M. and S. H. Duke (1990) Chloroplastic regulation of apoplastic **a-amylase** activity in pea seedlings. *Plant Physiol.* **93,** 131-140

Shropshire, W. Jr and H. Mohr (1983) Photomorphogenesis. *Encylopaedia of Plant Physiology.* Vol. 16, *New Series.* Springer Verlag, Berlin.

Spilatro, S. R. and J. Preiss (1987) Regulation of starch synthesis in the bundle sheath and mesophyll of *Zea mays* L. *Plant Physiol.* **83,** 621-627.

Sponga, F. C, G. F. Deitzer and A. L. Mancinelli (1986) Cryptochrome, phytochrome and photoregulation of

anthocyanin under blue light. *Plant Physiol.* 82, 952-955.

Subbaramaiah, K. and R. Sharma (1989) β-amylase from mustard (*Sinapsis alba* L) cotyledons: Immunochemical evidence for synthesis *de novo* during **photoregulated** seedling development. *Plant Physiol.* 89, 860–866.

Zieglar, P. (1988) Partial purification and characterization of the major endoamylasc of mature Pea leaves. *Plant Physiol.* 86, 659–666.

Ziegler, P. and E. Beck (1986) Exoamylase activity in vacuoles isolated from pea and wheat leaf protoplasts. *Plant Physiol.* 82, 1119–1121.

Zielinksi, R. E., W. M. Jeffrey and M. E. Jenkins (1989) Coordinate expression of rubisco activase and rubisco during barley leaf cell development. *Plant Physiol.* 90, 516-521.